FUNCTIONAL, STRUCTURAL AND MOLECULAR ALTERATIONS IN THE HEART AND KIDNEY DURING DIABETES MELLITUS

By

TEHREEM WAQAR

A thesis submitted in partial fulfilment for the requirements for the degree of Doctor of Philosophy at the University of Central Lancashire

February 2016

STUDENT DECLARATION FORM

Concurrent registration for two or more academic awards

I declare that while registered as a candidate for the research degree, I have not been a registered candidate or enrolled student for another award of the University or other academic or professional institution

Signature of Candidate _____

Type of Award _____

School _____

DECLARATION

I declare that I have not been an enrolled or registered candidate at any other academic or professional institution while being registered for the research degree at University of Central Lancashire. Furthermore, no material contained in this thesis has been utilised in any other submission for an academic award and is solely my own work.

ABSTRACT

Background: Diabetes mellitus (DM) is a major metabolic disorder leading to severe long term complications including cardiomyopathy, nephropathy, retinopathy and neuropathy that are common in type 1 DM (T1DM) and type 2 DM (T2DM). Epidemiological studies have demonstrated a role of hyperglycaemia (HG) in eliciting adverse cardiac and renal outcomes including heart failure (HF), diastolic and renal dysfunction. This study investigated the effect of HG on left ventricle (LV) and kidney structural remodelling, function and underlying molecular events associated with the two organs over a period of 2 and 4 months compared to age-matched control.

Methods: Molecular mechanisms underlying HG-induced remodelling changes including extracellular matrix (ECM) and myocyte apoptosis deposition, underlying cytokine induction, recapitulation of foetal genes, and transcriptional alterations that may influence the ECM and intracellular calcium $[Ca^{2+}]_i$ handling in the LV and kidney of T1DM as well as T2DM were examined in this study. LV and kidney isolations following 2 and 4 months of the development of T1DM were used to assess the remodelling changes and underlying transforming growth factor β1 (TGFβ1) activity, gene expression profile of the ECM and calcium mediators using histological, immunohistochemical and quantitative gene expression analyses compared to age-matched Wistar control rats.

Results: The results show that T1DM over 4 months can elicit severe structural and molecular changes in the LV and the kidney compared to 2 months of DM. The severity of these changes was significantly less in respective healthy age-matched control animals. The isolated ventricular cardiomyocytes from T1DM rats displayed altered cellular calcium (Ca^{2+}) homeostasis and $[Ca^{2+}]$i translating to alterations in mRNA abundance of key Ca^{2+} handling proteins, cardiac sarcoplasmic reticulum Ca^{2+}ATPase 2a (SERCA2a), ryanodine receptor (RyR2), Na^{2+}/Ca^{2+} exchanger, phospholamban (Plb), L-type Ca^{2+} channel proteins (Cav1.2 and Cav1.3), calmodulin2 (Calm2) and Ca^{2+}/calmodulin-dependant protein kinase II delta (CaMK2d) were significantly ($p<0.05$) altered in DM compared to age-matched control animals. The results showed LV and kidney remodelling in the T1DM rats with increased ECM deposition that translated into increased gene expressions of key components (collagen 1α, collagen 3α, fibronectin and elastin) and modulators i.e. MMP2 and MMP9 and their tissue inhibitor (TIMP4), connective tissue growth factor (CTGF), integrin 5α and connexin 43 (Cx43)

of the ECM. Molecular derangements underlying this phenotype included increased TGFβ1 transcription and activity, recapitulation of foetal gene phenotype atrial natriuretic peptide (ANP), brain natriuretic peptide (BNP) with marked hypertrophy, underscored by caspase-3 mediated cell apoptosis. Electron microscopic analysis revealed ultrastructural alterations in LV highlighted by increased mitochondrial number and altered mitochondrial population, whereas the kidney presented with increase glomerular basement membrane thickness in T1DM compared to controls. These data clearly show that adult vs young adult, in combination with STZ-induced T1DM, can elicit severe changes to both the heart and the kidney, respectively in structural, functional and biochemical alterations. The final part of the study revealed exercise training after 2-3 months may have beneficial effects in T2DM animals compared to sedentary control rats. Ventricular myocyte and shortening were generally well preserved despite alterations in mRNA gene expression encoding a variety of cardiac muscle proteins in the exercised trained adult GK diabetic rat. LV remodelling in GK rat presented with marked hypertrophy of cardiomyocytes and increased ECM deposition that altogether translated into increased ECM components and regulators which were reversed by exercise training.

Conclusions: The present results have demonstrated that T1DM, if left untreated, can lead to severe changes to both the heart and the kidney. These changes seem to occur at structural and molecular levels leading to dysfunction of the heart and kidney and the severity of the damage is enhanced over time. Data suggests that diabetic cardiomyopathy (DCM) may have possible origins in pro-fibrotic and pro-hypertrophic mechanisms. Moreover, this study demonstrates that physical exercise training continues to be one of the most valuable forms of non-pharmacological therapy in DM. Data concerning molecular signalling cascades and ECM phenotype is particularly significant as targeting features of structural remodelling may delay onset and severity of myocardial and renal complications.

TABLE OF CONTENTS

2. MATERIALS AND METHODS

LIST OF TABLES

LIST OF FIGURES

CHAPTER 3

CHAPTER 4

CHAPTER 5

CHAPTER 6

CHAPTER 7

CHAPTER 8

ACKNOWLEDGEMENTS

It is my pleasure to take this opportunity to convey my sincere thanks to numerous people who have made this thesis possible.

My deepest gratitude and appreciation is for my Ph.D. supervisor, friend and guide, Professor Jaipaul Singh, without whom I could not have reached the end of my research journey at UCLAN. His brilliant ideas, constant advice, mentorship, tremendous support and guidance have been of paramount value and have helped me grow as an independent thinker and researcher. Jai, your patience, inspiration, enthusiasm and generous contribution of resources and time are invaluable to me and I Thankyou for all that you have done for me.

Many thanks are due to several academics with whom I have had the opportunity and fortune to work with throughout my research and study. I am obliged to Professor Chris Howarth and Ernest Adeghate from the United Arab Emirates University (UAEU) who have provided me with great support and guidance constantly. My sincere thanks are due to Dr. Keshore Bidasee from the University of Nebraska Medical Centre (UNMC) who has guided me in the right direction in times of despair and for his encouragement and insight and Dr. Alicia D'Souza from University of Manchester, for her much appreciated help.

Collectively, I am thankful to my good friends and student colleagues from UCLAN and other institutions for providing a fun filled environment to relax and enjoy the research experience. Particular mention is for the technical support staff at UAEU, Anwar Qureshi for his help in conducting experiments and guidance, along with Saeed Tariq for his assistance. I owe a special thanks to Dr Simarjit Singhrao from UCLAN for her much appreciated support.

Most of all, this thesis could not have been possible without the encouragement, confidence and continuous support of my loving parents who have helped in every step of my journey, morally, emotionally, and financially. I am especially appreciative to my loving 2nd parents, who have provided me with invaluable love and prayers. Also, my grandmother for her most appreciated prayers and my siblings who have along with being irritating, provided me with moral support. Lastly, my heartiest acknowledgment is for my loving husband, Waqar Ahmed, whose tremendous encouragement, love and care erased all my worries. I dedicate this thesis to my parents and my 2nd parents.

ABBREVIATIONS

$[Ca^{2+}]_i$	Intracellular calcium concentration
*I*Ca,	Voltage-gated L-type Ca^{2+} channels
ACCORD	Action to Control Cardiovascular Risk in Diabetes
ACh	Acetylcholine
AGE	Advanced glycation end product
AV	Atrioventricular
αSKA	α-Skeletal actin
ANP	Atrial natriuretic peptide
ATP	Adenosine triphosphatase
BNP	B-type natriuretic peptide
BC	Bowmen Capsule
BMI	Body Mass Index
BW	Body weight
CHF	Congestive heart failure
Cl^-	Chloride ion
Ct	Cycle threshold
CICR	Calcium Induce Calcium Release
CHD	Coronary Heart Disease
CHF	Congestive Heart Failure
CKD	Chronic Kidney Disease
Col1α	Collagen Type 1α
Col3α	Collagen Type 3α
CRS	Cardio Renal Syndrome
Ca^{2+}	Calcium ion
CTGF	Connective tissue growth factor
CRP	C-reactive protein
Cx43	Connexin 43
cDNA	Complementary deoxyribonucleic acid
CVD	Cardiovascular disease
DAG	Diacylglycerol
DCCT	Diabetes Control and Complications Trial
DCM	Diabetic cardiomyopathy
DM	Diabetes mellitus
DN	Diabetic Nephropathy

ECG	Electrocardiogram
ECM	Extracellular matrix
ECC	Excitation-contraction coupling
EDV	End diastolic volume
EM	Electron Microscope
ESRD	End Stage Renal Disease
FN	Fibronectin
FITC	Fluorescein isothiocyanate
GAPDH	Glyceraldehyde-3-phosphate dehydrogenase
GBM	Glomerular basement membrane
GFR	Glomerular filtration rate
GFs	Growth factors
GTT	Glucose tolerance test
GLUT2	Glucose transporter 2
GK	Goto-Kakizaki
H&E	Hematoxylin and Eosin
HbA1c	Glycated haemoglobin
HF	Heart failure
HG	Hyperglycaemia
HW	Heart weight
Hz	Hertz
IFM	Interfibrillar mitochondria
K^+	Potassium Ion
LA	Left atrium
LV	Left ventricle
LVH	Left ventricle hypertrophy
LVEF	Left Ventricular Ejection Fraction
MI	Myocardial infarction
MMPs	Metalloproteinases
MPTP	Mitochondrial permeability transition pore
MODY	Maturity Onset Diabetes of the young
NA	Noradrenaline
NF-κB,	Nuclear Factor kappa-B
Na^+	Sodium Ion
NHS	National Health System

NCX	Na^+/Ca^{2+} exchanger
PIb	Phospholamban
PGs	Proteoglycans
PO	Pressure overload
PARP	Poly (ADP-ribose) polymerase-1
PKC	Protein kinase C
PBS	Phosphate buffered saline
PI3-K	Phosphatidylinositol 3-kinase
RASS	Renin-Angiotensin-Aldosterone System
ROS	Reactive Oxygen Species
RNA	Ribonucleic acid
RTqPCR	Quantitative real time polymerase chain reaction
RyR	Ryanodine receptor
SR	Sarcoplasmic reticulum
SERCA	Sarcoplasmic reticulum calcium ATPase
SHR	Spontaneously Hypertensive Rat
SSM	Sub-sarcolemmal mitochondria
SA	Sinoatrial
SR	Sarcoplasmic reticulum
SCD	Sudden cardiac death
STZ	Streptozotocin
TM	Tropomyosin
T1DM/IDD	Insulin-Dependent Diabetes Mellitus
T2DM/NIDDM	Non-insulin Dependent Diabetes Mellitus
TGFβ1	Transforming growth factor β1
TIMP	Tissue inhibitor of matrix metalloproteinase
Tm	Tropomyosin
TNFα	Tumour necrosis factor α
TnT, TnI, TnC	Troponin T, Troponin I, Troponin C
UKPDS	U.K. Prospective Diabetes Study
V	Volts
WRF	Worsening of renal function

CHAPTER 1

GENERAL INTRODUCTION

1.1 Functional anatomy of the mammalian heart

The mammalian heart is a four-chambered muscular organ located in the thoracic cavity medial to the lungs and posterior to the sternum, enclosed by the fibrous pericardium. The heart's pumping ability is central to the functioning of the circulatory system wherein blood is pumped through a network of blood vessels namely arteries, veins, arterioles, venules and capillaries. These blood vessels consist of a pulmonary circuit in which blood is carried to and from gas exchange surfaces of the lungs and a systemic circuit where deoxygenated blood is taken in through the veins and delivered to the lungs for oxygenation before pumping it into the various arteries (Vander *et al.,* 2007; Devereux *et al*., 2000; Sherwood, 2008).

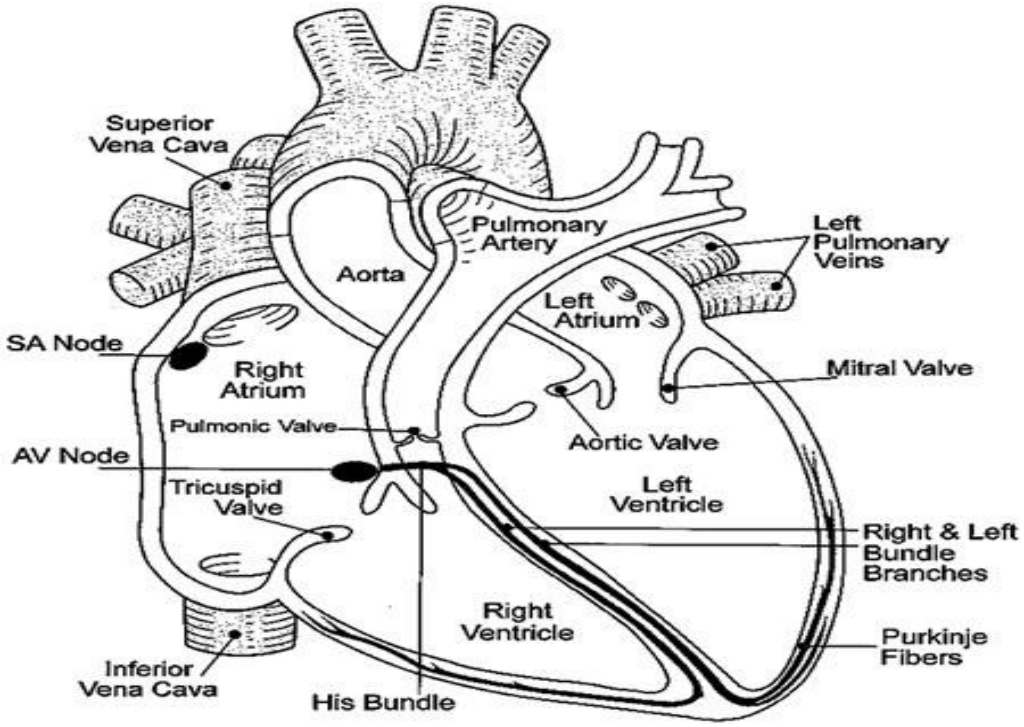

Figure 1.1: The mammalian heart. Components are described in the text (Image courtesy www.beyondbiology.org)

As shown in figure 1.1, the right and left atria and the right and left ventricles make up the four chambers of the mammalian heart. The chambers on the right are much smaller than the chambers on the left side of the heart and this difference in size is related to their functions and the size of the 2 circulatory loops namely, the systemic circuit and the pulmonary circuit. The right atrium is associated with the systemic circuit, receiving blood from the superior vena cava and the inferior vena cava and allows blood to flow

into the right ventricle passing through the right atrioventricular (AV) valve or tricuspid valve. Blood is pumped through the pulmonary circuit to be collected by the left atrium and emptied into the left ventricle (LV) through the left AV or bicuspid valve. Semi-lunar valves are situated between the ventricles and the major blood vessels of the heart and open and close passively due to pressure gradients. Blood pumped from the right atrium into the pulmonary trunk passes through the pulmonary valve and blood leaves the left ventricle through the aortic valve into the ascending aorta. The atria are separated by the inter-atrial septum and the ventricles by a much thicker inter-ventricular septum that houses electrical conduction tissue. Innervation of the heart is by both vagal and sympathetic fibres. The sino-atrial (SA) node and the atria are predominantly innervated by the right vagus, whereas the left vagus nerve supplies the AV node and the bundle of His (Vander *et al*., 2007). The ventricles of the myocardium are only sparsely innervated by vagal efferents. Nevertheless, the rhythmic contraction of the heart is initiated in the SA node and cardiac function is mediated by neural activation. The release of noradrenaline (NA) by sympathetic nerves and subsequent activation of beta adrenergic receptors result in positive chronotropy, inotropy and dromotropy as well as enhanced metabolism. In contrast, parasympathetic nerves (vagus) release acetylcholine (ACh) that acts on muscarinic cholinergic receptors in the heart leading to negative dromotropic, inotropic and chronotropic effects. The cardiac action potential that initiates contraction is generated in the SA node and spreads through the atria before converging upon the AV node for distribution to the ventricles by the specialised Bundle of His, right and left bundle branches and Purkinje fibre network.

The walls of the atria are thinner than those of the ventricles, particularly the LV whose wall is 3-4 times thicker than the right ventricle at a corresponding position (Vander *et al*., 2007). The walls of the heart typically contain three distinct layers namely the outer epicardium, (visceral pericardium) which is a serous membrane consisting of an exposed mesothelium and layer of smooth connective tissue that is attached to the myocardium (Koeppen and Stanton, 2008). The epicardium makes up the outer layer of the heart wall and consists of mainly a thin connective tissue membrane that helps to lubricate and protect the outside of the heart, forming the inner membrane portion of the pericardium. The endocardium, is the inner most layer of the wall, lining the inner surfaces of the heart (including valves), and consists of a simple squamous epithelial layer overlying a thinner areola tissue. The middle muscular wall and the thickest

section of the heart wall are the myocardium which contains several types of specialized cells, including ventricular and atrial cells or myocytes, nodal cells, smooth muscle cells and purkinje fibres that form both the atria and ventricles (Koeppen and Stanton, 2008). Cardiac myocytes account for 70% to 75% of the myocardium by cell volume but only 25% to 30% by cell number. Cardiac fibroblasts that synthesize proteins of the ECM are the most abundant cell type of the myocardium (Miner and Miller, 2006).

1.1.2 The extracellular matrix

The extracellular matrix (ECM) (Figure 1.2) is a highly organised structured non-cellular component present within all tissues and organs, providing fundamental physical scaffolding for the cellular constituents as well as playing a crucial role in initiating central biochemical and biomechanical cues that are requisite for tissue differentiation, morphogenesis and homeostasis (Frantz *et al*. 2010). The ECM is broadly differentiated into an epimysium encircling the endo- and epicardium, a perimysium that groups myofibrils into bundles and an endomysium that surrounds individual myocytes and provides connection to the vasculature (Fedak *et al*., 2005). The ECM is a highly dynamic structure that is persistently being remodelled, either by enzymatic or non-enzymatic actions and its molecular components undergoing multiple post-transductional modifications. Via these physical and biochemical characteristics, the ECM generates biochemical and mechanical properties of organs including their tensile strength and elasticity. In addition, the ECM consists of an essential morphological organisation and physiological function that directs the binding of growth factors (GFs) and interaction of cell-surface receptors which educe signal transduction and regulate gene transcription. Fibroblasts account for around 60-70% of the cells and are the key source of components of the ECM (Badylak., 2007). These are involved in regulation of the structure of the heart, as well as the mechanical, chemical and electrical signals between cellular and non-cellular components (Manabe *et al*., 2002). The ECM mainly comprises two individual classes of macromolecules: proteoglycans (PGs) and fibrous proteins. The most important fibrous ECM proteins include collagens, elastin, fibronectin and laminin (Jarvelainen *et al*., 2009; Schaefer and Schaefer., 2010; Alberts *et al*., 2007). The most abundant fibrous protein and the main structural component of the ECM are collagens I and II, synthesised by fibroblasts, comprising approximately 80% and 10% of the ECM, respectively. These collagens are the major stress-bearing element of the ECM which forms a 3D network

around bundles of myocytes in order to generate a stress-tolerant network. Collagens provide tensile strength, regulate cell adhesion and also support migration as well as chemotaxis and direct tissue development (Rozario and DeSimone., 2010). Fibronectin (FN) are intimately involved in the organisation of the interstitial ECM, playing a crucial role in directing cell attachment and function and is also classed as an extracellular mechano-receptor involved in cell migration (Smith *et al*., 2007; Rozario and DeSimone., 2010; Tsang *et al*., 2010). The ability to synthesize ECM components varies within the heart. Depending on the stimulus, myocytes produce type IV and VI collagens, laminin and proteoglycans and the mass of interstitial collagens types I and III and fibronectin are transcribed by surrounding fibroblasts that either live in the stoma or are recruited from neighbouring tissues (Banerjee *et al*. 2006; 2007; De Wever *et al*., 2008; Bosman and Stamenkovic., 2003). It is this calm network of collagens and elastin fibers which provide a healthy ECM enabled to resist tensile stresses. Thus, the ECM is a highly dynamic entity that constantly undergoes regulated remodelling whose fine structurisation is crucial for the maintenance of normal ECM function (Egeblad *et al*., 2010).

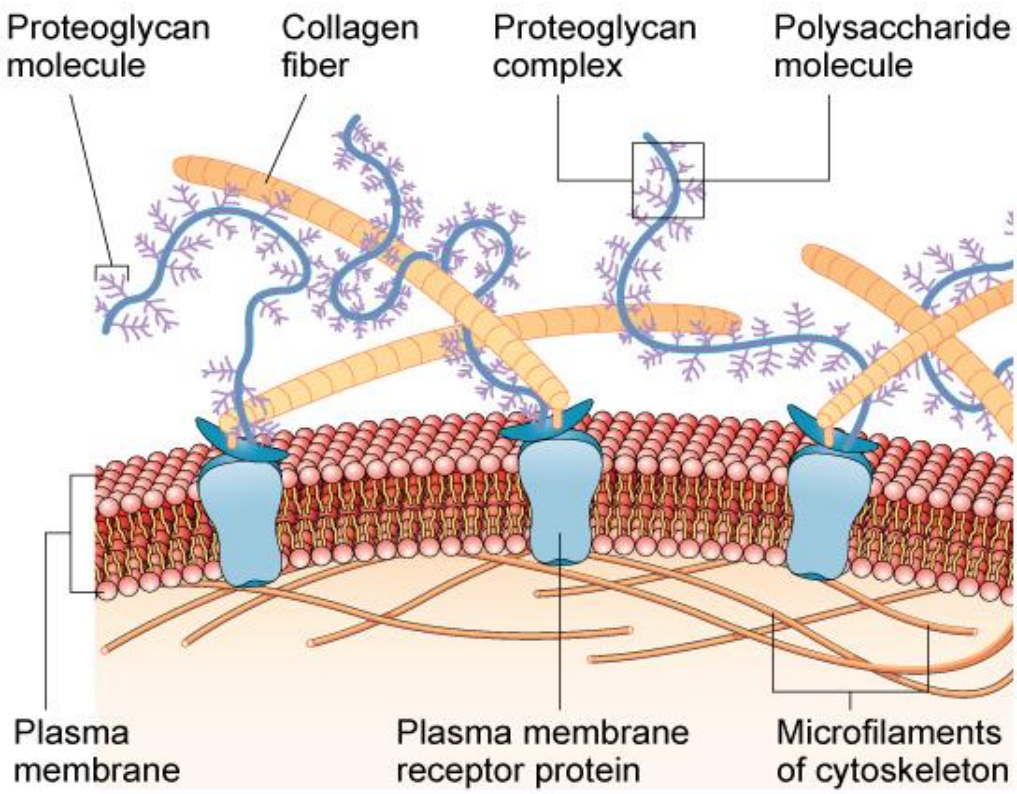

Figure 1.2: **Components of the extracellular matrix membrane.** This highlights the main components of the ECM. Contents are described in the text. (Image courtesy: http://naginata.cnx.rice.edu:9090/content/m10007/1.12).

ECM trans-membrane mechanoreceptors known as integrins constitute another important entity that transduces mechanical forces and changes in ECM structure, through signals from the extracellular compartment to the cytoskeleton and vice versa. Integrins consist of two different chains, α (120±150 kDa) and β (110±190 kDa), linked by non covalent bonds. These mechanoreceptors are involved in sending signals by ionic channels, hormone receptors and also GFs to participate in transduction processes including cell motility, differentiation and cell death (Spinale, 2007; Graham *et al*., 2008; Bowers *et al*., 2010). Figure 1.3 highlights a number of local and long-distance cell-cell communications that contribute to the maintenance of normal cardiac homeostasis and to response to hypertrophic stimuli. These include paracrine/autocrine and endocrine signals, direct cell-cell contacts via gap junction, and cell-matrix interactions between cells of the coronary vasculature, cardiomyocytes, fibroblasts, and other cell types. Perturbations in the balance of this network during sustained haemodynamic stress can lead to a variety of pathological sequelae, including heart failure resulting from inadequate vascular compensation for myocyte hypertrophy and

the development of cardiac fibrosis as a consequence of fibroblast proliferation and remodelling of the ECM (Tirziu *et al*., 2010).

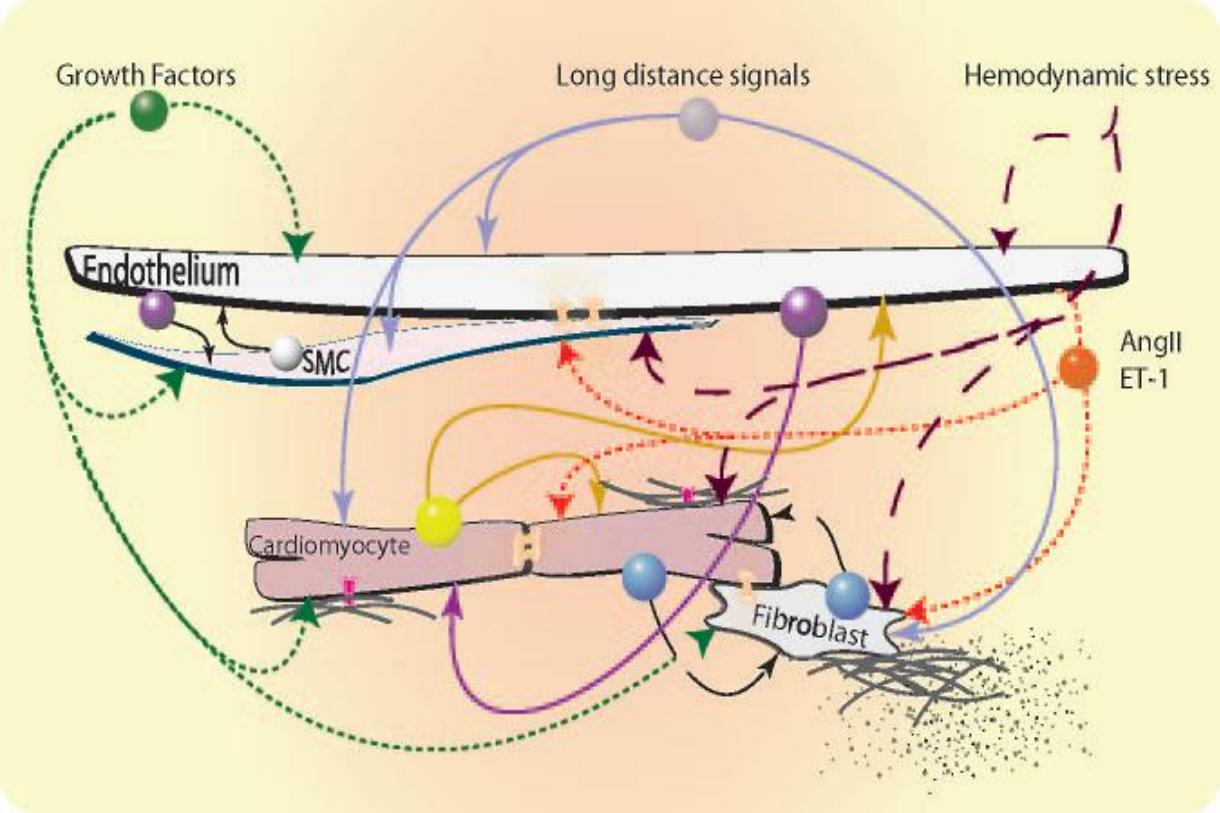

Figure 1.3: Cellular crosstalk paradigms in the heart. A diagram showing cell-cell communication mechanisms that contribute to the maintenance of normal cardiac homeostasis and responses to hypertrophic stimulus. Contents described in text. The green dot indicates growth factors, orange dot, stress enhancers (eg, AngII, ET-1); purple dot, endothelium signals; white dot, smooth muscle cells signals; yellow dot, cardiomyocyte signals; blue dot, cardiomyocyte-fibroblast signals (eg, TGF/CTGF); grey dot, endocrine signals; pink symbol, integrins; and gold symbol, connexins (Image adapted from Tirziu *et al*., 2010).

ECM homeostasis is maintained by coordinated action of the stimulators and inhibitors. Degradation of collagens occurs due to secretion of fibroblast metalloproteinases (MMPs) (Mott and Werb, 2004); which are capable of enzymatically digesting various ECM proteins. Different families of MMPs regulate the ECM in both normal and pathological conditions. Collagenases (MMP1) cleave collagens in fragments which in turn constitute the substrate of proteases including the gelatinases (MMP2, MMP9) that are responsible for the degradation of type IV collagen and fibronectin (Bowers *et al*., 2010). The activity of these MMPs is controlled at transcriptional level and also via activation and inhibition by other proteins including tissue inhibitors of metalloproteinases (TIMPs) (Cruz-Munoz and Khokha., 2008), together with the controlled activity of other enzymes, such as LOX, transglutaminases that crosslink and stiffen the ECM (Lucero and Kagan., 2006). These processes are directed by an excess of GFs that are bound to the ECM (Friedl., 2010; Macri *et al*., 2007; Murakami *et al*., 2008; Oehrl and Panayotou., 2008) which differentially adjust cell growth and migration and, comprise part of a tightly controlled feedback circuit that is essential for normal tissue homeostasis when released (Hynes., 2009). Modulation of these various components regulates mechanical, chemical and electrical signaling between cells (Miner and Miller, 2006).

1.1.3 The cardiomyocyte

Cardiomyocytes within the heart are required for contraction in unison to provide effective pump action of the heart to ensure adequate blood perfusion of the various organs and tissues of the body. Ventricular myocytes are single-nucleated elongated cells that have an inconsistent branching morphology of contractile myofibrils forming a striated appearance with an extensive capillary supply (Walker and Spinale., 1999). The intercalated discs of neighbouring cells are physically connected by types of cell junction i.e. gap junctions and desmosomes that together orchestrate and integrate cardiac electro-mechanical activity. Thus, the entire myocardium functions as a single unit, most commonly known as a ‘syncytium’ with a single contraction of the atria followed by a single contraction of the ventricles (Vander *et al*., 2007) (Figure 1.4).

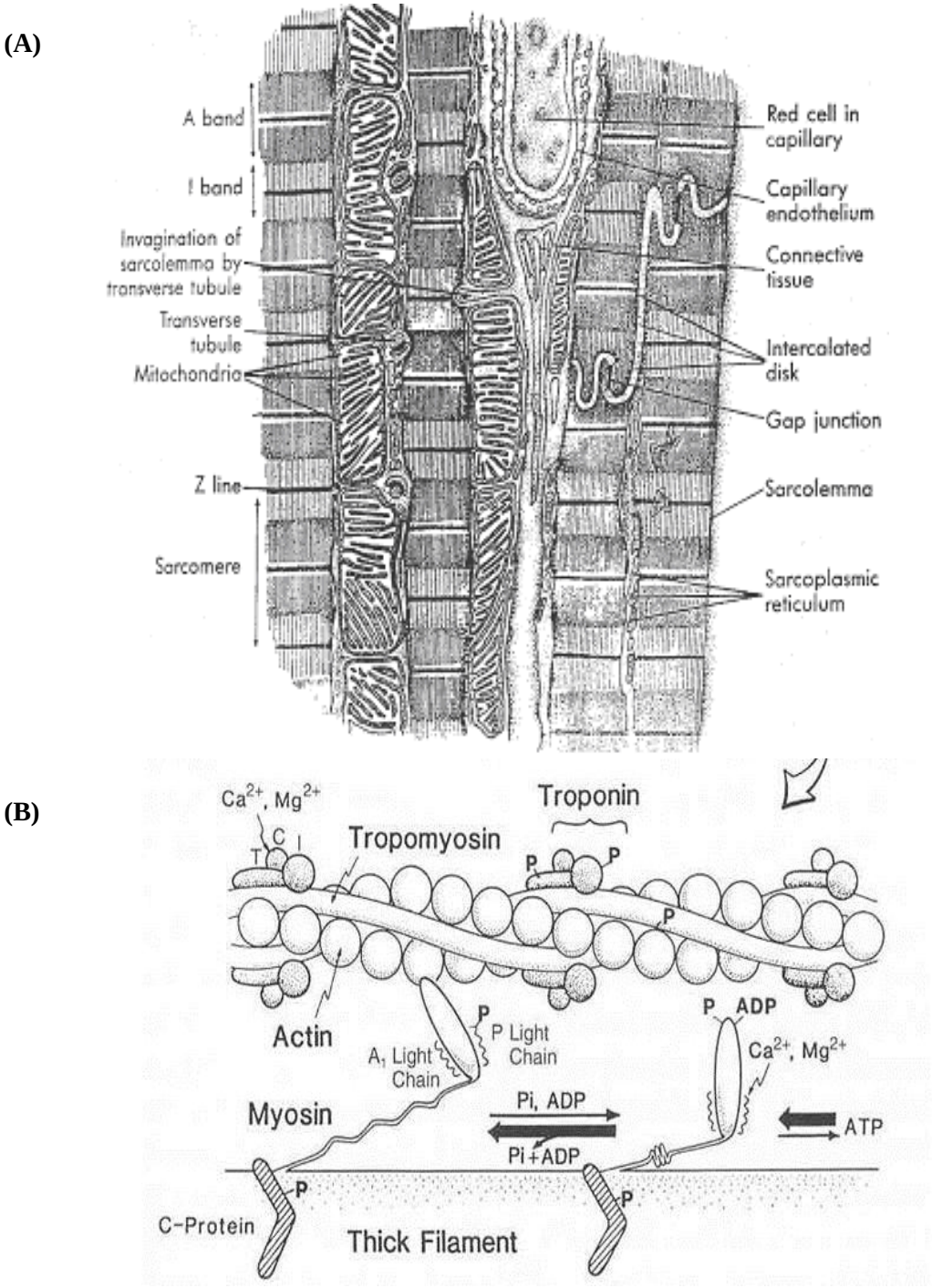

Figure 1.4: Functional anatomy of ventricular cardiomyocytes. Representative EM micrograph showing cardiomyocyte architecture **(A),** Cardiac myofilaments in cross bridge cycle underlying muscle contraction **(B)**. (Image Courtesy: (A) Koeppen and Stanton., 2008, (B) from http://www.ccbm.jhu.edu/doc/courses/BME_580_682)

The cardiomyocyte contains the sarcolemma, a specialized component of the cardiomyocyte which mainly serves as a lipid bilayer in combination with the plasma membrane and the basement membrane that contain membrane receptors, pumps and channels that regulate contractility. The sarcolemma forms the most specialized regions

of the myocyte, intercalated discs and the transverse tubular system. Each myocyte is connected to adjacent myocytes via intercalated discs. Intercalated discs form cell to cell junctions i.e. gap junctions and desmosomes serving as a strong mechanical link between myocytes as well as a path for low resistance allowing rapid conduction of action potentials between myocytes (Vander *et al*., 2007). Within the cardiomyocyte, each myofibril is enclosed with the sarcoplasmic reticulum (SR); a highly efficient Ca^{2+} handling organelle in an intracellular membrane network. The SR is specialized in regulation of cytosolic Ca^{2+} flux and forms specialized structural regions of the myocyte in close proximity with the sarcolemma and the T tubular system (Figure 1.3B). The SR is the major contractile source of Ca^{2+} in excitation-contraction coupling (ECC) with the help of the key sarcoplasmic proteins namely sarcoplasmic reticulum Ca^{2+} ATPase (SERCA), the regulatory protein of SERCA, phospholamban (Plb) and the Ca^{2+} release channels. Transverse tubules commonly known as T tubules, form invaginations of the sarcolemma into the myocyte forming a barrier between the intracellular and extracellular spaces. These T tubules play a major role in bringing in to close proximity sarcolemma ion channels and the SR Ca^{2+} discharge system and the SR calcium handling proteins, hence making the T-tubular system an important structural component in cell contractility. An important contractile unit present within the cardiomyocyte is known as the sacromere. This contains inter-digitating thick and thin filaments namely proteins actin, myosin, troponin complex and tropomyosin (Tm). The troponin complex is present within the thin filament and regulates the extent of cross-bridge formation along with contributing to the structural integrity of the sacromere. Troponin T binds the troponin complex to tropomyosin, anchoring the complex to the thin filament (Woodcock & Matkovich., 2005, Roderick and Bootman., 2007).

A more complete appreciation of the functional anatomy (contraction and relaxation) of myocyte ultra-structure comes from studies in ventricular myocytes.

The typical sequence and synchronous contraction of the atria and ventricles require the rapid activation of groups of cardiac cells. An activation mechanism is required to enable rapid changes in heart rate and also respond to the changes in autonomic tone. The propagating cardiac action potential fulfils these roles (Figure 1.5). In a resting cell, permeability is favoured for the entry of potassium ions (K^+) along with a relative impermeability to sodium ions (Na^+), calcium (Ca^{2+}) and chloride ions (Cl^-). Hence, the resultant resting membrane potential is highly negative at -90 mV. The 5 phases of a normal action potential are illustrated in figure 1.4). At phase 0, a rapid depolarisation

of the sarcolemma membrane occurs causing a transient opening of the fast Na^+ channels and slow Ca^{2+} channels. This leads on to a large influx of Na^+ into the cell via voltage-activated Na^+ channels, driving the membrane potential to +70 mV (Na^+ equilibrium) (Grant., 2009). Phase 1 represents the phase of rapid repolarisation, in correspondence with a rapid inactivation of the fast Na^+ channels along with a transient net external current of K^+ along the electrochemical gradient. This phase sets the potential for the next phase of the action potential to occur. Phase 2 represents a plateau phase which is the longest phase of a typical action potential. During this phase, a small influx of Ca^{2+} enters the cell after the initial depolarisation and triggers the release of Ca^{2+} from the SR via activation of the SR Ca^{2+} release channels resulting in a transient rise in cytosolic free calcium (Vander *et al.*, 2007). Phase 3 corresponds to the repolarisation of the action potential where a decay of the calcium transient occurs due to the reuptake of Ca^{2+} into the SR via the SERCA and the extrusion of Ca^{2+} from the cardiomyocyte primarily by the Na^+/Ca^{2+} exchanger (NCX). This phase occurs due to the closure of Ca^{2+} channels and the increased K^+ rectifier currents leading to a negative membrane potential. Phase 4 corresponds to the resting membrane potential where the sarcolemma becomes permeable to K^+ again and this condition is maintained by a combination of processes including Na^+/K^+ ATPase and the NCX as well as the activities of the inward K^+ rectifier (Grant., 2009; Vander *et al.*, 2007).

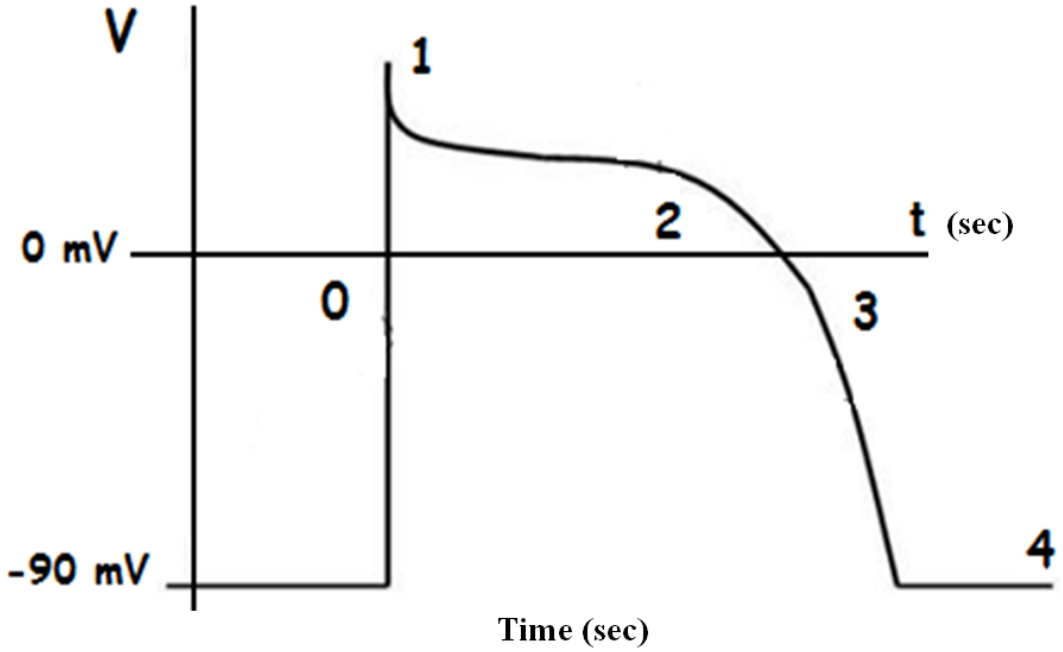

Figure 1.5: Diagram showing a typical action potential of a mammalian ventricular myocyte. Each number represents the four phases of the action potential. Phase 0, the upstroke, corresponds to rapid depolarization. The upstroke is followed by phase 1, a brief early repolarization, phase 2 or plateau, phase 3 or rapid repolarization, and phase 4, which corresponds to the resting membrane potential. (Image adapted from Grant., 2009).

Under resting conditions, lower intracellular Ca^{2+} favours the shift of the Tn-Tm complex towards the outer grooves of the actin filament and thereby blocks actin-myosin interaction. A rise in Ca^{2+} concentration during the action potential and subsequent binding of Ca^{2+} to TnC strengthens troponin C-troponin I interaction and detaches troponin I from the actin molecule by a conformational shift of the Tn-Tm complex, enabling cross bridge formation (Figure 1.6). Available literature suggests that thin filament activation is achieved by the movement of Tm over the surface of actin and this motion permits force generation and shortening. After cross bridge formation, i.e. the attachment of the myosin head of the thick filament to the actin molecules of the thin filament, the myosin head changes conformation 'pivoting' towards the M-line, with concomitant ATP hydrolysis to ADP that generates force causing the thin filament to slide over the thick filament and the sarcomere to shorten, collectively resulting in contraction. Binding of adenosine triphosphate (ATP) to the myosin head causes detachment of cross-bridges and (re)exposure of active sites making possible interaction with another cross-bridge. This highly dynamic phenomenon termed the 'sliding

filament theory' moves the filaments approximately 10 nm with an average velocity of 0.98 µm/s (Koeppen and Stanton., 2008) (Figure 1.5).

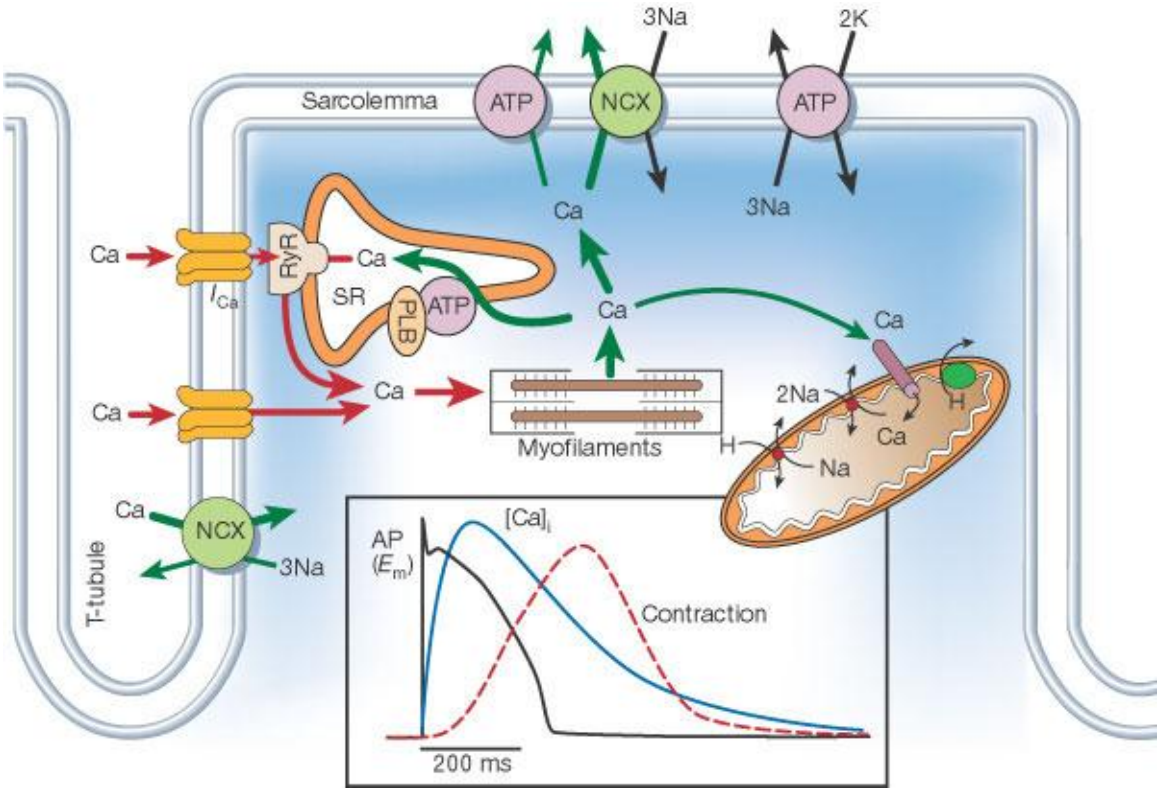

Figure 1.6: Diagram showing the processes involved in cardiac muscle contraction and relaxation (sliding filament). The insert shows relationship between the cardiac action potential, the Ca^{2+} transient and contraction (Taken from Bers, 2002).

1.1.4 Excitation contraction coupling (ECC) of the normal heart

The major function of the heart is to pump blood efficiently by virtue of an orchestrated contraction–relaxation cycle of the working cardiomyocytes (Figure 1.6). Contractility of these cardiomyocytes is regulated by a spatially defined program of ion channels and exchangers that precisely control Ca^{2+} entry in and out of the cell and the SR. Regulation of contractility, hence the control of Ca^{2+} release, is principally achieved via the electrical activity of the sarcolemma. Depolarization of the cardiac cell membrane sarcolemma, during a normal action potential is sustained in the plateau phase by the activation of voltage-gated L-type Ca^{2+} channels (ICa,L) mentioned earlier (Woodcock & Matkovich., 2005) (Figure 1.4). It is this small influx of Ca^{2+} via these channels that causes a much larger release of Ca^{2+} from the SR. Upon activation of the SR, there is a

transient rise in cytoplasmic Ca^{2+} concentration $[Ca^{2+}]_i$. This phenomena is commonly reffered to as the calcium transient $[Ca^{2+}]_i$ and this process is known as calcium induce-calcium release (CICR) and is generally accepted as the major mechanism of Ca^{2+} release from the SR. Ca^{2+} release from the SR is mediated by intracellular calcium receptors commonly known as ryanodine receptors (RyR), with type 2 RyRs being the most abundant intracellular Ca^{2+} channels in cardiomyocytes (Woodcock & Matkovich., 2005; Roderick and Bootman., 2007). Contraction is initiated when free Ca^{2+} increases contraction of the myofilaments via its interaction with troponin C and the thick and thin filaments, namely actin and myosin leading to cell shortening. Exclusion of Ca^{2+} from the cytosol is achieved by several mechanisms, including SR uptake via the sarco-endoplasmic reticulum Ca^{2+} transporter (and removal through the sarcolemma via the Na^{2+}/Ca^{2+} exchanger. (Bers *et al*., 2003; Hilgemann, 2004). These changes result in cyclic increases and decreases in Ca^{2+} and in contractility of the individual myocytes (Figure 1.7).

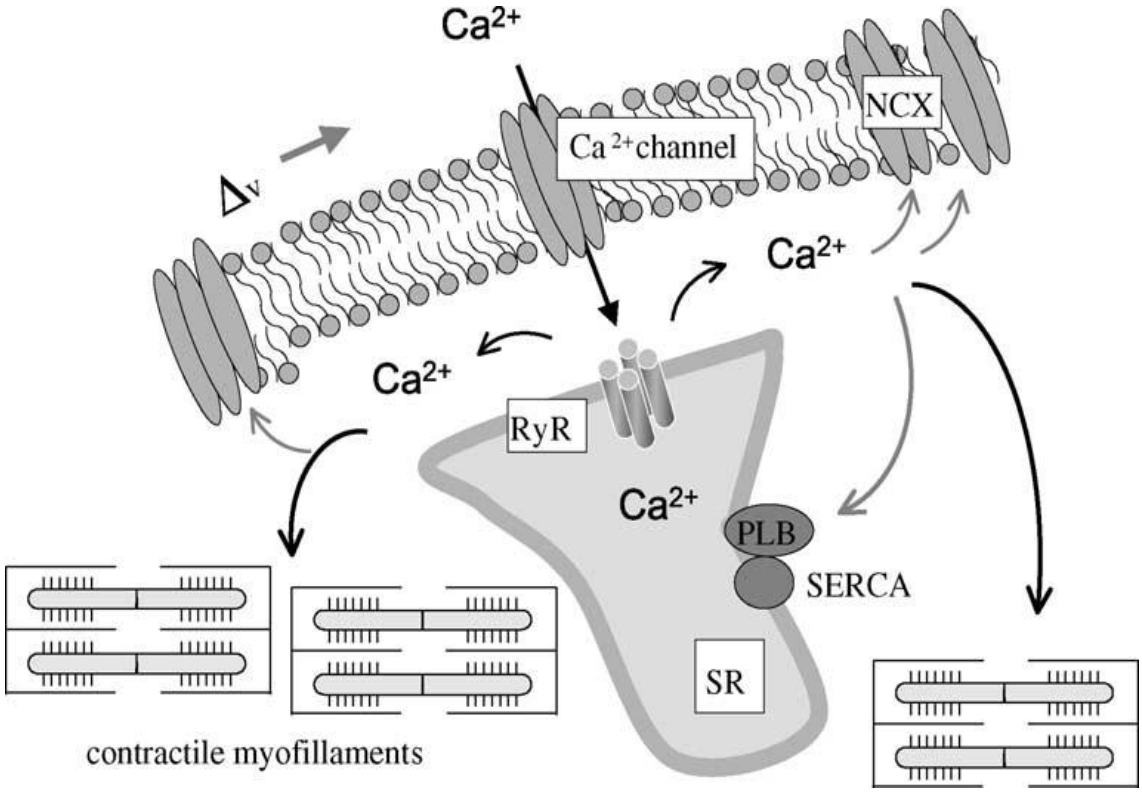

Figure 1.7: Schematic representation of Ca^{2+} regulation in cardiomyocytes. Depolarization of the sarcolemma opens the voltage-dependent Ca^{2+} channels and causes entry of Ca^{2+} from the extracellular milieu. The influx of Ca^{2+} via the L-type Ca^{2+} channels activates Ca^{2+}-activated Ca^{2+} release channels on the SR causing additional rises in Ca^{2+} and cycles of CICR. This high Ca^{2+} interacts with the myofilaments to enhance the interaction between actin and myosin leading to contraction of the cardiomyocyte. Upon relaxation, Ca^{2+} is lowered by re-uptake into the SR via the SERCA under the regulation of Plb. Ca^{2+} exits the cell via the NCX. (Image courtesy: Woodcock & Matkovich., 2005).

1.1.5 Mechanical events of the cardiac cycle

The cardiac cycle comprises of a series of alternate events that occur during each beat of the heart when the heart is in systole (contraction and emptying) and in diastole (relaxation and filling). Figure 1.7 shows the electro-mechanical events of a full cardiac cycle that starts with and ends with ventricular diastole. Systolic and diastolic events are described for the ventricles only as well as the activity of the left side of the heart. This is because events on the right side of the heart are identical with exemption of lower pressure in the right side of the heart.

As shown in figure 1.8A, atrial systole is the initiating step in the cardiac cycle. Initially the atria are in diastole, blood flows passively from the superior and inferior vena cava through the AV valve and into the ventricles. As the ventricles fill (mid ventricular diastole), the rate of flow slows and there is a parallel rise of ventricular pressure. This stage relates to the TP interval on the ECG. In the next phase, the late ventricular diastole, the SA node reaches threshold level and fires which becomes detectable on the ECG as the P wave while the impulse spreads throughout the atria. This depolarisation results in atrial contraction, blood squeezes into the ventricle. The AV valve remains open throughout atrial contraction although ventricular pressure rises simultaneously with the rise in atrial pressure slightly exceeding that in the ventricle. The point when the volume of blood averages130 ml in the ventricles marks the end of ventricle filling, known as the end diastolic volume (EDV), averages at about 135 ml (Sherwood, 2008). At this point ventricular systole (contraction) begins and this is shown as the QRS complex on the ECG where the impulse after atrial excitation travels to the AV node and His-Purkinje system to depolarise the ventricle. The modest delay between the QRS complex and the actual onset of ventricular systole is the time required for the EC coupling process. During the next phase, isovolumetric ventricular contraction, the AV valve is closed due to the change in pressure gradient within the ventricles that quickly exceeds that within the atria. At this point the aortic and pulmonary valves are not closed hence no ejection of blood occurs from the ventricles and ventricular pressure continues to rise as the volume remains constant. When the ventricular pressure exceeds aortic pressure, the aortic valve opens and ejection of blood occurs. The T wave on the ECG is the end of ventricular systole and as ventricles relax during repolarisation, pressure within the ventricles falls below aortic pressure which results in the closure of the aortic valve. During the isovolumetric relaxation stage, the AV valve is not yet

opened; therefore no change occurs in ventricular volume. When the pressure within the ventricles falls below that of the atria, the AV valve opens and ventricular filling begins again. Subsequently, this phase continues into later ventricular diastole where the SA node fires again and the cardiac cycle continues (Vander *et al.*, 2007; Sherwood., 2008).

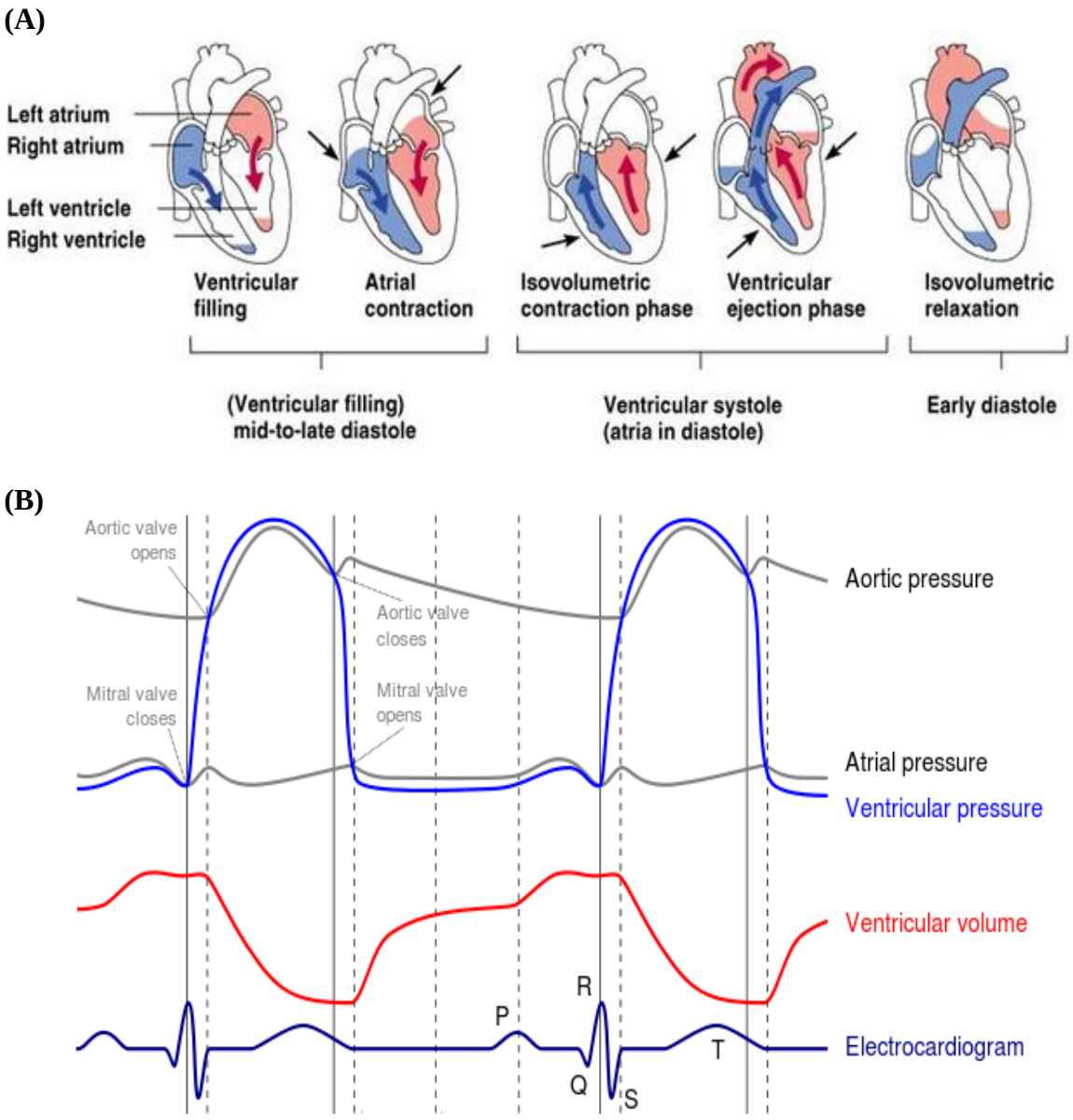

Figure 1.8: Mechanical events of the cardiac cycle. Present time frames of systole and diastole in the mammalian heart **(A)**.The main phases of the cardiac cycle including isovolumetric contraction, ejection, isovolumetric relaxation, rapid and slow filling and atrial contraction are shown. **(B)** Measurements of intravascular pressure in the aorta, LV, left atrium (LA) and LV volumes that underlie the phases of the cardiac cycle together with the corresponding electrical events of the electrocardiogram (ECG) (Image courtesy www.austincc.edu).

1.2 Heart failure

Heart failure (HF) or also known as Congestive heart failure (CHF) is a growing public health problem in industrialized nations. HF has been defined as 'a complex syndrome that can impair the ability for the normal functioning of the heart resulting from any structural or functional cardiac disorder (Dokken., 2008). HF can be classified into systolic and diastolic dysfunction to further emphasize the distinction between abnormal contraction and relaxation. Diabetic patients are particularly prone in developing HF with preserved systolic function (Fujisawa *et al*., 2004; Thorve *et al*., 2003) even in the absence of either demonstrable ischemia or elevated blood pressure, as a consequence of diabetic cardiomyopathy (Kakleas *et al*., 2009; Goldstein 2002). Systolic dysfunction arises due to compromised ability of heart defined as left ventricular ejection fraction (LVEF) <45%, whereas diastolic dysfunction is a result of abnormal ventricular filling and impaired relaxation (Gutierrez and Blanchard, 2004). This diastolic dysfunction is characterized by prolonged diastolic relaxation time. Increased left ventricular (LV) stiffness arises as an outcome of metabolic disturbances leading to the development of systolic dysfunction and subsequently HF (Mandavia *et al*., 2012; Zhang and Chen, 2012).

There has been recognition and confirmation of the presence of the clinical syndrome of HF with preserved LV ejection fraction (Owen *et al*., 2006). Patients with HF and normal ejection fraction are alleged to have abnormal diastolic function, in which abnormalities in both the active and passive phases of diastole are involved (Hyer & Shehata., 2005). Such failure may be an outcome of altered calcium handling in the early active phase of relaxation, including defects of the SERCA2a and related regulatory proteins such as phospholamban (Choi *et al.,* 2008). Changes in the visco-elastic properties of the heart, as a result of matrix accumulation, may also be seen to contribute to impaired ventricular filling in the later, passive phase of diastolic relaxation (Boudina & Abel., 2007). Although the mechanisms underlying these latter changes are incompletely understood, transforming growth factor β1 (TGFβ1), a growth factor with both pro-fibrotic and hypertrophic actions has been identified as a likely contributor (Rolo & Palmeira., 2006).

Sudden cardiac death (SCD) is mainly responsible for at least half of the deaths, where many progress to pump failure and congestion (Swedberg *et al*., 2005). SCD is reffered to someone who suffers a sudden, unexpected pulseless condition of cardiac etiology. The vast majority of patients have a sudden arrhythmic death. The assessment of sudden cardiac death has been difficult to accomplish as it is a dynamic event that occurs in the

general population in an unpredictable manner (Swedberg *et al*., 2005).Over the years, a standard definition for identifying the condition has not been employed in the large number of studies that have been conducted. The most accepted definition of SCD is sudden and unexpected death within an hour of symptom-onset (USRDS Annual Data Report., 2005; Herzog, 2007).

Currently, two well-established peaks in the age-related prevalence of sudden cardiac death occur, one during infancy representing the sudden infant death syndrome and the other between ages 75 and 85 years. However, the gender-related trends appear to have shifted, with an increase in the proportion of females who suffer sudden cardiac death. Earlier studies had reported 25:75 ratio of females to males (Chugh *et al*., 2004; Koplan & Stevenson, 2007). The Oregon experience shows that females, on a yearly basis, consistently make up approximately 40% of all SCD cases (Chugh *et al*., 2004). While the reasons for this changing trend merit further evaluation, one possibility is that this mirrors the altered gender distribution in prevalence of and mortality from, coronary artery disease (Gerber *et al*., 2006). The ability to non-invasively assess cardiac systolic function with echocardiography has brought with it the realisation that approximately 40% of hospitalisations for HF occur in patients with preserved left ventricular systolic function (Jacobson *et al*., 2009). Left ventricular function as reflected by ejection fraction and functional capacity are directly related to both total mortality and SCD in patients with heart disease. As such, LVEF has been used as a primary entry criterion for multiple clinical trials.

Furthermore, ventricular arrhythmias precipitating in cardiac arrest are the most common mechanisms of sudden death (Koplan & Stevenson, 2007). Approximately, half of all deaths from coronary artery disease occur suddenly, and in approximately half of these victims cardiac arrest is the first manifestation of the disease (Bowker *et al*., 2003). In the stages of the natural history of CAD, two major mechanisms of fatal ventricular arrhythmias exist. Acute coronary ischemia usually associated with plaque rupture and occlusion of one or more major coronary arteries is more likely to result in polymorphic ventricular tachycardia (Chugh *et al*., 2008). It is likely that such patients have relatively normal LV systolic function or mildly depressed LV function. Those with ischemic cardiomyopathy following one or more myocardial infarctions are more likely to have monomorphic ventricular tachycardias resulting from re-entrant loops around areas of

scarred myocardium. Either arrhythmia, if untreated, will eventually degenerate into ventricular fibrillation (Koplan & Stevenson, 2007).

The British Heart Foundation currently estimates that at least 4% of deaths in the UK are as a result of HF (www.heartstats.org). HF is greatly increased in patients with Diabetes Mellitus (DM), coronary heart disease (CHD), hypertension, use of cardiotoxins (alcohol, cocaine) and also in patients with a history of cardiomyopathy (Cohn *et al*., 2008). However, smoking remains a major public health issue in all European countries as well as eating foods high in fat, being obese, high cholesterol and sodium diets, and physical inactivity increase the risk of developing HF (www.bhf.org). Chronic heart failure currently affects 900,000 people in the UK and consumes almost 2% of the National Health Service (NHS) budget (www.heartstats.org). HF is a major burden on healthcare costs in the UK and other countries. The cost of health expenditure has now reached an all time high and these figures are set to rise as the prognosis of coronary artery disease improves and the population ages (Brown and Clark, 2013). The incidence and prevalence of HF increases with age and the average age of first diagnosis is 76 years (Hobbs et al., 2002). HF currently accounts for approximately 5% of all emergency medical admissions to hospital, and over the next 25 years the proportion will rise by 50% – largely due to an older population (National Institute for Health and Clinical Excellence, 2010 (www.nice.org.uk)).

1.2.1 Pathophysiology of the failing heart: Myocyte contractile dysfunction

HF has been recognized as a functional disorder in which the LV pump is impaired hence, contributing to increased burden of the heart on the contracting myocytes. Numerous cellular and molecular defects are associated with HF resulting in reduced myocyte contractility, LV pump failure, and electrophysiological dysfunction (Gupta et al., 2000). In the failing heart, cardiac myocytes undergo several changes leading to impaired contractile function. These include loss of myofilaments in myocytes, decreased gene expression of the α-myosin heavy chain (MHC), and cytoskeletal protein alteration (Gupta *et al*., 2000, Lowes *et al.*, 1997). Numerous studies emphasise the finding that depressed myocyte contractility may be the cause of alterations in the EC coupling process, including reduced activity of the SERCA pump which is responsible for calcium sequestration during cardiomyocyte diastolic relaxation (Borradaile et al., 2006; Lebeche et al., 2008; Minamino et al., 2010). Along with disregulated mitochondrial calcium

uptake due to mitochondrial dysfunction, reduced activity of NCX process and the sarcolemmal calcium-ATPase pump and reduced expression of the ryanodine receptor are all observed in T2DM. Together all these cause a calcium imbalance within the diabetic cardiomyocytes, which is characterized by calcium cytosolic overloading and reduced mitochondrial ATP production (Aroor *et al*., 2012ab; Lebeche *et al*., 2008; Minamino *et al*., 2010). This, in turn, leads to the prolonged diastolic relaxation time seen in initial diastolic dysfunction, and causes cardiomyocyte apoptosis and cell death as a result of the mitochondrial permeability transition pore (MPTP) response in the later stages (Gorman *et al*., 2012; Zhang and Chen., 2012). Altogether, these factors contribute to reduced rates of calcium cycling and diminished cellular contractile performance in CHF.

Nevertheless, it is not necessary that the reduced pump performance observed in the failing heart is only due to fundamental defects in the cardiomyocytes contractile ability. Other important factors also contribute to this abnormality including, ECM alterations, apoptosis (cell death), vascular alterations and neurohormonal disturbances can promote to progression of HF (Fedak *et al*., 2005). Currently, HF pathophysiology focus has shifted towards the notion that systolic and diastolic dysfunction are consequences of a structural increase in ventricular chamber volume (Swynghedauw et al., 2010). This notion is closely related to changes in ventricular geometry that seats the heart at a mechanical disadvantage, independent of functional changes at cellular level. Numerous studies have detailed about the history of HF due to progressive LV remodelling which leads to detoriated LV performance in HF patients. The following section outlines the cellular and molecular mechanisms underlying the fundamental process of LV remodelling.

1.2.2 Heart in response to stress: Cardiac structural remodelling

Structural and functional integrity of the heart is orchestrated by a fine balance between several neuro-hormonal and hemodynamic influences. Disruptions in this ‘fine tuning’ (e.g. in duress or injury) activate a complex, progressive process of diverse adaptive responses at transcriptional, molecular, cellular and functional levels that allow the heart to adjust to new working conditions and can be collectively termed ‘remodelling’ (Cohn *et al*., 2000). Cardiac remodelling may be broadly defined as alterations in cardiac structure resulting from altered hemodynamic load and/or cardiac injury. While remodelling may be physiological or pathological and by extension adaptive or maladaptive, in the present context the above definition excludes all aspects, gestational

or developmental as well as favourable remodelling that follows intensive exercise and is restricted to acquired structural rearrangement in the left myocardium (Fedak *et al*., 2005).

Cardiac remodelling is a common denominator in the aetiology of several primary cardiovascular diseases notably DM, coronary atherosclerosis, hypertension, cardiomyopathy and myocarditis (Swynghedauw, 1999). As shown in figure 1.9, HF may be seen as a progressive disorder that is initiated in response to an index event (i.e. diabetes mellitus (DM), hypertension, or myocardial infarction (MI) that may result in loss or damage of functioning myocytes or produce a decline in ability of the heart to function as a pump. Histopathologically, cardiac remodelling is characterised by structural rearrangement of normal chamber components, which involve cardiomyocyte hypertrophy, cardiac fibroblast proliferation, cardiac fibrosis and cell death (Pichler *et al*., 2012). Cardiac remodelling is widespread in numerous primary CVDs notably DM, atherosclerosis, cardiomyopathy and hypertension (D'Souza *et al*., 2011) and also to numerous pathological causes including, ischemia and inflammation. At the molecular level, myocardial ECM remodelling is mediated by the activation of a number of neurohormonal systems and inflammatory pathways are initiated, specifically the renin-angiotensin system (RAS), Transforming growth factor-beta 1 (TGFβ1) and beta-adrenergic systems (Rosenkranz., 2004; Fedak *et al*., 2005). Numerous proteins are involved in the disease progression of the failing heart of which include angiotensin II, aldosterone, TGFβ1, endothelin and tumor necrosis factorα (TNFα) (Fedak *et al*., 2005; Swynghedauw *et al*., 2010).

Thus far, a multitude of proteins, hormones, neurotransmitters and other mediators including norepinephrine, angiotensin II, endothelin, aldosterone, TGFβ1, tumor necrosis factor (TNF) have been implicated in disease progression of the failing heart (Maytin and Colucci, 2002; Fedak *et al*., 2005; Swynghedauw *et al.*, 2010). These processes are initially compensatory and beneficial, and in most instances, patients remain asymptomatic or minimally symptomatic following the initial decline in pumping capacity of the heart, or will develop symptoms only after the dysfunction has been present for some time (Maytin and Colucci, 2002). As such, the index event produces remodelling of the LV frequently along one of two patterns: hypertrophy or dilation.

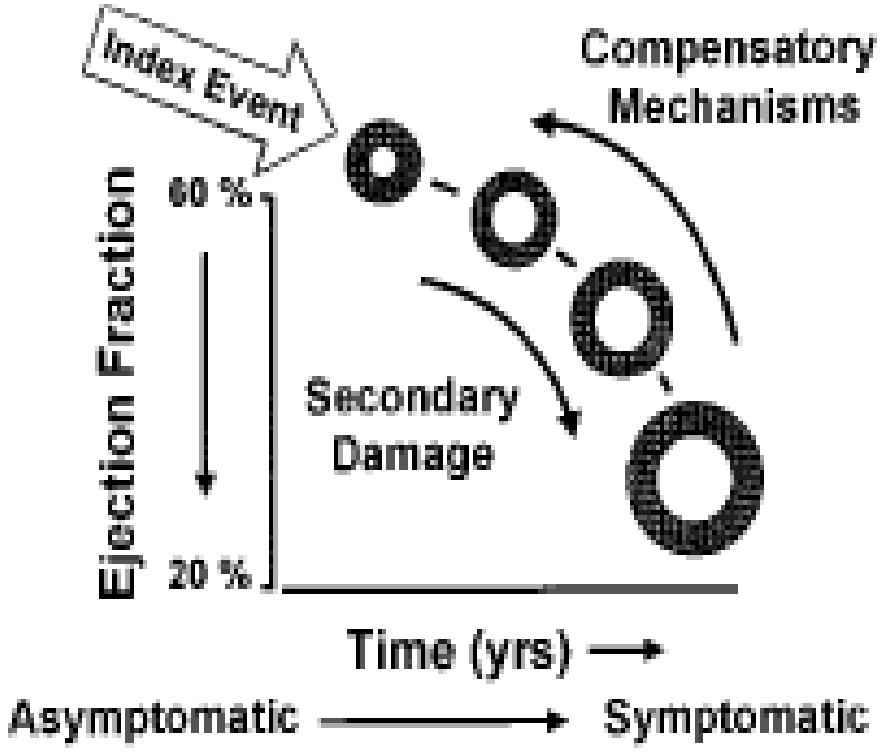

Figure 1.9: Heart failure pathogenesis. HF begins in response to an index event that produces an initial decline in pumping capacity of the heart following which a variety of compensatory mechanisms are activated to restore homeostatic CV function. Although beneficial in the short term, sustained activation of these systems can lead to worsening LV remodelling and cardiac decompensation that underscores the transition to symptomatic HF (Image: Mann *et al*., 2010).

Remodelling of the LV is visible as myocardial hypertrophy; an increase in LV mass without any effects on LV volume defined as ‘concentric remodelling’, associated with preserved function of the ventricles enabling greater force generation and high pressure. Along with LV dilation, defined as ‘eccentric remodelling’ and considerable increase in intraventricular volume with compared increase in LV mass which represents a compensatory response to supplement cardiac productivity (D’Souza *et al*., 2011; Albert *et al*., 2004). Current studies state that the development and progression of HF are initiated with an index event that produces impairment in the pumping capacity of the heart. As a result a number of compensatory mechanisms become active to restore this homeostatic change. These however, are beneficial in the short term but become

worse with sustained activation hence, worsening LV remodelling and eventually leading to HF (Mann *et al*., 2010).

Cardiac remodelling is a major feature of DCM. In this condition, over-production of ECM proteins leads to increased myocardial stiffness resulting in cardiac dysfunction, impairment of cardiac performance and ultimately cardiac failure (Li *et al*., 2011; Ahmed *et al*., 2006). Cardiac structural remodeling in the myocardium is widely associated with marked alterations in ECM structure and function is therefore a widely recognized alteration of the failing heart (Miner and Miller., 2006). Several experimental and clinical studies have given the notion of progressive fibrosis leading to HF progression. Fibrosis impairs electrical coupling of cardiomyocytes by separation of myocytes and ECM proteins. In addition, fibrosis leads to reduced capillary density and increased oxygen diffusion distances which eventually lead to myocyte hypoxia (Sabbah *et al*., 1995). Therefore, fibrosis is known to profoundly alter myocyte metabolism and performance and eventually ventricular function. Within the myocyte, in addition to the functional changes described in the previous section, the remodelling process is invariably associated with sarcomeric reorganisation. Dilation of the heart is associated with myocyte re-lengthening, mediated by the generation of new sarcomeres in series and an enhancement of the length-to-width ratio whereas a hypertrophic phenotype is the result of parallel addition of new sarcomeres. At the molecular levels, hypertrophy appears to be characterized by increased expression of adult isoforms of sarcomeric genes (i.e., αMHC, cardiac αSKA) and is often concomitant with increased natriuretic peptide synthesis (Hilfiker-Kleiner *et al*., 2006).

1.2.3 Molecular contributions in cardiac structural remodelling

Much experimental evidence suggests that the gradual loss of myocytes through programmed cell death (apoptosis) is known to contribute to LV remodelling and cardiac dysfunction in the heart (Wenker *et al.,* 2003; Foo *et al*., 2005). Particularly in relation to apoptosis, this point of view has received increasing support with the recognition that DNA damage characteristic of apoptotic cell death occurs in myocytes from failing hearts (Sabbah, 2000). Apoptosis can be characterised by the activation of caspase-8 and subsequently caspase-3. The apoptotic signal triggered by ligation of members of the death receptor family is promoted by sequential activation of caspase zymogens. Caspases are also known to promote systolic dysfunction by cleaving

myocardial contractile proteins. Treatment with caspase inhibitors have been proven to show improvement in myocardial contractile proteins and reduction in systolic dysfunction (Hilfiker-Kleiner *et al*., 2006). However, a definite role of apoptosis to be involved in the progression of the failing heart has not yet been established. Thus, it is difficult to establish a definitive statement on whether myocyte cell loss is an important contributor to HF pathogenesis, occurs early and continually in HF or, instead, only in end-stage heart.

Conversely, in the failing heart, activation of numerous humoral autocrine and paracrine pathways can determine the regulation of ECM metabolism and also the extent of myocardial remodelling. As a consequence, changes in ECM synthesis and degradation lead to disturbance of the composition of the collagen network in the heart. This disproportionate increase in synthesis/inhibition of the ECM proteins may result in cardiac fibrosis (Manabe *et al*., 2002). The ECM can be remodelled temporarily, reversibly and can fully adapt to the changes in the biomechanical load. However, continuous load can result in collagen deposition (fibrosis) which can render the heart electrically and structurally. Fibrosis represents a disproportionate accumulation of fibrillar collagen and it is a fundamental element of remodelling characteristic of the failing heart. Type I collagen is the fundamental collagen found in cardiac fibrosis, resulting in ventricle stiffness and moreover, it impedes contraction as well as relaxation of the heart (Pichler., 2012).

The underlying mechanisms and signalling pathways involved in ECM remodelling is of great importance. Oxidative stress, which is a major cause for all hyperglycaemia-induced diabetic complications, is associated with abnormal gene expression, altered signal transduction and also the activation of secondary messenger pathways leading to the development of myocyte cell death and cardiac fibrosis (D'Souza *et al*., 2011; Cai *et al*., 2006; Aneja *et al*., 2008). The physiological alterations associated with muscle tissue and cells include the presence of myocardial hypertrophy and impaired contraction. However, alterations associated with the ECM include excess deposition of collagens, abnormal glycosylation/crosslinking via AGE pathway as well as alterations in diastolic compliance (Aneja *et al*., 2008). Much emphasis is given to the metalloproteinases (MMPs) and the tissue inhibitors of metalloproteinases (TIMPs) in underlying LV dilatation. Degradation of collagens occurs due to MMPs which are capable of enzymatically digesting various ECM proteins. The activity of these MMPs

is controlled at transcriptional level and also via activation and inhibition by other proteins including tissue inhibitors TIMPs (Ahmed *et al.,* 2006). Once this balance is disrupted, progressive MMP activation leads to the degradation of the ECM, myocyte slippage as well as ventricular wall thinning leading to end stage HF (Maytin and Colucci., 2006). As such, the MMP/TIMP system is a key contributor to ECM turnover and its dysregulation plays a vital role in myocardial remodelling and progression to HF. Clinical studies have revealed that in the failing heart, whilst the activity of MMPs is increased, TIMPs are decreased (Li *et al*., 1997; Thomas *et al*., 1998); a scenario where MMP/TIMP balance is disturbed leading to changes in net proteolytic activity and a potentially deleterious outcome (Spinale., 2007). In support of this premise, pharmacological MMP inhibition in a pacing-induced animal model of heart failure improved LV dimensions and performance when administered early in the remodelling process (Spinale *et al*., 2007). Pharmacological inhibition and targeted deletion of MMPs in rats with HF have been shown to reduce the remodelling observed in experimental models, together show potential therapeutic relevance of MMP inhibition which may become understandable in the near future (Matsusaka *et al.,* 2006).

1.2.4 TGFβ1 in cardiac remodelling

A common histo-pathological finding in cardiac fibrosis is the accumulation and structural remodelling of the fibrillar collagen matrix of the heart. In ventricular tissue, fibrosis is responsible for a decrease in rate of relaxation, diastole suction and myocardial stiffness. TGFβ1 is the most important factor amongst many factors that contribute to this abnormal accumulation of fibrillar matrix (Pauschinger *et al*., 1999; Porter & Turner., 2009). TGFβ1, has come to light given constant myocardial upregulation in experimental models of MI and HF. This has also been discovered in patients with dilated or hypertrophic cardiomyopathy (Dobaczewski *et al*., 2010). TGFs are members of a superfamily of cytokines, consisting of three isoforms, of which TGF-β1 is the most prevalent. In their active form, all of the isoforms are dimers of 1 2-kD polypeptides that arise from a larger precursor through proteolytic processing. The activating stimuli for TGFβ1 are varied, including reactive oxygen species, integrin-mediated interactions and also MMP's 2 and 9, a phenomenon that couples matrix degradation with activation of a molecule that primarily mediates matrix integrity and stability (Porter & Turner.,2009). TGFβ1s are involved in a wide assortment of cell functions, including regulation of inflammation, ECM deposition, cell proliferation, differentiation as well as tissue growth

(D'Souza *et al.*, 2011). TGFβ1 acts to simultaneously stimulate the synthesis of ECM to inhibit the actions of proteases which cause matrix degradation in order to increase the expression of cell surface integrins that interact with matrix components. Through these particular effects, TGFβ1 rapidly causes the deposition of an exuberant ECM (Border., 1999). TGFβ1 plays a crucial role in the development of fibrosis. It stimulates fibroblast chemotaxis along with the production of collagen and fibronectin while inhibiting collagen degradation (Border., 1994). It can also induce expression of SM α-actin in fibroblasts hence it is considered to be involved in the factors held responsible for the formation of myofibroblasts (Sun & Weber., 2000). TGFβ1 stimulates the synthesis of individual matrix components including fibronectin and its variant forms including collagens, and proteoglycans. TGFβ1 concurrently inhibits matrix degradation by increasing the synthesis of proteases and also the levels of protease inhibitors. It is also known to increase the expression of integrins and alter their relative proportions on the surface of cells in a way that facilitates adhesion to matrix. Each of these events is found to be beneficial in tissue repair (Bujak & Frangogiannis, 2007). However, TGFβ1 also induces deposition of ECM at the sites of injury leading to scarring and fibrosis. In addition, the ability of TGFβ1 to induce its own production is found to be a major factor in the development of fibrosis and scarring into chronic, progressive conditions that alter the tissue structure (Rozenkranz., 2004; Bosman & Stamenkovic., 2003). In a previous study, Wu and Derynck (Wu & Derynck., 2009) reported a central role of TGFβ1 signalling in the ability of HG to induce hypertrophy in fibroblasts and epithelial cells. It was implicated that either blocking or enhancing the expression of the kinase activity of TGFβRI receptor can prevent the hypertrophic effects of HG. Exposure of cells to HG has been shown to elicit a rapid increase in cell surface levels of TGFβ1 receptors (TGFβRI/TGFβRII) along with the activation of a TGFβ1 ligand by MMP2 and MMP9. This autocrine signalling of TGFβ1 in response to HG leads to the activation of the pro-hypertrophic Akt-TOR pathway (Rozenkranz., 2004; Wu L, Derynck., 2009). Although, there is considerable evidence that TGFβ1 mRNA protein induction is up regulated in the remodelling myocardium, direct evidence of this is still lacking (Dobaczewski *et al.*, 2010). In order to achieve HF management, targeting the regulatory mechanisms of ECM homeostasis remains vital. The TGFβ1 system remains a promising therapeutic target for myocardial infarction and for conditions such as DCM that are associated with fibrosis and hypertrophy. Moreover, TGFβ1 inhibition has been shown to ameliorate the pro-fibrotic effects of this cytokine in animal models (Kuwahara *et al.*,2002). A recent study using tissue from failing and non-failing human hearts demonstrated a significant

increase in the transcript levels of TGFβ1 in the pathological heart tissue (Sivakumar *et al*., 2008), that were accompanied by significantly elevated levels of type I and III collagens. The key role of TGFβ1 in myocardial tissue remodelling and fibrosis has been extensively reviewed elsewhere (Lijnen *et al*., 2000; Bujak & Frangogiannis, 2007).

Collectively, structural remodelling in pathogenesis of HF is characterised by alterations in cardiomyocyte phenotype, defective EC coupling, disturbed intracellular Ca^{2+} handling and ECM degradation. These findings have been produced in vitro and experimental model systems and are produced in response to stimuli known to be associated with pathological remodelling. These include angiotensin, endothelin, factors like TGFβ1, inflammatory cytokines and oxidative stress. The complexities of this field and the challenged encountered in the translational study are outside the scope of this thesis but emphasises the 1,000 new drugs and devices that have been developed for the treatment of HF so far but only 9 received approval to be used in the clinical setting. The next section highlights the coexistence of CHF and DM and how their combined influence increases the risk of morbidity and mortality and provides complications in the therapeutic interventions (Van Melle *et al*., 2010).

1.2.5 Inflammation in HF and diabetes

Heart failure is a syndrome that has demonstrated increasing morbidity and mortality during the last decade. However, despite state-of-the-art cardiovascular treatment, chronic HF remains a progressive disorder, suggesting a role of key pathogenic mechanisms that remain unmodified by the present treatment modalities. Persistent inflammation may represent such unmodified mechanisms (Yndestad *et al*., 2006). Inflammation has been recognised to play an important role in HF and diabetes (Levine *et al*., 1990). Inflammatory process can cause myocardial damage, while inflammatory agents contribute to the worsening and progression of HF (Niessner *et al*., 2009). The first data concerning the relation between HF and inflammation were recorded in 1955, when a positive correlation was found between levels of C-reactive protein (CRP) and the severity of congestive HF (Elster *et al*., 1956). In 1990, Levine et al (1990) documented a positive correlation between TNF-α and chronic HF. Research carried out since then has produced new data concerning the relation between many cytokines including TGFβ1, TNF-α and HF. It seems that the HF syndrome is in large part due to an imbalance between increases in inflammatory and anti-inflammatory mediators (Oikonomou *et al*., 2011).

Inflammation occurs in the vasculature as a response to injury, lipid peroxidation, and perhaps infection. Various risk factors, including hypertension, diabetes, and smoking, are amplified by the harmful effects of oxidised low-density–lipoprotein cholesterol, initiating a chronic inflammatory reaction, the result of which is a vulnerable plaque and prone to rupture (Willerson & Ridker., 2004). Furthermore, inflammation plays a role in all stages of atherothrombosis, the underlying cause of approximately 80% of all SCD (Albert *et al*., 2002). Epidemiological and clinical studies have shown strong and consistent relationships between markers of inflammation and risk of future cardiovascular events. Recent data show that in patients with recent onset HF, increased TNF-α level are associated with a disturbance of left atrial function and an advanced degree of LV diastolic and systolic dysfunction (Chrysohoou *et al*., 2009). It has also been reported that TNF-α and other related molecules to cause apoptosis of myocardial cells via mechanisms of cell death (Haudek *et al*., 2007). This in turn, may be responsible for the molecular alterations occurring in the heart during diabetes.

The raised circulating levels of inflammatory cytokines in chronic HF may reflect immune activation and release from several tissues (heart, liver, lungs) and cell types (platelets, endothelium). Importantly, the myocardium itself may represent an important source for the inflammatory mediators found to be increased in the circulation during HF. Thus, the failing myocardium expresses enhanced levels of a range of inflammatory mediators including adhesion molecules, TNF-α, Interleukin-6-related cytokines and chemokines (Eiken *et al*., 2000; Damas *et al*., 2000). In fact, activation of the transcriptional factor nuclear factor (NF)-κB, a major mediator of inflammation within the failing myocardium, has anti-apoptotic rather than pro-apoptotic effects (Valen *et al*., 2001). This local inflammation may not only contribute to the pathogenesis of HF in an autocrine/paracrine manner, but release from the heart may contribute to the systemic inflammatory phenotype of HF. In addition, chronic inflammation is thought to accelerate the progression of diabetes, and great efforts have been made to understand the molecular mechanisms by which inflammation promotes the development of cardiovascular and metabolic diseases (Esser *et al*., 2014). Several conditions that are driven by inflammatory processes are also associated with diabetes, including rheumatoid arthritis, gout, psoriasis and Crohn's disease, and various anti-inflammatory drugs have been approved or are in late stages of development for the treatment of these conditions (Donath, 2014).

Patients with chronic HF are characterised by systemic inflammation, as evident by increased circulating levels of several inflammatory cytokines with increasing levels according to the degree of disease severity (Yndestad *et al*., 2006; (Oikonomou *et al*., 2011). Although the mechanisms for the systemic inflammation is unknown, a growing body of evidence suggest that the systemic inflammation may play a role in the development and progression of diabetes and consequently, HF (Willerson & Ridker., 2004). Inflammation influences not only the myocardial function, but also by inducing pathogenic consequences in other organs and tissues, thereby contributing to additional aspects of the HF syndrome (Willerson & Ridker., 2004). Further studies are necessary in order to investigate the role of inflammation in diabetes and HF in order to seek possible therapeutic approaches.

1.3 Diabetes mellitus

1.3.1 Importance of studying diabetes mellitus

Currently, more than 350 million people worldwide suffer from DM which is likely to increase to 450 million within the next 15-20 years (Choi *et al*., 2008) making it one of the five leading causes of death in developed countries. It was previously estimated that, the number of adults with diabetes worldwide would increase from 135 million in 1995 to 320 million by 2025 [Boudina & Abel., 2007; Rolo & Palmeira., 2006). They also claimed that patients with DM are likely to have increased risk of cardiovascular disease (CVDs). The UK was reported to have over 3 million people diagnosed with DM with a further 850,000 people still underdiagnosed, which has almost doubled since 2012. In terms of total expense, it costs about £850 billion to diagnose, treat and care for DM patients worldwide. It is now apparent that more women have been diagnosed with diabetes in the age range of 45 and 65 years (Diabetes UK, 2007). The prevalence of diabetes is higher in the developed countries. However, the major increase in people with diabetes occurs in the developing countries such as China, India, Africa and the Middle East. Throughout the developing world, increasing rates of diabetes represents an emerging epidemic with marked pathological consequences which are likely to drive previously unpredicted rates of vascular target organ complications (Diabetes UK, 2007; Tuttle., 2005). Adults with diabetes are at a 2 to 4 fold increased risk of cardiovascular events relative to those without diabetes (Schalkwijk & Stehouwer., 2005). With such high rates of morbidity and mortality reaching epic proportions, DM in the 20th century represents one of the supreme medicinal, sociological and

economical challenges today. It is also particularly noteworthy that 1 billion people in the world are prediabetic and they will eventually form the complete diabetic status within time. In addition HG is closely associated with age and it is the aging population who are most likely to become diabetic.

DM is universally characterised by micro-angiophatic complications, consisting of micro-vascular (nephropathy, retinopathy and neuropathy) and macro-vascular (ischaemic heart disease, cerebrovascular diseases and peripheral vascular diseases) complications (Rehman *et al.*, 2007). DM is a heterogeneous metabolic disorder characterised by chronic HG due to malfunctioning of insulin secretion, its action or both (Jacobsen *et al.*, 2009). Current diagnosis of the disease is based on glucose levels (WHO, 2006); random venous plasma glucose levels above 11.1mmol/L on two occasions and/or fasting plasma glucose ≥7 mmol/l (126 mg/dL) is required for a diagnosis of DM. A two-hour blood glucose ≥ 11.1mmol/L (200 mg/dL) on administration of an OGTT (2 hour venous plasma glucose after ingestion of 75 g oral glucose load) compared to normal glucose tolerance value of <7.8 mmol/L is used to further confirm DM.

1.3.2 Diabetes mellitus classification

DM is classified into Insulin-Dependent Diabetes Mellitus (T1DM/IDDM) and Non-insulin Dependent Diabetes Mellitus (T2DM/NIDDM) on the basis of the history, aetiology and clinical presentation of the patient (Fujisawa *et al.*, 2004). T1DM is a lifelong metabolic disorder characterised mainly by a deficiency in endogenous insulin production due to cellular-mediated autoimmune destruction of insulin-producing β-cells of the endocrine pancreas. Due to the lack of insulin production, there is an increase in ketone production in the body leading to metabolic ketosis followed by diabetic coma and death. Consequently, the patient becomes dependent on exogenous insulin administration (Thorve *et al.*, 2003). T1DM is the most common childhood disease in the developed world and it is treated with a complex regime of insulin injections, diet and exercise (Kakleas *et al.*, 2009). Individuals with TIDM usually present with severe symptoms of polyuria (increased urinary frequency), polydipsia (increased thirst), polyphagia (hunger), weight loss, ketoacidosis and coma. Exogenous insulin is the only treatment available to maintain blood glucose levels and prevent end-

organ complications for survival (Canivell and Gomis., 2014). Despite several advances in the field, T1DM is currently refractory to prevention, barring toxic immunosuppression (Mordes *et al*., 2008). On the other hand**,** T2DM is the most prevalent form of diabetes and can develop at any age but most predominantly diagnosed after the fourth decade of life. T2DM is characterised by insulin resistance (IR) which plays a major role in metabolic abnormalities, such as dyslipidemia and hypertension (Goldstein, 2002). T2DM is a polygenic disorder along with T1DM which may be triggered by genetic and environmental factors including life style habits such as obesity, diet and decreased physical activity. These factors increase insulin resistance together with progressive β cell failure, result in rising glycemia (Throve et al., 2003; Hyer & Shehata., 2005; Bergman, 2009). Nevertheless, the management of T2DM is more complex and the majority of patients require hypoglycemic agents to maintain desired blood glucose levels. When therapeutic management including diet, exercise hypoglycemic agents fail to attain acceptable glycaemic state, different endogenous insulin formations are necessary (Kaul *et al*., 2012). Another type of diabetes is maturity-onset diabetes of the young (MODY) which occurs before 25 years of age (accounts for 0.6-2% of all diagnosed cases of DM) and is associated with a defect in insulin secretion with minimal or no impairments in insulin action (McDonald and Ellard., 2013).

1.3.3 Cardiovascular disease in diabetes dellitus

Cardiovascular disease (CVD) directs to dysfunction of the heart and/or the blood vessels, or the blood itself and includes the clinical manifestations of microvascular and macrovascular disease, coronary heart disease (CHD), stroke, and peripheral vascular disease (Bertoni *et al*., 2003). CVD is a major cause of mortality, morbidity and disability in people with DM, calculating for up to 44% of fatalities in people with T1DM and 52% in people with T2DM (Diabetes UK, 2010). Recent British Heart Foundation surveys show that at present, there are an estimated 7 million people living with CVD in the UK (www.bhf.org) with CVD being the main cause of deaths before the age of 65 in Europe: accounting for over 680,000 deaths each year. Conversely, the total cost of premature death, lost productivity, hospital treatment and prescriptions relating to cardiovascular disease is estimated at £19 billion each year in the UK (ww.bhf.org). CVDs account for up to 80% of premature excess mortality in diabetic

patients (Winer & Sowers., 2004). In a recent study, (Ceriello & Testa., 2009) it has been suggested that diabetes may now be considered a CVD due to its high level of morbidity and mortality attributed to CVD resulting from DM. It has been established that CVD is the leading cause of morbidity and mortality in less developed countries as well as developed countries (Boudina & Abel., 2007; Winer & Sowers., 2004; Rana *et al*., 2009). Whilst medications such as insulin and many others, including hypoglycaemic drugs can control many aspects of diabetes, an assortment of complications affect the vascular system, heart, kidney and peripheral nerves and the eyes in the body. These are very common and the cost is extremely high in terms of the quality of life for the diabetic patients (Rolo & Palmeira., 2006). Although cardiovascular mortality has decreased in the general population, it has risen by 23% among women with diabetes over the past 3 decades and autopsy studies have found that 75% of patients with diabetes presented with high-grade atherosclerosis, despite being asymptomatic before death (Gora *et al.,* 2002). CHD is a priority in Scotland where prevalence of the associated risk factors is high and around 7.5% of men and 4.9% of women are living with CHD (Scottish Health Survey 2011). Surveys carried out in the UK and other countries show that almost 20% of the elderly have HF with 31% of deaths occurring before the age of 65 in men and 26% of deaths occurring before the age of 65 in women from CHD (www.heartstats.org, Wells and Gordon., 2008).

1.3.4 Diabetic cardiomyopathy in heart failure

A high proportion of diabetic patients (both type 1 and type 2) develop a unique cardiomyopathy. This "diabetic cardiomyopathy" (DCM), as the name suggests, initiates with asymptomatic left ventricular diastolic dysfunction (slowing of relaxation kinetics) and on progression of the disease, systolic function becomes compromised, which results in an increase in the incidence of morbidity and mortality. DCM develops as a result of changes to cardiac structure and function in the absence of hypertension and coronary artery disease (Boudina & Abel., 2007; Pires & Moreira., 2012; Fang *et al.,* 2004,2005). The diastolic dysfunction characterizing early DCM may lead to subsequent progressive fibrosis, impaired calcium handling in the heart leading to contractile dysfunction, cardiac autonomic neuropathy and increased mitochondrial and endoplasmic reticulum stress contributing further to the reduced cardiac energetics (Aroor *et al*., 2012a; Mandavia *et al*., 2012; Zhang and Chen, 2012). Initially, the term

DCM was introduced based upon the findings of post mortem patients with heart failure in the absence of other complications (Fang *et al*., 2004). It has recently been reported that 56% of diabetic patients have had DCM (Somaratne *et al*., 2011). A high prevalence of heart failure is seen in individuals with diabetic cardiovascular complications, with DCM as one of the key determinants (Tziakas *et al*., 2005). These cardiovascular complications compromise cardiac performance ultimately resulting in cardiac failure (Loganathan *et al*., 2006). The aetiology and pathophysiology of DCM are poorly understood and are multifactorial in nature.

Diabetic macro-vasculopathy is most commonly coupled with structural (glycation of wall components) and functional changes (endothelial cell dysfunction and increased arterial stiffness) (Rehman *et al*., 2007) vasoconstriction and inflammation via specific cytokines (TGF-β1). In turn, these ultimately promote the progression of left ventricular hypertrophy; a self-governing risk factor for cardiovascular (CV) mortality and important mechanisms in the development of DCM (Winer &Sowers., 2004; Fang *et al*., 2004). These studies have shown that conventional cardiac risks such as hypertension, atherosclerosis and dyslipidemia are more frequent in diabetic patients and further aggravate cardiac function. More specifically, DCM is identified by impaired myocardial relaxation dynamics or diastolic dysfunction (Boudina & Abel., 2007) left ventricular hypertrophy (LVH) (Rolo & Palmeira., 2006) interstitial fibrosis (Diabetes UK, 2007) and microvascular dysfunction (Tuttle., 2005) in the absence of significant hypertension, coronary artery disease (CAD) and valvular disease (Choi *et al*., 2008; Schalkwijk & Stehouwer., 2005) accompanied by comorbidities such as obesity. These complications often precede the development of systolic dysfunction, hypertension, CAD and heart failure (Choi *et al*., 2008; Rolo & Palmeira., 2006). Diabetic patients are prone to the development of left ventricular (LV) dysfunction that is different from that seen in chronic diseases such as hypertension and chronic ischemia in which the ventricle is not prominently hypertrophied (Shizukuda *et al*., 2002). Numerous mechanisms have been proposed to contribute to this clinical situation, including oxidative stress (Fostermann & Munzel., 2006) microvascular abnormalities, and decreased SR calcium uptake. However, the molecular mechanisms that cause this cardiac dysfunction are still largely undefined. It has been suggested that diastolic dysfunction may be due to myocellular hypertrophy and myocardial fibrosis. In turn at cellular level, these are associated with defects in calcium transport,

myocardial contractile protein collagen formation and fatty acid metabolism (Bertoni *et al*., 2003).

More recently, it has been suggested that DCM is a very common condition and its aetiology is largely due to HG which in turn causes LV hypertrophy. Therefore, the occurrence of DCM in DM patients is found to be elevated, and this DCM is due to diastolic dysfunction which is caused by myocardial fibrosis that occurs in response to HG (Ghosh & Bradham., 2010). Current evidence suggests that persistent HG-induced mitochondrial oxidative stress (MOS) is a significant contributor to DCM (Boudina & Abel, 2010; Dobrin & Lebeche., 2010). Certainly, the activity of several anti-oxidant enzymes is decreased in the diabetic heart in both humans and rats (Johansen *et al*., 2005). Of note, DCM appears to have an extensive preclinical course. Chronic, uncontrolled hyperglycemia has been indicated as an important contributor to the multifactorial pathogenesis of DCM (Schalkwijk & Stehouwer., 2005, D'Souza *et al*., 2011). Additionally, alterations in myocardial substrate metabolism precede lipotoxicity and increased oxidative stress–contributing pathological factors in DCM (Winn & Sowers., 2004). Despite considerable research into the pathophysiology of DCM, cardiovascular complications are generally only detected once overt clinical disease has developed.

1.3.5 Hyperglycemia and heart failure

HG is the most important factor that presents with increased risk of developing cardiovascular events together with HF and in particular it is a hallmark of DM. HG is most commonly recognized as the causal link between diabetes and diabetic complications and the target for antidiabetic therapy along with glycated haemoglobin (HbA1c) (Rolo & Palmeira., 2006; Fostermann & Munzel., 2006; D'Souza *et al*., 2011; Edwards *et al*., 2008)**.** Brief episodes of HG induce numerous maladaptations at cellular, subcellular and molecular levels in vascular tissues as an independent risk factor and also worsen cardiac performance and cell survival (Filippo *et al*., 2006). HG and HF significance is better appreciated with a clinical data background. Increased levels of HbA1c are an important risk factor in glycaemic burden. In a U.K. Prospective Diabetes Study (UKPDS) study, it was postulated that for every 1% increase in HbA1c, a 14% rise was shown for MI with a 16% rise in the risk for HF (Stratton *et al*., 2000) and a 19% increase in the incident of HF in an ongoing study in Scotland (Wong *et al*.,

2010). HG still remains the most common factor which leads to the development of chronic diabetic complications that are of high risk and are long-term (Chen *et al*., 2008). HG also has adverse effects on left ventricular function. A study demonstrated that acute HG is not merely a marker of severe myocardial damage, but a potential direct cause of abnormal left ventricular function (Ceriello., 2008). Numerous mechanisms of HG are claimed to be responsible for the generation of diabetes-induced heart disease. These include metabolic abnormalities such as cellular overload of fatty acid metabolites, defective glucose transport, structural alterations in the form of microangiopathy and altered calcium metabolism in cardiomyocytes (Doron., 2003; Asbun & Villareal., 2006; Masoudi & Inzucchi., 2007). The Diabetes Control and Complications Trial (DCCT) and the UKPDS have established that HG is the initiating cause of diabetic complications, relatively tissue damage. It has been shown that these processes are modified by both genetic determinants and independent factors, such as hypertension. The mechanisms that mediate the tissue damaging effects of HG are of great interest. DM selectively damages cells like endothelial and mesengial cells whose glucose transport rate does not decline as a result of HG, leading to an increase in glucose inside the cell. There is much evidence that these complications must involve mechanisms that occur inside these cells.

Despite several associations between increasing dysglycemia and CV risk, it is not clearly identified that the lowering of blood glucose demonstrates improvements in HF prognosis or delays HF onset in patients with DM (Goldfine and Backman., 2008). Optimizing glycaemic control is therefore a primary therapeutic target for reducing CVD risk in patients with diabetes (Voulgari *et al*., 2010, Schindler *et al*., 2007) as shown by the UKPDS metformin trail (UKPDS study group, 1998). However, recent trials including the ACCORD (Action to Control Cardiovascular Risk in Diabetes) (ACCORD study group, 2008) have demonstrated that tight control of glucose in patients may not improve mortality but may as well in fact increase it (Nathan *et al*., 2005).

1.3.6 Role of HG and its biochemical pathways in contractile dysfunction

Various mechanisms of HG are responsible for the generation of diabetes-induced heart disease, including metabolic abnormalities such as cellular calcium overload and altered calcium metabolism in cardiomyocytes leading to contractile dysfunction (D'Souza *et al*., 2011, 2014; Doron., 2003; Masoudi & Inzucchi., 2007; Asbun & Villareal., 2006; Brownlee., 2001,2005). One major contributor to HG-induced diabetic abnormalities is increased reactive oxidative stress (ROS) along with depleted antioxidant defences and raised levels of reactive oxygen species. ROS damage in the mitochondria together with poly (ADP-ribose) polymerase-1 (PARP) activation leads to the inhibition of the cytosolic enzyme glyceraldehyde-3-phosphate dehydrogenase (GAPDH) which initiates a series of cellular processes, by activating pathways leading to HG-associated cellular/tissue damage (Giacco & Brownlee., 2010) Inhibition of GAPDH, diverts glucose from glycolytic pathways into alternative biochemical pathways, including advanced glycation end product (AGE) formation, hexosamine, polyol pathway flux, and protein kinase C (PKC) activation (Scott & King., 2004) (Figure 1.10). Increased formation of AGE are involved in forming irreversible cross-links with macromolecules such as collagen leading to myocardial fibrosis, inactivation of sarcoplasmic SERCA2a and RyR2 calcium release channel, together with impaired cardiac contractility, relaxation and ventricular stiffness (Boudina &Abel., 2010; Dobrin & Lebeche., 2010; Doron., 2003; Candido *et al*., 2003; Young *et al*., 2009; Brownlee., 2004). Increased polyol pathway flux is associated with reduced levels of intracellular glutathione and a growth in cardiac cell apoptosis (Cai *et al*., 2002). Furthermore, inhibition of this pathway has been claimed to provide protection for the heart from ischemic injury (Guo *et al*., 2007). The hexosamine biosynthetic pathway is known for reducing SR SERCA2a mRNA and protein expression, along with reduced SERCA2a promoter activity via increased nuclear O-GlcNAcylation. As a result, this leads to prolonged calcium transients and impaired myocardial relaxation (Schleicher & Weigert., 2000; Mohora *et al*., 2007).

Finally, the activation of PKC via de nova synthesis of lipid second messenger diacylglycerol (DAG) can also lead to vascular alterations at pathological, cellular and functional levels these include, basement membrane thickening, extracellular matrix expansion, vascular permeability, enzymatic alterations such as Na^+–K^+–ATPase, and MAP kinase, multifocal fibrosis, myocyte necrosis, decreased left ventricular

performance and left ventricular hypertrophy (Belke & Dillmann., 2004). Impaired calcium handling and cellular efflux of calcium may further contribute to either impaired relaxation, or diastolic dysfunction. Overall, HG, via multiple biochemical pathways can result in myocardial, cellular and functional changes which contribute to the development of a cardiomyopathy which subsequently leads to HF.

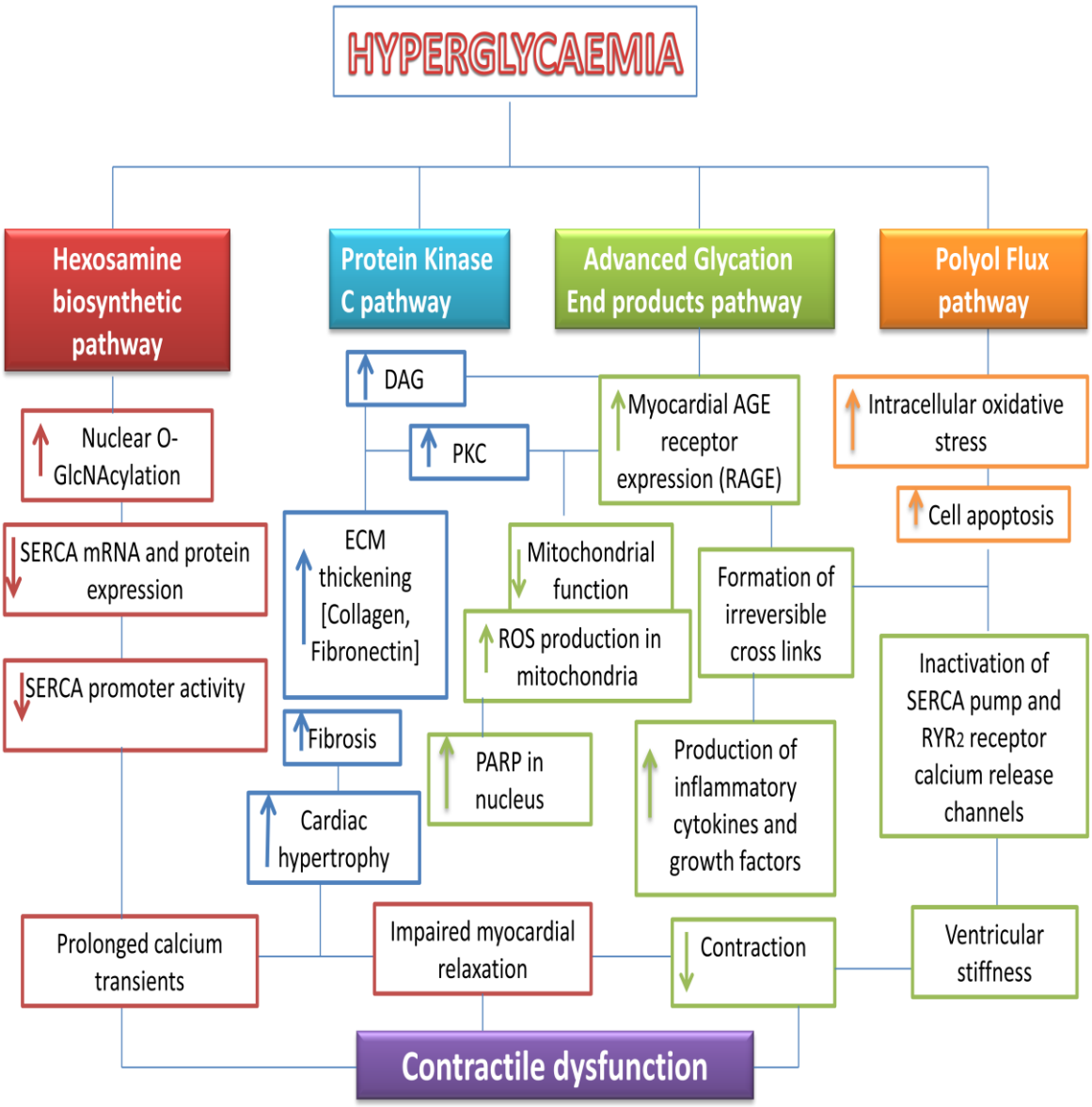

Figure 1.10: A schematic representation highlighting the role of hyperglycaemia and its biochemical pathways (Hexosamine biosynthetic pathway, Protein Kinase C (PKC) pathway, Advanced glycation end-products pathway and the Polyol flux pathway in the development of cardiac dysfunction**.** See text for discussion. DAG; diacylglycerol, ECM; Extracellular Matrix, PARP; poly (ADP-ribose) polymerase-1, SERCA; sarcoplasmic reticulum Ca^{2+}-ATPase.

1.4 The kidney

The kidneys, are the part of the endocrine system, in particular the main constituents of the urinary system. The kidneys play a fundamental role in regulating and maintaining the composition and volume of the extracellular fluid. They are essential in maintaining the acid-base balance by excretion of H^+ ions when the fluid becomes too acidic or excreting bicarbonate ions when the bodily fluid becomes too basic. The kidneys are highly vascular organs since they receive approximately 25% of the cardiac output. The main function of the kidneys is to produce urine, usually an ultrafiltrate of blood, which is then modified by selective reabsorption and specific secretions by the cells of the kidney. The final urine is conveyed by the ureter in the urinary bladder, where it is stored until discharge via the urethra. Constituents of final urine contain water and electrolytes as well as waste products including urea, uric acid, and creatinine, and breakdown products of various substances. The kidneys are large, bean shaped organs located in either side of the spinal column in the retroperitoneal space of the posterior cavity (Figure 1.11). Each kidney in humans measures approximately 10 cm long and 6.5 cm wide and 3 cm thick. Embedded within the renal fascia and thick protective layer of perirenal adipose tissue lays an adrenal gland. The medial border of the kidney is concave and contains a deep vertical tissue known as helium, through which the renal vessels and nerves pass through from the expanded funnel-shaped origin of the ureter, known as the renal pelvis. The kidney surface is covered by a highly organised connective tissue capsule which consists of two distinct layers; an outer layer known as the cortex, and an inner layer known as the medulla. The medulla is the location of renal pyramids that point towards the renal pelvis and terminate at a minor calyx where urine is collected (extension of the ureter) and is composed of connective and muscular tissue. There stipend appearance is the result of straight segments of the nephrons that span the pyramid. The renal pelvis is the location which leads out of the kidney to the ureter.

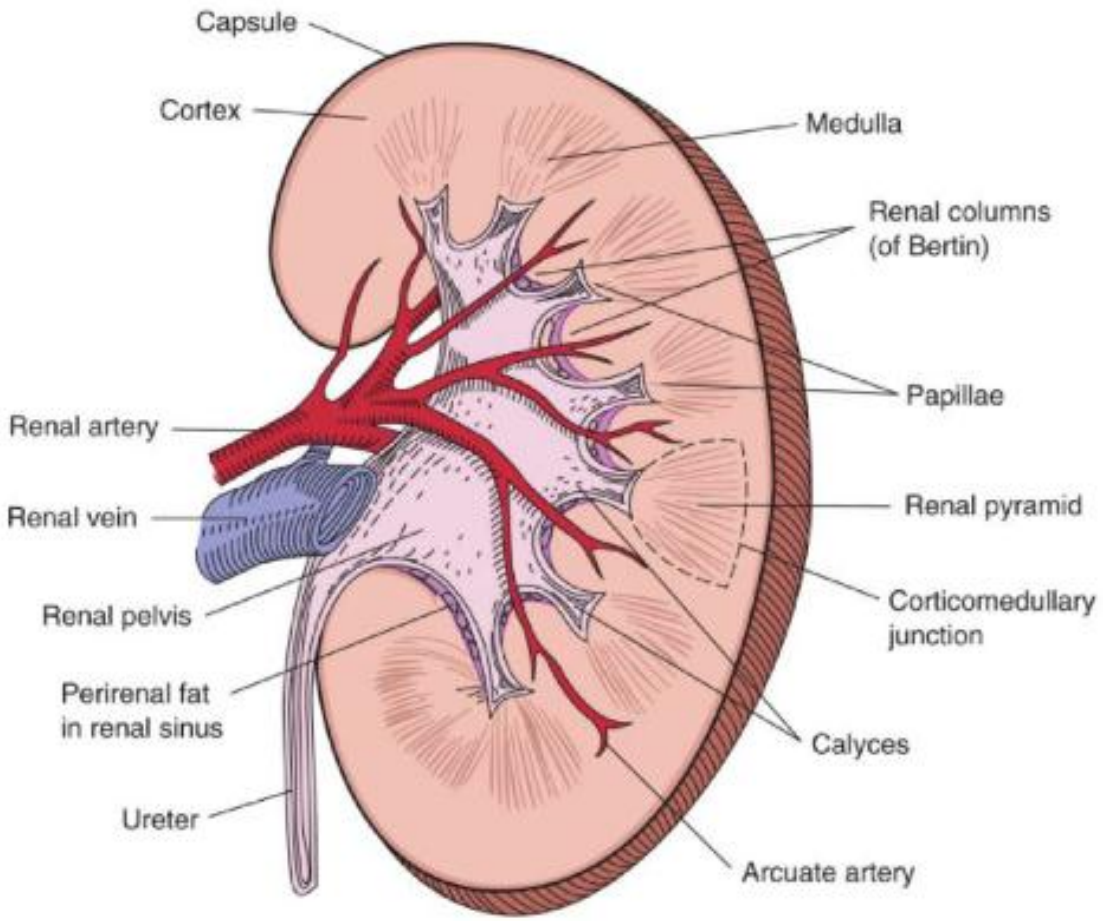

Figure 1.11: Anatomy of the human kidney. The diagram represents a hemisection of a kidney, revealing its structural organisation. The components are described in the text (Image courtesy: www.kidneyatlas.org).

The nephron is the fundamental structural and functional unit of the kidney (Figure 1.12). Each human kidney contains approximately 2 million nephrons. Nephrons are responsible for the production of urine and correspond to the secretory part of other glands. The collecting ducts are responsible for the final concentration of the urine. The renal corpuscle represents the beginning of the nephron which consists of the glomerulus. Glomerulus are the tuft of capillary composed of 10-20 capillary loops and surrounded by 1 double-layered epithelial cup known as the renal or Bowman's capsule (BC). The BC is the initial portion of the nephron where blood flowing through the glomerular capillaries undergoes filtration to produce the glomerular ultrafiltarate. The glomerular capillaries are supplied by the afferent arteriole and are drained by the efferent arteriole that branches, forming a new capillary network to supply the kidney tubules (Miner, 2003).

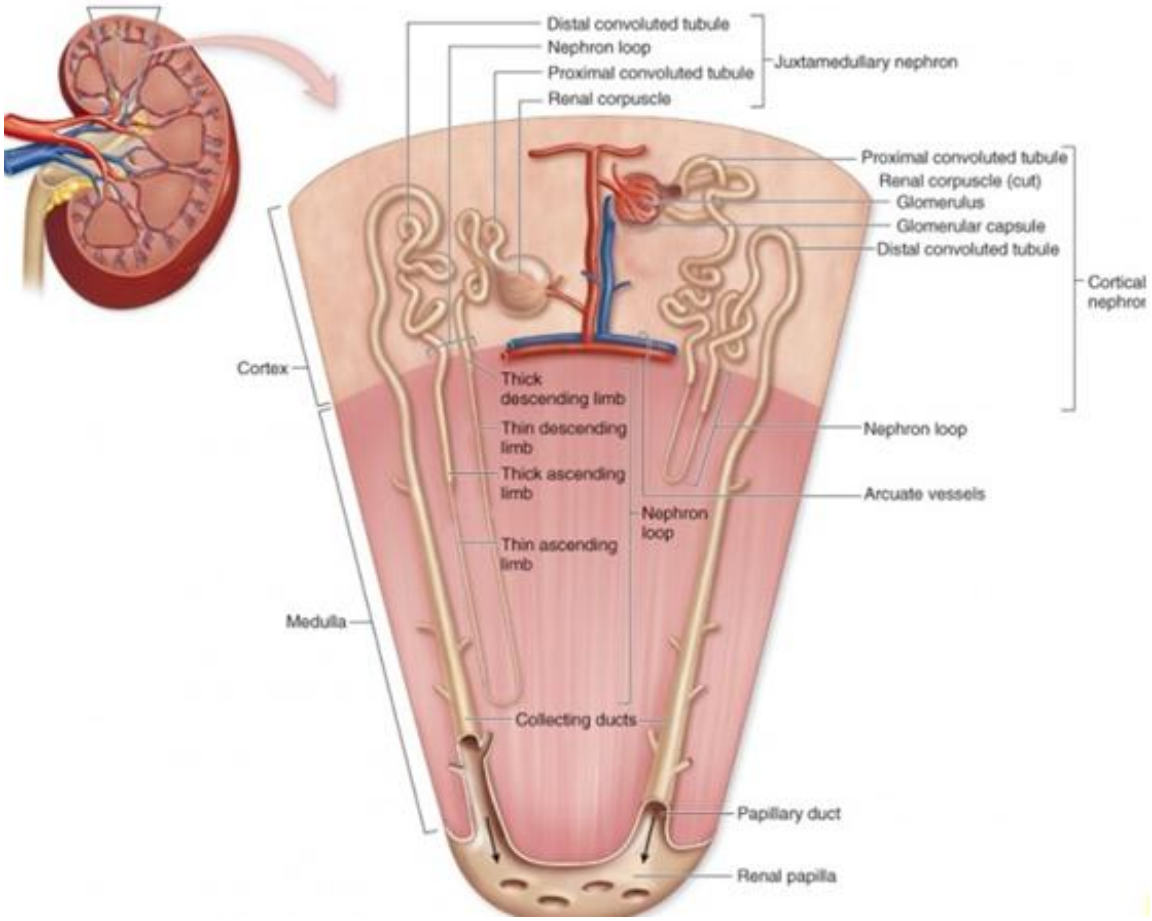

Figure 1.12: Anatomy of the Nephron. Components are described in the text (Image courtesy: www.kidneyatlas.org).

Beginning from the BC, the sequential parts of the nephron consist of firstly, the proximal convoluted tubule; the site of early reabsorption of water, ions, glucose and amino acids and by the end of which 60% of original water is reabsorbed and 65% of original ions. The proximal convoluted tubule is attached to the thick descending limb, thick descending limb, thin ascending limb and thick ascending limb that together form a hairpin like structure known as the loop of Henle, by the end of which 80% of original water is reabsorbed and 65% of original ions. This leads to the distal convoluted tubule that empties into the collecting duct that lies in the medullary ray via a short connecting tubule (Gattone, 2007). Nephrons can be classified by their location. Most nephrons are located almost completely within the cortex, known as cortical nephrons. Nephrons that are found close to the boundary between the cortex and the medulla, and whose loops of

Henle are mainly within the medulla are known as juxtamedullary nephrons. The juxtamedullary nephrons make up one eight of the total nephron count. Their renal corpuscle occur in proximity to the base of a medullary pyramid and have long loops of Henle and long ascending thin segments that extend into the inner region of the pyramid.

1.4.1 Diabetic Nephropathy (DN)

Diabetic nephropathy is microvascular complication leading to kidney dysfunction and end-stage renal disease (ESRD) (Kato *et al*., 2006). It is suggested that the Diabetes Control and Complications Trail (DCCT) that approximately 30% patients with T1DM and 25-40% of patients with T2DM develop DN, irrespective of glycemic control (DCCT, 1995; Dronavalli *et al*., 2008). In addition, the disease often involves siblings and even more so, some ethnic groups. DN is a clinical syndrome characterised by the occurrence of persistent microalbuminuria in concomitance with T1DM and T2DM. In T1DM, initially, the patient shows hyperfiltration, represented by high values of glomerular filteration rate (GFR), approximately doubling of the normal value, and occasional occurrence of microalbuminuria. Later, during a course of approximately 20 years, the patient shows a gradual decline of the GFR and persistence of microalbuminuria that comes before mild and subsequently moderate proteinuria. The final step of the natural history of the disease is characterised by severe proteinuria with or without nephrotic syndrome and chronic renal insufficiency that declines to ESRD (Schena & Gesualdo, 2005). Risk factors for development of DN include HG, hypertension, positive family history of nephropathy and hypertension, and smoking. Key elements in the primary care of diabetes include glycemic control, blood pressure control, and screening for microalbuminuria. In general, the goal for glycaemic control is a blood glucose level as close to normal (HbA1c <7%) as possible without causing dangerous hypoglycaemia. Blood pressure control is at least as important as glucose control, especially after the onset of renal damage, and blood pressure should be consistently <130/85. Screening for DN usually involves yearly monitoring for urinary albumin excretion >30 mg per day.

The general characteristics of DN include renal glomerular hypertrophy, basement membrane thickening, and fibrosis due to accumulation of ECM proteins and regulators (Ziyadeh, 1993; Steffes *et al*., 1989; Decleves & Sharma, 2010; Kato *et al*., 2012) and clinical features include proteinuria, albuminuria, and progressive glomerular dysfunction

(Yamamoto *et al*., 1993; Sharma *et al*., 1997; Kato *et al*., 2006; Kato *et al*., 2007). Glomerular basement membrane (GBM) thickening is a characteristic early change in type 1 (Drummond *et al*., 2002) and type 2 DN (Perrin *et al*., 2006) and it increases with duration of disease. GBM thickening may already be present in type 1 diabetes patients who are normoalbuminuric (Perrin *et al*., 2006) Furthermore, in patients with proteinuria and isolated GBM thickening, but without overt diabetes, 20% were positive for a blood test for diabetes at the time of biopsy, whereas 44% were diagnosed with diabetes at 6 months, and 70% at 2 years after the biopsy was taken (Mac-Moune *et al*., 2004). Long-term glucose control and urinary albumin excretion (UAE) correlate strongly with basement membrane thickness (Bangstad *et al*., 1994). Advanced DN is characterized by macroalbuminuria (>300mg/day), a progressive decline in glomerular filtration rate, decreasing creatinine clearance, glomerulosclerosis, and interstitial fibrosis (Kato et al., 2006; Raptis & Viberti, 2001). Although poor glycaemic control is an important risk factor, glycaemia does not fully explain why only a subset of diabetic patients progress to end stage renal disease (ESRD).

DN is associated with an excessive accumulation of ECM proteins in the mesangial, reffered to as glomerulosclerosis, which narrows the glomerulus lumen. These ECM depositions are closely related with loss of kidney function and reduced survival rates (Kato *et al*., 2007). The thickening of the glomerular basal membrane is associated with increases in collagen type IV, laminin, and proteoglycans (Burns *et al*., 2006; Wan *et al*., 2010). Similarly, increases in collagen types IV, V, VI, fibronectin, and laminin, as well as proteoglycans have been identified in the mesengium (Wang *et al*., 2010, Wang *et al*., 2011; Sengupta *et al*., 2008). Several decades of extensive research has elucidated various pathways to be implicated in the development of diabetic kidney disease. These include haemodynamic factors, the renin-angiotensin-aldosterone system (RAAS), the intracellular signaling molecule protein kinase C, TGFβ1 (described previously), insulin like growth factors, vascular endothelial growth factor, AGE products, RAAS, and platelet-derived growth factor are believed to be involved in the pathogenesis of DN (Raptis & Viberti, 2001; Kato et al., 2006; Kato *et al*., 2007).

1.4.2 Kidney and heart failure

In addition to the above, HF and kidney disease are two of the most important conditions affecting morbidity and mortality of adult subjects. Their prevalence is still growing because of ageing of the general population and better treatment of acute conditions (Metra & Voors, 2012). Hypertension, DM, and atherosclerosis are coexisting risk factors both for HF and chronic kidney disease (CKD). In addition, there is much evidence that both HF and CKD may affect each other, leading to further progression of the disease (Metra & Voors, 2012). Thus, an impairment of kidney function is present in 30–60% of the patients with HF and is an independent prognostic factor (Colombo *et al*., 2011). Episodes of acute decompensated HF is found in upto 64% of patients hospitalised with renal dysfunction (Heywood *et al*., 2007). Furthermore, historical analysis indicates that the mean creatinine level at admission has risen in recent decades (Owan *et al*., 2006). In addition, worsening of renal function (WRF) may also be related with poorer outcomes in these patients (Ruggenenti & Remuzzi, 2011). Hemodynamic abnormalities such as venous congestion and a low cardiac output, neurohormonal and inflammatory activation, atherosclerosis, and diuretic treatment may all contribute to WRF in patients with HF. Impaired kidney function is, on its turn, associated with abnormalities in mineral metabolism, anaemia, formation of AGE-products, further inflammatory and neurohormonal activation, reduced use of life saving therapies, such as inhibitors of RAAS (Lazzarini *et al*, 2011; Metra & Voors, 2012).

1.5 Animal models used in this study

STZ-induced model of type 1 diabetes mellitus

Current pathophysiology and pathogenesis of cardiac disease in DM can be understood by experimenting in the rodent model system. This model shares many phenotypic similarities with human disease, making significant correlates possible for physiology and metabolism. The fact that human tissue cannot be invasively tested due to ethical and logistical constraints limits the opportunities to study DM in depth. Hence, rat models are used to provide enormously invaluable opportunities to study the mechanisms underlying the pathophysiology of DM in detail. Advantages of using the rodent models include short generation intervals, their adaptability to invasive testing and the ability to provide controlled conditions for chemical, microbiological, genetic and environmental factors to be studied (Kahn, 2005).

Animal models of diabetes can be characterised in two main types: chemically induced type 1 diabetes and genetically determined diabetes (Dhalla *et al*. 1985). Chemically induced type-1 diabetes is the most common model of animal and DM which involves the administration of agents by producing toxic effects which cause β cell necrosis of the pancreas. This model was firstly described in 1943 by Bailey and Bailey, and Dunn *et al*. 1943, who accidentally developed the diabetogenic potential of alloxan in an attempt to create an experimental model for uremia. Alloxan is a structurally similar pyrimidine which is synthesised by chemical combination of two uric acid molecules. However, alloxan has been shown to elicit non specific necrotic effects. Hence, streptozotocin (STZ) has been more widely used as the diabetogenic agent of choice due to its specific action on β cells resulting in lesions that accurately resemble β cell destruction characteristics of T1DM (Weiss. 1982, Smith *et al.* 1983, Ikebukuro *et al*. 2002). STZ is also reported to have a greater specificity to β cells, a longer half life and is associated with lower mortality rates making it the agent of choice for chemical induction of experimental diabetes in this study (Lenzen, 2008).

In 1993, Rakieten and colleagues introduced the induction of DM by selective destruction of insulin-producing β cells of the pancreas with a single, rapid injection of STZ (Rakieten *et al*. 1993). STZ, [2-deoxy-2(3-methyl-3-nitrosourea)1-D-glucopyranose] is an antimicrobial glucose moiety consisting of a very reactive nitrosoureas product of *Streptomyces achromogens* and has been widely used as a chemotherapeutic alkylating agent. This procedure of DM induction has been published in more than 7,600 reports, making it the second most used animal model of human disease, following the spontaneously hypertensive rat (SHR) (Wei *et al*. 2003). Clinically, symptoms of diabetes are clearly seen in rats within 2-4 days following single intravenous or intraperitoneal injection of 60 mg/kg STZ (Ganda *et al.* 1976, Weiss. 1982, Elias *et al*. 1994, Arora *et al*. 2009). βeta cell toxicity of STZ has been associated with the glucose moiety of its chemical structure, enabling STZ to enter the cell via the low affinity glucose transporter GLUT2 present within the plasma membrane (Elsner *et al*. 2007)**.** A study by Weiss (1982) hypothesized that the reduction of NAD in pancreatic cells is mediated by the diabetogenic action of STZ. STZ mediated alkylation damages the DNA which is then repaired by an excision repair process. This process requires the activation of NAD dependent enzyme, poly (ADP-ribose) synthetase which is continuously activated in the beta cell, thus depleting the cell of NAD. This loss of NAD leads to termination of cellular function, thus leading to cell death. This model of βeta cell damage is referred to

as the Okamoto model. In addition, DNA alkylation, reactive oxygen species (ROS), including the superoxide (O_2•-), hydrogen peroxide (H_2O_2), hydroxyl radical (HO•), and nitric oxide (NO•) have all been discovered to play important roles in the mechanisms of DNA damage through STZ-induced cytotoxicity (Bolzan and Bianchi. 2002). It has been hypothesised by Turk and colleges in 1993, that potentially, diabetogenic STZ acts as an intracellular NO donor which generates 3',5'-cyclic guanosine monophosphate (cGMP) and NO all of which contribute in DNA damage by inhibiting aconitase (Turk *et al*., 1993). STZ is also found to participate in xanthine metabolism which has been associated with increases in ROS that further speed up cell death and insulin synthesis inhibition. Collectively, these mechanisms lead to defaults in insulin biosynthesis and secretion, glucose transport and metabolism in DM which resembles human hyperglycemic DM.

The Goto-Kakizaki rat

The Goto-Kakizaki (GK) rat is a non-obese, spontaneously T2DM model that was created by repetitive breeding of Wistar rats with poorest glucose tolerance (Goto *et al*., 1975). The pathogenesis of diabetes in the GK rat includes, impaired insulin secretion in response to glucose both *in vivo* and in isolated pancreas, reduced pancreatic β cell mass and pancreatic insulin stores, IR in adipose tissue, muscle and liver, moderate but stable fasting HG and late complications manifesting as nephropathy and neuropathy (Yashushi *et al*., 2007; Howarth *et al*., 2007). T2DM in the GK rat is polygenic, and at least six independent genetic loci are involved in pathogenesis of the disease (Gaugier *et al*., 2006). GK rats have a stable, inheritable form of T2DM and do not develop marked obesity, hypertension or hyperlipidemia and have been used in many studies (Portha *et al*., 1991; Zhou *et al*. 1995; Darmellah *et al*., 2007).

1.5.1 Working hypothesis, aims and specific aims of the study

Working hypothesis: Hyperglycaemia, as in Type 1 Diabetes mellitus, can lead to remodelling of the heart and kidney and associated changes in endogenous inflammatory markers, function and cellular calcium homeostasis.

Main aim: The main aim of this study was to investigate the effect of T1DM-induced hyperglycemia on cardiac remodelling measuring factors and events which are associated with cardiac hypertrophy, stiffness, contraction and dysregulation of cellular calcium transport. In doing so, the important question that arose was if these changes are occurring in the heart, are they simultaneously occurring within the kidneys? Hence, another major objective of this study was to examine the occurrence of transcriptional reprogramming of key genes that execute hypertrophic/fibrotic gene programs during pathological remodelling of the heart and the kidneys to access similarities or differences in the pathological responses adopted by these two specialised organs.

Specific aims of the research:

1. To induce type 1 diabetes mellitus in young adult male Wistar rats using a single intraperitoneal (ip) injection containing Streptozotocin (STZ) and to investigate the general characteristics of the animals at 2 and 4 months post STZ-administration.

2. To investigate if DM-induced HG can produce impairments in myocyte contractility and altered $[Ca^{2+}]_i$ handling. This was achieved by measuring ventricular myocyte shortening and intracellular calcium transients in single cardiomyocytes.

3. To measure gene expression of intracellular calcium transport proteins in STZ-induced rat hearts at 2 and 4 months post STZ-administration and age-matched control animals.

4. To investigate if LV and left kidney structural remodelling was occurring as a result of uncontrolled DM-induced HG, characterised principally by ECM proliferation and apoptotic cell death in the STZ-induced diabetic rats at 2 and 4 months post STZ-administration and age-matched control animals.

5. To measure ECM components and regulators in the LV and left kidney at 2 and 4 months post STZ-administration and age-matched control animals.

6. To investigate involvement of endogenous inflammatory markers (TGFβ1) and signalling molecules such as atrial natriuretic peptide (ANP) and brain natriuretic peptide (BNP) in the LV and left kidney at 2 and 4 months post STZ-administration and age-matched control animals.

7. To investigate the effect of exercise training in 10-11 month old T2DM model of GK rats and age-matched Wistar control animals following 2-3 months of treadmill exercise training measuring myocyte contractility, altered $[Ca^{2+}]_i$ handling, intracellular calcium transport proteins, ECM proliferation, apoptotic cell death, gene expression of ECM components and regulators, signalling molecules as well as the involvement of TGFβ1 cytokine activation.

8. To analyse the data and write up the PhD thesis.

CHAPTER 2

MATERIALS AND METHODS

2.1 Materials

Animals: Several Male Wistar rats 4 months and 30 male GK and 30 male Wistar control rats aged 8 months at the start of the experiment.

Drugs and reagents: Streptozotocin, 10 % formalin, ethanol, histoclear, histamount, poly-L-lysine coated slides, H&E stain, Masson's Trichrome stain, Periodic Acid Schiff stain, homogenisation buffers,fura-2-AM, liquid nitrogen, β-mercaptoethanol, TBST buffer, PBS buffer, Citrate buffer, isolation buffers and solutions, Collagenase, Proteinease, Protein kinase.

Equipment: Microtome, cryostat, Confocal laser microscope, Video-edge detection system, Plate reader, ND-100 Nano-Drop, Applied Biosystems 7900 HT Sequence Detection System, Electron microscope, Langendorff perfusion apparatus, -80˚C and -20˚C freezers, Temperature controlled centrifuge, Conventional microwave oven, Humidified chamber, spatula, scissors, weighing dish, PCR 96 well plates, plate sealer, ELIZA plates, homogeniser, sonicator, polytron, mini centrifuge columns, 0.5 ml epindorff tubes, pipette tips, pipettes, multichannel pipettor, RNA zap, RNAase free water, OneTouch glucose meter, distilled water.

Antibodies and kits: SignalStain Apoptosis (Cleaved Caspase-3) IHC detection kit, TGFβ1 Enzyme-linked ImmunoSorbant Assay (ELIZA) kit, Superscript III reverse transcriptase, 2X Power SYBRGreen Master Mix, RNA extraction kit, DNAse 1 kit, FITC-conjugated Lectin, FITC-conjugated anti-mouse IgG, Anti-Alpha Skeletal Muscle Actin antibody, Goat anti-rabbit IgG, Lowery protein assay.

Software: Image J, IBM SPSS Statistics 22, Fig.P software.

2.2 Methods

2.2 Investigational design: In the first series of experiments functional, structural and molecular investigations were performed in the LV and kidneys of 2 and 4 month old STZ- induced type 1 diabetic and aged-matched control Wistar rats. Subsequently, in another series of experiments, similar variables were investigated in adult GK rats at 8 months of age compared to aged matched male Wistar controls. These animals were divided into four subgroups, where two subgroups of GK and control rats received exercise training whilst the other 2 subgroups continued on a sedentary lifestyle.

2.3 Experimental models: The project obtained relevant clearance from the Animal Ethics Committees at the University of Central Lancashire, UK and College of Medicine & Health Sciences, United Arab Emirates University, UAE. All procedures were carried out in accordance with the 'UK Animals (Scientific Procedures) Act 1986'. Animals were housed in groups (3 or 4 in 1 cage) under institutional regulations at standard animal housing conditions. Animals were kept at an average room temperature of 24˚C, a relative humidity of 50% and a 12-hour day and night cycle. All rats were allowed unlimited access to water and commercial chow (unless indicated). All rats were regularly monitored throughout the experimental period for any signs of suffering or disease.

2.3.1 Induction of diabetes: One week after arrival in the animal house, young male Wistar rats (2 months of age) were rendered diabetic by a single intraperitoneal injection (i.p.) of Streptozotocin (Sigma-0130) (60 mg kg^{-1} body weight) dissolved in citrate acid buffer (0.1 M citric acid, 0.1 M sodium citrate in distilled water, pH 4.5). Control animals received an equal volume (0.3 ml) of the citrate buffer alone. Rats were caged separately and fed routinely on a normal diet and water until after 2 months or 4

months of diabetes, when they were humanely killed for experimentation. DM was confirmed 4-5 days following STZ injection and on the day of experiments, prior to killing the rats, using a glucose meter (One Touch II glucose meter, Lifescan inc).

2.3.2 GK model and exercise training: Thirty male GK (Taconic, Germantown, NY, USA) and 30 male Wistar control rats aged 8 months were divided into four subgroups (15 animals each). Two subgroups of GK and control rats received exercise training whilst the other two subgroups of GK and control rats continued a sedentary lifestyle. Animals were exercised on a treadmill (EXER-4, Columbus Instruments, Columbus, OH, USA) according to previously described protocol with minor modifications (Howarth *et al*., 2009; Howarth *et al*., 2008). Exercise training sessions were given daily for 1 hour each and repeated 5 days per week for a period of 2-3 months. Each training session began with a 10 minute warm-up during which the belt speed was gradually increased from zero to required training speed. For the duration of week 1, the training belt speed was 10 m/minute, during weeks 2-3 belt speed was increased to 15 m/minute and during week 4 the belt speed was maintained at 15 m/minute and the belt gradient was increased from 0˚ to 10˚. Thereafter, the training belt speed was increased to 20 m/minute. Two months into the exercise training programme, animals were subjected to a glucose tolerance test (GTI) (applied when animal in resting stage). After an overnight fast, animals were given an i.p injection of glucose (2 g glucose per kg body weight) and blood glucose was measured using a glucose meter (One Touch II glucose meter, Lifescan inc) 120 minutes following the glucose challenge.

2.4 Sample collection

Animals were weighed throughout the time course of the study and prior to the end of the experiment, with regular checks for any signs of distress. Animals were humanely

killed by a blow to the head followed by cervical dislocation and hearts rapidly removed by midsternal incision. Blood samples were taken directly from the heart by cardiac puncture. Blood was collected in tubes containing 25 mM Ethylenediaminetetraacetic acid (EDTA) and rapidly put on ice following centrifugation at 3,000 rpm for 5 minutes. Blood plasma was removed, transferred to a new tube, and centrifuged again at 12,000 rpm for 5 minutes to remove residual red blood cells and platelets and stored at -80°C until use. After the excision of the heart, blood was removed from the chambers and blotted dry and the weight was recorded. Only the left kidney was removed carefully by locating it under the matter, blotted dry, weighed and either frozen in liquid N_2 for protein assay/gene expression and stored at -80°C or processed for light/electron microscopy. The LV was isolated and either frozen in liquid N_2 for protein assay/gene expression study and stored at -80°C or processed for light/electron/confocal microscopy. For all animals, body weight, heart weight and kidney weight was measured immediately after isolation and non-fasting blood glucose was measured prior to experiments.

2.5 Histological studies

Tissues were processed for histological examination according to previously described techniques (D'Souza *et al*., 2011). Briefly, LV and kidney tissue samples were fixed in 10% formalin and dehydrated in alcohol (30, 50, 70, 90 and 100% Ethanol) for specific time periods. Samples were than embedded in paraffin wax and sectioned at 4 µm using HM325 microtome. Samples were re-hydrated and stained with hematoxylin and eosin stain (H&E) as described below for general examination and with Masson's trichrome stain for the determination of ECM deposition according to previously established methods (D'Souza *et al*., 2011). Pre-staining procedure of dewaxing and hydration involved the flooding of slides with Histoclear twice for 3 minutes and a series of

100%, 70% and 50% absolute alcohol changes for 3 minutes each and washed in tap water, prior to staining. For H&E stain, the slides were firstly stained with Harris' haematoxylin (Sigma Aldrich, HHS128) for 5 minutes and washed in tap water. Scott's tap water was used to blue the section for 3 minutes. Alcoholic eosin (Sigma Aldrich, HT110132) was applied to the slides for 2 minutes prior to dehydrating through changes of alcohol and Histoclear. It was essential at this stage to give sufficient time, to avoid any air bubbles being trapped on the tissue. The slides were then mounted in histamount (Agar Scientific, AGR1351). For the Masson Trichrome staining, slides were firstly stained with Weigert's haematoxylin (Sigma Aldrich, HT1079) for 15 minutes and Ponceau red for 5 minutes, washing with water in between. Phosphomolybdic acid was applied for 5 minutes and drained. Finally, light green stain was used on the slides for 5 minutes and the slides were dehydrated and mounted. In addition, Periodic Acid Schiff (PAS) stain was performed on kidney sections to highlight the basement membrane. Briefly, sections were oxidized in 0.5% periodic acid solution for 5 minutes and rinsed in distilled water. Sections were then placed in Schiff reagent for 15 minutes and sections were observed for a light pink colour followed by washing in lukewarm water for 5 minutes. Sections were counterstained with Mayer's hematoxylin for 1 minute followed by washing in tap water, dehydration and mounting. Morphometry was performed by digital image analysis using a PC digital image camera (Digital Sight DS-5M, Nikon Corp, Japan) mounted on an Axiolab Zeiss light microscope (Carl Zeiss Corp, Germany) with a 40X objective. Extent of ECM proliferation in the LV and Kidney was assessed by using a freely available colour image analysis system (NIH Image J 1.37 V). The programme was calibrated using a graduated slide (Graticules LTD). Application of a plugin known as colour segmentation was applied to calculate the percentage of interstitial fibrosis present in the Masson's trichrome stained LV and kidney sections. Image J was programmed to identify shades of a specific colour (green

for collagen) on the stained sections. Collagen area fraction was calculated as the ratio of area of fibrotic tissue to total area of myocardial tissue based on operator's threshold settings. Approximately, 30-40 selected fields in each group were included in the analysis.

2.5.1 Immunohistochemistry

To investigate the activation of the apoptotic pathway, activity of caspase-3, the primary effector of cardiomyocyte apoptosis, was estimated using a commercially available caspase-3 detection kit (SignalStain Apoptosis (Cleaved Caspase-3) IHC detection kit, Cell Signaling Technology, 12692) and manufacturers' instructions. Caspases have earlier been described to possess proteolytic activity which enabled them to cleave proteins at aspartic acid residues, functioning as endonucleases leading to programmed cell death (Rai *et al*., 2005). Briefly, paraffin embedded tissue sections were deparaffinised in Histoclear and rehydrated in alcohol (95% and 100% Ethanol). Antigen unmasking was achieved by heating sections in 10 mM sodium citrate buffer at pH 6 for 10 minutes using a conventional microwave. Following antigen unmasking, tissue sections were allowed to cool for 30 minutes and then washed in distilled water three times for 5 minutes each. Thereafter, sections were incubated in 3% hydrogen peroxide for 10 minutes followed by washing in water twice for 5 minutes each. Sections were then washed in Tris Buffered Saline with Tween 20 (TBST) (prepared according to manufacturer's instructions). Each section was then blocked with blocking solution (1x TBST/5% normal goat serum) and incubated for 1 hour at room temperature. A negative control was also prepared using the control present within the kit and incubated in the same conditions. Sections were incubated over night at 4˚C with polyclonal rabbit anti-active caspase 3 antibody diluted in antibody diluent (1:500) supplied within the kit and washed in TBST wash buffer three times for 5 minutes each.

This specifically recognised the large fragment (17/19 kD) of activated Caspase-3. SignalStain Boost Detection Reagent supplied within the kit was equilibrated to room temperature. Sections were covered with 1-3 drops of this detection reagent and incubated in a humidified chamber for 30 minutes at room temperature, followed by washing with TBST for 5 minutes each. A volume of 30 µl of chromagen concentrate (supplied in kit) was added to 1 ml of Signal Stain DAB Diluent (supplied in kit) and mixed well before use. A volume of 100-400 µl of this DAB was then applied to each section and monitored closely for acceptable staining intensity, approximately 1-10 minutes. When desired staining was achieved (red-brown in colour) immunohistochemical staining with caspase 3 was monitored by light microscopy, post immersion of slides in tap water, counterstained with Hematoxylin (Sigma Aldrich, MHS32) as per manufacturer's instructions. Slides were dehydrated through a series of alcohol changes and Histoclear and then coversliped with Permount. A semiquantitative analysis of the apoptotic cells that were on average of 30-40 LV groups, defined as caspase-3 positive cells/area (mm^2) were obtained using Image J and the utilization of a plugin known as Deadeasy Caspase that was designed to quantify cleaved caspase-3 mediated apoptosis (Forero *et al*. 2009). Photomicrographs were imaged at X400.

2.5.2 Electron microscopy

Freshly isolated LV and kidney samples from 2 and 4 month old STZ-induced diabetic rats and 8 month old GK rat subgroups with age matched controls were cut to 4 mm x 4 mm size, transferred into Karnovsky's fixative (16% paraformaldehyde, 50% EM grade glutaraldehyde, 0.1 M sodium phosphate buffer) at pH 7.2 in 7 ml glass vials with lids attached and endorsed to rotate on a rota mixer for 4-5 hours at room temperature. Samples were than washed in 0.1M phosphate buffer 3 times for 15 minutes each and stored at 4^{o}C until ready for further processing. For post fixation, 1 ml of buffered 1%

osmium tetroxide in 0.1 M sodium cacodylate and allowed to mix for 1 hour at room temperature on a rotamixer. Subsequently, the samples were washed in distilled water and dehydrated in graded ethanol and processed as follows: 15 minutes each in 30%, 50%, 70%, 80%, 90%, 95% ethanol, and 2 changes in absolute ethanol and propylene oxide for 15 minutes each. Polymerisation resin was then carefully prepared by the following balanced composition: Agar 100 epoxy resin, 23 ml; Dodecenylsuccinic anhydride (DDSA), 14 ml, Methylnadic anhydride (MNA), 13 ml and Tri (Dimethylaminomethyl phenol (DMP-30), 1.1 ml. Tissues were then immersed in an appropriate agar and propylene oxide ratio ranging from 1:1/1:2/1:3 for 1 hour each followed by embedding in pure resin using flat molds. These molds were then placed in a desiccator for 2-3 hours to remove the air bubbles followed by polymerization at 61°C for 24 hours. Five blocks with transverse and longitudinally directed myocytes were selected from each investigational group. Randomly selected, semithin sections, (1~tm thick) were cut with glass knives and stained with Toluidine blue for examination by light microscopy in order to exclude abnormal tissues from ultrastructural studies. Thereafter, semithin sections were stained with methylene blue and examined in the light microscope to select appropriate areas for the preparation of ultrathin sections. Ultrathin sections were cut with a diamond knife (DuPont) on an LKB III ultratome and picked up on mesh copper grids. Sections were carefully stained with saturated uranyl acetate solution in 50 percent ethanol for 15 minutes followed by lead citrate solution for two minutes. A JEM 1010 electron microscope was used to examine the ultrathin sections at an accelerating voltage of 60 kV. Subsequently, electron micrographs were printed on 8 x 10 inch photographic paper at 7,000 X and 14,000 X magnifications.

Electron microscopy quantitative measurements

Quantitative sarcomere measurements were made using commercially available Image J software. A total of thirty measurements of sarcomere length were recorded from each

treatment group and age-matched control hearts. Image J drawing tool was used to draw a point to point perpendicular line of each sarcomere in a single composed stack and obtained vales were then averaged for each experimental group. Mitochondrial count was performed using manual counting of clearly visible mitochondria in each micrograph; values obtained were averaged for each experimental group. Similarly, Subsarcolemmal mitochondria (SSM) were identified by counting those that directly abut the sarcolemma and Interfibrillar mitochondria (IFM) were identified by those situated between the myofibrils. Mitochondria that were attached or transformed into a single shape were discarded from the analysis. Similarly, GBM width was measured by using the Image J drawing tool to obtain the average GBM measurement from the control groups across both treatment times (300-400 nm) and the software was calibrated accordingly. Approximately, 6-7 points of the GBM were measured for each experimental group running in a clockwise order to ensure the same point was not measured twice. Measurements were taken from GBM loop visible in each micrograph to gain statistically significant data. Values obtained were averaged for each experimental group and expressed as Mean±S.E.M.

2.5.3 Immunofluorescence and confocal laser scanning microscopy

In order to process paraffin sections for immunofluorescence microscopy, sections were deparaffinised in Histoclear and dehydrated through a series of alcohols followed by antigen unmasking as described previously. Paraffin embedded LV sections were firstly blocked in 5% normal goat serum (NGS) and incubated overnight in either Fluorescein isothiocyanate (FITC) conjugated Lectin (Sigma Aldrich, 6171) 1 µg/µl or Anti-Alpha Skeletal Muscle Actin antibody (αSKA) (Abcam, ab28052) (1:100). Tissues were further incubated with secondary antibody; FITC-conjugated anti-mouse IgG (Sigma Aldrich, M0659) at a dilution of 1:100 for 1 hour at room temperature. Sections

were washed in three changes of PBS for 5 minutes each and mounted with mounting medium with Propidium Iodide (Vector Laboratories, H1300). Slides were examined using a laser scanning confocal microscope (LSM 510, Carl Zeiss, UK) for detection of FITC (excitation Bandpass 450-490 nm, emission low-pass 515 nm) and final material captured as 512 x 512 pixel images with a magnification at X400 and constant setting where possible. Commercially available programme Image J was used to measure cell size or florescence intensity. Background fluorescence was determined by replacement of primary antibody/robe with 5% NGS in PBS to facilitate specificity of staining pattern. Lectin labelling identified single cardiomyocytes which enabled accurate measurement of individual myocyte diameter. Briefly, short axis diameter was measured 3 times on transverse sections by using the drawing tool on Image J to draw a point to point perpendicular line and obtained vales were then averaged for each experimental group. In order to measure the fluorescence intensity of anti-αSKA labelled sections, gain and threshold settings were kept constant for each experimental group. For all scans of control and diabetic myocardial tissue, the photo multiplier tube settings were 450-550, pinhole setting of 60 μm, with a laser voltage setting of 20 mW. Quantification of fluorescence signal for anti-αSKA labelled sections was analysed by transforming confocal micrographs in grey luminance values that ranged from 0-255 (corresponding from black to white) and splitting these to RGB channels on Image J. Fluorescence intensity was evaluated as the sum of pixel intensity values via utilising the green channel. Total fluorescence intensity for each field was inferred and obtained value was subtracted from background signal using a negative control stained slide and this corrected value was then expressed as labelling intensity/unit area of field. Averaged values for each section were expressed as Mean±S.E.M.

2.6 mRNA quantification by Quantitative Reverse transcriptase Polymerase chain reaction

Quantitative reverse transcription polymerase chain reaction (RTqPCR) is a highly sensitive method for comparing the quantification of mRNA levels and gene expression patterns in sample populations. This study employed the two-step SYBR green I RT-PCR protocol to quantify mRNA expression of numerous target genes in 'real time' RTqPCR assays. The general principal of PCR involved the amplification of DNA at the end of the reaction, where as RTqPCR amplified DNA as the reaction progresses in real time. The primer sequences, experimental conditions, design and techniques detailed below had previously been validated (Yanni *et al*., 2010).

2.6.1 mRNA isolation and generation of Cdna

Briefly, frozen LV and kidney samples were cut into 10 µm sections using a cryostat, making sure the samples did not thaw. The work bench was cleaned with Rnase Zap to ensure surface was RNA free. Total RNA was isolated from sections using Qiagen muscle RNA extraction procedure and manufacturer's instructions (Qiagen, Hilden, Germany). Briefly, 10 µl of β-mercaptoethanol was added to 1 ml of 'RLT' buffer provided. A stock of carrier RNA was prepared by dissolving 310 µg of carrier RNA in 1 ml Rnase free water. A working solution of 4 ng/µl was made up by adding 5 µl of stock carrier RNA to 34 µl of RLT followed by addition of 6 µl of this dilution to 54 µl of RLT. The RDD/DNase I solution for each sample was prepared by addition of 70 µl of RDD to 10 µl of DNase I. The samples were homogenised using a polytron and 155 µl of RNA/RLT/B-ME mix was added to each sample. This step brought the samples to room temperature and prevented guanidinium salt from gelling on the frozen sections and inhibititing RNAase. A volume of 5 µl of proteinase K was then added to digest proteins in the tissue. Next, the samples were centrifuged at 13000 rpm for 5 minutes

and supernatant dissolved in β-mercaptoethanol-'RLT' mix and vortexed. This step was a modification which increased salt concentration in the homogenate, producing more reliable yields. After addition of 100% ethanol and vortexing, the samples were applied to the Qiagen-provided columns in aliquots, centrifuged for 15 seconds at 13000 rpm for after each aliquot and flow through discarded. DNAse was then diluted in the provided buffer, added to the columns and left for one hour at room temperature to digest. After 3 rounds of centrifugation and addition of 'RW' buffer, the column was dried and eluted by spinning down. A second elution gave a final volume of approximately 90 µl that was left to precipitate overnight at -20˚C. After 30 minutes of spinning in the cold at 13000 rpm, the resulting RNA was ethanol precipitated and pellets were dissolved in 10 µl, RNAse free water. Thereafter, the concentration and purity of RNA samples was measured at A260 and the ratio of absorbance at 260 and 280 nm with a Nanodrop ND-1000 spectrophotometer (Nanodrop Techologies, USA).

The isolated RNA (and resulting cDNA) samples were not pooled and kept separately. A total of 125 ng total RNA from each sample was reverse transcribed with Superscript III reverse transcriptase (Invitrogen, 18080-044) in a 20 µl reaction according to the manufacturer's instructions. Using random hexamer priming to each 8 µl of RNA a 2 µl solution consisting of Hexamers/deoxyribonucleotide triphosphate (dNTP) in buffer containing manufacturer provided RT buffer mix (25 mM $MgCl_2$, 0.1M DTT, RNase OUT and Superscript III reverse transcriptase). The tubes were then heated to 65°C for 10 min and transferred onto ice immediately for 3 minutes to denature the RNA. A volume of 10 µl of the RT/buffer master mix was added while samples were on ice. Samples were then incubated at 25°C for 10 min in the PCR machine, for first priming, 50°C for 50 min, for further synthesis and 85°C for 15 min, to stop the reaction.

Aliquots of neat cDNA were diluted (2 µl into 18 µl H_2O) giving a 1:10 ratio for direct use in qPCR.

2.6.2 Quantitative PCR

RTqPCR was achieved using an ABI Prism 7900 HT Sequence Detection System (Applied Biosystems, Foster, USA). The size of qPCR products and specificity of primers were tested in the laboratory previously by running samples on 2 % agarose gels containing ethidium bromide and visualised by UV light. For this study commercially available primers (Table 2.1) were utilized which gave amplicons of similar size. The reaction mixture consisted of 1 µl of cDNA, 1x Qiagen assay, 1x SYBR Green Master Mix (Applied Biosystems, 4367659) and the final volume of 10 µl was made up with DNAse-free water. All samples were run in triplicate for significance. The reaction conditions were: denaturation step of 95°C for 10 min, 40 cycles of amplification and quantification steps of 95°C for 30 s, 60°C for 30 s and 72°C for 1 min. The melt curve conditions were: 95°C for 15 s, 60°C for 15 s and 95°C for 15 s. PCR assay validity was assessed by examining RNA amplification data represented in figure 2.1A showing a melting curve obtained post PCR reaction and figure 2.1B showing a dissociation curve examined to eliminate Primer-dimers or other contaminants.

Table 2.1: Commercially available primers used in the study

Target transcript	**Species**	**Qiagen catalogue number**
ANP	Rat	QT00366170
BNP	Rat	QT00183225
$Ca_V1.2$	Rat	QT01571822
$Ca_V1.3$	Rat	QT00194306
Calm2	Rat	QT01169840
Camk2d	Rat	QT01708595
CTGF	Rat	QT00182021
Collagen type 1	Rat	QT01621417
Elastin	Rat	QT01575924
Fibronectin 1	Rat	QT00179333
GAPDH	Rat	QT00199633
Integrin alpha 1	Rat	QT00193172
Integrin alpha 5	Rat	QT00431053
Integrin beta 1 (fibronectin receptor beta)	Rat	QT00187656
Matrix metallopeptidase 2	Rat	QT00996254
Matrix metallopeptidase 9	Rat	QT00178290
NCX	Rat	QT01592451
Procollagen, type III, alpha 1	Rat	QT01083537
Pln_1 (phospholamban)	Rat	QT01290058
RyR2 (ryanodine receptor)	Rat	QT02348003
SERCA2a	Rat	QT01082508
Transforming growth factor β1	Rat	QT00190953
Vimentin	Rat	QT00178724
18SrRNA	Rat	QT00199374

Connexin 43 custom designed primer sequence:

Forward primer: 5’-GGAATGCAAGAGAGGTTGAAAG-3’

Reverse Primer: 5’-GGCATTTGGAGAAACTGGTAGA-3’

This primer was designed using Primer 3® software, Whitehead Institute for Biomedical Research, Cambridge, MA, USA.

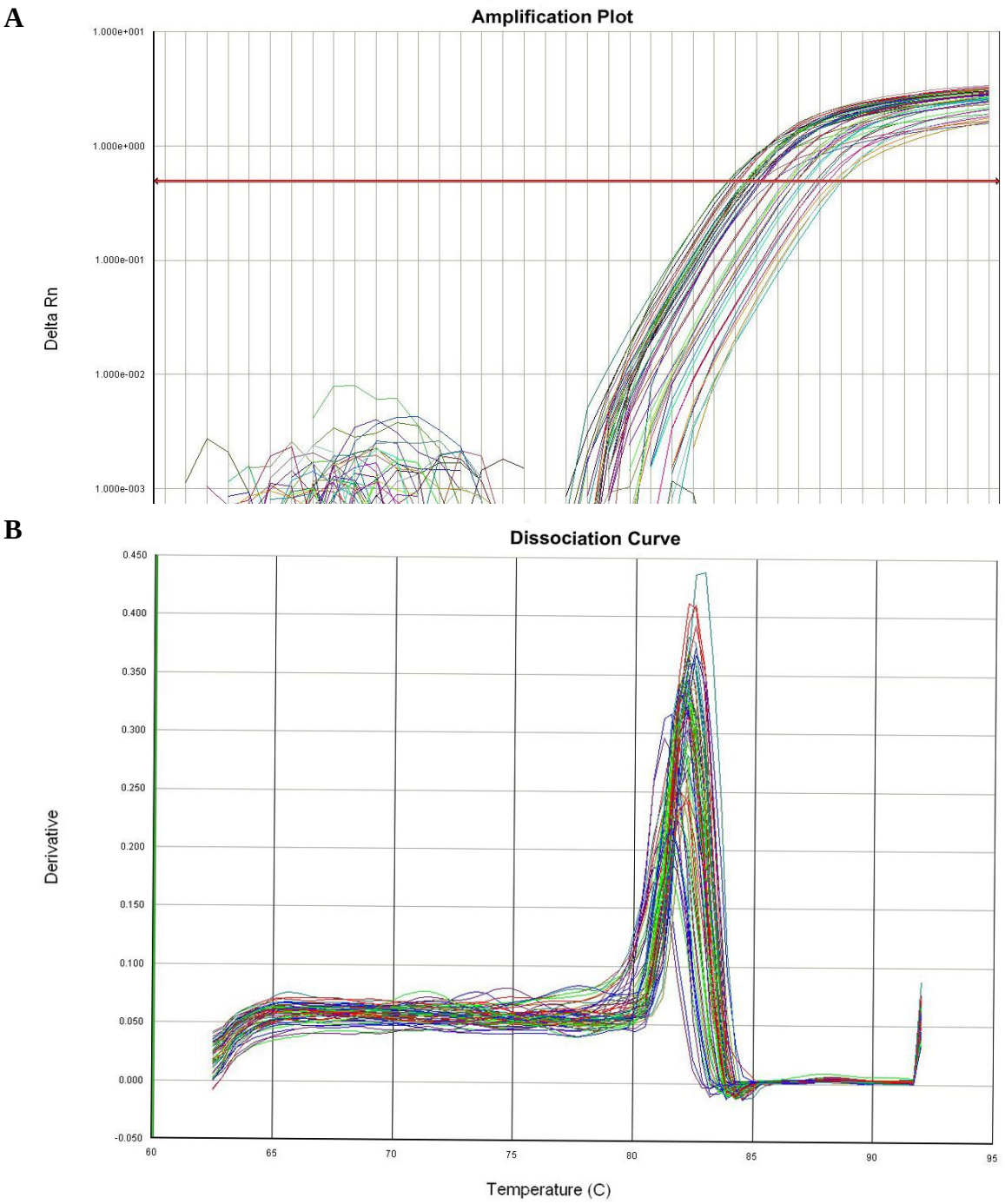

Figure 2.1: Representative validation plots of RTqPCR methodology. GAPDH RTqPCR amplification (A) and dissociation curve (B) used to validate experimental condition for each primer set (Rat GAPDH is shown in figure). Traces are typical of 5-6 different experiments.

2.6.3 Gene expression analyses

Gene expression was analysed using SDS 2.1.1 software (Applied Biosystems) by a double standardisation method known as the modified $2^{-\Delta\Delta Ct}$ method that adjusts for PCR efficiency differences (Skern *et al.*, 2005). This model calculated changes in gene expression by a comparison of the cycle threshold (Ct) values for the samples of interest with a control/calibrator sample. Thereafter, the Ct values of both the calibrator and the samples of interest were normalized to an appropriate endogenous housekeeping gene. GAPDH and 18S ribosomal RNA were analysed to determine the housekeeping gene whose amplification efficiency is equal to other PCR targets of this study. This was a requirement for the $2^{-\Delta\Delta Ct}$ calculation validity. GAPDH was chosen as the housekeeping gene in the present study. To analyse gene expression, for each run, ratios relative to the calibrator (reference standard sample) were determined based on the respective delta Cts and an average efficiency value was obtained. These ratios were then averaged over all three runs and related to the average content of GAPDH cDNA in each sample to correct for variations in input RNA. Expression levels were articulated as value of mRNA abundance relative to average GAPDH content.

2.7 Functional studies in the STZ-induced type 1 diabetic rat and GK study subgroups

Solutions and reagents for cell isolation:

1. Physiological salt solution (cell isolation solution): 130 mM NaCl (VWR, 102415-R), 1.8 mM $MgCl_2$ (VWR, 220933-M), 5.4 mM KCl (VWR, 1019842), 0.4 mM NaH_2PO_4 (102494-C), 5 mM, 4-(2-hydroxyethyl)-1-piperazineethanesulfonic acid (HEPES) (Sigma, C-0780); 10 mM creatine (Sigma,C-0780), 10 mM glucose and 20 mM, taurine (Sigma, T-0625) set to pH 7.3 by using 4 M NaOH (16g NaOH/100ml Milli-Q) (VWR, 10252).

2. Normal Tyrode solution (Cell perfusion solution): 140 mM NaCl; 5 mM KCl; 1 mM $MgCl_2.6H_2O$ (VWR, 10194-V), 10 mM glucose; 5 mM HEPES; 1mM $CaCl_2$ set to pH 7.4 by using 4 M NaOH (16g NaOH/100ml Milli-Q).

2.7.1 Ventricular myocyte isolation

Ventricular myocyte isolation was performed by utilising a combination of mechanical and enzymatic techniques, which have been previously described by Howarth *et al*., 2001 and Howarth *et al*., 2007 (see figure 2.1). Figure 2.2 shows the heart mounted on a cannula ready for perfusion. Briefly, the isolated hearts were immediately washed in 20 ml of isolation solution 'A' (0.75 mM Ca^{2+}) to remove excess blood and tissue. The weight of the hearts was recorded prior to perfusion. Hearts were perfused by the Langendorff method utilising solution A. Rate of perfusion was kept constant at 8 ml g^{-1} heart min^{-1} to allow for the differences in heart weight between the age-matched control and STZ-treated animals as well as the GK study subgroups. Once the preparation was stable with coronary vessels cleared of blood, the heart beat became rhythmic, this was a trigger point for the perfusion of nominally Ca^{2+} free isolation was switched to solution 'B' which contained Ethylene glycol tetraacetic acid (0.01 mM) for 4 minutes. This was an essential step to remove the Ca^{2+} from the heart in order to break down intercalating discs to stop the heart in a diastole state. The heart was then perfused with an enzyme salt solution 'C' which contained 0.05 mmol/L Ca^{2+}, 0.75 mg/mL collagenase (type 1; Worthington Biochemical Corp., Lakewood, NJ, USA) and 0.075 mg/ml protease (type X1V; Sigma Taufkirchen, Germany). The purpose of this solution was to breakdown the collagen fibers holding the cells together. Solution C was recirculated and the total enzyme perfusion time was 6 minutes. The perfusion was carried out at 37˚C and solutions were gassed with 100% medical oxygen. Following perfusion with the enzyme, the heart was removed from the perfusion apparatus and the

ventricles were excised, minced and gently agitated at 300 oscillations/min in a 5 ml collagenase solution supplemented with 1% Bovine Serum Albumin (BSA) for 4 minutes. Cells were than filtered through gauze (300 μm aperture, Cadish precision meshes, London) and suspended in 10 ml of isolation solution A. The cell filtrate was centrifuged at 400 rpm for 1 minute, and the supernatant was removed. The resulting cell pellet was resuspended in physiological salt solution containing 0.75 mM Ca^{2+}. The process was repeated 4 times and ventricular isolates from the 2^{nd}, 3^{rd} and 4^{th} repetition were stored at 4°C prior to use (not exceeding 1-2 hours). Experiments were performed during a period of 1-6 hours after isolation.

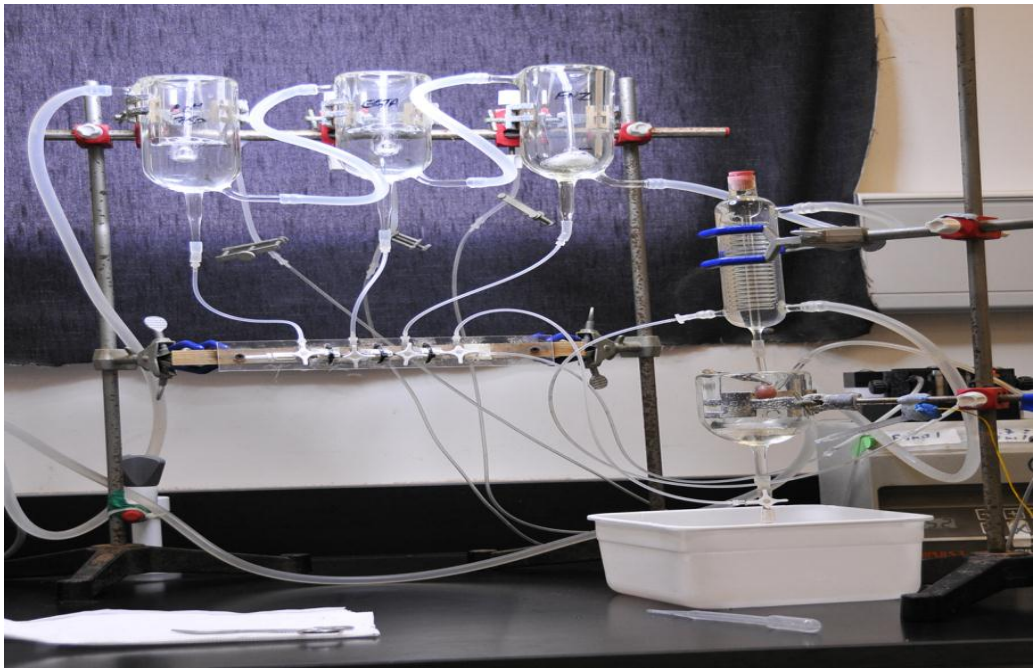

Figure 2.2: A photograph showing isolation apparatus for ventricular myocyte isolation. Photograph was taken in United Arab Emirates University laboratory.

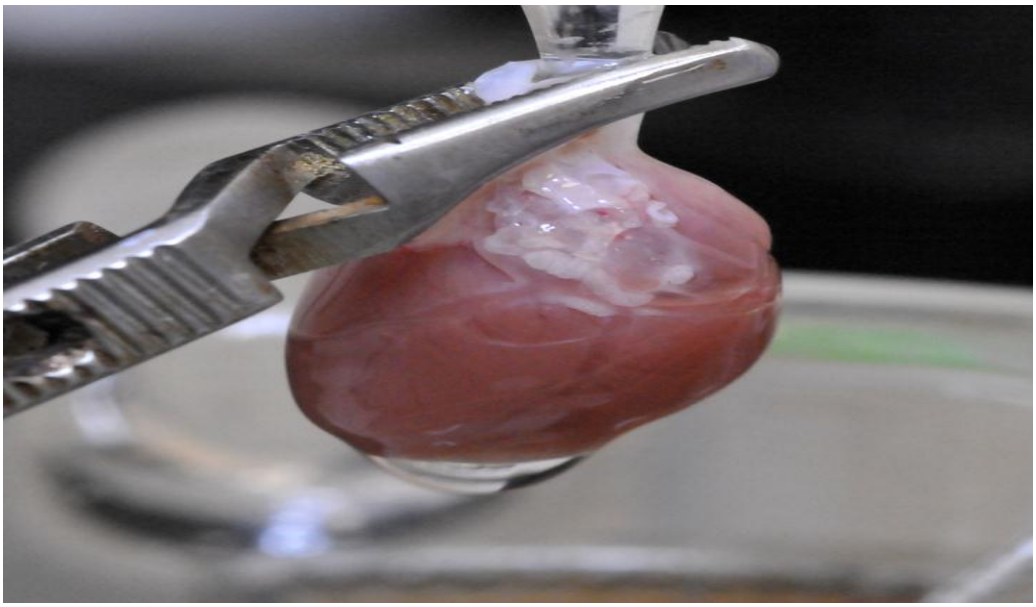

Figure 2.3: A photograph showing an isolated rat heart on the cannula of Langendorff apparatus. Photograph was taken in United Arab Emirates University laboratory.

2.7.2 Measurement of shortening in ventricular myocytes

Freshly isolated ventricular myocytes were allowed to settle on the glass bottom of a Perspex chamber mounted on the stage of an inverted microscope (Axiovert 35, Zeiss, Gottingen, Germany) with a 40X objective lens. Myocytes were superfused at 3-5 ml/min with a HEPES-based tyrode solution maintained at 35-37°C using a micro pump and a heating system coupled to a temperature controller (Luiggs & Neumann, Germany). Myocytes were field stimulated at 1 Hz (S88 stimulator, Grass-Telefactor, USA) using 2 platinum electrodes at 0.2 to 1 Hz positioned at either side of the chamber. Ventricular myocyte shortening was measured using a video edge detection system (VED-114, Crystal Biotech, Northborough, MA, USA) and data were acquired and analysed using SignalAverager (version 6.37, Cambridge Electronic Design, Cambridge, UK). Resting cell length (RCL), time to peak shortening (TPK), time from peak shortening to half-relaxation (THALF) and amplitude of shortening (expressed as % of resting cell length) were recorded.

2.7.3 Measurement of intracellular calcium transients $[Ca^{2+}]_i$

To measure $[Ca^{2+}]_i$ transients, previously described methods by Howarth *et al* (2007) were employed. Briefly, ventricular myocytes were firstly loaded with a fluorescent indicator fura-2-AM (F-1221, Molecular probes, The Netherlands) by addition of a volume of 6.25 µl of a 1.0 mM stock of fura-2-AM dissolved in dimethylsulfoxide (DMSO) to a 2.5 ml normal Tyrode solution containing fresh myocytes to give a final fura-2-AM solution of 2.5 µmol/l. Myocytes were gently agitated for 10 min at room temperature and then centrifuged at 400 rpm for 1 minute. After centrifuging, the solution containing myocytes was resuspended in normal tyrode solution to remove excess fura-2-AM and incubated for 30 min to ensure complete hydrolysis of the

intracellular ester. Intracellular $[Ca^{2+}]_i$ transients were measured by alternately exposing the myocytes to light at 340 and 380 nm using a monochromator (Cairn Research, Faversham, UK). The fluorescence emission at 510 nm was recorded by a photomultiplier tube and the ratio of emission at the 2 excitation wavelengths (340/380 ratio) to provide an index of $[Ca^{2+}]_i$ concentration. Resting fura-2 ratio, TPK of Ca^{2+}transient, THALF decay of the Ca^{2+} transient and the amplitude of the Ca^{2+} transient were recorded. Data were collected and analysed using SignalAverager (version 6.37, Cambridge Electronic Design, Cambridge, UK).

2.8 Transforming growth factor β1 immunoassay

Protein extraction

LV and kidney samples from 6 STZ-induced type 1 diabetic rats and aged matched Wistar control rats at 2 and 4 months and 6 LV and Kidney samples from each GK subgroups at 8 month old were weighed and homogenised in buffer recommended by ELIZA kit manufacturers. Sample homogenate was sonicated and centrifuged at 14,000 g for 1 minute at 4˚C. The supernatant was collected and aliquotted into tubes and further assayed for protein concentration or stored at -80˚C. Homogenisation buffer consisted of 0.5% Triton X-100, 2 µg/ml Aprotinin (Sigma Aldrich, A6013) in PBS, 137 mmol/L NaCl, 2.7 mmol/L KCl, 10mmol/L Na_2HPO_4, 1.76 mmol/L KH_2PO_4 at pH 7.4.

Modified Lowry protein assay

Protein concentration in tissue homogenates of LV and kidneys were assayed employing the modified Lowry method previously described (Lowry *et al*., 1951). Briefly, protein in BSA standards (0, 1, 2, 5, 10 and 20, diluted from a 20 mg/ml stock BSA) or samples was reacted with 1% cupric sulfate ($CuSO_4$) and 2% Sodium

potassium tartate in 1 N NaOH and 2% Na_2CO_3 (solution 1) resulting in the formation of a tetradentate copper-protein complex. This was further reduced to a 2 N Folin-Ciocalteu Reagent mixed with distilled water in a 1:1 ratio (solution 2). The final reaction mix contained 0.5 ml of distilled water, 5 µl of sample or BSA, 2 ml of solution 1 and 0.2 ml of solution 2 in a culture tube at room temperature for 20-30 minutes. Protein containing tubes changed colour to a blue water-soluble product. Thereafter, 200 µl of from each tube was transferred to a 96 well clear plate and absorbance was measured at 660 nm with a microplate reader (Micro Quant, Biotech Instruments). The linearity range for protein detection was given as 1-1,500 µg/ml.

Total and active Transforming growth factor β_1 detection by Enzyme-Linked ImmunoSorbant Assay (ELIZA)

The TGFβ_1 E_{max} Immunoassay system (Promega, Madison, WI) is a sandwich ELIZA designed for the sensitive and specific detection of biologically active and/or total TGFβ_1 in an antibody sandwich format with ≤ 3% cross reactivity with other TGFβ_1 isoforms (TGF$\beta_{2/3}$). Detection of endogenous TGFβ_1 in plasma, LV and kidney homogenates (extracted as mentioned above) from age-matched control and STZ-induced and GK subgroups was achieved using manufacturer's protocol.

Briefly, a Nunc MaxiSorp™ 96 well flat-bottom plate (Thermo Scientific, 439454) was coated with TGFβ_1 monoclonal antibody in freshly prepared coating buffer (0.025 M sodium bicarbonate, 0.025 M sodium carbonate, pH 9.7) at 1:1000 and incubated overnight at 4˚C. TGFβ_1 block buffer was prepared by adding stock TGFβ_1 Block 5X buffer (manufacturer supplied) and incubated at 35˚C for 35 minutes without shaking in order to block nonspecific binding. Plates were then washed once with Tris buffered saline-tween (20 mM Tris-HCl (pH 7.6) 150 mM NaCl and 0.05% Tween 20). Thereafter, all washes were performed with this buffer. TGFβ_1 standard curve was

prepared in duplicate by accurately diluting the manufacturer supplied TGFβ$_1$ standard 1:1000 in TGFβ$_1$ Sample 1X buffer (manufacturer supplied) to achieve a concentration of 1000 pg/ml. A standard curve were prepared from 0-1000 pg/ml (0, 15.6, 31, 62, 125, 250, 250, 500, 1000 pg/ml) and data shown in figure 2.3.

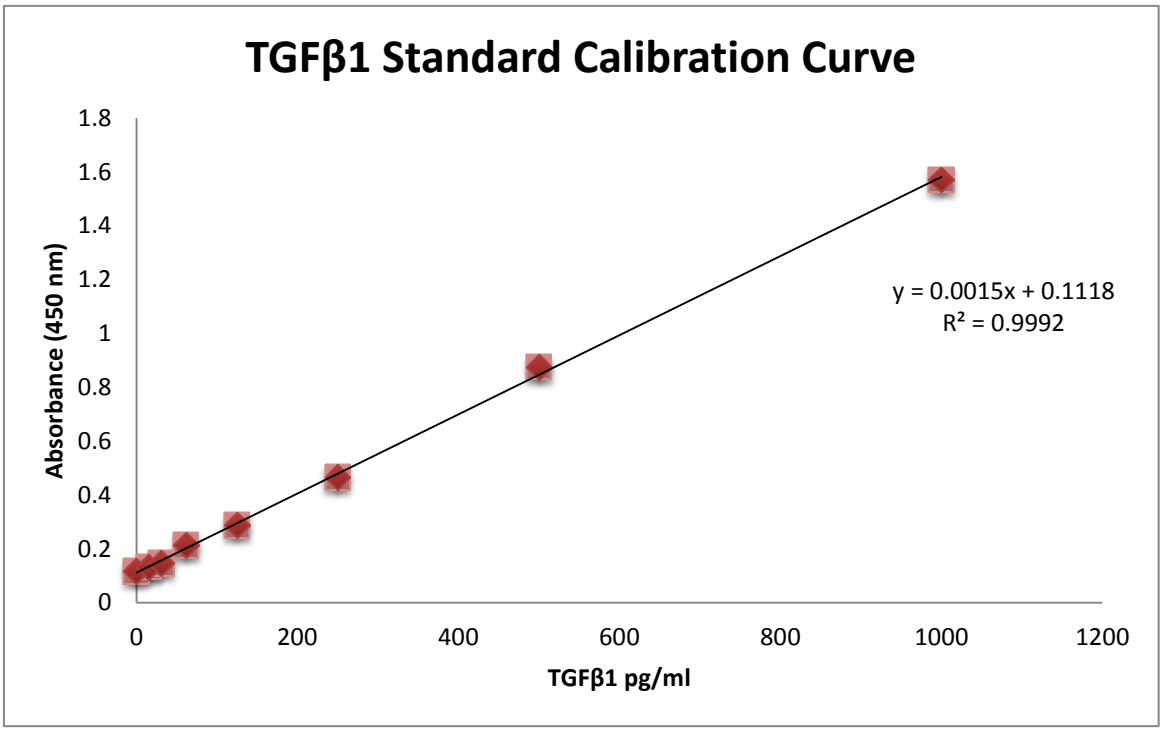

Figure 2.3: A typical TGFβ$_1$ standard calibration curve.

Sample preparation was achieved by dividing plasma, LV and kidney homogenates in 2 equal fractions to assay for total *and* active TGFβ$_1$. One fraction was acid-treated in order to activate total TGFβ$_1$ as described in the manufacturer's protocol. Briefly, either plasma or tissue homogenates were diluted in 1:5 in Dulbecco's PBS (in grams (g): 0.2 KCL, 8.0 NaCl, 0.2 KH_2PO_4, 1.15 Na_2HPO_4, 0.1 $MgCl_2 \cdot 6H_2O$ and 0.13 $CaCl_2 \cdot 2H_2O$) and acidified to pH below 3.0 by adding 1 N HCl/50 µl of sample and incubated at room temperature for 15 minutes. Following incubation, samples were neutralized to pH 7.6 by addition of 1 N NaOH/50 µl of sample. These amounts varied for plasma samples as they contained much more carrier protein than tissue homogenates. Hence, the fraction of samples with acid treatment represented total TGFβ$_1$ in sample whereas

samples without acid treatment represented the biologically active TGFβ_1 in the sample. In accordance with the protocol, a volume of 100 µl of either acid treated or naturally processed samples were added to the coated plate and incubated for 90 minutes at room temperature with shaking (500±100 rpm). For post incubation, plate was washed with wash buffer 5 times by filling each well with the wash buffer. Flicking out the contents and tapping the plate 3 times on a paper towel. Samples were diluted in Sample Buffer prepared according to manufacturer protocol and optimal concentrations were achieved by testing a series of dilutions. LV and kidney homogenates were diluted 1:2 and plasma samples were diluted 1:25. After washing, the specifically bound polyclonal antibody was detected by diluting 10 µl stock Anti- TGFβ_1 pAb in 10 ml of Sample 1X Buffer (1:1000) and 100 µl of this was pipetted in each well using a multichannel pipettor and incubated for 2 hours at room temperature whilst shaking (500±100 rpm). Subsequently, the plate was washed 5 times as previously described and TGFβ_1 HRP conjugate was added at a dilution of 1:100 with Sample 1X Buffer and incubated for 2 hours at room temperature with shaking (500±100 rpm). Unbound conjugate was subsequently removed by washing 5 times and subsequently, samples were incubated with 100 µl of TMB One Solution (chromagen substrate) (manufacturer supplied) for 15 minutes at room temperature which produced a blue colour in the wells. The reaction was stopped using 100 µl of 1 N HCl which changed the colour to yellow. This colour change was measured at 450 nm using a microplate reader (Anthos Hill, Biochrome Ltd, UK). The colour change was proportional to the amount of TGFβ_1 in the samples. The samples were analysed in duplicate and the results were obtained by extrapolation from the TGFβ_1 standard curve and expressed as ratio of Active:Total TGFβ_1 for plasma samples and pg/mg of total protein for LV and kidney homogenates.

2.9 Statistical analysis

Quantitative data acquired from these experiments were statistically analysed. Using different statistical tests, data plotted as graphs were expressed as mean±SEM of 3 or more experiments. The statistical significance of differences between age-matched control and STZ-induced diabetic data as well as the GK study data were compared by Independent samples Student's *t*-test using IBM SPSS statistics 22 software (SPSS Inc., Chicago, IL, USA). Unless stated otherwise, statistical comparisons were performed using one-way ANOVA followed by Bonferroni corrected t-tests for multiple comparisons. A value of $p<0.05$ was taken as statistically significant and values <0.01 were taken as highly significant and these have been illustrated in text. Lines over bars indicate significance. Statistical analysis was performed on 3 or more different animals where n= the number of control or diabetic rats.

CHAPTER 3

ASSESSMENT OF THE GENERAL CHARACTERISTICS, CARDIOMYOCYTE CONTRACTILE FUNCTION AND CALCIUM HOMEOSTASIS IN STZ-INDUCED TYPE 1 DIABETIC RAT

3.1 Abstract

Diabetes is a major disorder which can lead to numerous long term complications. If left untreated, patient with DM can develop complications such as HF and DCM. There is much evidence that the diabetes-induced HG can alter cellular Ca^{2+} homeostasis and subsequently contraction. This chapter investigated the role of HG in diabetic heart disease with emphasis on cardiomyocyte contractile function and employed Wistar rats which were rendered diabetic by a single intraperitoneal injection (i.p.) with 60 mg/kg body weight of STZ dissolved in citrate buffer while the control animals received an equivalent volume of citrate buffer alone. Following 2 and 4 months of the development of T1DM, animals were humanely killed and hearts were perfused with the Langendorff perfusion method. Video edge detection system and micro-spectrofluorimetry were utilised in order to measure contraction and Ca^{2+} transients respectively, in electrically stimulated ventricular myocytes at 2 and 4 months post STZ-induction compared to age –matched control animals. The general characteristics of animals revealed that STZ-induced diabetic rats weighed significantly (p<0.01) less than their age-matched controls and this reduction in weight was more with increasing age at 2 and 4 months post STZ-treatment. Heart weights were also significantly lower and there was an increase in the HW/BW ratio. A significant elevation in plasma blood glucose levels was observed in diabetic animals after 2 months and 4 months of treatment. Moreover, cell viability measured by the percentage (%) of viable myocytes was significantly (P<0.01) decreased at 2 months and at 4 months STZ-treated hearts compared to age-matched controls. Time-dependent effects of STZ-induced diabetes after 2 and 4 months of treatment revealed significant increases in RCL and reductions in TPK relaxation, exhibiting prolonged relaxation times in 2 and 4 months duration of STZ-induced DM compared to age-matched controls. Conversely, alterations in Ca^{2+} homeostasis manifested as prolonged TPK and rate of decay of Ca^{2+} transient at 2 and 4 months post STZ-induction compared to control. Moreover, these alterations were more severe with age highlighting the severity of ageing in T1DM. Altogether, these results have indicated that T1DM can result in the development of cardiac disease that is characterised by alterations in contractility and Ca^{2+} homeostasis in ventricular cardiomyocytes.

3.2 Introduction

During the last decade, accumulating evidence has been presented revealing that altered calcium homeostasis is of significant relevance for the pathophysiology of myocardial dysfunction and HF. Various mechanisms have been postulated as a result of many clinical and experimental studies and many outcomes have been identified from reduced Ca^{2+} transients and altered intracellular calcium cycling, reduced amplitude of Ca^{2+} transients with reduced systolic calcium concentrations and increased diastolic calcium levels in isolated myocytes, together with decreased rates of SR calcium uptake in the failing human heart in type 1 DM (Bracken *et al*., 2003; Howarth and Singh, 1999; Qureshi et al., 2001; Singh *et al*., 2003; Pandit et al., 2003). Abnormal $[Ca^{2+}]_i$ homeostasis has also been implicated in DCM and may precede clinical manifestation. Studies in cardiomyocytes have shown that diabetes results in impaired $[Ca^{2+}]_i$ homeostasis due to altered SERCA and NCX activity (Sheikh *et al*., 2012).

This study employed the use of cardiomyocytes to investigate contraction and $[Ca^{2+}]_i$ homeostasis is very useful and as such the STZ-induced T1DM rat has been widely used as a model of DCM. Belke and colleagues investigated contractile performance and Ca^{2+} transients in Langendorff-perfused hearts and isolated cardiac myocytes (Belke *et al*., 2004). The study demonstrated that diabetic mouse hearts presented with decreased rates of contraction, relaxation, and pressure development along with Ca^{2+} transients significantly lower diastolic and systolic levels of calcium in myocytes from diabetic hearts. However, extensive discrepancy exists in previously published literature regarding contractile dysfunction in T1DM. Isolated cardiomyocytes from STZ-induced diabetic hearts have been reported to have either increased (Howarth et al., 2007, 2001), depressed/unaltered (Yu *et al*., 1994; Ren & Davidoff, 1997; Tamada *et al*., 1998; Choi *et al*., 2002) contractile kinetics. Similarly, much variation exists in results from $[Ca^{2+}]_i$ homeostasis studies as resting Ca^{2+} has been shown to be either increased (Yaras *et a*l., 2005), decreased (Hayashi & Noda, 1997; Howarth *et al*., 2005; Howarth and Qureshi, 2006), or unaltered (Howarth *et al*., 2002; Howarth *et al*., 2004). Nevertheless, these variations in results may be due to different experimental conditions, frequency of stimulation and/or voltage times (Zhang *et al*., 2008) the ageing process or the duration of diabetes.

This study was specifically designed to investigate the duration of STZ-induced DM, employing two time points, namely 2 and 4 months to identify the contribution of

diabetes-induced HG towards contractile characteristics and cellular calcium homeostasis in isolated cardiomyocytes compared to age-matched controls.

3.3 Methods

Methods are described in Chapter 2.

3.4 Results

1. General characteristics of the experimental model

General characteristics of the STZ-treated rats and age-matched Wistar control are shown in Table 3.1 from post STZ treatment, it was observed that STZ-induced diabetic rats weighed significantly (p<0.01) less than their age-matched controls and this reduction in weight is more with increasing age (270±5.78** *vs.* 343±9.99) at 2 months and (221±13.02***vs.* 378±10.63) at 4 months post STZ-treatment. Similarly, heart weights were also significantly lower along with an increase in the HW/BW ratio at 2 and 4 months. Plasma blood glucose levels were significantly elevated in diabetic animals after 2 months (443±12.2** *vs.* 98±3.79) and 4 months (446±18.8** *vs.* 97±3.04) of treatment (p<0.01). Cell viability measured by the percentage (%) of viable myocytes was significantly decreased (P<0.01) at 2 months (46.2±7.5% *vs.* 69.0±5.8%) and at 4 months (29.5±1.2% *vs.* 51.4±3.5%) STZ-treated hearts compared to age-matched controls. These data are in accordance with previously published glucometry values (Singh *et al*., 2006; D'Souza *et al*., 2011; Howarth *et al*., 2007; Bracken *et al*., 2003).

Animals	Fasting Blood Glucose (mg/dl)	BW (g)	HW (g)	HW/BW ratio (g/100g body weight)	Cell Viability (% rod cells)
Control (n=6) 2 months	98±3.79	343±9.99	1.15±0.22	0.33±0.02	69.0 ±5.8
Diabetic (n=6) 2 months	443±12.2**	270±5.78**	0.98±0.30*	0.36±0.05*	46.2 ±7.5**
Control (n=9) 4 months	97±3.04	378±10.63	1.18±0.30	0.31±0.03	51.4±3.5
Diabetic (n=9) 4 months	446±18.8**	221±13.02**	0.94±0.33*	0.42±0.02*	29.5±1.2**

Table 3.1: **Heart- General characteristics of rats at 2 and 4 months post STZ-administration**. All data were obtained prior to the end of the treatment period. Data are given as Mean ±S.E.M, *$p<0.05$ **$p<0.01$, unpaired Student's t-test. Numbers in bracket indicate number of animals used for experiments.

2. Time-dependent effects of STZ-induced diabetes on the kinetics of contraction in ventricular myocytes isolated from rat heart

Figure 3.1A represents typical traces of cell contraction observed at 2 and 4 months in control and STZ-treated ventricular myocytes stimulated at 1 Hz and figure 3.1B depicts fast time-base recordings of unloaded shortening in STZ-treated and age matched control ventricular myocytes. Figure 3.2 describes the time-dependent effects of STZ-induced diabetes and age matched control after 2 and 4 months of treatment on amplitude of shortening (expressed as % of RCL), resting cell length (RCL), time to half relaxation shortening (THALF) and time to peak relaxation shortening (TPK) in electrically stimulated ventricular myocytes at 1 Hz. The results indicate that a significant ($p<0.05$) increase was seen in RCL (Figure 3.2A) from control 2 months to control 4 months (125.8±2.68 *vs.* 136.3±3.42*) and a significant ($p<0.01$) decrease was seen in STZ-induced diabetic ventricular myocytes at 4 months of treatment time compared to aged matched controls, (120±2.97** *vs.* 136.3±3.42). A significant ($p<0.05$) reduction was seen in TPK relaxation shortening (Figure 3.2B) from control 2 months to control 4 months of treatment time (116.6±3.12 *vs.* 100.8±2.63). Nevertheless, TPK relaxation shortening remained unchanged at 2 months of treatment time, however a significant ($p<0.01$) increase was seen in 4 months STZ-treated ventricular myocytes compared to age matched control, (100.8±2.63 *vs.* 134.6±5.10**). No significant differences were observed between the two groups and treatment times for THALF relaxation shortening (Figure 3.2C) and amplitude of shortening (Figure 3.2D). THALF relaxation shortening (Figure 3.2C) did show a reduction at 2 months and an increase at 4 months in STZ-induced diabetic ventricular myocytes compared to age matched controls, but this did not reach significance ($p<0.05$).

A

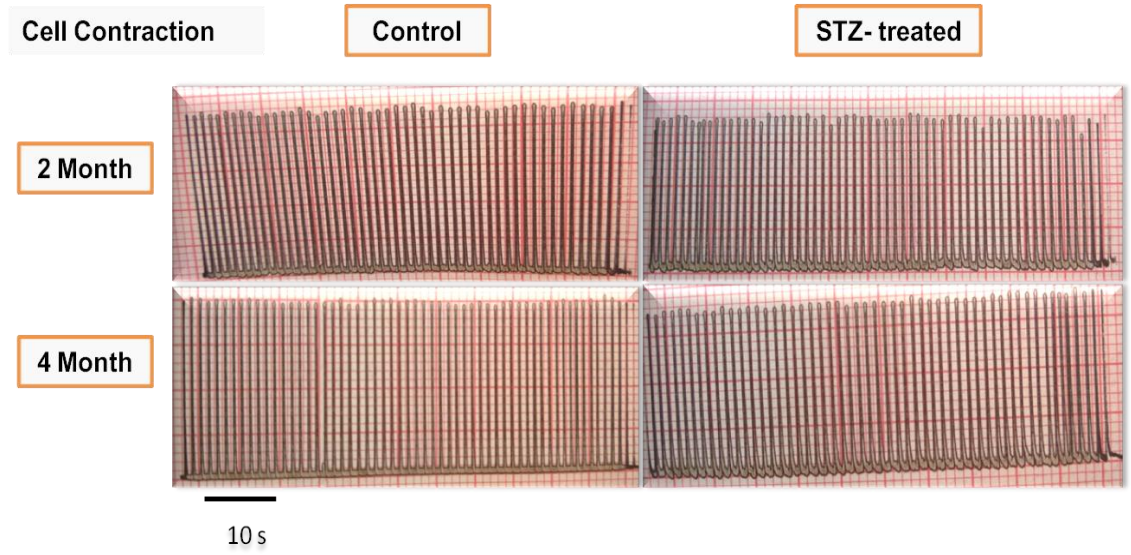

B

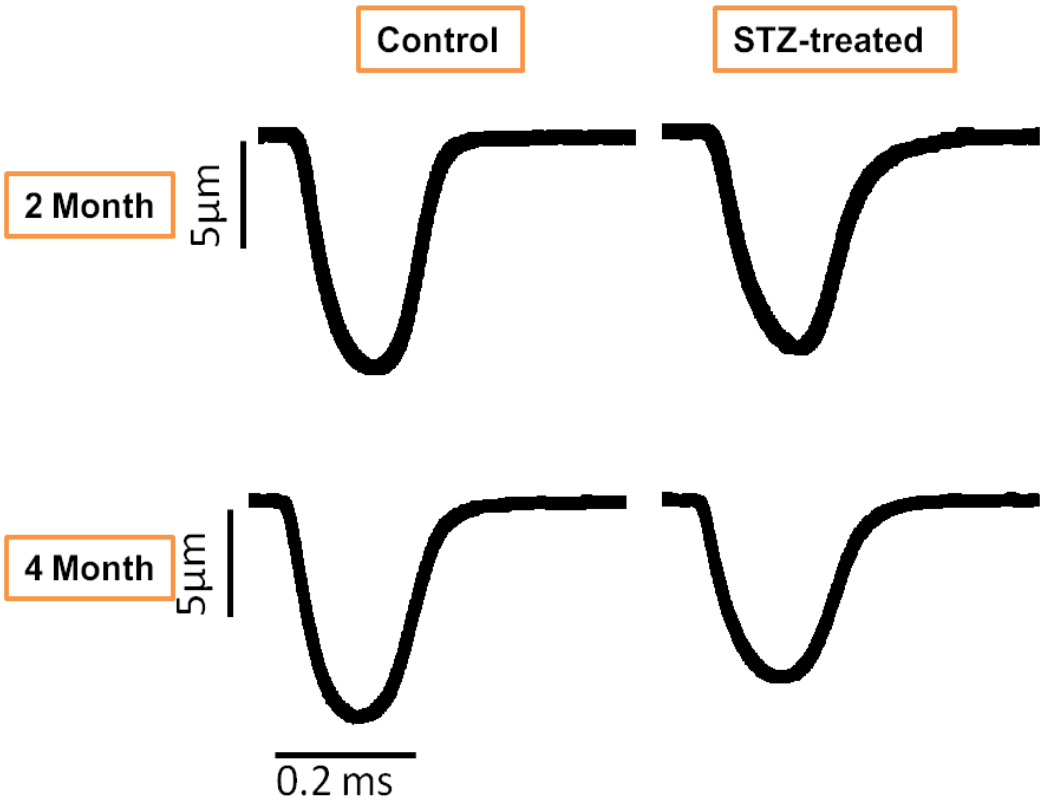

Figure 3.1: Ventricular cardiomyocyte contractility. Representative traces showing ventricular cardiomyocyte contraction at 2 and 4 month of STZ-induced diabetes **(A)** and representative fast time-base recordings of unloaded shortening in STZ-treated and age matched control ventricular myocytes **(B)**. Traces are typical of 35-50 myocytes from 3-4 rats.

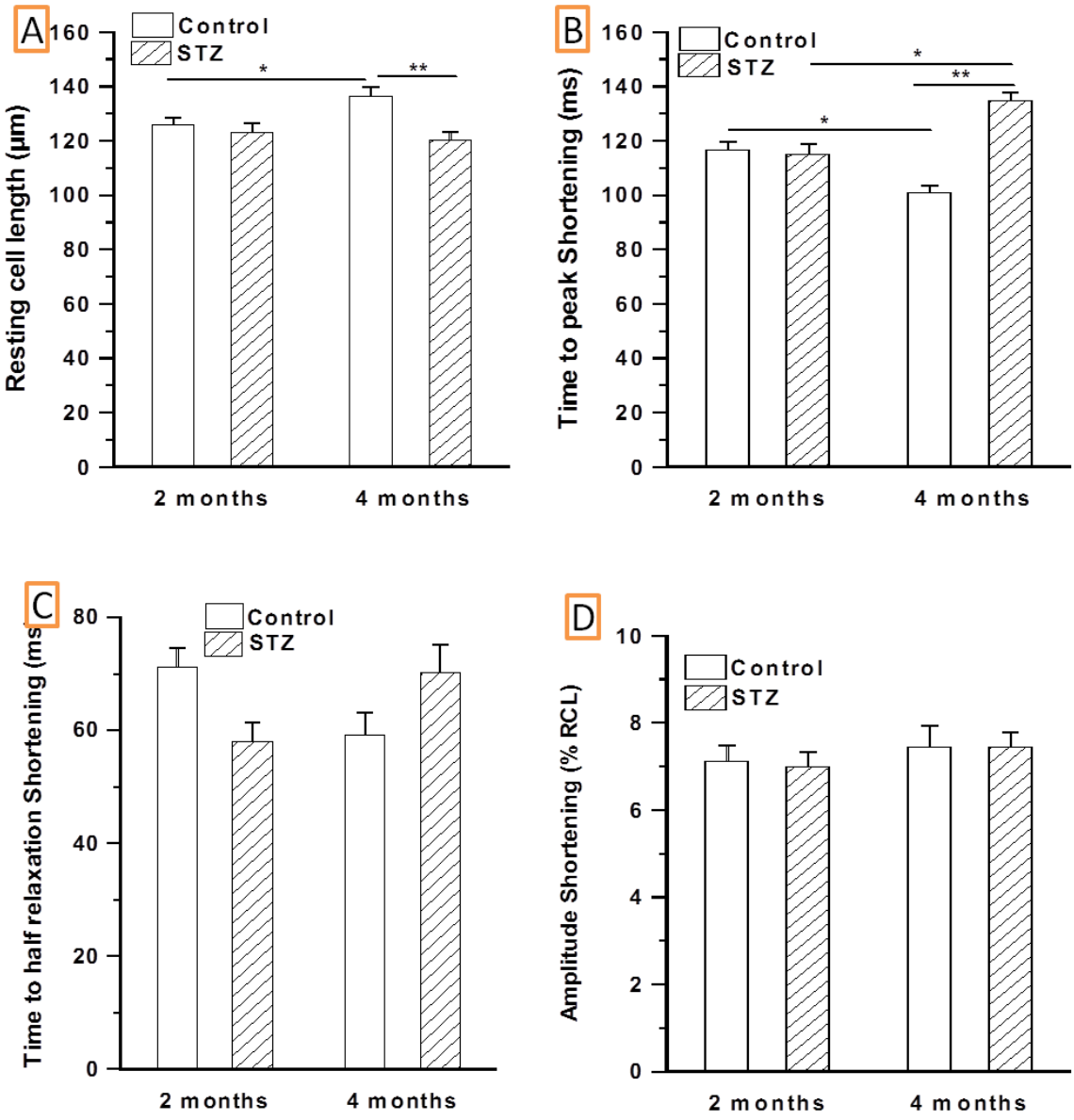

Figure 3.2: Contractility in ventricular cardiomyocytes. Time-dependent effects of STZ-induced diabetes and age matched control after 2 and 4 month of treatment on Resting cell length **(A)**, Time to peak relaxation shortening **(B)**, Time to half relaxation shortening **(C)** and Amplitude of shortening **(D)** in electrically stimulated myocytes at 1 Hz. perfused at 35-37^{o}C in a solution containing 1 mM Ca^{2+}. Data are Mean±S.E.M and is representative of 35-50 cells from 4-5 hearts. Lines over the bars indicate significance *P< 0.05, ** P< 0.01, One-way ANOVA followed by Bonferroni corrected t-tests for multiple comparisons.

3. Calcium homeostasis in ventricular myocytes

Figure 3.3 depicts representative fast time-base recordings of Ca^{2+} transients in ventricular myocytes at 2 and 4 months of control and STZ-treated rats. Figure 3.4 shows time-dependent effects of STZ-induced diabetes and age-matched control after 2 and 4 months of treatment on calcium homeostasis including resting fura-2, amplitude of Ca^{2+} transient, time to peak Ca^{2+} transient and rate of Ca^{2+} decay. The results indicate that there were no significant differences seen in resting fura-2 ratio (Figure 3.4A) and time to peak Ca^{2+} transient (Figure 3.4B) at 2 and 4 months of STZ-treatment compared to aged matched controls. However, a significant ($p< 0.01$) increase in THALF Ca^{2+} transient (Figure 3.4C) was seen at 2 months after STZ-treatment compared to age matched control (170.2±6.09** *vs.* 151.2±4.34) along with an increase at 4 months after STZ-treatment compared to age matched control (174.6±5.41** *vs.* 156.4±6.91). Amplitude of the Ca^{2+} transient (Figure 3.4D) was significantly ($p< 0.05$) higher between the two control groups, at 2 months control (0.30±0.01) and at 4 months control (0.44±0.02*). A similar trend was seen between the STZ-treatment groups, at 2 months (0.33±0.02) after STZ-treatment and at 4 months (0.39±0.03*) after STZ-treatment.

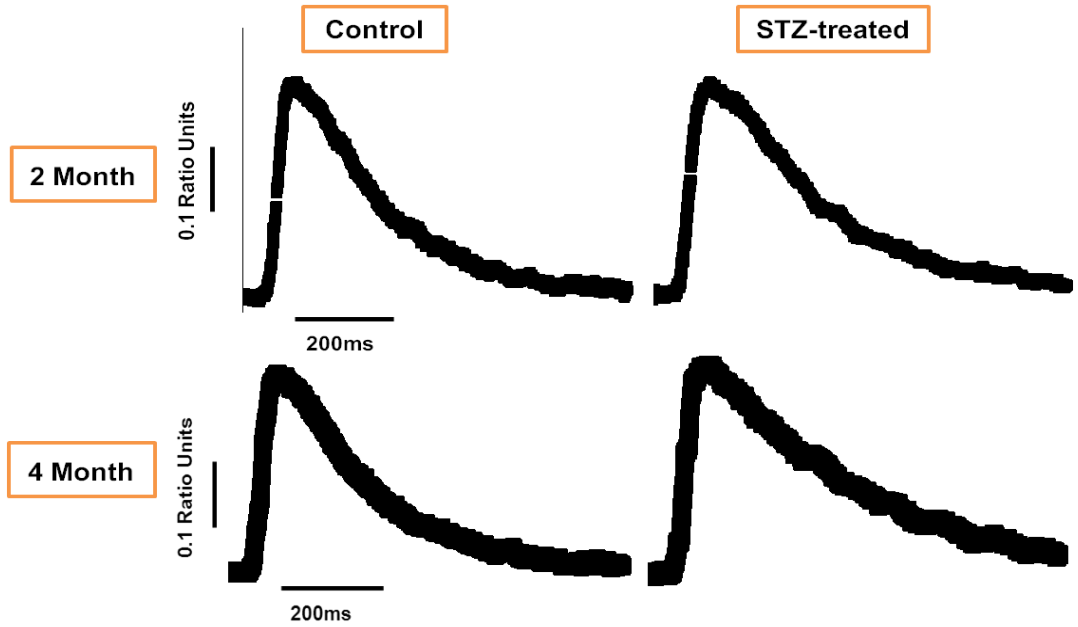

Figure 3.3: Cellular calcium changes. Fast time base recordings of representative Ca^{2+} transient in electrically stimulated (1 Hz) ventricular myocytes isolated at 2 and 4 months from age-matched control and STZ-induced diabetic rat hearts superfused with a solution containing 1 mM Ca^{2+} at 35–37 ^{o}C. Traces are typical of 35-50 myocytes obtained from hearts of 3-5 rats.

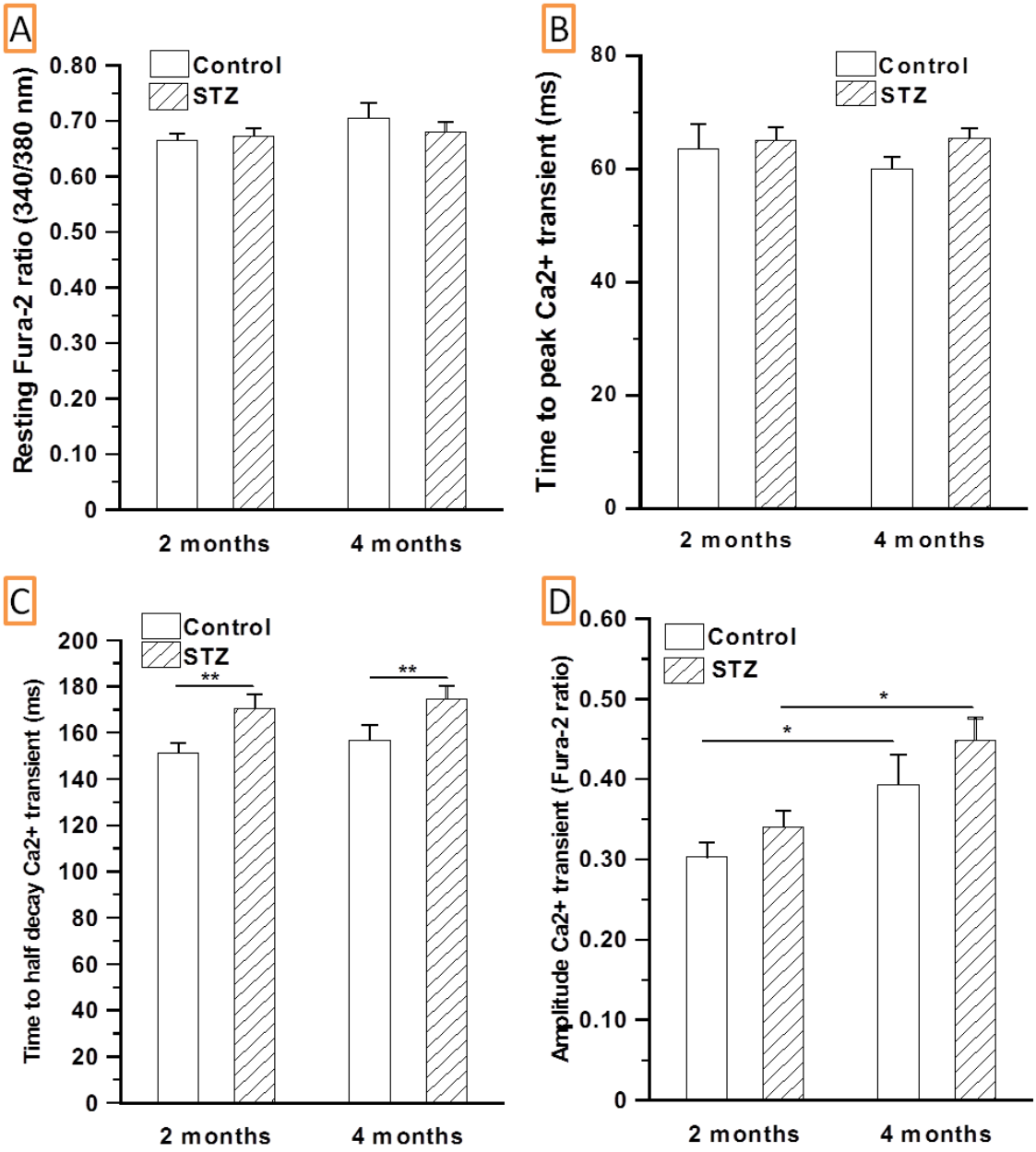

Figure 3.4: $[Ca^{2+}]_i$ transient kinetics in ventricular cardiomyocytes. Time-dependant effects of STZ-induced diabetes and age matched control after 2 and 4 month of treatment on Ca^{2+} homeostasis, Resting Fura-2 ratio **(A)**, Time to peak Ca^{2+} transient **(B)**, Time to half Ca^{2+} transient **(C)** and Amplitude of Ca^{2+} transient decay **(D)** in ventricular myocytes stimulated at 1 Hz and perfused with a solution containing 1 mM Ca^{2+} at 35-37^{o}C. Data are Mean±S.E.M and are representative of 35-50 cells from 4-5 hearts. Lines over the bars indicate significance *P< 0.05, **P< 0.01, One-way ANOVA followed by Bonferroni corrected t-tests for multiple comparisons.

3.5 Discussion

Summary of key findings:

1. STZ as a model of T1DM revealed marked differences in the general characteristics of the diabetic rats in comparison to age-matched controls.
2. Significant elevations in blood plasma glucose and reductions in body weight, heart weight, heart weight to body weight ratio and cell viability in STZ-induced diabetic rat hearts at 2 and 4 months compared to age-matched controls.
3. STZ-induced T1DM rat heart showed significant alterations in ventricular cardiomyocyte contractility, accompanied by disruption of the excitation contraction coupling process.
4. Significant alterations in $[Ca^{2+}]_i$ homeostasis manifested as prolonged time to peak and prolonged rate of decay in Ca^{2+} transients in diabetic cardiomyocytes compared to age-matched controls.
5. T1DM can result in the development of cardiac disease that is characterised by alterations in contractility and Ca^{2+} homeostasis in ventricular cardiomyocytes.

Diabetes is a major global disorder which can lead to numerous long term complications and if left untreated it can lead to DCM, one of the major complications of DM. The precise mechanism underlying DCM is not fully understood, but there is much evidence that the diabetes-induced HG can alter cellular Ca^{2+} homeostasis and subsequently contraction. The STZ-induced rat model was employed in this study to investigate DCM. A single dose of STZ (between 40 and 60 mg Kg^{-1}) administered to young adult rats is sufficient to initiate a stable model of T1DM (Szkudelaki, 2001). STZ disrupts and destroys pancreatic β-cells, leading to alterations in glucose and insulin (Szkudelaki, 2001). It has been reported that two hours, post injection of STZ, there is a fall in plasma insulin level leading to a rise in blood glucose. Normally, this should be followed by a transient decrease in blood glucose and concurrent elevation in levels of circulating insulin 6 hours later. Finally, blood chemistry stabilises to a state of hyperglycaemia and hypoinsulinaemia (West *et al.* 1996). Therefore, induction of diabetes results in a state of β-cell necrosis that is manifested by a temporary return of responsiveness, which appears to be followed by a permanent disruption and/or destruction of the β-cells. Following a short incubation of up to 3 days, STZ-induced rats present symptoms, which include severe hyperglycaemia, polyuria, polyphagia and

polydipsia. Within the next two weeks, the rats start to show symptoms of muscle wastage increased food consumption, decrease in muscle mass and after a number of weeks some rats appear to acquire a cataract like condition (a feature associated with T1DM) (Bracken *et al.* 2003).

Streptozotocin as a model of T1DM

A wide variety of animal models have been developed which closely approximate the clinical condition of DM. Rat models are used to provide enormously invaluable opportunities to study the mechanisms underlying the pathophysiology of DM in detail. This study employed the use of type 1, or most commonly known as STZ-induced diabetic model, to investigate the changes in their general characteristics (body weight, heart weight, heart weight to body weight ratio) and blood glucose in comparison to their age-matched controls. STZ is a diabetogenic agent which once administered, produces toxic effects which cause β cell necrosis of the pancreas and hyperglycemia and hypoinsulinaemia. Symptoms of diabetes are clearly seen in rats within 2-4 days following single intravenous or intraperitoneal injection of 60 mg/kg STZ (Ganda *et al.* 1976, Weiss. 1982, Elias *et al.* 1994, Arora *et al*. 2009). The results of this investigation have revealed marked differences in the characteristics of the diabetic rats in comparison to age-matched controls. Significant elevations in blood plasma glucose (Table 3.1) are seen which are consistent with previous studies employing STZ-treated rats (Singh *et al*., 2006; D'Souza *et al*., 2011; Howarth *et al*., 2007; Bracken *et al*., 2003). STZ-induced diabetic rats weighed significantly less than their age-matched controls and this reduction in weight was seen to be more with increasing age at 2 months and at 4 months post STZ-treatment which is in correlation with previous studies. Similarly, heart weights were also significantly lower along with a reduction in the HW/BW ratio at 2 and 4 months of treatment (Ren & Davidoff, 1997; Tamada *et al*., 1998; Singh *et al*., 2006; Howarth *et al*., 2007). The reason for the reduction in the weight of these animals are postulated to be due to the fact that STZ-induced rats undergo severe changes in body mass, muscle tone and eating/drinking habits and these changes are observed due to destruction of the β cells that produce Insulin. These changes lead to altered physiological properties in the body's infrastructure and most importantly changes in heart functioning (D'Souza *et al*., 2011; Howarth *et al*., 2007; Choi *et al*., 2002).

Dysfunction of the excitation contraction coupling process

This study has demonstrated defects in contractile function in ventricular myocytes from 2 and 4 months after STZ-induced T1DM which are congruent with previous clinical findings (Choi *et al*., 2002, Howarth *et al*., 2007; Ren & Davidoff, 1997). In order to discuss the results of the present study, it is of paramount importance to briefly explain the process by which contraction and relaxation of the heart is regulated.

The major function of the heart is to pump blood efficiently by virtue of an orchestrated contraction–relaxation cycle of the working cardiomyocytes. Contractility of these cardiomyocytes is regulated by a spatially defined programme of ion channels and exchangers that precisely control Ca^{2+} entry in and out of the cell and the SR. Regulation of contractility and hence, the control of Ca^{2+} release is principally achieved via the electrical activity of the sarcolemma. Depolarization of the cardiac cell membrane, during a normal action potential is sustained in the plateau phase by the activation of voltage-gated L-type Ca^{2+} channels (Woodcock & Matkovich, 2005). It is this small influx of Ca^{2+} via these channels that triggers a much larger release of Ca^{2+} from the SR. Upon activation of the SR, there is a transient rise in cytoplasmic Ca^{2+} concentration $[Ca^{2+}]_i$. This phenomena is commonly reffered to as the $[Ca^{2+}]_i$ and this process, known as CICR is generally accepted as the major mechanism of Ca^{2+} release from the SR. Ca^{2+} release from the SR is mediated by intracellular calcium receptors commonly known as RyR, with type 2 RyRs being the most abundant intracellular Ca^{2+} channels in cardiomyocytes (Woodcock & Matkovich, 2005; Roderick & Bootman, 2007). Contraction is initiated when free Ca^{2+} causes the interaction of the myofilaments via TC and the thick and thin filaments, namely actin and myosin leading to cell shortening. Exclusion of Ca^{2+} from the cytosol is achieved by several mechanisms, including SR uptake via the SR Ca^{2+} transporter and removal through the sarcolemma via the NCX (Bers *et al*., 2003; Hilgemnn, 2004). These changes result in cyclic increases and decreases in Ca^{2+} and in contractility of the individual myocytes.

Impairments in this mechanical function may be due partly to alterations in $[Ca^{2+}]_i$ homeostasis that manifests as prolonged time to peak and prolonged rate of decay in Ca^{2+} transients in diabetic cardiomyocytes compared to controls (Zhang *et al*., 2008). However, experimental findings are inconsistent as mentioned previously and undergo

much debate. Nevertheless, this disturbed Ca^{2+} homeostasis may be explained by the reduced activity of SERCA2a and the decreased ability of the SR to take up calcium (Boudina and Abel, 2007). In HF, this reduced SR content may be due to either reduced Ca^{2+} pumping by SERCA or increased SR Ca^{2+} leak via RyRs. In addition, increased NCX function can participate with SERCA during $[Ca^{2+}]_i$ decline, hence extruding more Ca^{2+} from the cell and depleting the SR (Bers *et al*., 2003). In the new balanced state, a generously proportioned fraction of activating Ca^{2+} also enters the cell at each beat in HF (e.g. smaller Ca^{2+} release causes less Ca^{2+} inactivation). Numerous previous studies have documented impaired activity of SERCA and/or other regulatory proteins including NCX (Ren and Bode, 2000; Hilgemnn, 2004).

The results of this study have been presented with prolonged amplitude which could possibly relate to the slower $[Ca^{2+}]_i$ kinetics due to the sustained depolarisation (achieved by inhibition of Ca^{2+} extrusion by NCX) observed in STZ-induced diabetes causing the decreased rate of return of $[Ca^{2+}]_i$ to resting levels (Zhang *et al*., 2008). Additionally, previous experiments in our laboratory discovered a significant increase in Ca^{2+} content when measured in LV isolations from STZ-induced diabetic rat heart with a concomitant increase in blood plasma Ca^{2+} (Singh *et al*., 2006). In turn, this can be associated with increased Ca^{2+} influx through leak channels in heart muscle cells and reductions in the NCX activity (Dhalla *et al*, 1996) and reductions in SERCA2a activity (Takeda *et al*., 1996).

Defects in ventricle contraction and relaxation have been observed in isolated myocytes (Ren & Davidoff, 1997) with the severity of dysfunction increasing with the duration of diabetes similar to the observations made in this study which showed significant increase in prolonged contractile function at 4 months after STZ-induction compared to 2 months. The altered time-course of shortening and relaxation in myocytes from diabetic rats observed in this study at 2 and 4 months after STZ treatment is in agreement with previously published studies (Choi *et al*., 2002; Ren & Davidoff, 1997, Tamada *et al*., 1998). Ventricular myocytes from 2 and 4 months of STZ treatment presented with unchanged resting $[Ca^{2+}]_i$ levels and $[Ca^{2+}]_i$ amplitude. These results are consistent with some previous studies performed on ventricular myocytes under identical conditions (Zhang, 2008; Howarth *et al*., 2002). However, other studies showed reduced $[Ca^{2+}]$i amplitude and peak but it should be noted that the experimental conditions were not identical (Yaras *et al*., 2005; Kotsanas et al., 2000).

Conclusion

In conclusion, this study has demonstrated that T1DM can result in altered mechanical function and cellular $[Ca^{2+}]i$ homeostasis in ventricular myocytes from STZ-induced diabetic rats after 2 and 4 months duration of STZ-diabetes compared to age- matched control. The findings discussed in this chapter suggest that cardiac dysfunction in STZ-induced diabetes is attributable to changes at cellular level described previously i.e. EC coupling. However, a little is known about the contribution of ventricular remodelling and alterations observed in contractile proteins including NCX, SERCA2a, L-type calcium channels and structural alterations that contribute to such cardiac dysfunction. Additionally, a large body of evidence associates cardiac remodelling in DM to be a crucial factor that leads to myocardial ECM hyperplasia in clinical and experimental HF. As such, the next chapter addresses these contractile proteins and explores various features of ventricular remodelling to determine the scope of cardiac changes in remodelling in DM that may contribute to this decline in the cardiac pumping function.

CHAPTER 4

STRUCTURAL AND MOLECULAR LEFT VENTRICLE REMODELLING IN THE STZ-INDUCED TYPE 1 DIABETIC RAT

4.1 Abstract

Background: This study tested the hypothesis that HG can elicit marked structural remodelling of the LV with TGFβ1 playing a pivotal role in the process.

Methods: LV from 2 and 4 months after STZ-induction and age-matched controls were used to access remodelling changes and underlying TGFβ1 activity, gene expression analysis of ECM mediators and regulators, ultrastructural analysis and gene expressions analysis of cardiomyocyte contractile proteins.

Results: LV remodelling in STZ-induced type 1 diabetic rats at 2 and 4 months of DM duration characterised by elevated ECM deposition and consequently altered gene expression profile of ECM key components (Collagen 1α, Collagen 3α, Fibronectin and Elastin) together with elevated levels of key mediators (MMP9, Integrin 5α, TIMP4, CTGF) and reduced expressions of Cx43 and MMP2 of the ECM. Electron microscopic analysis revealed ultrastructural alterations in LV highlighted by increased mitochondrial number and altered mitochondrial population. Additionally, elevations in ANP and BNP marked the recapitulation of foetal gene phenotype together with increased caspase-3 immunoreactivity observed in the LV of STZ-induced type 1 diabetic rats compared to age-matched controls. Cardiomyocyte contractile proteins revealed marked reductions in gene expression of SERCA2a, RyR2, Pln, L-type Ca^{2+} channel proteins (Cav1.2, CaV1.3) and calcium/calmodulin-dependant protein kinase II delta (CaMK2d), together with increases in NCX and calmodulin2 (Calm2) gene expression underlying the contractile dysfunction observed in STZ-induced type 1 diabetic rat model. These changes were correlated with parallel transcriptional findings of increased TGFβ1 activity, gene expression in the LV and elevated active TGFβ1 in the plasma of STZ-induced type 1 diabetic rat. Collectively, these changes were more severe in DM of 4 months compared to 2 months and their respective age-matched controls.

Conclusions: This is the first report describing LV structural remodelling in STZ-induced type 1 diabetic rat model over two time periods, where all experimental groups had age-matched control animals for comparisons. The results of this study clearly show that adult vs young adult, in combination with STZ-induced T1DM, can elicit severe changes to LV via structural, functional and biochemical alterations. TGFβ1 activity may represent a key agent in the process.

4.2 Introduction

Structural remodelling of the myocardium has been widely studied in literature using ex-vivo and in-vivo experiments. Remodelling has been the focus of numerous investigations studying DCM in rodent and primate models of the disease (Asghar *et al*., 2009). HG is the primary diagnostic feature of DM and the target for anti-diabetic therapy together with HbA1c, the principal marker of glucose control (Schainberg *et al*., 2010). In recent years HF has been defined as the sustained progression of LV myocardial remodelling that leads to impairments of chamber performance and medical manifestations (Fedak *et al*., 2005). It has been postulated that endothelial dysfunction, endomyocardial fibrosis, direct toxic effect of HG on cardiomyocytes, alterations in myocyte size and autonomic neuropathy play important roles in the development of DCM (Wang *et al*., 2006). The roles of HG in metabolic abnormalities and subcellular defects to the myocardium are believed to cause the development of DCM (Cai *et al.*, 2001). The latter stage of the disease has also been postulated to bring abnormal gene expression and programmed cell death by apoptosis and necrosis (Hilfiker-Kleiner *et al*., 2006). Similarly, to human pathophysiology (Cosyns, 2007), the STZ-treated diabetic rat model has also been widely used to study LV remodelling.

Nevertheless, there seems to be an assortment of discrepancies amongst experimental findings from many studies regarding the development of structural remodelling. In numerous structural studies, the structural manifests of the disease reflect as early as 6-12 weeks, with some studies demonstrating changes in the first week of disease induction (Thompson, 1988). Contrasting studies in the STZ-induced model of T1DM have demonstrated both hypertrophy (Feng *et al*., 2008) and atrophy (Nemoto *et al*., 2006) with regards to cardiomyocyte size. Common findings in the diabetic heart biopsies included, interstitial fibrosis, myocyte hypertrophy, and ECM deposition (Van Van Heerebeek *et al*., 2008). Furthermore, one of the proposed mechanisms whereby HG may induce LV structural remodelling is via activity of the pro-fibrotic and pro-hypertrophic cytokine TGFβ1 that stimulates ECM protein production and thereby the resultant cardiac complications. TGFβ1 has the capacity to initiate a pro-fibrotic programme in the heart which in turn, effects the transcriptional profile of the ECM as well as key mediators of intracellular calcium $[Ca^{2+}]_i$ and consequently regulates the expression of foetal genes including natriuretic peptide expression (Parker *et al*., 1990;

Lijnen and Petrov, 2002; Kapoun *et al*., 2004; Porter & Turner, 2009) to initiate adverse LV remodelling.

It is of interest to appreciate the interpretation of existing experimental evidence on structural remodelling in DCM which has been associated with factors such as simultaneous presence of hypertension and differences in disease duration. Thus, the present study was undertaken in order to access and confirm the development of LV histopathological changes as a result of HG in the rat heart at 2 and 4 months post STZ-treatment compared to the respective age-matched controls. This study focuses on the myocardial matrix remodelling accompanied by structural and molecular alterations that lead to the onset of ventricular remodelling in HF. The study of such complex process of myocardial remodelling is of considerable clinical importance, especially because pharmacological, cellular, and mechanical interventions could be used to target this process and reverse the mechanisms that lead to progressive left ventricular dysfunction (Segura *et al*., 2014). In this chapter, data are presented to investigate the hypothesis that HG can elicit LV remodelling that is characterised by ECM proliferation with resulting ECM gene expression profile, together with concomitant increases in circulating active TGFβ1 as well as the gene expression of cardiac Ca^{2+} handling proteins that may be responsible for the altered mechanical, functional and cellular $[Ca^{2+}]_i$ homeostasis presented in chapter 3.

4.3 Methods

Methods are described in Chapter 2

4.4 Results

The general characteristics of rats are described in Chapter 3.

1. Histopathology of the LV after 2 and 4 months of STZ-treatment

Optical analysis using the H & E stain on LV sections by light microscopy revealed general disorganised architecture of the myocardium characterised by hypertrophied cardiomyocytes, disarray of myofibres and scared myofibrils in the STZ-induced diabetic groups at 2 and 4 months compared to age-matched controls which revealed an organised cardiomyocyte muscle structure with striation pattern clearly visible in both groups (Figure 4.1).

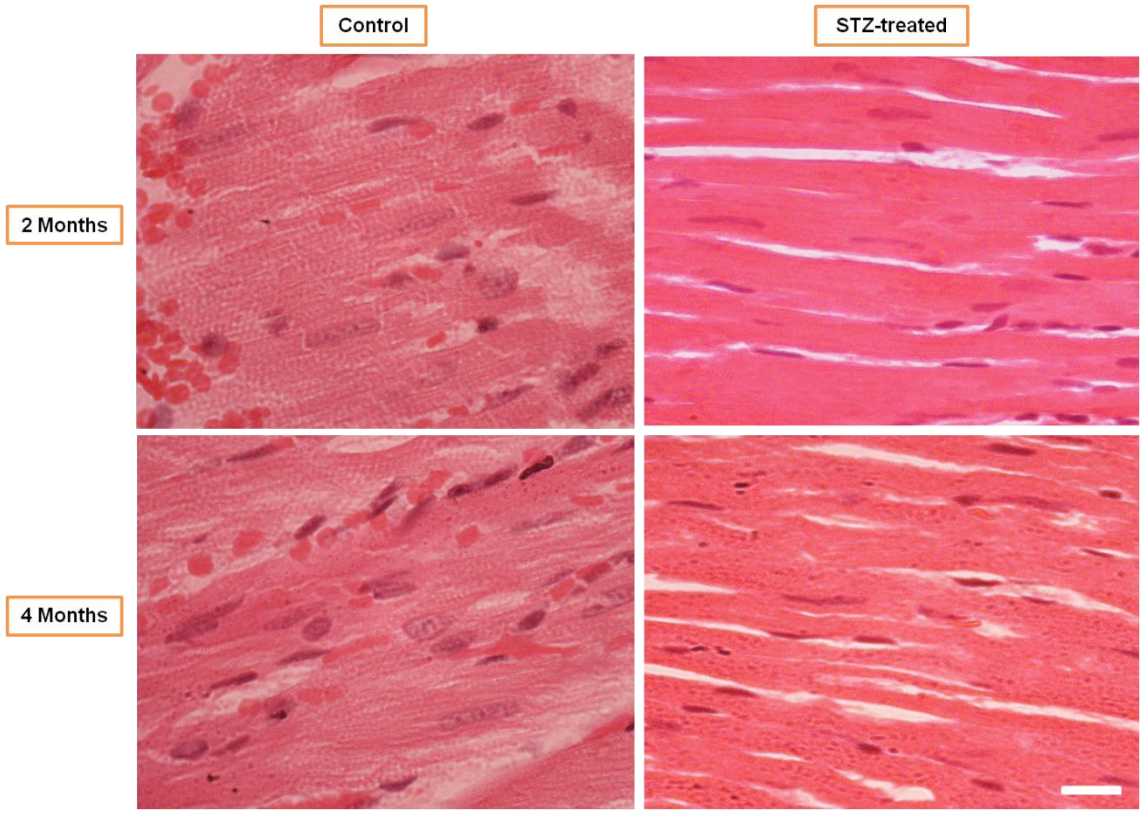

Figure 4.1: Left ventricle histology. Representative light photomicrographs detailing LV histopathology, showing H & E stained LV myocardial sections at 2 and 4 months of STZ-treated and age-matched controls. Both groups demonstrated frequent architectural distortion together with irregular myofibril pattern arrangement with thinner fibers in the STZ-treated rats compared to an organised muscle fiber structure present in age-matched controls. Original Magnification X1000 oil immersion. Photomicrographs are typical of 35-45 fields/experimental groups consisting of 6-9 animals per group. The bar represents 10 µm and calibration is the same for all micrographs.

2. Evaluation of myocyte diameter after 2 and 4 months of STZ-treatment

Figure 4.2 represents the effect of 2 months (A) and 4 months (B) of STZ-treatment on rat ventricular myocyte diameter compared to age-matched controls. Image analyses of FITC-conjugated Lectin stain showed a significant change in cardiomyocyte diameter in the diabetic group at both treatment times (C). Myocyte diameter was significantly (p<0.05) smaller in the STZ-treated rats compared to age matched controls, at 2 months (10.60±0.25 *vs.* 12.21±0.23 µm) and at 4 months (9.14±0.26 *vs.* 11.87±0.22 µm). This reduction is greater in the 4 months STZ-treated rats compared to 2 months STZ-treated rats. Lines and asterisks above the bars show significance (p<0.05) (See Figure 4.2C).

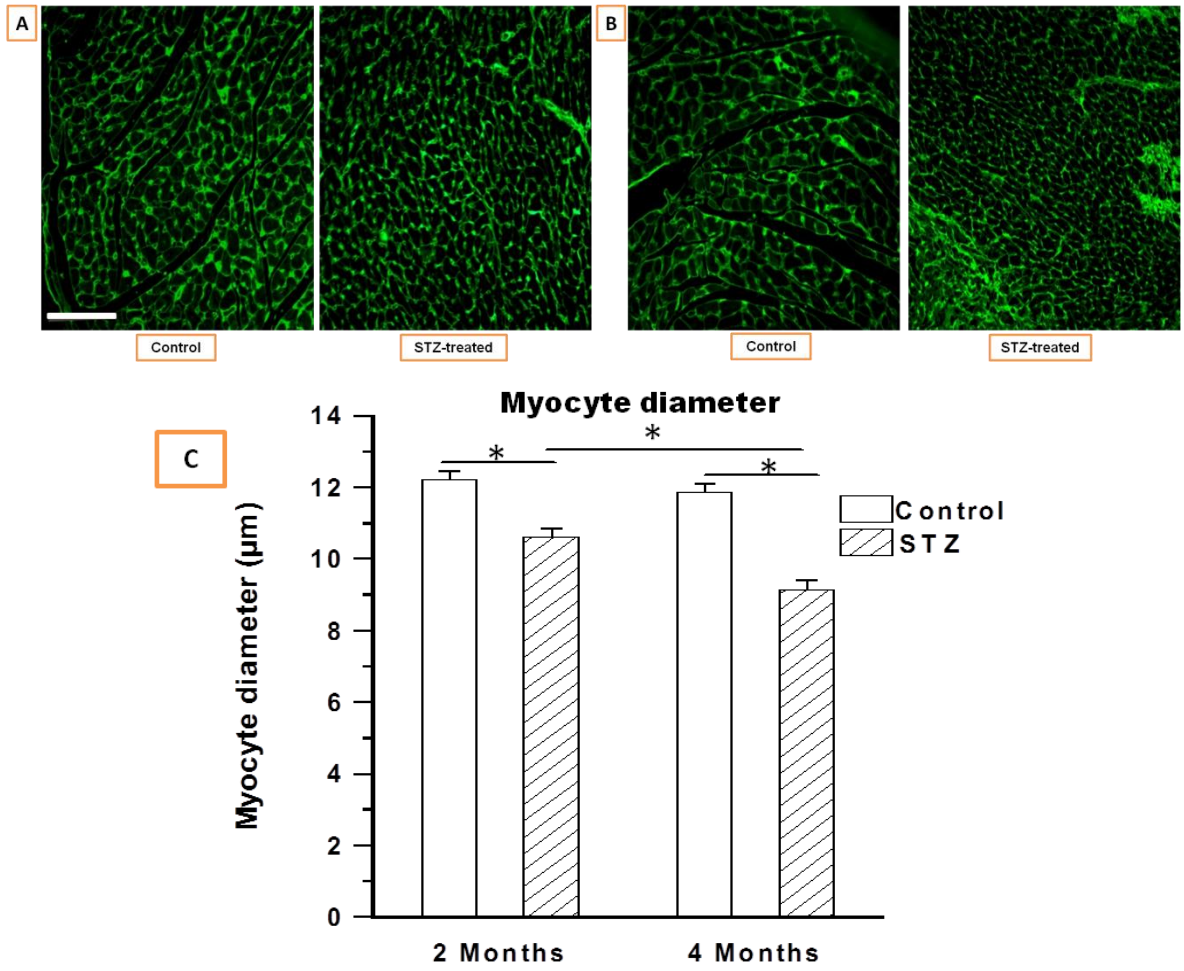

Figure 4.2: Myocyte diameter. Representative fluorescence light micrographs showing FITC-conjugated Lectin staining of individual cardiomyocytes at 2 months **(A)** and at 4 months **(B)** after STZ-treatment and age-matched controls. Original magnification X 200. Photomicrographs are typical of 35-40 experimental groups consisting of 5-8 animals per group. Scale bar in first image represents 20 µm and calibration is the same for all micrographs. Cardiomyocyte transverse diameter measured by Image J **(C)**. Bar chart data are Mean±S.E.M, *p< 0.05, One-way ANOVA followed by Bonferroni corrected t-tests for multiple comparisons.

3. Examination of myocardial fibrosis after 2 and 4 months of STZ-treatment

Light microscopy photomicrographs of Masson's Trichrome stained STZ-treated rats demonstrated significantly increased ECM deposition in both interstitial and perivascular regions (Figure 4.3) in comparison to age-matched controls. Quantitative analysis of interstitial fibrosis in STZ-treated rats revealed significantly greater myocardial area coverage as compared to age-matched controls occupying 5.06±0.40% *vs.* 2.19±0.37% (p<0.05) at 2 months and 7.29±0.44% *vs.* 3.39±0.39% (p<0.05) at 4 months post STZ-treatment. This change was significantly (p<0.05) different between 2 and 4 months of STZ-treatment time (see Figure 4.3C).

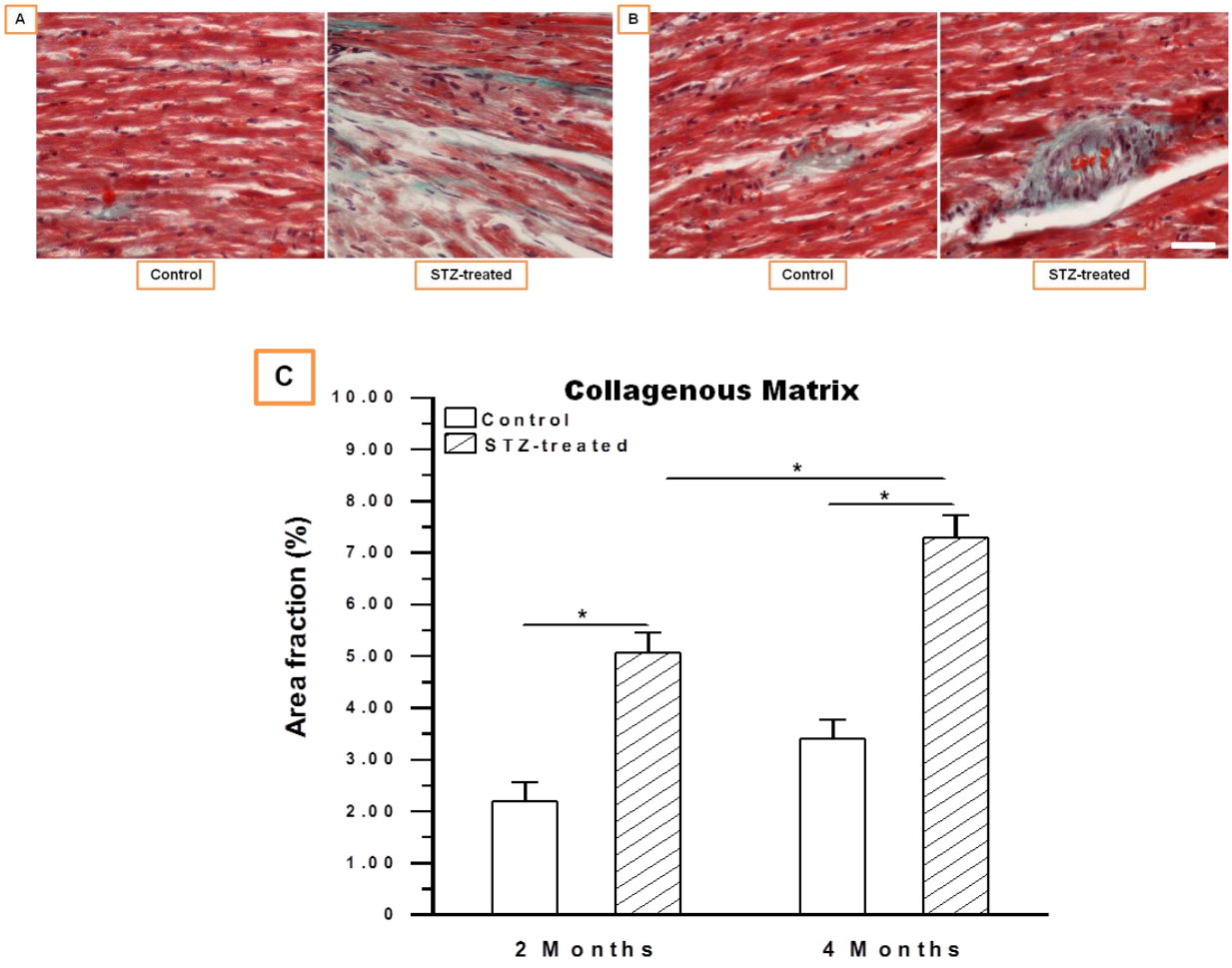

Figure 4.3: Investigations of ECM deposition in LV myocardium. Representative light micrographs of Masson's Trichrome stained myocardial sections from 2 months after STZ-treatment **(A)** and 4 months after STZ-treatment **(B)** and quantitative assessment of interstitial fibrosis using Image J analysis tool **(C)**. Original Magnification X400, Photomicrographs are typical of 35-47 fields/experimental groups consisting of 6-9 animals per group. Scale bar indicates 10 µm. Bar chart data are Mean±S.E.M, *P< 0.05, One-way ANOVA followed by Bonferroni corrected t-tests for multiple comparisons.

4. Localisation of Apoptosis after 2 and 4 months of STZ-treatment

DM is frequently associated with apoptotic mechanisms causing cardiac myocyte loss in the failing heart (Sabbah, 2000; Elmore, 2007). Hence, the activation of caspase-3, a key effector involved in the apoptosis process was assessed. Figure 4.4 shows the distribution (A) and (B) and quantification of caspase-3 (C) in age-matched control and diabetic LV of 2 and 4 months old rats. Cleaved (active) caspase-3 revealed significant (p<0.05) increases in the immunoreactivity within the hearts of STZ-treated diabetic rats compared to age-matched controls (5.56±0.44 *vs.* 1.29±0.39) positive cells/mm^2 (p<0.05) at 2 months and (8.99±0.46 *vs* 1.89±0.40) positive cells/mm^2 at 4 months after STZ-treatment (Figure 4.4 C). This increase was significant (p<0.05) between the two treatment times.

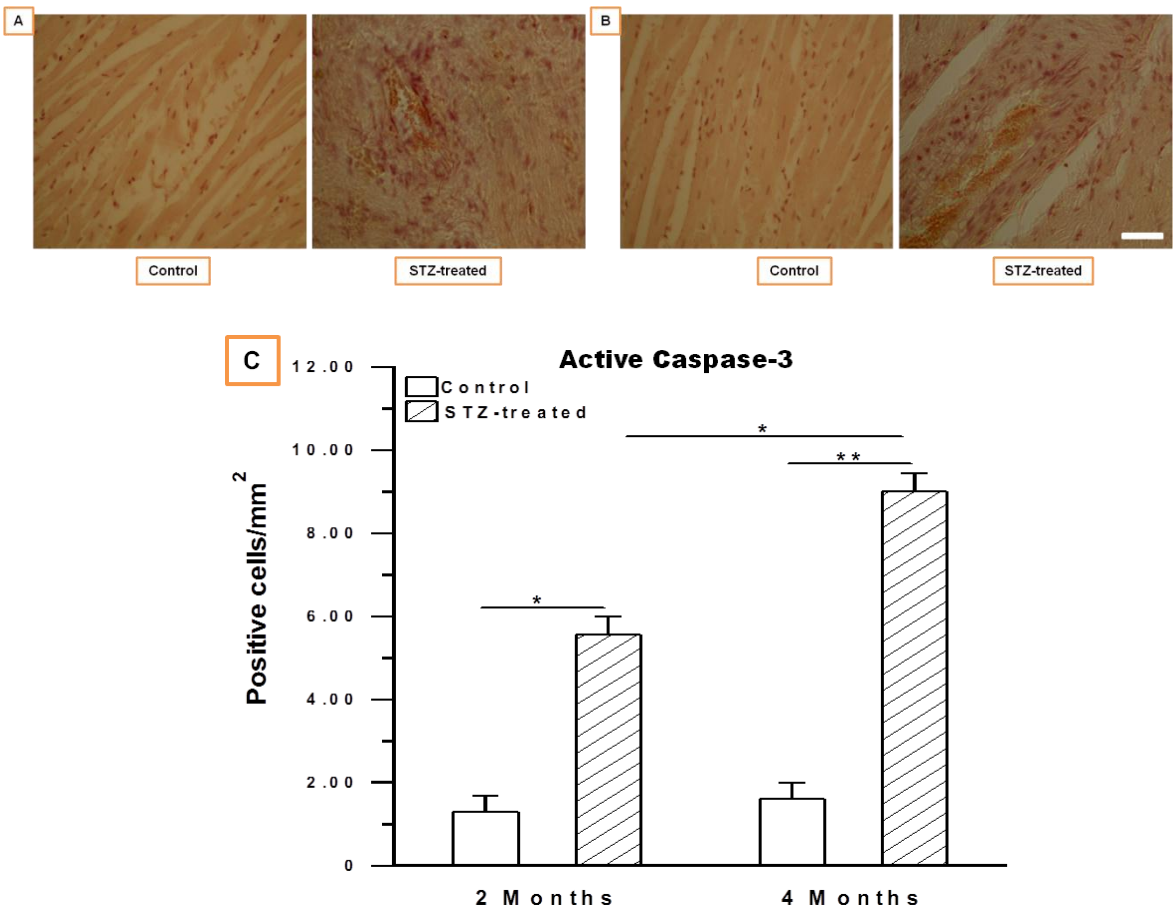

Figure 4.4: Myocyte apoptosis. Active Caspase-3 positive cells (brown staining) in the LV from 2 months after STZ-treatment **(A)** and 4 months after STZ-treatment **(B)** and quantitative assessment of immunoreactivity using Image J analysis tool **(C)**. Magnification X400, Photomicrographs are typical of 15-20 fields/experimental groups consisting of 5-6 animals per group. Scale bar indicates 20 µm and is true for all photomicrographs. Bar chart data are Mean±S.E.M, *p<0.05, **p<0.01, One-way ANOVA followed by Bonferroni corrected t-tests for multiple comparisons.

5. Ultrastructural investigations after 2 and 4 months of STZ-treatment

Figure 4.5 shows the ultrastructure changes in LV cardiomyocytes at 2 and 4 months after STZ-treatment compared to the vasculature of age-matched control animals. Electron micrographs show disorganised cytoarchitecture and altered intercalated discs compared to controls in the LV from 2 months **(A)** and 4 months **(B)** after STZ-treatment and micrographs showing altered mitochondrial distribution at a higher magnification in LV from 2 months **(C)** and 4 months **(D)** after STZ-treatment compared to age-matched control**.** Figure 4.5E Quantitative assessment of cardiomyocyte sarcomere length (µm) **(E)** using Image J analysis tool revealed significant ($p< 0.05$) increase at 4 months after STZ-treatment (2.37±0.12 *vs.* 2.01±0.08 µm) compared to age-matched control. However, this significance was not observed in cardiomyocytes at 2 months after STZ-treatment (2.15±0.10 *vs.* 1.93±0.06 µm) compared to age-matched control.

Recent studies have identified mitochondria as the target and origin of major pathogenic pathways which lead to the progression of myocardial dysfunction and HF (Hoppel *et al*., 2009; Rosca and Hoppel, 2010). Mitochondria of cardiomyocytes consist of two spatially disparate populations: Subsarcolemmal mitochondria (SSM) that abut the sarcolemma while the Interfibrillar mitochondria (IFM) are trapped within the contractile apparatus (Riva *et al*., 2005). Thus, both mitochondrial populations were quantified at 2 and 4 months after STZ-treatment using Image J analysis tool. Quantification of electron photomicrographs (Figure 4.5F) revealed significant ($p<0.05$) increases in mitochondrial number in LV of 2 months (32.86±4.92 *vs.* 15.07±1.14) and 4 months (57.80±5.26 *vs.* 20.37±1.23) after STZ-treatment compared to control, revealing an age-related affect in mitochondrial number. The results for the quantification of the two distinct mitochondria population revealed no significant ($p<0.05$) differences in the SSM population in LV of 2 and 4 months of STZ-treated rat hearts compared to control (Figure 4.5G). However, the IFM population (Figure 4.5H) revealed a significant ($p<0.05$) increase in IFM population (Figure 4.5H) after 2 (24.33±2.49 *vs.* 11.47±1.16) and 4 months (36.33±2.58 *vs.* 22.27±2.92) of STZ-treatment compared to age-matched control. Together, these alterations in mitochondrial morphology have previously been associated with changes in mitochondrial bioenergetics, such as decreased oxidative phosphorylation as well as metabolic remodelling and increased oxidative stress (Rosca and Hoppel, 2010).

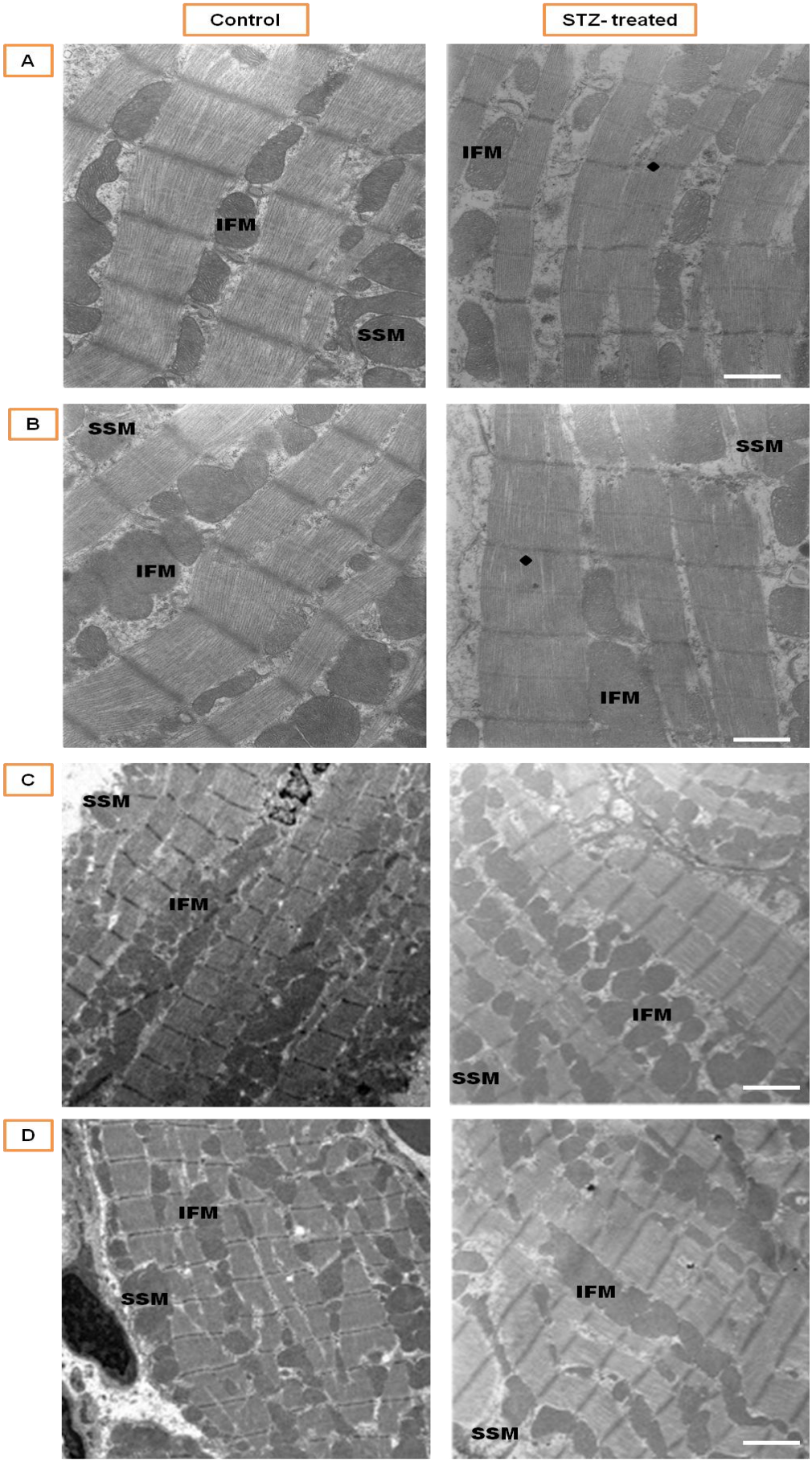
Control
STZ- treated
A
IFM
SSM
IFM
B
SSM
IFM
SSM
IFM
C
SSM
IFM
IFM
SSM
D
IFM
SSM
IFM
SSM

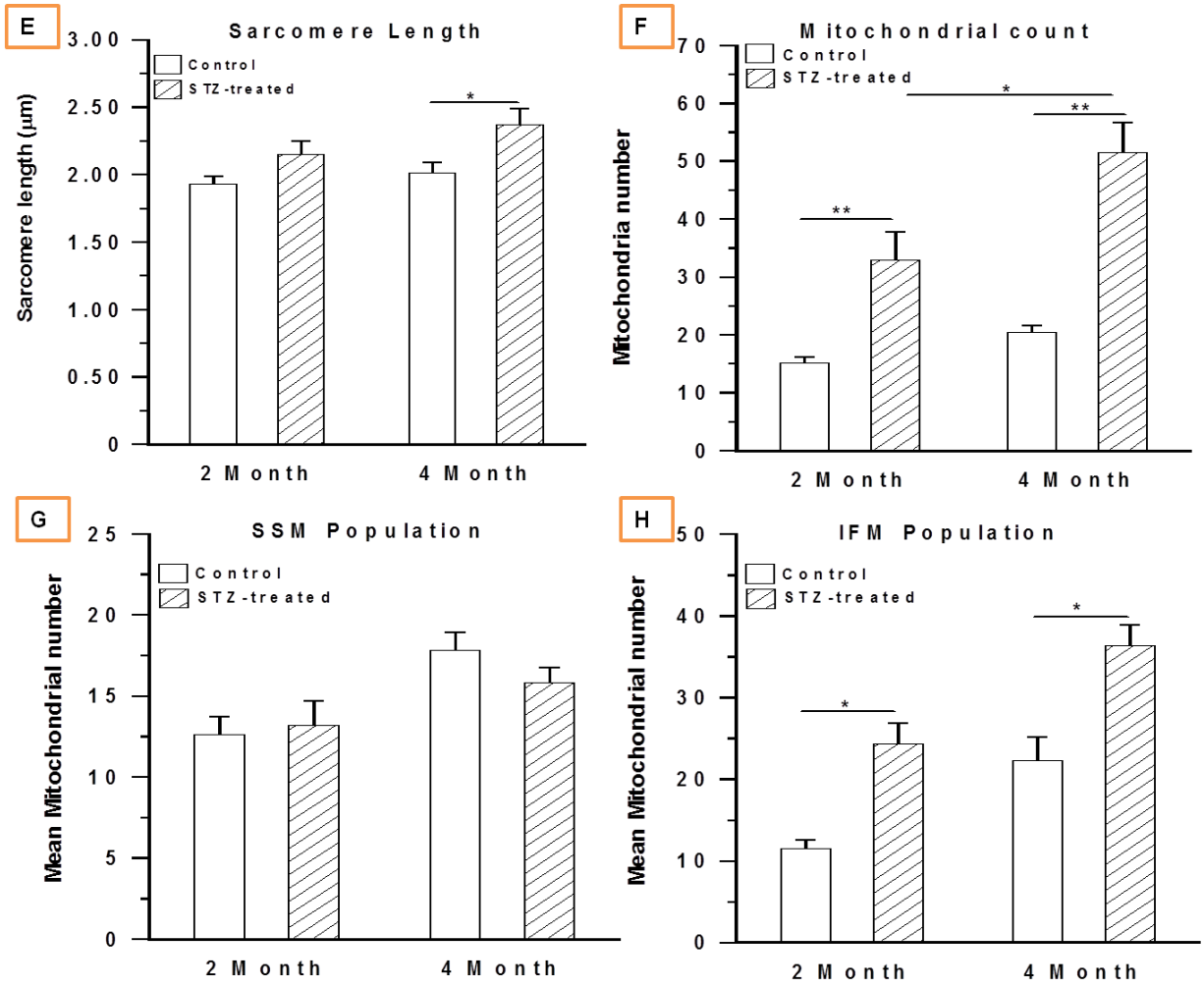

Figure 4.5: Myocyte ultrastructure and quantitative investigations. Representative electron micrographs showing disorganised cytoarchitecture and altered intercalated discs compared to controls in the LV from 2 months after STZ-treatment **(A)** and 4 months after STZ-treatment **(B) (**Magnification 14,000 X) and micrographs showing altered mitochondrial distribution in LV from 2 months after STZ-treatment **(C)** and 4 months after STZ-treatment **(D) (**Magnification 7,000 X)**.** Quantitative assessment of Sarcomere length (µm) **(E),** Mitochondrial count **(F),** SSM population **(G)** and IFM population **(H)** using Image J analysis tool. Micrographs are representative of 25-35 photomicrographs from 5-6 animals. Scale bar in the lower right indicates 1µm and calibration is correct for all micrographs. Diamond; altered intercalated disc, SSM; Subsarcolemmal mitochondria, IFM; Interfibrillar mitochondria. Data are Mean±S.E.M, *p<0.05 **p<0.01, One-way ANOVA followed by Bonferroni corrected t-tests for multiple comparisons.

6. Molecular events underlying structural remodelling in the LV of STZ-induced diabetic rats after 2 and 4 months of STZ treatment.

a. Transcriptional profile of ECM

ECM alterations are accepted as hallmarks of the diabetic heart as well as in other organs (Brownlee *et al*., 2001). Production of fibrosis is an adaptive response of the heart to pathophysiological stimuli and various mechanisms have been suggested through by HG and TGFβ1 contribute pathological remodelling of LV, mainly via transcriptional regulation of ECM components (Elmore, 2007).

Figure 4.6 represents gene expression of ECM components Collagen 3α, Collagen 1α, Fibronectin and Elastin quantified using qRT-PCR. The results show significant ($p<0.05$) increases in Collagen 3α (after 2 months; (1.15±0.08 *vs.*0.58±0.06) and 4 months; (1.55±0.10 *vs.* 1.00±0.08 ratio units) (Figure 4.6A), and Collagen 1α (after 2 months; (0.99±0.09 *vs.* 0.51±0.06 ratio units) and 4 months; (1.12±0.10 *vs.* 0.59±0.08 ratio units) (Figure 4.6B) after 2 and 4 months of STZ-induced diabetes compared to age-matched control. Collagen 3α revealed an adult vs young adult effect as there was a significant ($p<0.05$) increase between the two age groups. Similarly, Fibronectin (Figure 4.6C) and Elastin (Figure 4.6D) were significantly increased at 2 months (fibronectin; 1.35±0.08 *vs.* 1.00±0.05 ratio units), (elastin; 0.89±0.03 *vs.* 0.59±0.04 ratio units) and 4 months (fibronectin; 1.55±0.10 *vs.* 1.11±0.08 ratio units), (elastin; 1.16±0.09 *vs.* 0.93±0.03 ratio units) after STZ-induction compared to age-matched control. Surprisingly, both of the ECM components revealed an adult vs young adult effect that was significantly ($p<0.05$) evident.

Furthermore, these changes were accompanied by divergent alterations in ECM regulators. Figure 4.7 represents gene expression of ECM regulators; matrix metalloproteinases (MMP2, MMP9), tissue inhibitor of metalloproteinase (TIMP4), connective tissue growth factor (CTGF), Connexin 43 and Integrin 5α. Increased expression of MMPs upregulation was evident at 2 months and 4 months after STZ-induction. MMP2 (Figure 4.7A) was significantly ($p<0.05$) down-regulated at 2 months (0.56±0.12 *vs.* 1.12±0.10 ratio units) and 4 months (0.65±0.15 *vs.* 1.19±0.09 ratio units) after STZ-induction compared to age-matched controls. In comparison, MMP9 (Figure 4.7B) was also significantly ($p< 0.05$) up-regulated at 2 months (1.14±0.15 *vs.* 0.59±0.10 ratio units) and 4 months (2.08±0.17 *vs.* 0.88±0.12 ratio units) ($p<0.05$) after

STZ-induction compared to age-matched control.. MMP9 was significantly ($p<0.05$) increased between the two age groups indicating an adult vs young adult effect. Interestingly, endogenous MMP tissue inhibitor TIMP4 (Figure 4.7C) was up-regulated at 2 months (1.20±0.16 *vs.* 0.57±0.09 ratio units) and 4 months (1.99±0.10 *vs.* 0.88±0.08 ratio units) after STZ-induction compared to age-matched control and this difference was significantly evident between the two age groups. mRNA gene expression level for CTGF (Figure 4.7D), an important downstream effector of TGFβ1 was significantly increased at 2 months (1.00±0.10 *vs.* 0.55±0.05 ratio units) and 4 months (1.07±0.11 *vs.* 0.67±0.10 ratio units) after STZ-induction compared to age-matched controls. Additionally, a significant ($p<0.05$) decrease in gap junction protein Cx43 (Figure 4.7E) was evident in the STZ-induced diabetic rat LV only after 4 months (0.87±0.99 *vs.* 1.34±0.09 ratio units) of STZ-induction compared to age-matched control. However, no significant change was observed at 2 months (1.00±0.12 *vs.* 1.20±0.11 ratio units) of STZ-induction compared to age-matched control. Finally, mRNA levels of Integrins, Integrin 5α (Figure 4.7F) was significantly ($p<0.05$) increased at 2 months (1.00±0.11 *vs.* 0.45±0.10 ratio units) and 4 months (1.35±0.10 *vs.* 0.49±0.09 ratio units) after STZ-induction compared to age-matched control. Integrin 1α was also studied, but remained unaffected by the disease. Taken together, gene expression profile of ECM components and regulators were variously effected, where ECM component alterations paralleled ECM regulating agents (MMP2-up-regulated and MMP9-down-regulated) and tissue inhibitors (TIMP4-up-regulated) representing a mechanism to re-compensate the LV. It can also be suggested that age might also be an important factor involved in the severity of disease, as observed in gene expression of some ECM components and regulators.

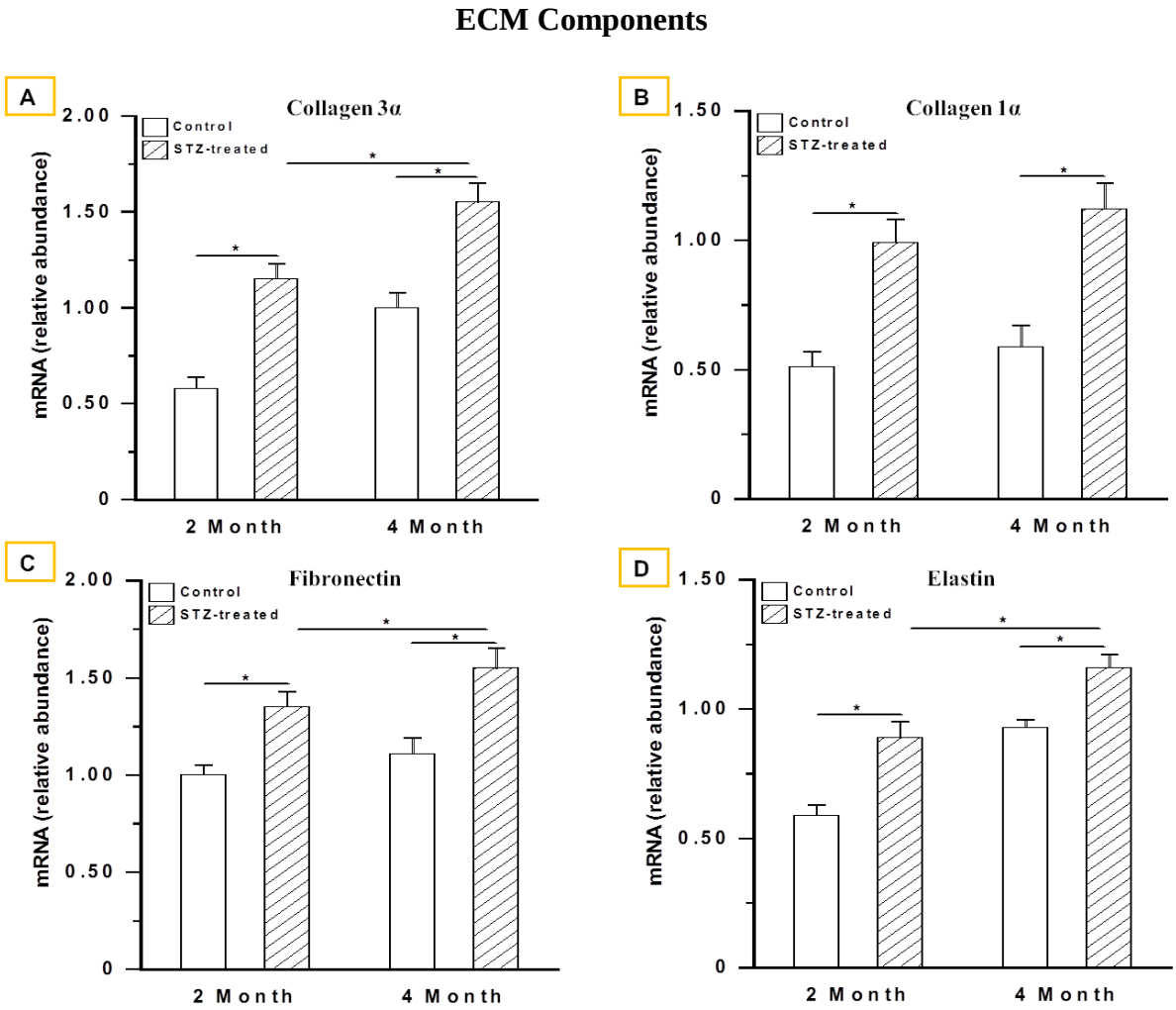

Figure 4.6: ECM components gene expression. Summarised data showing gene expression for ECM components Collagen 3α **(A)**, Collagen 1α **(B)**, Fibronectin **(C)** and Elastin **(D)** in the LV of STZ-treated and age-matched controls at 2 and 4 months post STZ-treatment. Results are representative of 8-9 animals/per group conducted in triplicates. RT-PCR amplification was normalised to that of GAPDH. Data are expressed as Mean±S.E.M. Lines over bars indicate significance *p<0.05, One-way ANOVA followed by Bonferroni corrected t-tests for multiple comparisons.

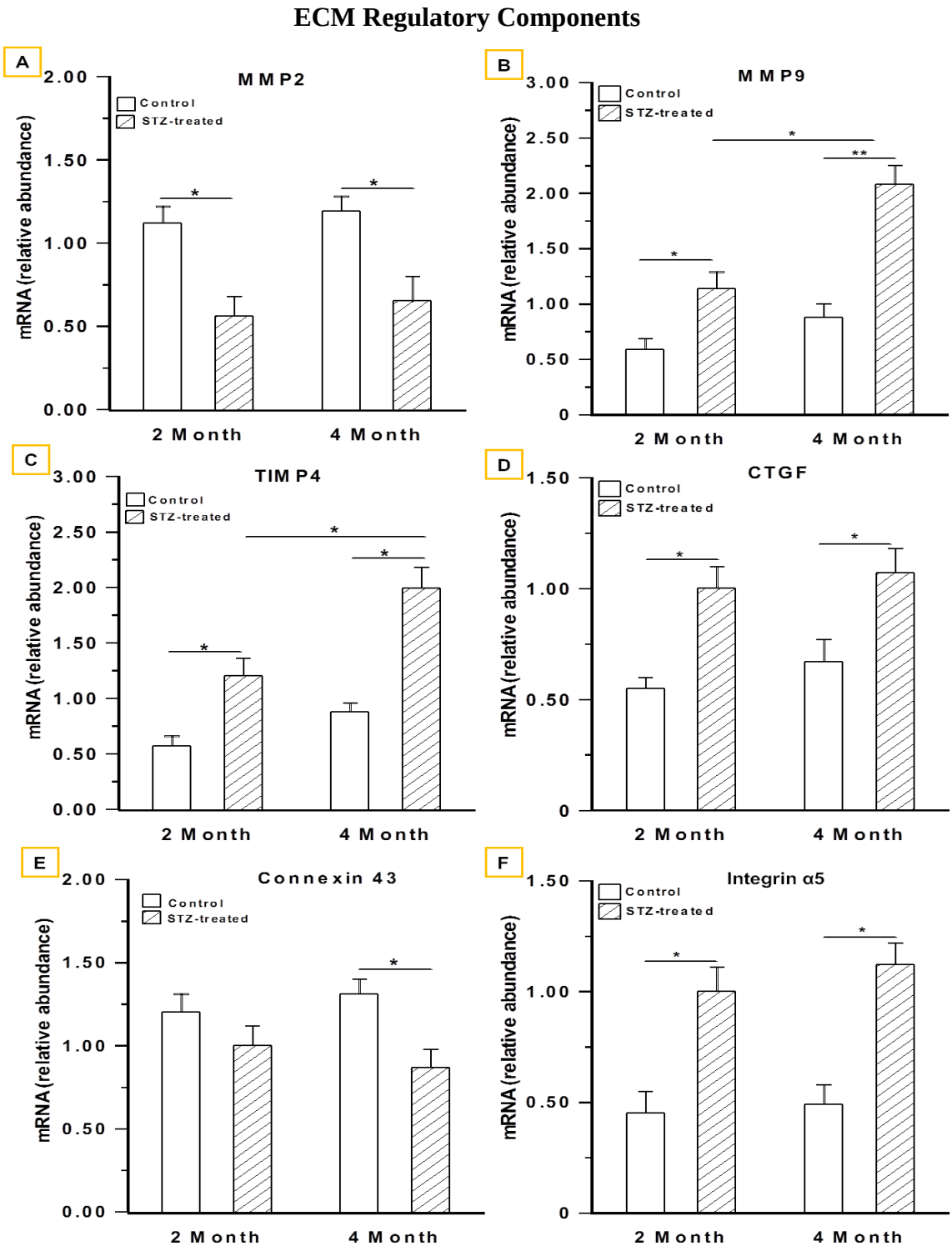

Figure 4.7: **ECM regulatory components gene expression.** Summarised data showing gene expression for ECM regulators MMP2 **(A)**, MMP9 **(B)**, TIMP4 **(C)**, CTGF **(D)**, Connexin 43 **(E)** and Integrin 5α **(F)** in the LV of STZ-treated and age-matched controls at 2 and 4 months post STZ-treatment. Results are representative of 8-9 animals/per group conducted in triplicates. RT-PCR amplification was normalised to that of GAPDH. Data are expressed as Mean±S.E.M. Lines over bars with asterisk indicate significance * $p<0.05$, ** $p<0.01$, One-way ANOVA followed by Bonferroni corrected t-tests for multiple comparisons.

b. Foetal gene phenotype of natriuretic peptides

Figure 4.8 A and B show increased expression of atrial natriuretic peptide (ANP) and brain natriuretic peptide (BNP) quantified by qRT-PCR, respectively. Ventricular hypertrophy is characterised by an increase in the synthesis of ANP and BNP release from the ventricles (Magga *et al*., 1998; Howarth *et al*., 2005). These peptides are considered sensitive biomarkers for cardiac hypertrophy. Furthermore, TGFβ1 has been shown to stimulate these foetal cardiac genes. Furthermore, these peptides are extensively used as an indirect marker for myocardial injury/overload (D'Souza *et al*., 2011). The gene expression analysis results revealed that ANP was significantly up-regulated at 2 months (0.89±0.09 *vs*. 0.47±0.06 ratio units) and 4 months (1.35±0.11 *vs.* 0.59±0.09 ratio units) after STZ-induction compared to age-matched control. This was significantly different between the two age groups, indicating an adult vs young adult effect. On the other hand, BNP was significantly ($p<0.05$) up-regulated at 4 months (0.99±0.11 vs. 0.58±0.09 ratio units) after STZ-induction compared to age-matched control. However, no significance ($p<0.05$) was observed at 2 months (0.59±0.09 vs. 0.44±0.06 ratio units) after STZ-induction but a significant up regulation can be observed between the two age groups.

c. Gene expression of $[Ca^{2+}]_i$

Myocardial response to either injury or mechanical load involves alterations in gene expression of the foetal gene programme (D'Souza *et al*., 2011). It is well known that characteristics of pathological remodelling frequently involve alterations of foetal genes that regulate Ca^{2+} handling and cardiac contractility (Hilfker-Kleiner *et al*., 2006). Hence, Figure 4.9 represents gene expression of fundamental calcium proteins involved in Ca^{2+} handling (L-type calcium channel proteins, (SERCA2a, NCX, Pln, RyR2, calmodulin2 (Calm2) and calcium/calmodulin-dependent protein kinase II delta (CaMK2d) were measured after 2 and 4 months of STZ-induced diabetes compared to age-matched control. Figure 4.9 represents gene expression of L-type calcium channels (Cav1.2 and Cav1.3). Gene expression of Cav 1.2 (Figure 4.9A) was significantly ($p<0.05$) down-regulated after 4 months (0.68±0.13 *vs*. 1.12±0.10 ratio units) of STZ treatment compared to age-matched controls. However, no significance was observed at 2 months (1.00±0.11 *vs.* 1.09±0.09 ratio units) post STZ-induction. A significant ($p<0.05$) downregulation was observed between the two age groups, representing an adult vs young adult effect as with age the Cav1.2 activity was reduced. Similarly, gene

expression of Cav1.3 (Figure 4.9B) was also reduced by 4 months (0.81±0.14 *vs.* 1.12±0.08 ratio units) of STZ-induction compared to age-matched controls. No significance was observed at 2 months (0.89±0.11 *vs.* 1.00±0.09 ratio units) after STZ-induction. Figure 4.9 C represents gene expression for NCX protein which was significantly ($p<0.05$) up-regulated after 2 (0.78±0.13 *vs.* 1.09±0.09 ratio units) and 4 months (0.51±0.15 *vs.* 1.19±0.12 ratio units) of STZ-induction compared to age-matched controls. However, gene expression for SERCA2a pump (Figure 4.9 D) represented with a significant ($p<0.05$) down regulation at 2 months (0.89±0.15 *vs.* 1.15±0.10 ratio units) and 4 months (0.58±0.14 *vs.* 1.25±0.11 ratio units) after STZ-induction compared to age-matched controls and this reduction was significantly different between the two age groups. Similarly, gene expression for Pln protein (Figure 4.9E) revealed significant ($p<0.05$) reduction at 2 months (0.84±0.13 *vs.* 1.22±0.12 ratio units) and 4 months (0.63±0.14 *vs.* 1.19±0.11 ratio units) after STZ-induction compared to age-matched controls. This trend seemed to correspond with RyR2 receptor protein (Figure 4.9F) expression as down-regulation was observed at 2 months (0.68±0.13 *vs.* 1.09±0.09 ratio units) and 4 months (0.44±0.15 *vs.* 1.11±0.06 ratio units) after STZ-induction compared to age-matched control. Down-regulation of RyR2 was significantly ($p<0.01$) different between the two age groups. Finally, expression of genes regulation ion channels (Calm2, Figure 4.9G) and calcium homeostasis (CaMK2d, Figure 3.13H) were measured. A significant ($p<0.05$) upregulation of Calm2 was observed after 4 months (0.89±0.09 *vs.* 0.65±0.06 ratio units) of STZ-induction compared to age-matched control, with no change observed at 2 months (0.77±0.05 *vs.* 0.68±0.03 ratio units) after the STZ-induction. However, CaMK2d significantly ($p<0.05$) down-regulated after 2 months (0.55±0.12 vs. 0.79±0.07 ratio units) and 4 months (0.48±0.13 vs. 0.69±0.08 ratio units) of STZ-induction compared with age-matched control.

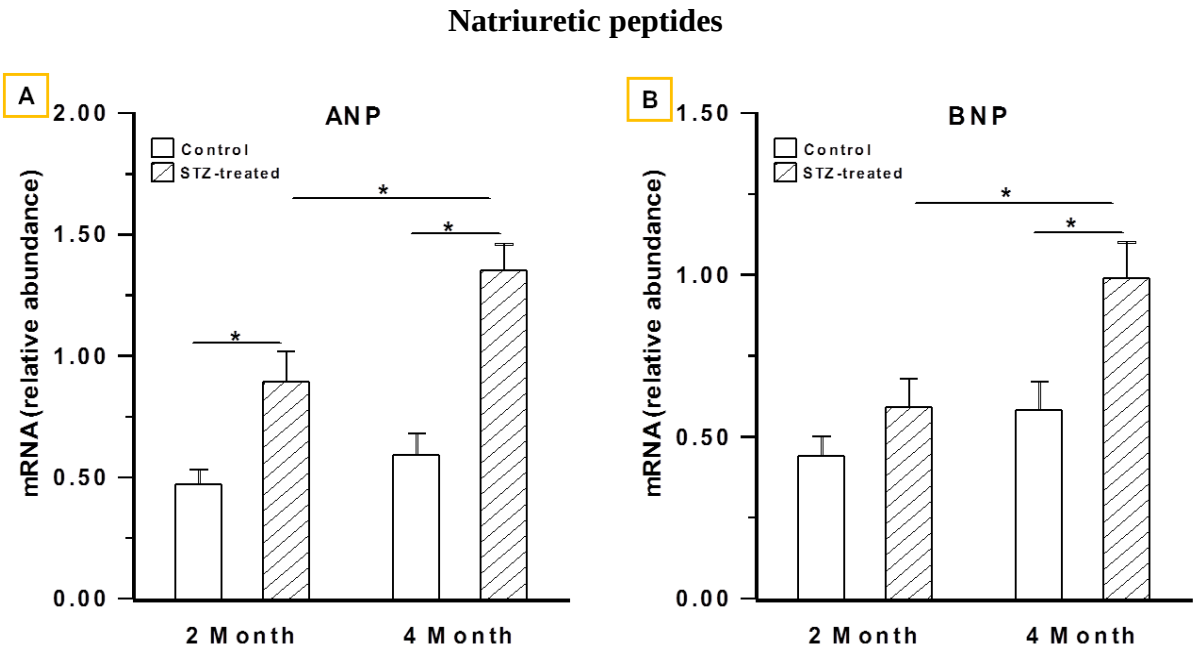

Figure 4.8: ANP and BNP gene expression. Summarised data showing ANP **(A)**, and BNP **(B)** gene expression in the LV of STZ-treated and age-matched controls at 2 and 4 months post STZ-treatment. Results are representative of 8-9 animals/per group conducted in triplicate. RT-PCR amplification was normalised to that of GAPDH. Data are expressed as Mean±SEM. Lines over bars with asterisk indicate significance * $p<0.05$, ** $p<0.01$, One-way ANOVA followed by Bonferroni corrected t-tests for multiple comparisons.

$[Ca^{2+}]_i$

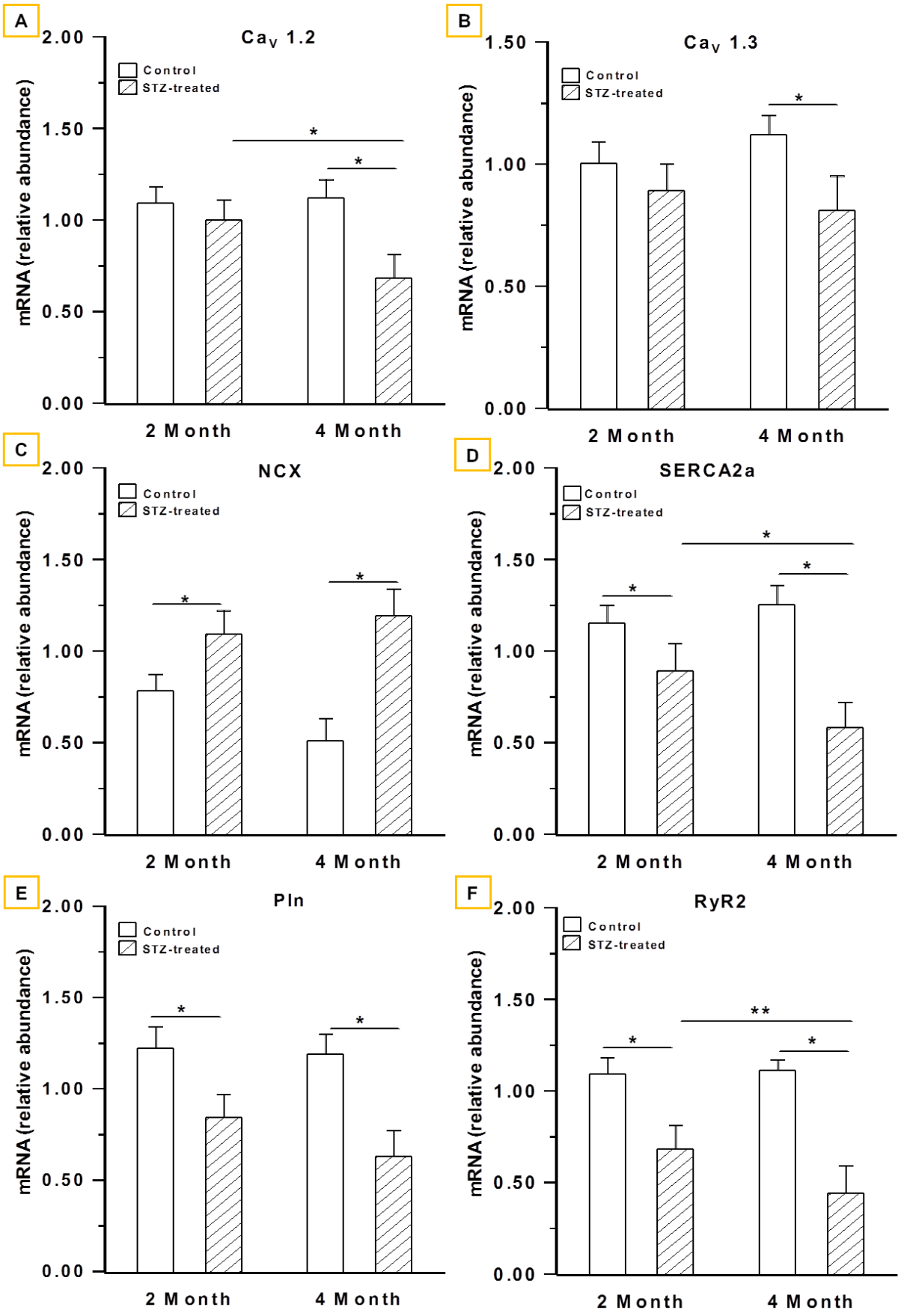
A
Ca$_V$ 1.2
Control
STZ-treated
mRNA (relative abundance)
2.00
1.50
1.00
0.50
0.00
*
*
2 Month
4 Month
B
Ca$_V$ 1.3
Control
STZ-treated
mRNA (relative abundance)
1.50
1.00
0.50
0.00
*
2 Month
4 Month
C
NCX
Control
STZ-treated
mRNA (relative abundance)
2.00
1.50
1.00
0.50
0.00
*
*
2 Month
4 Month
D
SERCA2a
Control
STZ-treated
mRNA (relative abundance)
2.00
1.50
1.00
0.50
0.00
*
*
*
2 Month
4 Month
E
Pln
Control
STZ-treated
mRNA (relative abundance)
2.00
1.50
1.00
0.50
0.00
*
*
2 Month
4 Month
F
RyR2
Control
STZ-treated
mRNA (relative abundance)
2.00
1.50
1.00
0.50
0.00
**
*
*
2 Month
4 Month

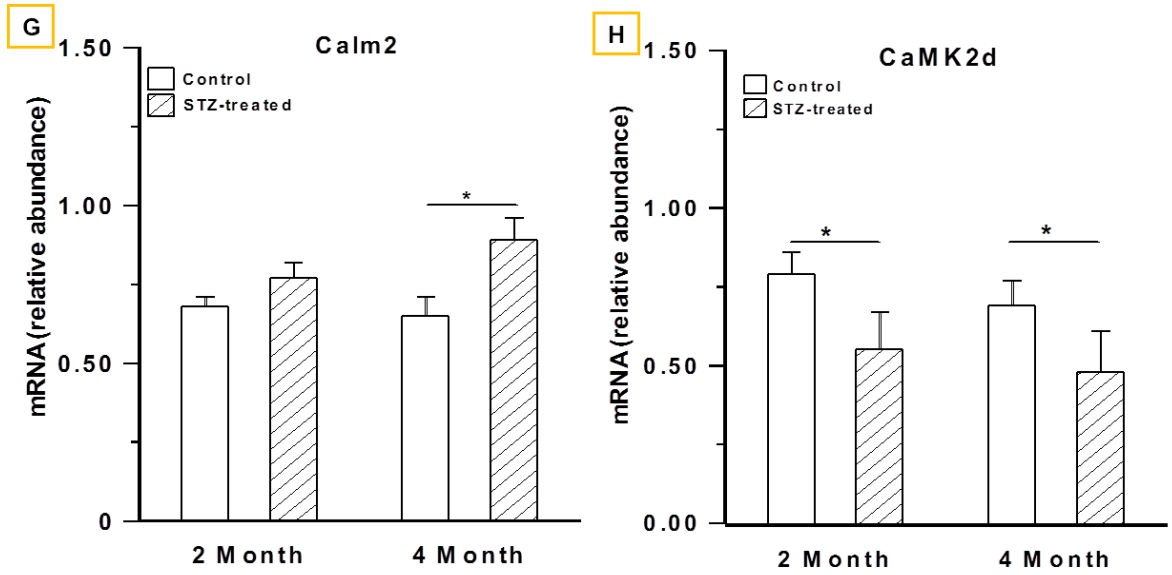

Figure 4.9: **$[Ca^{2+}]_i$ gene expression.** Summarised data showing gene expression for various $[Ca^{2+}]$i mediators CaV1.2 **(A)**, CaV1.3**(B)**, NCX **(C)**, SERCA2a **(D)**, Pln **(E)**, RyR2 **(F),** Calm2 **(G)** and CaMK2d **(H)** in the LV of STZ-treated and age-matched controls at 2 and 4 months post STZ-treatment. Results are representative of 8 animals/per group conducted in triplicate. RT-PCR amplification was normalised to that of GAPDH. Data are expressed as Mean±S.E.M. Lines over bars with asterisk indicate significance * $p<0.05$, ** $p<0.01$, One-way ANOVA followed by Bonferroni corrected t-tests for multiple comparisons.

7. Molecular events characterising extracellular matrix proliferation in the LV after 2 and 4 months of STZ-treatment

Figure 4.10 shows an increased TGFβ1 mRNA gene expression and active TGFβ1 in plasma and LV samples from rats at 2 and 4 months of STZ-treatment compared with age-matched controls. Total and active TGFβ1 concentration in the LV and plasma was evaluated by ELIZA. Active TGFβ1 significantly ($p < 0.05$) increased in plasma after 2 months (2.72±0.20 *vs.* 1.15±0.04ng/ml) of STZ-induced diabetes compared to control whereas no significant differences were observed after 4 months (2.36±0.06 *vs.* 2.18±0.07 ng/ml) of STZ-treatment (Figure 4.10A). Total TGFβ1 levels were significantly ($p < 0.05$) increased in STZ-induced diabetic LV at 2 months (16.25±0.29 *vs.* 8.45±0.11 pg/mg of total protein) and 4 months (20.98±0.25 *vs.* 10.13±0.14 pg/mg of total protein) after STZ-treatment compared to age-matched control (Figure 4.10B). These differences were significantly ($p<0.05$) apparent between the two treatment groups. Similarly, active TGFβ1 levels in LV were significantly ($p<0.01$) increased after 2 months (22.65±0.25 *vs.* 14.28±0.17 pg/mg of total protein) and 4 months (25.54±0.24 *vs.* 15.69±0.15 pg/mg of total protein) of STZ-induction compared to age-matched control and this significance was apparent between the two age groups (Figure 4.10C). TGFβ1 gene expression was also significantly ($p<0.05$) different between the two age groups (after 2 months; (1.23±0.14 vs. 0.48±0.11) and after 4 months; (1.89±0.19 vs. 0.89±0.13) in STZ induced diabetic rat LV compared to age-matched control (Figure 4.10D).

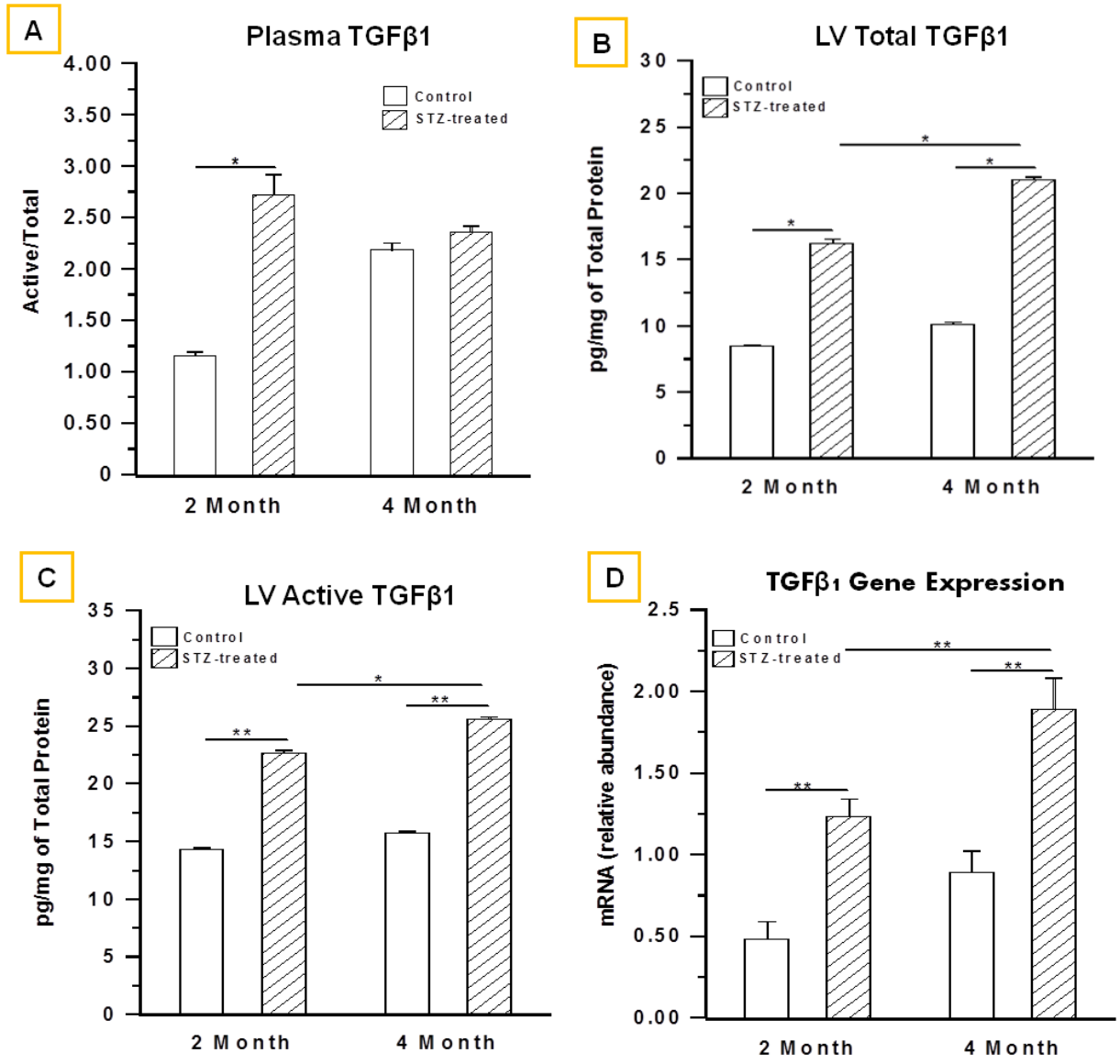

Figure 4.10: **TGFβ1 protein level and gene expression profile.** Summarised Data from ELIZA showing ratio of active: total TGFβ1 protein in plasma **(A)**, total TGFβ1: total extracted LV protein **(B)** and active TGFβ1: total extracted LV protein **(C)** at 2 and 4 months of STZ-treatment with age-matched control animals (n=3/group). mRNA gene expression of TGFβ1 **(D)** at 2 and 4 months of STZ-treatment with age-matched controls. The results of both ELIZA and qRT-PCR are representative of 3 individual experiments conducted in triplicate. RT-PCR amplification was normalised to that of GAPDH. Data are expressed as Mean±S.E.M. Lines over bars indicate significance * $p<0.05$, ** $p<0.01$, One-way ANOVA followed by Bonferroni corrected t-tests for multiple comparisons.

4.5 Discussion

Summary of key findings:

1. LV remodelling in STZ-induced T1DM rats at 2 and 4 months of DM duration is characterised by significant elevations in ECM deposition, increased apoptotic cell death and reduced cardiomyocyte diameter compared to age-matched control animals.
2. Ultrastructural alterations in sarcomere length, mitochondria number and population, suggesting a role of mitochondrial dysfunction in cardiac failure.
3. T1DM presented with molecular alterations in key ECM components and regulatory mechanisms.
4. Significantly increased expression, activity and plasma levels of TGFβ1 in fibrotic remodelling of the myocardium.
5. Significant alterations in gene expression of key calcium-cycling proteins including SERCA, Plb, NCX and Ryr2.
6. Left ventricular ECM proliferations, biochemical and morphological changes have been demonstrated to affect the function of the myocardium leading to reduced cardiac pump function in T1DM, encompassing an adult vs young adult phenomenon.

Diabetes mellitus (DM) is projected to embrace 480 million people by 2030 (Shaw *et al*., 2010). Cardiovascular diseases account for three quarters of the deaths in diabetic population (Westermann *et al*., 2009; Yu *et al*., 2012). Persistent HG is fundamental in the pathophysiology of DCM, typically designated by increased cardiac cytokine (Huynh et al., 2010; Pieres and Moreira., 2012) inflammation, apoptosis as well as changes in the composition of the ECM with enhanced cardiac fibrosis (Pieres and Moreira., 2012; Westermann *et al*., 2007).

A notable finding in this study was that significant cardiac atrophy was observed in STZ-induced type 1 diabetic rats at 2 and 4 months compared to respective age-matched controls characterised by reductions in cardiomyocyte diameter (Figure 4.2) and reduced heart weight (Chapter 3, Table 1). This finding is in accordance with previous studies representing atrophy in myocytes to be closely linked with nutrient deficiency (Nemoto et al., 2006; Kawaguchi *et al*., 1999). A previous study in STZ-diabetic rat hearts also found reduced myocyte diameter together with reduced f-actin labelling

suggesting that the amount of myofilament protein per myocyte is reduced (Zhang et al., 2013; Ward & Crossman, 2014). The findings of this study are consistent with previous studies conducted in STZ-diabetic rat hearts (Kawaguchi *et al*., 1999; Cagalinec *et al*., 2013). It has been suggested that the role of decreased phosphorylation of anabolic hormone Akt (also known as protein kinase B) to be involved in the atrophy of organ sizes, particularly the heart (Abel, 2005; Bilim *et al.,* 2008). Other studies report a hypertrophic role of Akt and its downstream effector mTOR in STZ-induced diabetes (Yang *et al*., 2007).

Ultrastructural defects in T1DM

Ultrastructural study of the LV in STZ-induced diabetes in this study revealed some important results that require some explanation. Firstly, sarcomere length was increased only after 4 months of STZ-duration while after 2 months of STZ-duration no significant effects were seen. Previous studies in STZ-diabetic hearts revealed no change in sarcomere length, however both width and volume were markedly reduced (Ward & Crossman, 2014). Additionally, a significant increase was observed in mitochondrial number at 2 and 4 months after STZ-induction compared to respective age-matched controls. Cardiac mitochondria are complex highly organized cellular organelles, which play central roles not only in energy homeostasis but also in various biosynthetic, signaling, and cell death pathways (Rosca and Hoppel, 2010). A number of previous studies reported with similar findings of increased mitochondrial number (Bugger *et al*., 2009). Mitochondria of cardiomyocytes consist of two spatially disparate populations: one abuts the sarcolemma (SSM), and the other is trapped within the contractile apparatus (IFM) (Riva *et al*., 2005), hence both of these populations were quantified. The results of this study revealed significant increases in the IFM population at 2 and 4 months post STZ-induction compared to age-matched controls which were increased with age. On the other hand, there was a reduction in cardiac SSM population in diabetic rats. SSM are more susceptible to Ca^{2+} overload-mediated cytochrome c release and mitochondrial damage compared to IFM population (Palmer *et al*., 1986). In contrast, cardiac IFM experience an age-related increased susceptibility towards mitochondrial permeability transmission pore opening (Hofer *et al*., 2009). These alterations in mitochondrial morphology are associated with changes in mitochondrial bioenergetics, such as decreased oxidative phosphorylation measured in isolated mitochondria (Rosca and Hoppel, 2010). Furthermore, these data emphasise the

importance of studying both mitochondrial populations when attempting to elucidate the contribution of mitochondrial dysfunction to cardiac failure.

ECM deposition in STZ-induced LV

An important finding in this study was the ECM deposition in the STZ-treated LV intertisium; a fundamental component of the pathological alterations observed during DM (Ban and Twigg, 2008). As mentioned previously, cardiac structural remodelling in the myocardium is widely associated with marked alterations in ECM; a widely recognized alteration of the failing heart (Miner and Miller, 2006). Several experimental and clinical studies have given the notion of progressive fibrosis leading to HF progression. This finding is in agreement with previous studies detailing DM to exaggerate LV remodelling via ECM deposition counteracted mainly by interstitial and perivascular fibrosis (green staining) can be seen in figure 4.3 in LV of diabetic rats at 2 and 4 months compared to respective age-matched controls (Adeghate *et al*., 2004; Miner and Miller., 2006). Cardiac fibrosis is an important determinant of the increase in diastolic LV stiffness in diabetic patients with reduced LV ejection fraction (Van Heerbeek *et al*., 2008). Collagen deposition and ECM alterations are accepted as hallmarks of the diabetic heart as well as other organs (Brownlee *et al*., 2001). The production of fibrosis is an adaptive response of the heart to pathophysiological stimuli and various mechanisms have been suggested by which HG and its biochemical pathways contribute towards pathological remodelling of LV (Elmore, 2007).

TGFβ1 increase in fibrotic remodelling

Increased matrix turnover in DM is associated with TGFβ1, a fibrogenic cytokine of the ECM that plays a fundamental role in the development of cardiac fibrosis (Xiao & Zhang, 2008; Desmouliere et al., 1993; Kuwahara *et al*., 2002). Stimulation of TGFβ1 enhances the synthesis of ECM proteins including collagens type II and III (Van Linthout *et al*., 2008) elastin and fibronectin as shown in this study (Figure 4.6A-D) and suppresses ECM degradation by the inhibition of MMPs and synthesis of protease inhibitors, especially TIMPs (Figure 4.7A-C). TGFβ1 is postulated to activate intracellular pathways linking TGFβ1 signals to plasma membrane serine/threonine kinase receptors with the final activation of cytoplasmic effectors, such as Smad proteins. Phosphorylation of Smad2 and its subsequent translocation to the nucleus are

the critical steps in cell signaling through this pathway (Boudina & Abel, 2010; Dorbin & Lebeche, 2010). Thus, in the transition from hypertrophy to heart failure, there is an increase of TGFβ1 expression associated with abnormal accumulation of ECM components (Masson *et al*., 2000). Moreover, increased nuclear factor –Kappa B (NFκ-B) expression (not measured in this study) is also known to activate TGFβ1 as well as fibronectin thus, fostering increased ECM synthesis in diabetes (Soetikno *et al*., 2011).

Additionally, altered activity of collagen degrading MMPs are postulated to be involved in matrix turnover as previously mentioned (Martin and Colucci, 2006; Matsusaka *et al*., 2006). The findings of increased MMP9 transcription with increasing age, as observed in this study, is consistent with findings from a previous study (Halade *et al*., 2013). A large number of studies on MMP9 highlight the importance of this enzyme in the list of prospective and important biomarkers, which could be used in combination with other biomarkers to improve diagnosis or accelerate drug discovery (Halade *et al*., 2013, Yabluchanskiy *et al*., 2013). Upregulation of MMPs has been reported previously in dilated cardiomyopathies (Seeland *et al*., 2007) and this is based on the phenomenon that total matrix collagen content is a function of synthesis and degradation and thus degraded products of matrix proteins may stimulate collagen synthesis and deposition of poorly structured fibrotic tissue in the myocardium (Li *et al*., 1997). Conversely MMP2 was observed to be down-regulated with age and this is consistent with previous studies (Van Linthout *et al*., 2008; Bollano *et al*., 2006; Wang *et al*., 2007), whereas MMP9 remained unchanged (Bollano *et al*., 2006).

In this study, an overall increase in TGFβ1 activity was observed in LV of 2 and 4 months after STZ-induction compared to respective age-matched controls (Figure 4.10A-C). Elevated TGFβ1 activity correlated with parallel findings of increased TGFβ1 gene expression that is consistent with previous findings with correlations to fibrosis and recapitulation of foetal cardiac genes (Schultz *et al*., 2002). Elevated active TGFβ1 reported in this study is predominantly important as TGFβ1 is used as a risk stratification tool for myocardial fibrosis in HF pathogenesis post MI (Sovari *et al*., 2010). Collectively, these changes were more severe in DM of 4 months compared to 2 months and their respective age-matched controls. However, the association between such events requires further clarification before prognosis of TGFβ1 can be determined.
This study also found an up-regulation in ANP and BNP levels in LV at 2 and 4 months post STZ-induction compared to age-matched controls which is consistent with

previous studies (Wu *et al*., 1998; Lukowicz *et al*., 2005; Howarth *et al*., 2005). Up-regulated expression of ANP and BNP are regarded as sensitive markers for LV dysfunction and hypertrophy and an approved marker for decompensated HF (Lukowics *et al*., 2005). However, other studies found circulating ANP levels to be either elevated (Ortalo *et al*., 1987; Black *et al*., 1988) or unchanged (Hebden et al., 1988) in rats with diabetes produced by STZ. However the effects of diabetes on cardiac ANP synthesis still requires clarification.

Furthermore, an increase in gene expression of CTGF at 2 and 4 months post STZ-induction and respective age-matched control animals (Figure 4.7D) was found. CTGF is another potent pro-fibrotic protein that is reported to mediate tissue and organ fibrosis thus contributing to structural and functional abnormalities in the diabetic heart (Leask *et al*., 2002; Way *et al*., 2002). Notably, CTGF expression is increased in type I DM and is accompanied by increased expression of fibronectin and collagen type 1 (James *et al*., 2013) as demonstrated in this study. This study showed significantly reduced Cx43 gene expression in STZ-induced LV in both age groups respective to age-matched controls. It is postulated in rat studies of STZ-induced diabetes that Cx43 in structural remodelling may partially account for sinus arrhythmias, ventricular arrhythmias, and prolonged QT/QRS conditions found in human diabetes (Howarth *et al*., 2007; Howarth *et al*., 2008; Wright *et al*., 2012). The underlying mechanism by which Cx43 achieves this has been proposed to involve the activation of PKC by HG which in turn leads to phosphorylation of Cx43 and impaired ventricular contraction (Inoguchi *et al*., 2001). Reduced levels of Cx43 have been associated with mutations in Lamin A/C gene (*LMNA*) causing dilated cardiomyopathy (Sun *et al*., 2010). It is thought that the altered distribution of Cx43 and consequent interruption of gap junctional communication within the myocardium lead to decreased velocity of electrical conduction, generation of re-entry arrhythmias, and arrhythmias causing sudden death (Severs et al., 2008). Additionally, an increased expression of integrin α5 was observed at 2 and 4 months post STZ-induction compared to respective age-matched control animals.

Caspase-3 activity increases in STZ-induced T1DM

Pathogenesis of HF is associated with marked pathological alterations in the myocardium including programmed cell death, loss of myocardial contractile tissue and reparative fibrosis are considered as the major contributing factors. Of most interest, is

the loss of myocardial cells through a highly regulated process of apoptosis occurring during the remodelling of the failing heart and is subjected to play a central role in the journey from compensated hypertrophy to HF causing a reduction in myofibril mass and subsequently cardiac dysfunction (Sharma *et al*., 2007; Elmore, 2007). Furthermore, apoptosis has been reported to contribute to the loss of cardiomyocytes, an event that is followed by collagen deposition following activation of myofibroblasts thus replacing the space of damaged cardiomyocytes. Hence, fibrosis subsequent to apoptosis is acknowledged as a poor prognosis outcome in patients with diabetes (Rizk *et al*., 2014). In the present study, immunohistochemical quantification of cleaved (active) caspase-3 revealed significant ($p<0.05$) increases in the immunoreactivity within the hearts at 2 and 4 months after STZ-treatment compared to age-matched controls and this increased with age (Figure 4.3). This is in correlation with previous studies of apoptotic cell death in STZ-treated rats and cultured myocytes in response to HG (Cai and Kang., 2003; Cai et al., 2002; Formigli *et al*., 2000; Sperandio et al., 2000). Figure 4.3 represents key characteristic features of apoptosis including cell shrinkage and pyknosis (chromatin condensation) (Elmore, 2007). Apoptotic cells display a number of biochemical modifications such as protein cleavage, protein cross-linking, DNA breakdown, and phagocytic recognition that collectively result in the distinctive structural pathology described in the study (Hengartner, 2000).

Activation of caspase-3 is mediated by multiple pathways that can be divided into mitochondria-dependent and independent pathways (Roy, 2000; Reed & Tomaselli, 2000). Of much interest is the mitochondrial cytochrome *c* release in the activation of caspase-3 (Bertoni *et al*., 2003). A pharmaceutical inhibitor of caspase-3, Ac-DEVD-cmk, which specifically inhibits caspase-3 activity, has been used in a variety of experimental approaches to inhibit apoptosis (Ghosh *et al*., 2010). This inhibitor thus provides a valuable tool to dissect the caspase-3–dependent apoptotic pathway (Cai *et al*., 2002). A short list of potential methods of anti-apoptotic therapy includes stimulation of the IAP (inhibitors of apoptosis proteins) family of proteins, caspase inhibition, PARP (poly [ADP-ribose] polymerase) inhibition, stimulation of the PKB/Akt (protein kinase B) pathway (Elmore, 2007).

Alterations in gene expression of calcium-cycling proteins

The results of this study revealed significant reductions in gene expression analysis of some key calcium-cycling proteins including SERCA2a, Pln, RyR2, L-type Ca^{2+} channel proteins and CaMK2d at 2 and 4 months post STZ-induction. These reductions were more severe with age. Conversely, gene expressions of NCX and Calm2 were found to be increased. These results are explained below.

Altered SERCA function in T1DM

In cardiac muscle, the SR has been shown to be the most active subcellular organelle implicated with the sequestration of activator calcium. SERCA 2a ATPase, together with sarcolemmal NCX, are responsible for lowering $[Ca^{2+}]_i$, leading to the relaxation of muscle. Experiments have shown that calcium binding and/or uptake by cardiac SR is altered in a variety of physiological and pathological states (Okunade et al., 2004; Liu *et al*., 2006). Lacombe and colleagues reported that diabetes-induced diastolic dysfunction, together with preserved overall systolic performance, is coupled with abnormalities of intramyocyte calcium regulation (Lacombe et al., 2007). Their findings included, prolonged Ca^{2+} transient decay, reduced intra-SR Ca^{2+} stores, reduced Ca^{2+} sparks, and decreased SERCA2a protein content, which were all consistent with decreased SR Ca^{2+} reuptake during the relaxation phase of cardiac myocytes. The decrease in SR Ca^{2+} load was found to be combined with decreased EC-coupling efficiency and these factors may contribute to the decrease in Ca^{2+} transient amplitude and Ca^{2+} spark frequency. One alternative mechanism for this approach could be defined as a compensatory mechanism via reduced SR Ca^{2+} leak which will enhance SR Ca^{2+} load (Searls *et al*., 2010; Zhong *et al*., 2001) leading to the conclusion that impaired calcium reuptake during the diastolic phase, may results from an impaired SERCA pump function as demonstrated in this study with a decrease in gene expression of SERCA2a (Figure 4.9D). Similar to the results observed in this study, SERCA2a mRNA expression and protein level and activity have been demonstrated to be down-regulated in STZ type 1 DM and the alteration of SERCA expression is accompanied by functional changes (Zarain-Herzberg *et al*.,1994; Zhong *et al*., 2001). Studies from many laboratories have demonstrated that the expression level of SERCA is significantly decreased in pressure overload (Po) induced hypertrophy and HF (Aoyagi *et al*., 1999). In addition to animal studies on cardiac diseases, there is considerable

evidence for alterations in SR Ca^{2+} transport and function. In end stage human HF, intracellular Ca^{2+} measurements using Fura-2 have shown markedly prolonged Ca^{2+} transients in both Ca^{2+} release and uptake phases in muscle samples from human hearts (Periasamy & Huke, 2001). In another study, substantial reduction of SERCA2a ATPase was observed in the diabetic Ren-2 rats (Connelly *et al*., 2007). Nevertheless, a true relation between SERCA levels and muscle function cannot be defined because too many changes occur in parallel within the heart and myocytes during progression to HF. Studies using these animal models do not allow a precise cause-effect relationship between SERCA pump level and cardiac contractility. Hence, many studies have now begun to investigate long term changes in cardiovascular function. Upon examining the abundance of the inhibitory protein Pln, which is a regulator of SERCA2a ATPase, a reduction of the active, phosphorylated form of Pln was observed in the diabetic state which is similar to that seen in human hearts and STZ-induced type 1 diabetic heart in this study. Thus, it was predicted to reduce calcium transport and prevent actomyosin dissociation contributing to delayed relaxation and reduced contractility (Fredersdorf *et al*., 2012). These studies further demonstrated that an alteration in the Pln-to-SERCA ratio can affect SR Ca^{2+} transport, having profound effects on myocardial contractility (Periasamy & Jenssen, 2008).

Altered RyR2 function in T1DM

During the past decade numerous discoveries have been made of RyR2 gene mutations which underlie the arrhythmogenesis leading to sudden cardiac death which has added a new focus to the role of RyR2 dysfunction in cardiac disease (Mackrill, 2010; Kushnir *et al*., 2010; Priori *et al*., 2001; George *et al*., 2007). CaMK2d, a predominant cardiac isoform, is an important regulator of cardiac myocyte Ca^{2+} homeostasis and shares functional targets with PKA with respect to EC coupling. Recently, constitutive CaMK2d phosphorylation of RyR2 has been hypothesized to participate in the pathogenesis of HF. This is based on the observation that transgenic mice demonstrating an overexpression of CaMK2d have increased CaMK2d dependent phosphorylation of RyR2 and hence develop cardiac hypertrophy as well as signs of dilated cardiomyopathy (Kushnir *et al*., 2010; Zhang *et al*., 2003). There is considerable controversy about which RyR2 sites are phosphorylated by PKA and/or CaMK2d and the functional impact on SR Ca^{2+} leak in HF. It has been shown that blocking of

CaMK2d (but not PKA) inhibits SR Ca^{2+} leak and significantly enhances SR Ca^{2+} content in HF myocytes. Although this does not prove which CaMK2d target (e.g, RyR2-Ser2815, Ser2809, or other) is responsible for the enhanced leak it raises the possibility that CaMK2d could be an alternative or additional target in the treatment of HF (Ai *et al*., 2005).

Altered NCX function in T1DM

Upon measurement of protein levels of NCX relative to SERCA, it was discovered that this ratio was increased by a factor of 3 in end stage failing myocardium, indicating a relative dominance of NCX over the SERCA Ca^{2+} transport. This finding leads to the discovery of two distinctly interesting phenotypes, (1) an increase in protein levels of NCX in end stage failing hearts, (2) a predominant decrease in SERCA protein levels in end stage failing heart (Hasenfuss & Schillinger, 2004). Earlier studies using dogs (O'Rourke *et al*., 1999) have demonstrated an upregulation of NCX at protein and mRNA levels with a down-regulation of SERCA which resulted in increased Ca^{2+} removal by NCX, meanwhile studies in rabbits (Yao *et al*., 1998) showed the opposite effect down-regulation of NCX at protein and mRNA level and decreased SERCA activity, and similar effect in another study (Pogwidz *et al*., 1999). Another study in AKITA murine model of Type 1 DM also showed increased NCX expression (LaRocca *et al*., 2012). Despite inconsistencies, many studies have shown that increased expression of the NCX is reported as a common feature in HF (Schillinger *et al*., 2000; Goldhaber, 2011).

Concluding Remarks

In conclusion, this study was conducted to access structural remodelling changes in LV after 2 and 4 months of STZ-induced DM and age-matched controls. The results have indicated that HG can produce marked alterations in the LV myocardium architecture expressed as fibrosis proliferation, apoptotic cell death atrophy of cardiomyocytes, mitochondrial alterations, and altered cardiomyocyte calcium-cycling proteins and these changes are more severe with age. The extent to which remodelling changes observed in this study and the degree of LV functional impairment are the subject of ongoing enquiry. The involvement of TGFβ1 in these transcriptional changes cannot be disregarded. TGFβ1involment is closely associated with marked changes in contractility accompanied by the alterations in $[Ca^{2+}]_i$ transients kinetics (Ramos-Mondragon *et al*., 2008) observed in this study.

Current therapy should be based on strict glycaemic control and, when appropriate, on antihypertensive treatment and lipid-lowering drugs. These pharmacological approaches ameliorate the prognosis of diabetic cardiomyopathy by reducing risk factors and improving the 'environment', but do not directly affect the underlying fibrosis (Heerbeek *et al*., 2008). A direct antifibrotic agent is still far from being identified and tested in the clinical arena regardless of the mechanism, ECM proliferations; biochemical or morphological, have been demonstrated to effect the function of the myocardium leading to reduced cardiac pump function in DM (Ban and Twigg, 2008).

CHAPTER 5

STRUCTURAL REMODELLING IN THE LEFT KIDNEY OF STZ-INDUCED TYPE 1 DIABETIC RAT

5.1 Abstract

Background: One main long term complication of DM is diabetic nephropathy, possibly due to the hyperglycaemia (HG). This study tested the hypothesis that HG can elicit marked structural remodelling and hypertrophy in the left kidney.

Methods: Left kidney was isolated from 2 and 4 months after STZ-induction and age-matched controls to access remodelling changes and underlying TGFβ1 activity, gene expression analysis of ECM mediators and regulators and ultrastructural analysis employing electron microscopy.

Results: Left kidney remodelling in STZ-induced type 1 diabetic rats at 2 and 4 months of DM duration presented with elevated ECM deposition and consequently altered gene expression profile of ECM key components (Collagen 1α, Collagen 3α, Fibronectin and Elastin) together with elevated levels of key mediators (MMP9, Integrin 5α, TIMP4, CTGF, Vimentin) and reduced expressions of Cx43 and MMP2 of the ECM. Electron microscopic analysis revealed ultrastructural alterations in the left kidney highlighted by an increase in glomerular basement membrane width. Additionally, recapitulation of foetal gene phenotype represented with marked hypertrophy, highlighted by increased ANP and BNP gene expression. Furthermore, increased caspase-3 immunoreactivity was observed in the left kidney of STZ-induced type 1 diabetic rats compared to age-matched controls. These changes were correlated with parallel transcriptional findings of increased TGFβ1 activity, gene expression in the left kidney and elevated active TGFβ1 in plasma of STZ-induced type 1 diabetic rat. Collectively, these changes were severe in DM of 4 months compared to 2 months and their respective age-matched controls.

Conclusions: This is the first report describing kidney structural remodelling in STZ-induced type 1 diabetic rat model over two time periods, where all experimental groups had age-matched control animals for comparisons. The results of this study clearly show that adult vs young adult, in combination with STZ-induced T1DM, can elicit severe changes to kidney structural and biochemical alterations leading to DN. TGFβ1 activity may represent to a key agent in the process.

5.2 Introduction

Diabetes-associated nephropathy is the pathological entity that has been best characterised and studied. It is well established that the chronic exposure of the kidney to hyperglycemic conditions favours the development of extensive structural damage (Decleves & Sharma, 2010). DN is a microvascular complication that leads to kidney dysfunction and end-stage renal disease (ESRD) (Kato *et al*., 2006). The characteristics of DN include renal glomerular hypertrophy, basement membrane thickening, and fibrosis due to accumulation of ECM proteins and regulators (Ziyadeh, 1993; Steffes *et al*., 1989; Decleves & Sharma, 2010; Kato *et al*., 2012) and clinical features include proteinuria, albuminuria, and progressive glomerular dysfunction (Yamamoto *et al*., 1993; Sharma *et al*., 1997; Kato *et al*., 2006; Kato *et al*., 2007).

DN does not develop in the absence of HG, even in the presence of a genetic predisposition (Schena & Gesualdo, 2005). Nevertheless, HG is a crucial factor in the development of DN because of its effects on glomerular and mesangial cells, but alone it is not causative. Mesangial cells are crucial for maintenance of glomerular capillary structure and for the modulation of glomerular filtration via smooth-muscle activity (Schena & Gesualdo, 2005). HG is associated with an increase in mesangial cell proliferation and hypertrophy, as well as increased matrix production and basement membrane thickening. Several *in vitro* studies have demonstrated that HG is associated with increased mesangial cell matrix production and mesangial cell apoptosis (Mishra *et al*., 2005; Lin *et al*., 2006).

One mechanism whereby HG can elicit unfavourable remodelling changes is via the activation of the pro-fibrotic cytokine TGFβ1. This concept is reinforced by previous experimental and clinical studies highlighting the functional linkage of HG-stimulated elevations in protein synthesis, in particular of ECM proteins with increased TGFβ1 signalling in the kidney (Ziyadah, 2004). Additionally, the role of TGFβ1 in DN has been highlighted in resultant increases in renal mesangial cells, kidney hypertrophy and cell survival (Deshpande *et al*., 2013). TGFβ1 plays a major role in glomerular alteration in diabetic sclerosis via induction in transient actin cytoskeleton disassembly in mesangial cells, high production of fibronectin, collagen types I and IV, and mesangial cell hypertrophy. Thus, TGFβ1 may be considered as an important therapeutic target in DN.

The present study was undertaken in order to access and confirm the development of histopathological changes as a result of HG in the rat left kidney at 2 and 4 months post STZ-treatment compared to the respective age-matched controls. This study focuses on the myocardial matrix remodelling accompanied by structural and molecular alterations that lead to the onset of structural remodelling in the kidney. The study of such complex processes of remodelling is of considerable clinical importance, especially because pharmacologic, cellular, and mechanical interventions could be used to target this process and reverse the mechanisms that lead to DN. This chapter investigated the hypothesis that HG can elicit kidney remodelling that is characterised by ECM proliferation, kidney hypertrophy, HG-induced cell death by caspase-3 mediated apoptosis as well as ECM gene expression profile with concomitant increases in circulating active TGFβ1.

5.3 Methods

Methods are described in Chapter 2

5.4 Results

1. Characteristic evaluation of the experimental model

General characteristics of the STZ-treated rats and age-matched Wister control are shown in Table 5.1. The data for fasting blood glucose and body weights of the animals are repeated here for comparison. Post STZ treatment, it was observed that the STZ-induced diabetic rats weighed significantly (p<0.01) less than their age-matched controls and this reduction in weight is more with increasing age (270±5.78 *vs.* 343±9.99) at 2 months and (221±13.02 *vs.* 378±10.63) at 4 month post STZ-treatment as mentioned earlier in Chapter 3. However, kidney weight was significantly increased in STZ-treated rats at 2 months of DM (4.22±0.13 *vs.* 3.25±0.12) compared to age-matched control and this increase was higher at 4 months of DM (4.45±0.16 *vs.* 3.08±0.13) compared to age-matched control. Similarly, kidney weight to body weight ratio was significantly (p<0.01) increased at 2 months of DM (1.56±0.02 *vs.* 0.94±0.01) and at 4 months of DM (2.01±0.03 *vs.* 0.82±0.01) compared to their age-matched controls showing kidney hypertrophy. Plasma blood glucose levels were significantly elevated in diabetic animals after 2 months (443±12.2 *vs.* 98±3.79) and 4 months (446±18.8 *vs.* 97±3.04) of treatment (p<0.01).

Animals	Fasting Blood Glucose (mg/dl)	Body Weight (g)	Kidney weight (g)	Kidney Weight/Body Weight ratio (g/100g body weight)
Control (n=6) 2 months	98±3.79	343±9.99	3.25±0.12	0.94±0.01
Diabetic (n=6) 2 months	443±12.2**	270±5.78**	4.22±0.13**	1.56±0.02**
Control (n=8) 4 months	97±3.04	378±10.63	3.08±0.13	0.82±0.01
Diabetic (n=8) 4 months	446±18.8**	221±13.02**	4.45±0.16**	2.01±0.03**

Table 5.1 Kidney- General characteristics of rats at 2 and 4 months post STZ-administration. All data were obtained prior to the end of the treatment period. Data are given as Mean±S.E.M, *$p<0.05$ **$p<0.01$, unpaired Student's t-test. Numbers in bracket indicate number of animals used for experiments.

2. Histopathology of the Kidneys after 2 and 4 months of STZ-treatment

Figure 5.1 shows the histopathology of the left kidney at 2 and 4 months after STZ-induction compared to age-matched controls. Kidney optical analysis using the H & E stain by light microscopy revealed general disorganised architecture of the kidney characterised by expansion in glomerular borders, tubular atrophy and increased vacuolization of renal tubular epithelial cells in the STZ-induced diabetic group compared to age-matched controls which revealed an organised, intact glomeruli, bowman's capsule and tubular structure is clearly visible in both groups (Figure 5.1).

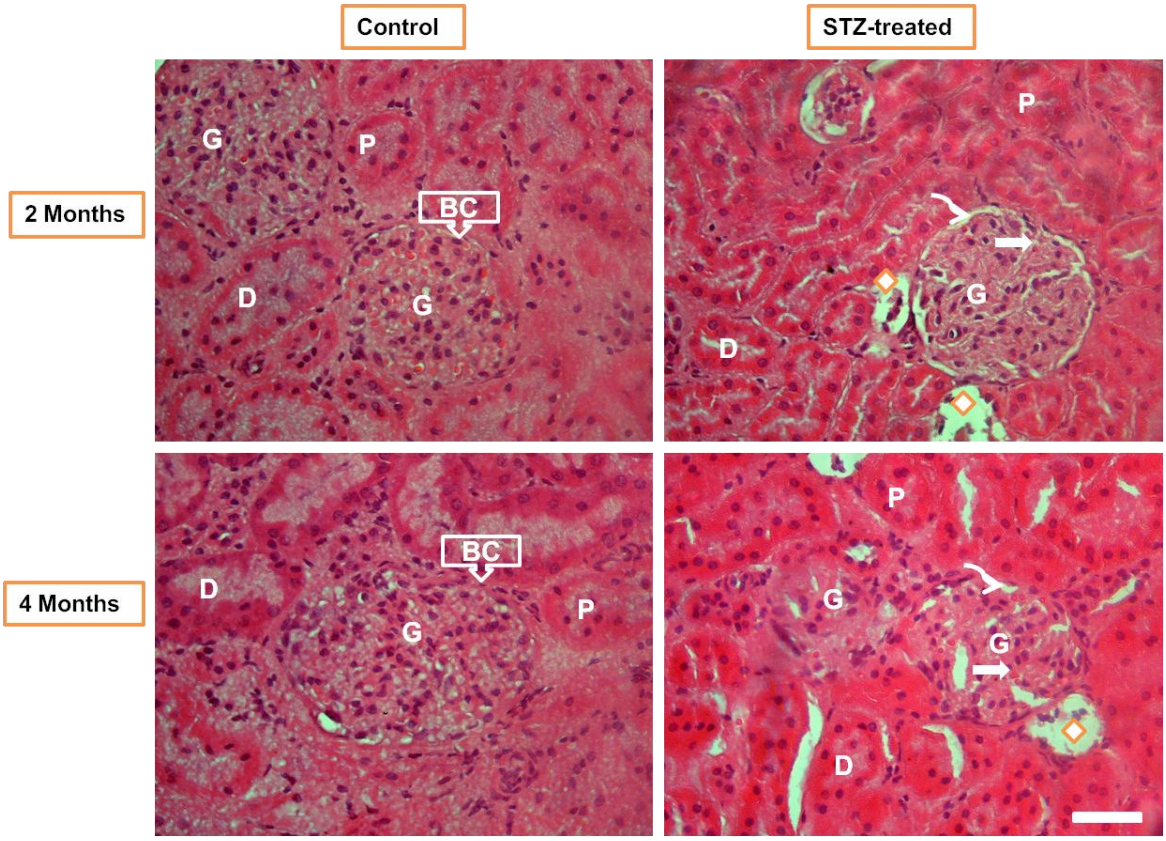

Figure 5.1: Kidney histology. Representative light photomicrographs detailing kidney histopathology in H & E stained kidney sections at 2 and 4 months of STZ-induced diabetes and age-matched controls. General glomeruli are intact and organised in structure. Original magnification X400. Photomicrographs are typical of 20-25 fields/per group. Scale bar in the right hand corner is 20 µm and calibration is the same for all micrographs. D: Distal tubulus, P: Proximal tubulus, G: Glomerulus, BC: Bowman's capsule, Tailed arrow: expanded glomerulus borders in DM group, Block arrow: RBC that make statis in glomerulus and interstisium, Diamond; clear cells.

3. Examination of the glomerular basement membrane in kidneys after 2 and 4 months of STZ-treatment

Figure 5.2 shows glomerular basement membrane examination, highlighted by Periodic Acid Schiff (PAS) stained sections in the left kidney at 2 and 4 months after STZ-induction compared to age matched controls. Light microscopy revealed thickened glomerular basement membranes in both STZ-treated groups compared to age-matched control groups (Figure 5.2). Increased mesengial expansion is clearly visible in both groups as the earliest morphological change in diabetic nephropathy due to increased deposition of the mesangial matrix together with a mild increase in mesangial cellularity, and mesangial cells hypertrophy (Wolf *et al*., 2003, Alsaad and Hersenberg, 2007).

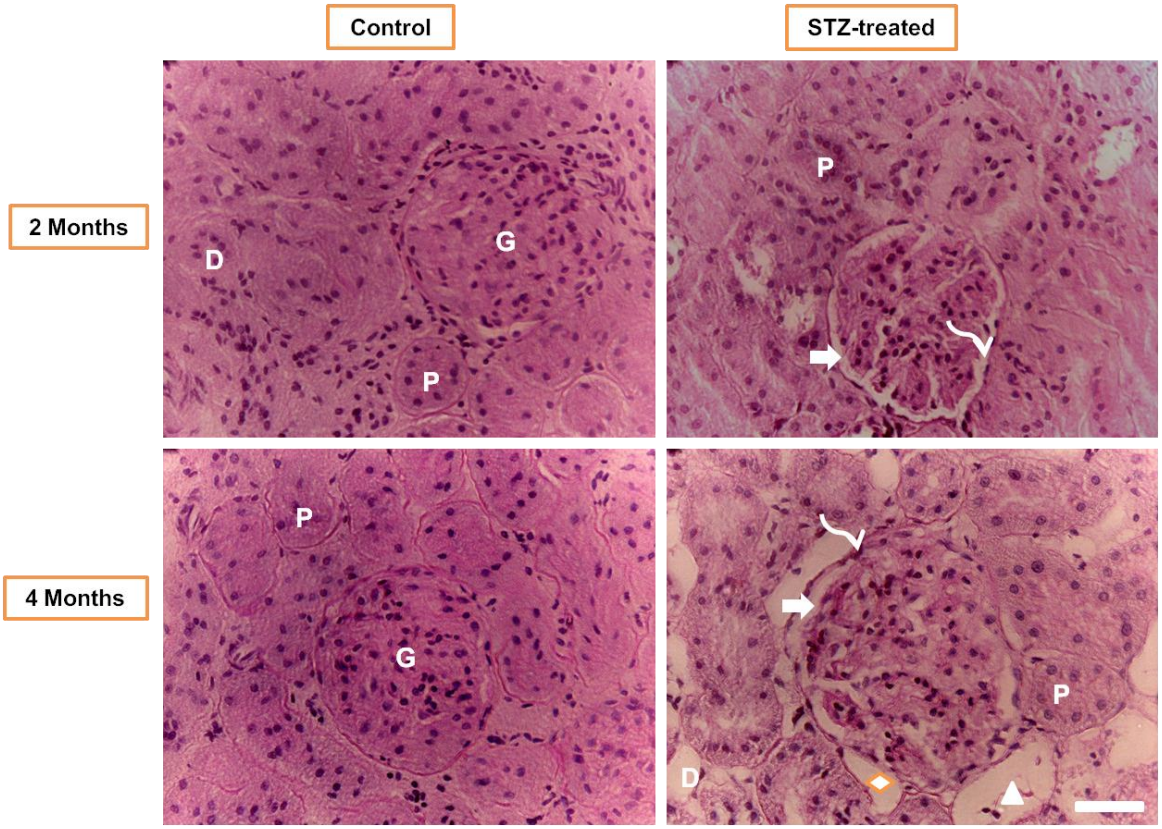

Figure 5.2: Investigations of glomerular basement membrane. Representative light micrographs of PAS stained kidney sections from 2 and 4 months after STZ-treatment. Glomerular basement membrane is seen to be increased in STZ-treated kidneys in comparison to age-matched controls. Original Magnification X400, Photomicrographs are typical of 35-47 fields/experimental groups consisting of 6-9 animals per group. Scale bar indicates 20 µm. D; Distal tubulus, P; Proximal tubulus, Tailed arrow; thickened basement membrane of glomerulus, Block arrow; increased Bowman's space, Diamond; clear cells of tubulus Triangle; Dilated tubulus.

4. Examination of kidney fibrosis after 2 and 4 months of STZ-treatment

Figure 5.3 shows results from light microscopy photomicrographs of Masson's Trichrome stained sections in the left kidney after STZ-induction compared to age matched controls. STZ-treated rats demonstrated significantly increased ECM deposition in both glomerulus and tubulus regions (Figure 5.3A and B). Quantitative analysis of fibrosis (C) in STZ-treated rats revealed significantly greater glomerular area coverage as compared to age-matched controls occupying 5.89±0.51% *vs.* 2.41±0.44% (p<0.05) at 2 months and 7.66±0.53% *vs.* 3.36±0.46% (p<0.01) at 4 months post STZ-treatment. This change was significantly (p<0.05) different between 2 and 4 months of STZ-treatment time.

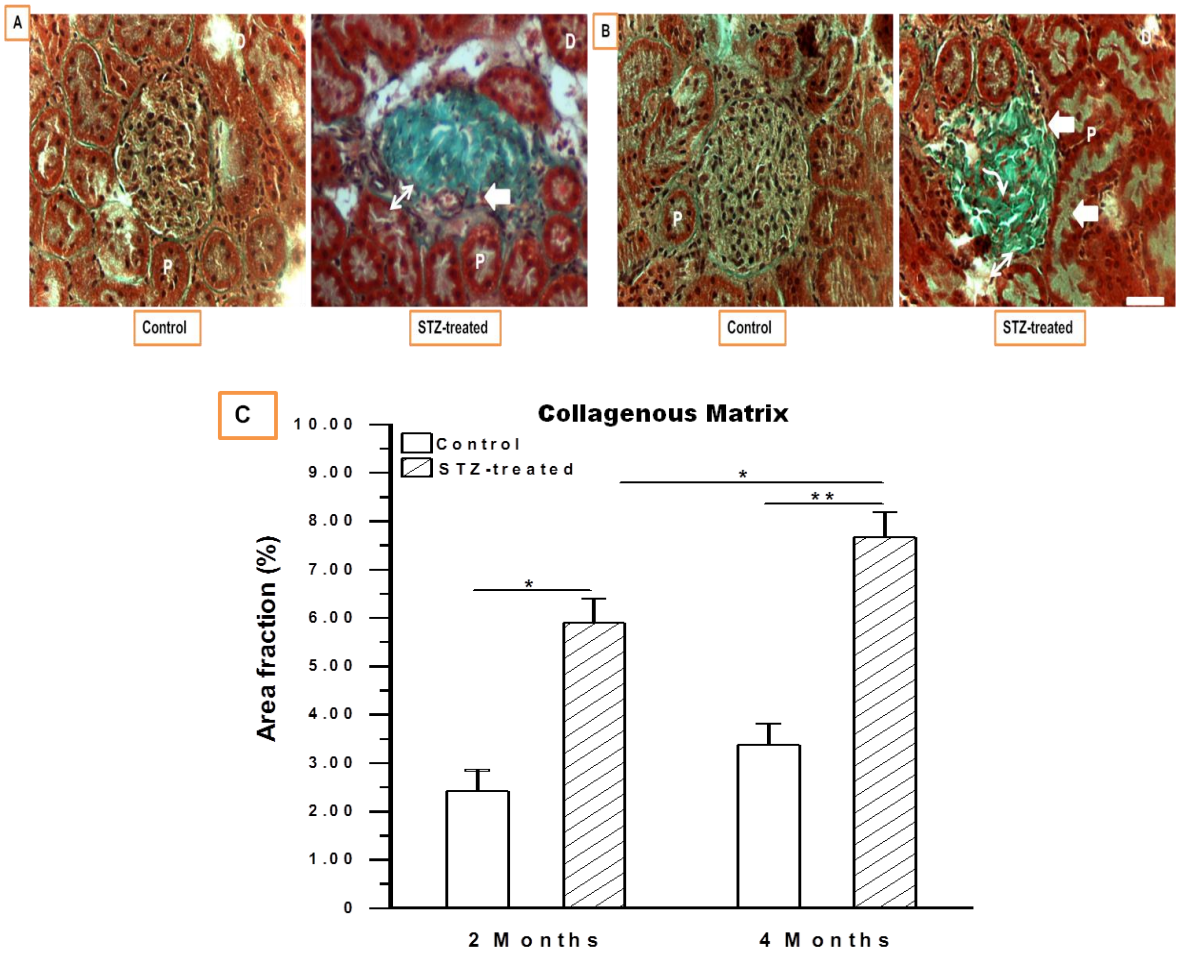

Figure 5.3: Investigations of ECM deposition in the kidney. Representative light micrographs of Masson's Trichrome stained myocardial sections from 2 months after STZ-treatment **(A)** and 4 months after STZ-treatment **(B)** and quantitative assessment of interstitial fibrosis using Image J analysis tool **(C)**. Original Magnification X400, Photomicrographs are typical of 35-47 fields/experimental group consisting of 6-9 animals per group. Scale bar indicates 10 µm. Bar chart data are Mean±S.E.M, *p< 0.05, **p< 0.01 One-way ANOVA followed by Bonferroni corrected t-tests for multiple comparisons.

5. Assessment of apoptosis in the kidneys after 2 and 4 months of STZ-treatment

Figure 5.4 represents significantly (p<0.05) increased immunoreactivity of cleaved (active) caspase-3 within the left kidney of STZ-treated diabetic rats compared to age-matched controls at 2 months (8.96±0.89 *vs.* 1.89±0.39) positive cells/mm^2 (p<0.05) and 4 months (9.66±1.00 *vs* 2.49±0.50) positive cells/mm^2 after STZ-treatment (Fig 5.4 C). This increase was significant (p<0.05) between the two treatment times.

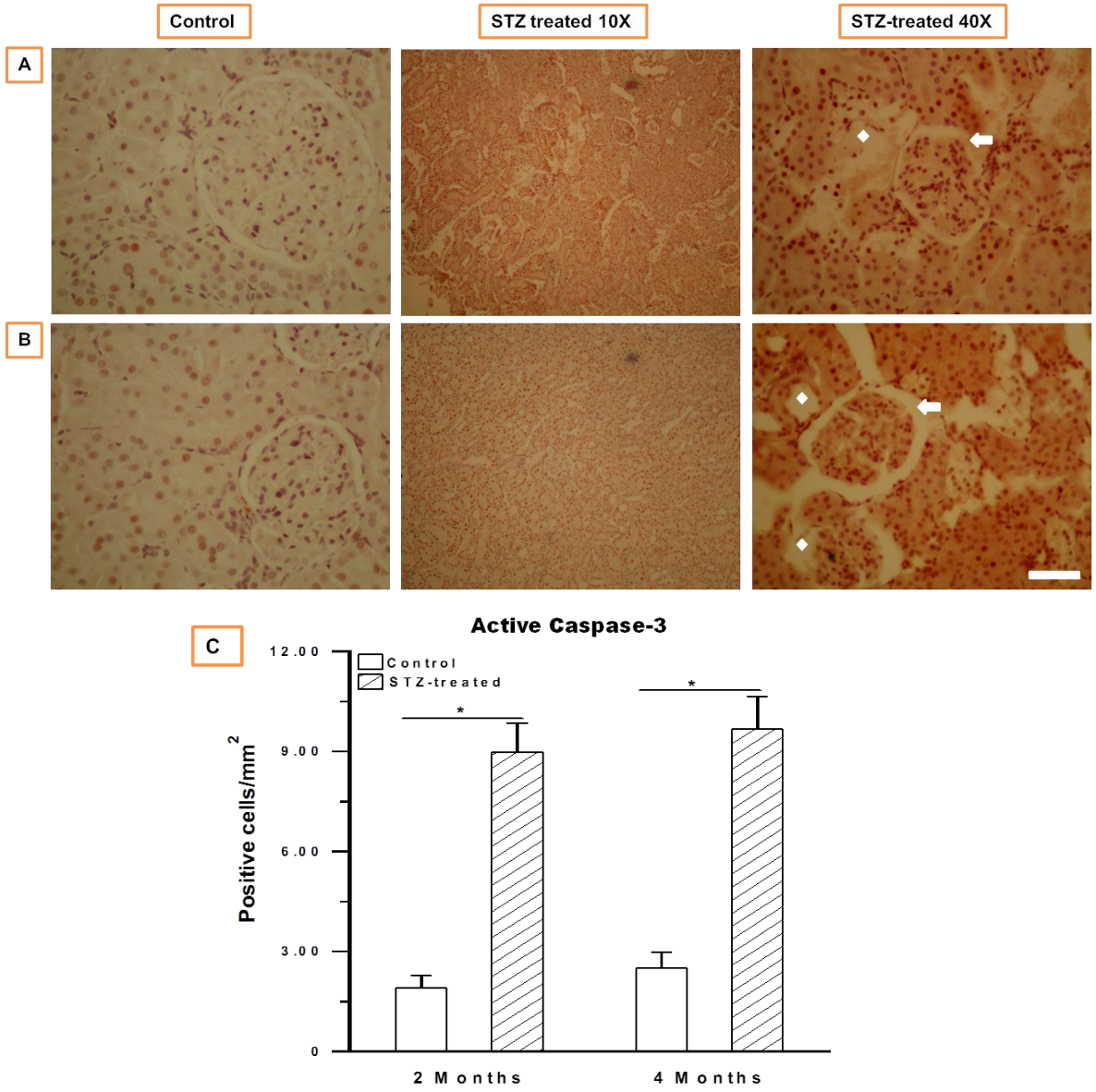

Figure 5.4: Kidney apoptosis. Active Caspase-3 positive cells (brown staining) in the kidneys from 2 months after STZ-treatment **(A)** and 4 months after STZ-treatment **(B)** and quantitative assessment of immunoreactivity using Image J **(C)**. Photomicrographs are typical of 15-20 fields/experimental groups consisting of 5-6 animals per group. Diamond; clear cells of tubulus, Block arrow; Thickened basement membrane and small glomerular size. Scale bar indicates 20 µm and calibration is the same for all photomicrographs. Bar chart data are Mean±S.E.M, *p< 0.05, One-way ANOVA followed by Bonferroni corrected t-tests for multiple comparisons.

6. Ultrastructural study of the kidneys after 2 and 4 months of STZ-treatment

Figure 5.5 represents the electron microscopic images of the left kidney at 2 and 4 months after STZ-induction compared to age-matched controls (Figure 5.5A). The earliest ultrastructural abnormality in diabetic nephropathy is postulated to be diffuse thickening of the GBM (Mauer *et al*., 1984; Drummond and Mauer, 2002). A variable degree of mesangial expansion by extracellular matrix deposition and increased mesangial cellularity is present in both STZ-induced groups (Steffes *et al*., 2001). A reduction in podocyte number (podocytopenia), along with a reduced podocyte per glomerulus ratio can also be seen in both groups after STZ-induction. Diffuse foot process effacement and podocyte detachments are another hallmark of DN (Dalla *et al*., 2003), are visible in both STZ-treated groups. Quantitative assessment of GBM width **(B)** using Image J analysis tool revealed significant ($p < 0.05$) increase at 2 months (510±1.35 *vs.* 330±1.15 µm) and 4 months after STZ-treatment (540±1.50 *vs.* 348±1.15 µm) compared to age-matched controls.

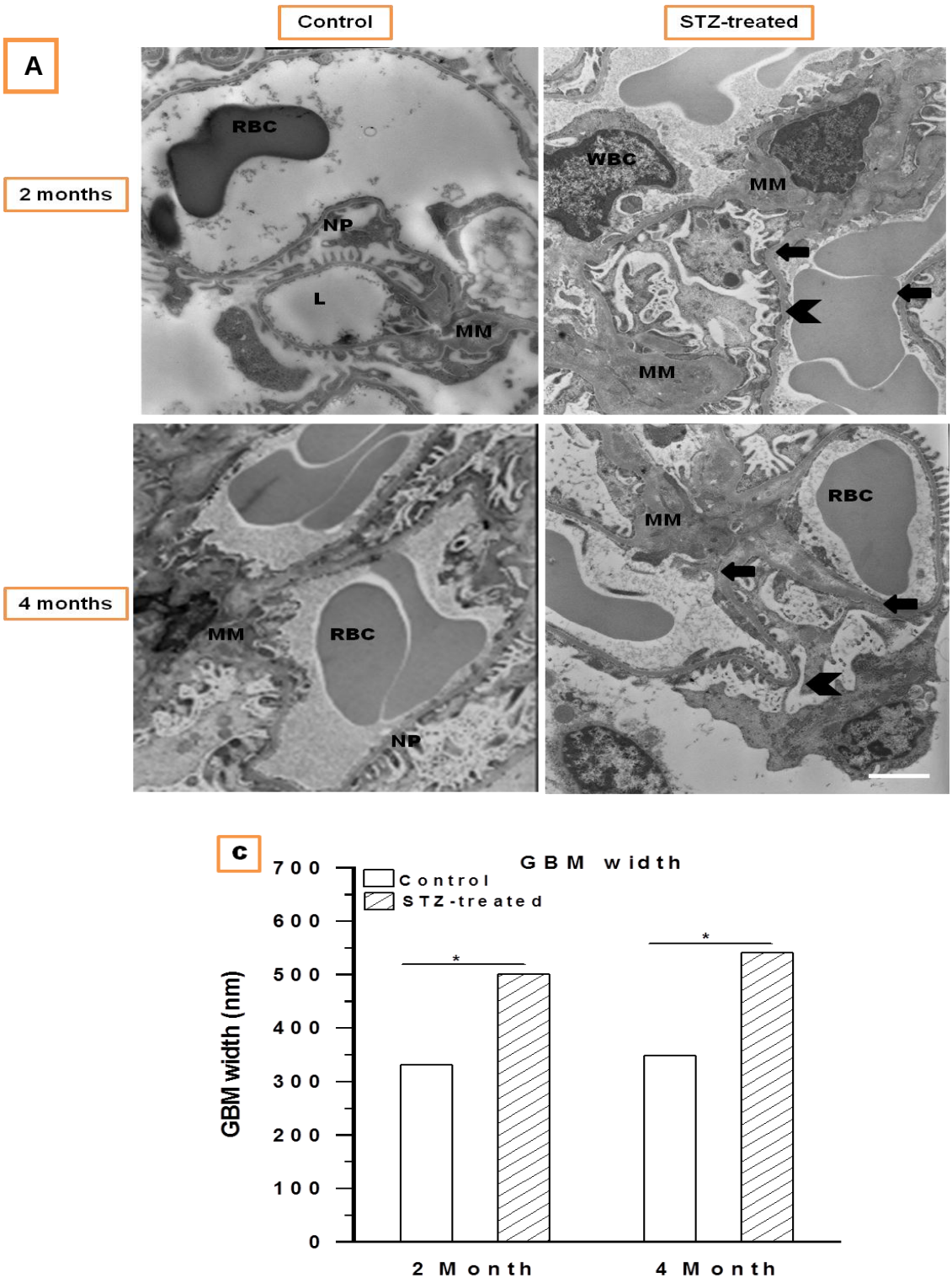

Figure 5.5: Kidney ultrastructure. Representative TEM electron micrographs showing increased mesangial matrix and glomerular basement membrane (GBM) together with increased detachment of podocytes in the kidneys from 2 and 4 months after STZ-treatment **(A)** and quantitative assessment of GBM (nm) using Image J analysis tool **(B)**. Original magnification X14,000. Electron micrographs are representative of 35-45 photomicrographs studied from 5-6 animals. Scale bar in the lower right indicates 1µm. MM; Mesangial Matrix, Block arrow; Thick GBM, NP; Normal Podocyte, Chevron; Podocyte detachment. Bar chart data are Mean±S.E.M, **P*< 0.05, One-way ANOVA followed by Bonferroni corrected t-tests for multiple comparisons.

7. Molecular events underlying structural remodelling in the Kidneys of STZ-induced diabetic rats after 2 and 4 months of STZ treatment.

a. Transcriptional profile of ECM

Figure 5.6 represents gene expression of ECM components collagen 3α, collagen 1α, fibronectin and elastin quantified using qRT-PCR. Significant (p<0.05) increase in collagen 3α after 2 months (1.00±0.12 *vs.*0.61±0.09) and 4 months (1.45±0.13 *vs.* 0.68±0.07 ratio units) (Figure 5.6B). Similarly, collagen 1α was also increased after 2 months (0.89±0.14 *vs.* 0.53±0.10 ratio units) and 4months (1.23±0.13 *vs.* 0.58±0.11 ratio units) (Figure 4.6A) of STZ-induced diabetes compared to age-matched control. Both type of collagens showed significant (p<0.05) differences between the two age groups indicating that collagen expressions are changed over time due to the duration of diabetes. Fibronectin (Figure 5.6C) and Elastin (Figure 5.6D) were significantly increased at 2 months (fibronectin; 1.26±0.14 *vs.* 0.92±0.07 ratio units), (elastin; 0.98±0.13 *vs.* 0.55±0.05 ratio units) and 4 months (fibronectin; 1.59±0.11 *vs.* 0.92±0.07 ratio units), (elastin; 1.09±0.12 *vs.* 0.59±0.08 ratio units) after STZ-induction compared to age-matched control. However, only fibronectin revealed an adult vs young adult effect that was significantly (p<0.05) evident. Furthermore, these changes were accompanied by divergent alterations in ECM regulators. Figure 5.7 represents gene expression of ECM regulators MMP2, MMP9, TIMP4, CTGF, Connexin 43, Integrin 5α and Vimentin. Kidney mRNA gene expression for MMP2 (Figure 5.7A) revealed a significant (p<0.05) down-regulation at 2 months (0.56±0.12 *vs.* 1.00±0.11 ratio units) and 4 months (0.58±0.13 *vs.* 1.13±0.10 ratio units) after STZ-induction compared to age-matched control. On the other hand, MMP9 (Figure 5.7B) was significantly (p<0.05) up-regulated at 2 months (1.16±0.11 *vs.* 0.86±0.02 ratio units) and 4 months (1.31±0.12 *vs.* 0.91±0.10 ratio units) after STZ-induction compared to age-matched controls. Interestingly, endogenous MMP tissue inhibitor TIMP4 (Figure 5.7C) was up regulated at 2 months (1.00±0.12 *vs.* 0.67±0.06 ratio units) and 4 months (1.32±0.11 *vs.* 0.93±0.05 ratio units) after STZ-induction compared to age-matched control and this difference was significantly (p<0.05) evident between the two age groups. mRNA gene expression level for CTGF (Figure 5.7D), was significantly (p<0.05) increased at 2 months (1.11±0.14 *vs.* 0.57±0.04 ratio units) and 4 months (1.23±0.15 *vs.* 0.79±0.08 ratio units) after STZ-induction compared to age-matched controls. Additionally, a significant (p<0.05) down-regulation in gap junction protein Cx43 (Figure 5.7E) was evident in the STZ-induced diabetic rat kidney after 2 months (0.89±0.12 *vs.* 1.28±0.06

ratio units) and at 4 months ($p<0.01$) (0.45±0.14 *vs.* 1.39±0.09 ratio units) of STZ-induction compared to age-matched control and this difference was significantly evident between the two age groups. Additionally, mRNA level of Integrin 5α (Figure 5.7F) was significantly ($p<0.05$) increased at 2 months (1.08±0.13 *vs.* 0.49±0.06 ratio units) and 4 months (1.19±0.15 *vs.* 0.55±0.09 ratio units) after STZ-induction compared to age-matched control. Integrin 1α was also studied but remained unaffected by the disease. Finally, mRNA level of vimentin (Figure 5.7G) was significantly ($p<0.05$) up-regulated at 2 months (1.08±0.13 *vs.* 0.49±0.06 ratio units) and 4 months (1.19±0.15 *vs.* 0.55±0.09 ratio units) after STZ-induction compared to age-matched control. Taken together, gene expression profile of ECM components in the kidneys revealed marked changes that were accompanied by parallel alterations in ECM regulating agents (MMP2 and MMP9) and tissue inhibitor (TIMP4), gap junction proteins and vimentin expression. Imbalance in these expressions could lead to abnormal ECM deposition which remains as one of the hallmarks of DN.

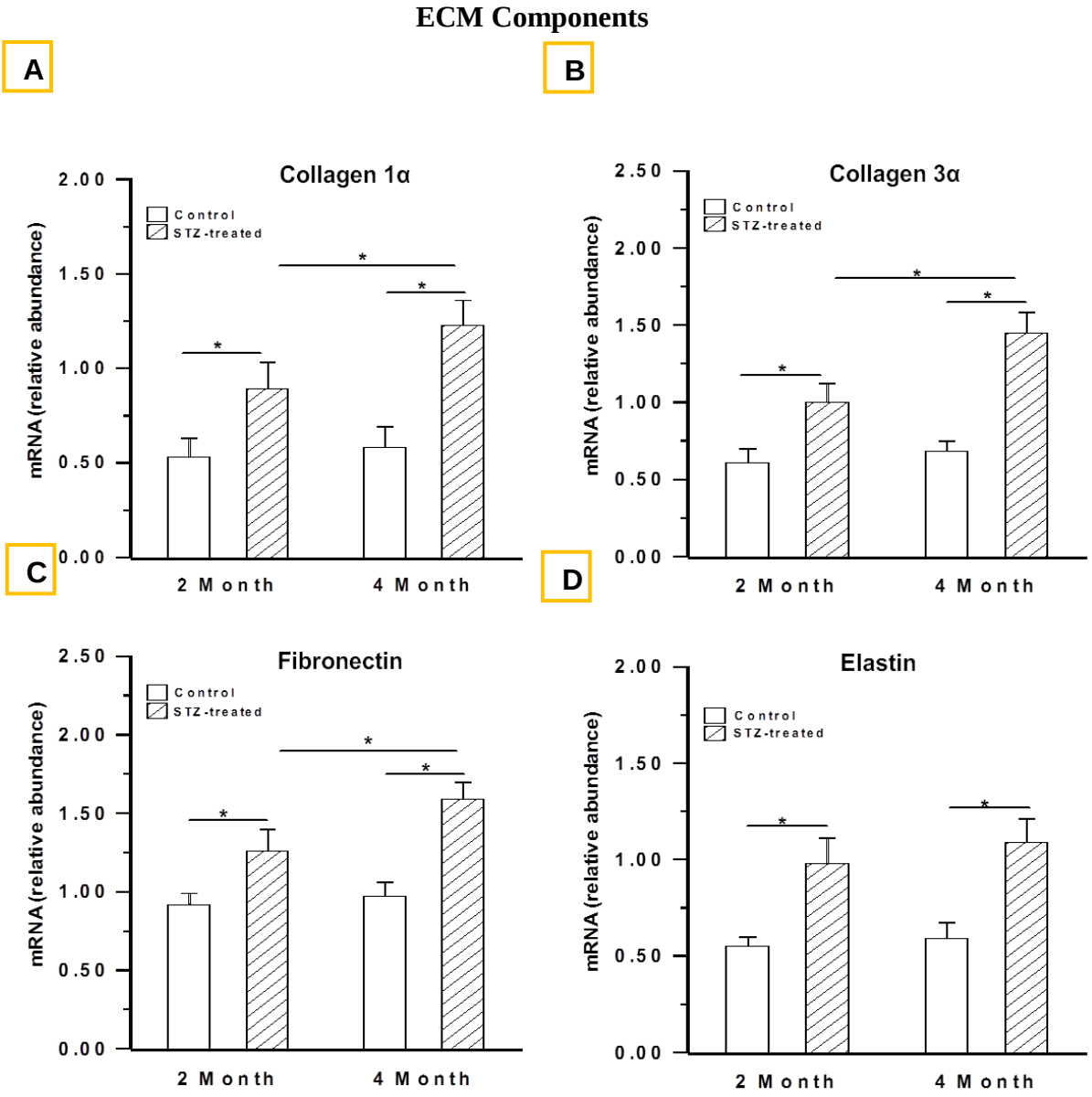

Figure 5.6: ECM components gene expression. Summarised data showing gene expression for ECM components Collagen 1 **(A)**, Collagen 3 **(B)**, Fibronectin **(C)** and Elastin **(D)** in STZ-treated and age-matched controls at 2 and 4 months post STZ-treatment. Results are representative of 8 animals/per group conducted in triplicate. RT-PCR amplification was normalised to that of GAPDH. Data are expressed as Mean±S.E.M. Lines over bars indicate significance * $p<0.05$, One-way ANOVA followed by Bonferroni corrected t-tests for multiple comparisons.

ECM Regulatory Components

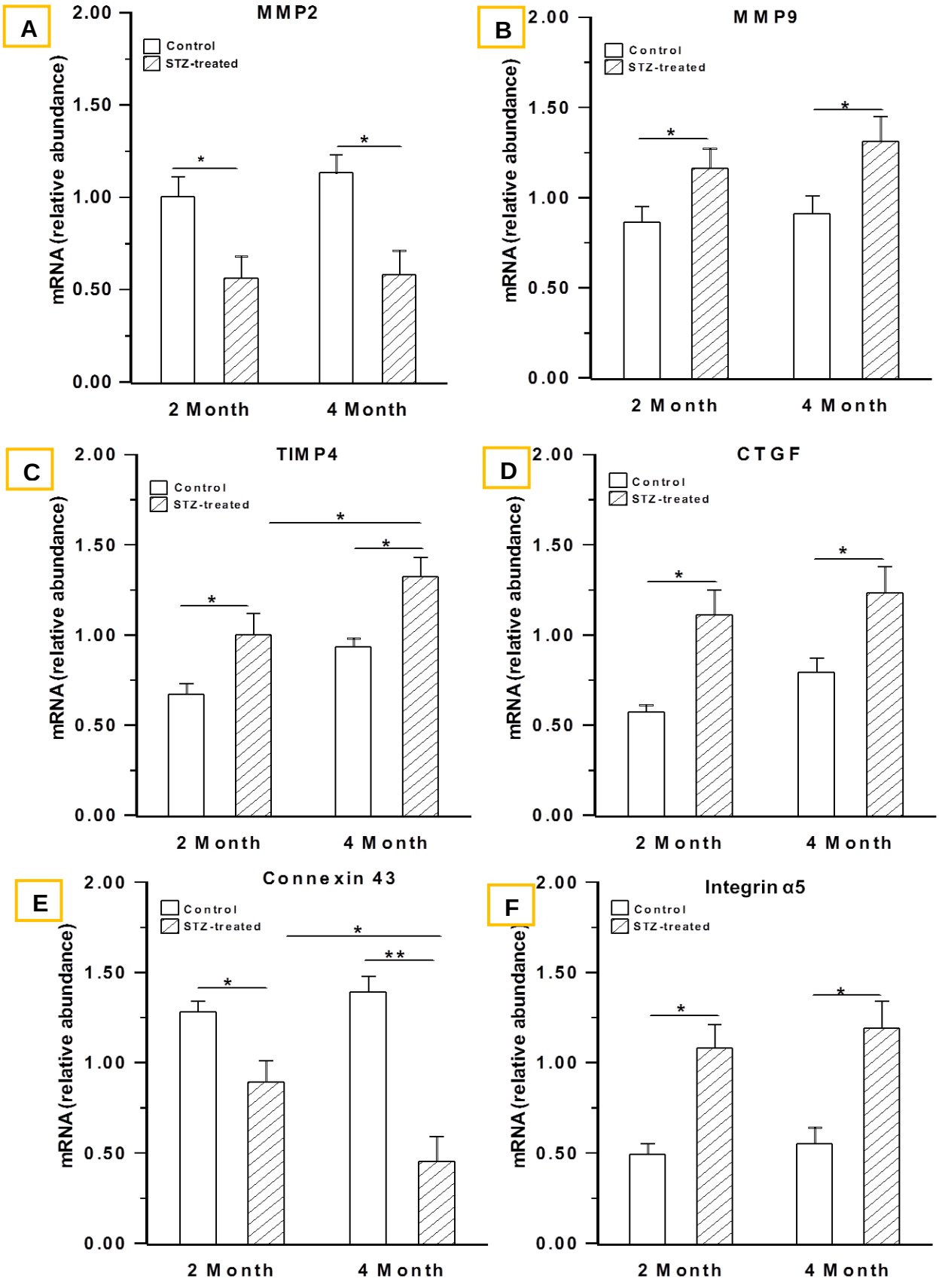

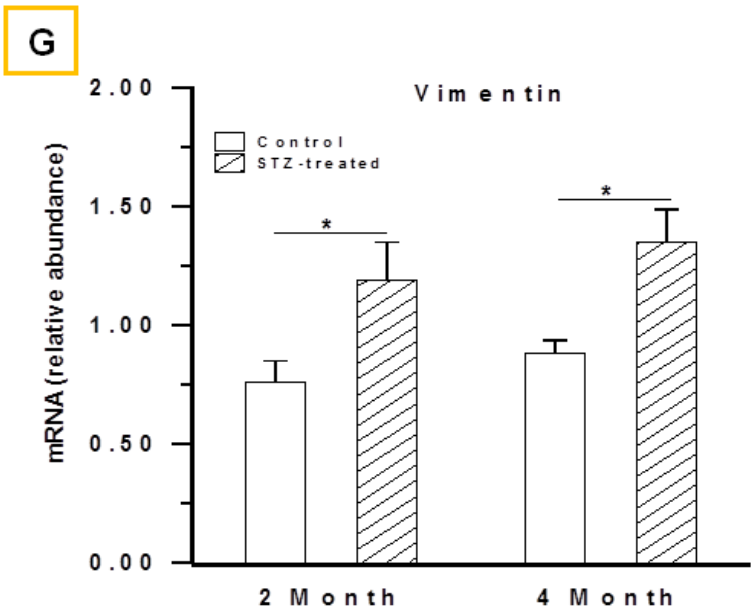

Figure 5.7: **ECM regulatory components gene expression.** Summarised data showing gene expression for ECM regulators MMP2 **(A)**, MMP9 **(B)**, TIMP4 **(C)**, CTGF **(D)**, Connexin 43 **(E)**, Integrin 5α **(F)**, and Vimentin **(G)** in STZ-treated and age-matched controls at 2 and 4 months post STZ-treatment. Results are representative of 8 animals/per group conducted in triplicate. RT-PCR amplification was normalised to that of GAPDH. Data are expressed as Mean±S.E.M. Lines over bars with asterisk indicate significance * $p<0.05$, ** $p<0.01$, One-way ANOVA followed by Bonferroni corrected t-tests for multiple comparisons.

8. Assessment of hypertrophy in kidneys

Hypertrophy biomarkers ANP and BNP were assessed in STZ-induced and age-matched controls at 2 and 4 months post STZ-treatment. Gene expression analysis revealed that ANP was significantly (p<0.05) up-regulated at 2 months (1.55±0.16 *vs.* 0.56±0.09 ratio units) and 4 months (2.50±0.14 *vs.* 0.67±0.06 ratio units) after STZ-induction compared to age-matched control. There was a significant (p<0.05) difference between the two age groups, indicating an adult vs young adult effect. On the other hand, BNP was significantly (p<0.05) up-regulated at 4 months (0.89±0.12 vs. 0.55±0.09 ratio units) after STZ-induction compared to age-matched controls. However, no significance (p<0.05) was observed at 2 months (0.55±0.13 vs. 0.49±0.66 ratio units) after STZ-induction (Figure 5.8B).

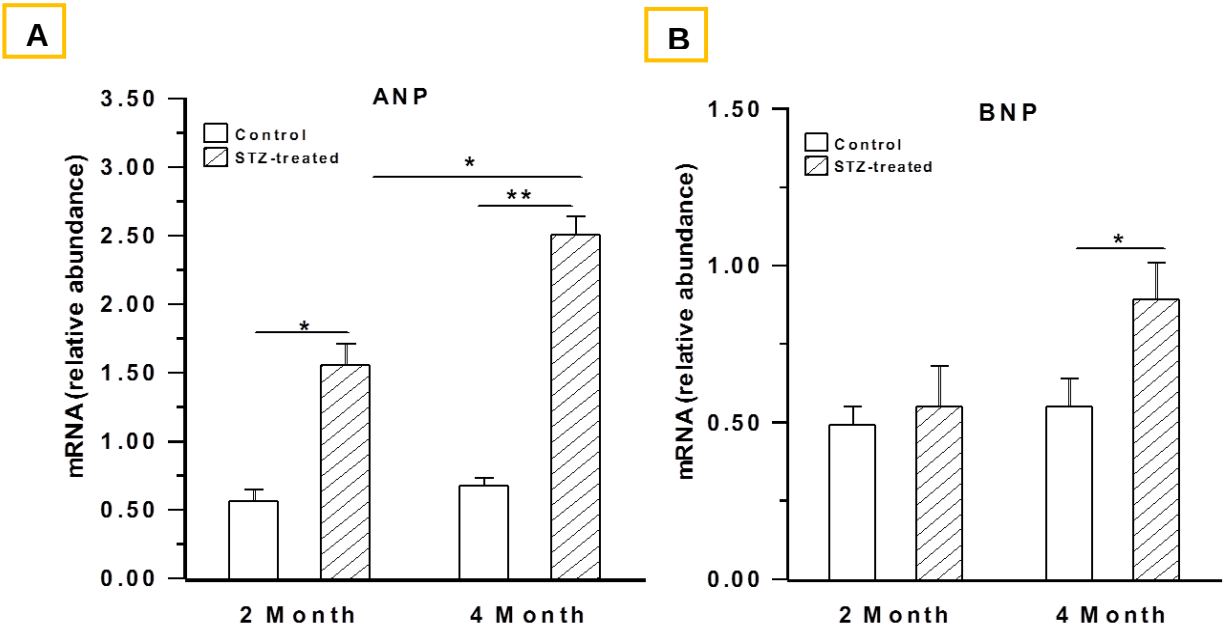

Figure 5.8: Hypertrophy biomarkers ANP and BNP gene expression. Summarised data showing ANP **(A)**, and BNP **(B)** gene expression in STZ-treated and age-matched controls at 2 and 4 months post STZ-treatment. Results are representative of 8 animals/per group conducted in triplicates. RT-PCR amplification was normalised to that of GAPDH. Data are expressed as Mean±SEM. Lines over bars with asterisk indicate significance * p<0.05, ** p<0.01, One-way ANOVA followed by Bonferroni corrected t-tests for multiple comparisons.

9. Molecular events characterising extracellular matrix proliferation in the Kidneys after 2 and 4 months of STZ-treatment

Figure 5.9 represents an increased TGFβ1 mRNA gene expression and active TGFβ1levels in plasma and kidney samples from rats at 2 and 4 months of STZ-treatment compared with age-matched controls. Total and active TGFβ1 concentration in kidneys and plasma was evaluated by ELIZA. Active TGFβ1 significantly ($p< 0.05$) increased in plasma after 2 months (2.72±0.20 *vs.* 1.15±0.04 ng/ml) of STZ-induced diabetes compared to control whereas no significant differences were observed after 4 months (2.36±0.06 *vs.* 2.18±0.07 ng/ml) of STZ-treatment (Figure 5.9A). Total TGFβ1 levels were significantly ($p<0.05$) increased in STZ-induced diabetic LV at 2 months (9.53±0.12 *vs.* 3.44±0.20 pg/mg of total protein) and 4 months (11.92±0.32 *vs.* 4.73±0.15 pg/mg of total protein) after STZ-treatment compared to age-matched control and this significance was apparent between the two age groups (Figure 5.9B). Similarly, active TGFβ1 levels in kidneys were significantly ($p<0.01$) increased after 2 months (60.75±0.38 *vs.* 28.83±0.35 pg/mg of total protein) and 4 months (59.68±0.32 *vs.* 36.33±0.28 pg/mg of total protein) of STZ-induction compared to age-matched control (Figure 5.9C). However, these differences were not significantly different between the two age groups. TGFβ1 gene expression was also significantly ($p<0.05$) different between the two age groups (after 2 months; (1.25±0.13 vs. 0.55±0.05) and after 4 months; (1.79±0.15 vs. 0.88±0.08) in STZ induced diabetic rat LV compared to age-matched control this significance was apparent between the two age groups (Figure 5.9D).

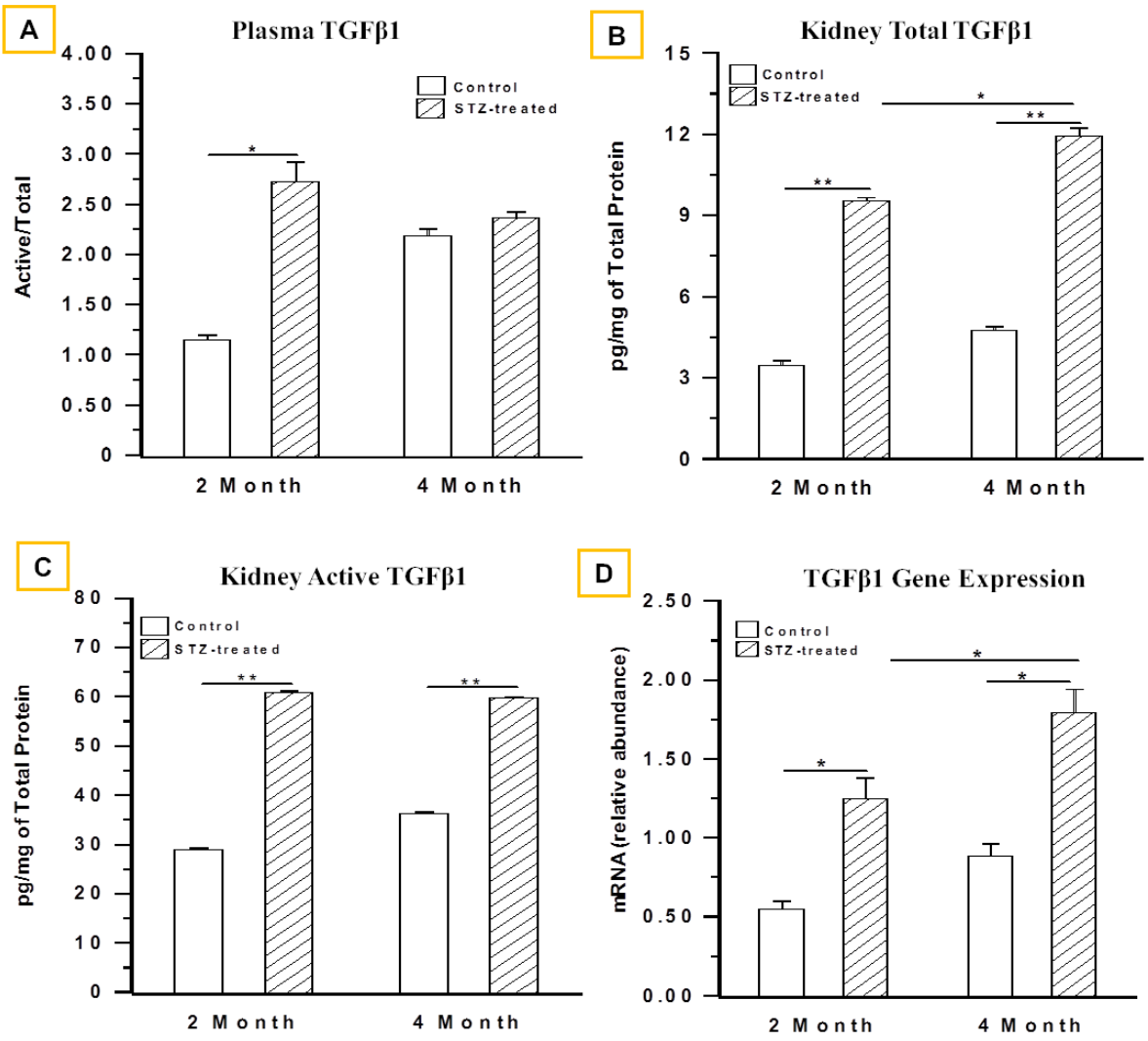

Figure 5.9: **TGFβ1 protein level and gene expression profile.** Summarised data from ELIZA showing ratio of active:total TGFβ1 protein in plasma **(A)**, total TGFβ1: total extracted kidney protein **(B)** and active TGFβ1: total extracted kidney protein **(C)** at 2 and 4 months of STZ-treatment with age-matched control animals (n=3/group). mRNA gene expression of TGFβ1 **(D)** at 2 and 4 months of STZ-treatment with age-matched controls. The results of both ELIZA and qRT-PCR are representative of 3 individual experiments conducted in triplicate. RT-PCR amplification was normalised to that of GAPDH. Data are expressed as Mean±S.E.M. Lines over bars indicate significance * $p<0.05$, ** $p<0.01$, One-way ANOVA followed by Bonferroni corrected t-tests for multiple comparisons.

5.5 Discussion

Summary of key findings:

1. Kidney remodelling in STZ-induced T1DM rats at 2 and 4 months of DM duration is characterised by significant elevations in ECM deposition and apoptotic cell death compared to age-matched control animals.
2. Ultrastructural alterations revealed significant increases in GBM membrane.
3. Significant molecular alterations in key ECM components and regulatory mechanisms, indication of a remodelling process occurring in the kidneys.
4. Significantly increased expression, activity and plasma levels of TGFβ1 in fibrotic remodelling of the kidney.
5. Kidney hypertrophy marked elevations in ANP and BNP is evident in STZ-induced T1DM rats at 2 and 4 months of DM compared to age-matched controls.
6. Adult vs young adult in STZ-induced T1DM can elicit severe changes to kidney structural and biochemical alterations leading to DN. TGFβ1 activity may represent to a key agent in the process.

Diabetic nephropathy

DN is a major microvascular complication of diabetes and a leading cause of death among diabetic patients. In this study the morphological and molecular consequences of HG-induced diabetes have been characterised in the left kidney of STZ-induced type 1 diabetics rats compared to age-matched controls. Preliminary experiments in the laboratory revealed similar results in the right kidney, thus it was decided to undertake all the studies employing only the left kidney. Firstly, the general characteristics of rats revealed marked elevations in blood glucose levels in STZ-induced rats as described previously in chapter 3. Of note here, is the significant increase in kidney weight observed in the STZ-induced rat at 2 and 4 months after STZ-induction compared to control. Conversely, kidney weight to body weight ratios were significantly increased compared to respective age-matched controls and this increase was more severe with age. The increase in kidney size refers to renal hypertrophy which is the hallmark of DN (Wolf, 2004; Border *et al*., 1996; Branton & Kopp, 1999). This increase in size is primarily due to glomerular and tubular hypertrophy, although some low-grade proliferations of glomerular cells are present in the early stage (Border *et al*., 1996;

Caramori *et al*., 2006). Glomerular hypertrophy is in part the result of glomerular cell hypertrophy and recent studies have suggested that the diabetic milieu *per se*, hemodynamic changes and local growth factors such as TGFβ1 and angiotensin II (ANG II) are mediators in the pathogenesis of glomerular cell hypertrophy (Wolf, 2004; Hoffman *et al*., 1998; Leehy *et al*., 2000). The results of this study are consistent with previously published reports on renal hypertrophy (Brever *et al*., 1996).

In addition, previous *in vitro* studies have demonstrated that high glucose, TGFβ1 and ANG II, mediators of DN, are closely linked with the Akt pathway (Mahimainathan *et al*., 2006; Chuang *et al*., 2007; Song *et al*., 2007; Kaatla *et al*., 2008). Owing to these findings, the activity of Akt under diabetic conditions has been heavily investigated, but discrepancies remain, some have demonstrated an increase in Akt phosphorylation (Mahimainathan *et al*., 2006; Gorin *et al*., 2005; Nagai *et al*., 2005) whereas others have have reported reduced activity of Akt (Tejada *et al*., 2008; Rane *et al*., 2010). The reasons for the divergence of changes in Akt activity under diabetic conditions are not clear, but differences between the duration of diabetes or of high-glucose stimulation or the species of animals may contribute to these disparities. Additionally, this study revealed marked elevations in ANP and BNP gene expression levels which are suggested to be sensitive biomarkers for hypertrophy. The findings of an up-regulation in ANP and BNP levels in the left kidney at 2 and 4 months post STZ-induction compared to age-matched controls which is consistent with previous studies (Shin *et al*., 1997). Additionally, BNP level is also a predictor of cardiac events in diabetes (Bhalla *et al.,* 2004). The Breathing Not Properly study found a weak but significant correlation between glomerular filtration rate (GFR) and BNP, and suggested higher cut off points for patients with GFR\60 ml/min/1.7 m2 (Daniels & Maisel, 2007). Therefore, monitoring of ANP and BNP can play an important role in the management of DN.

Ultrastructural alterations in STZ-induced T1DM

Ultrastructural analysis employed in this study revealed an increase in GBM thickness in kidney from 2 and 4 months of STZ-induced diabetes compared to age-matched control animals. Previous literature suggests that GBM thickening is a characteristic early change in type 1 (Mauer *et al*., 1984; Drummond & Mauer, 2002) and type 2 DN (White & Bilous, 2000) and increases with duration of disease (Perrin *et al*., 2006; Tervaret *et al*., 2010). GBM thickening is a consequence of ECM accumulation, with

increased deposition of normal ECM components together with altered expression of the regulators of EM, similar to the findings of this study (Figure 5.6). It is described that such an increase in GBM results from an increased production of these proteins, their decreased degradation, or the combination of both. GBM thickening has previously been described as a "prediabetic" lesion in studies with patients with proteinuria without overt diabetes, thus GBM thickening may already be present in T1DM patients (Drummond & Mauer, 2002). Another hallmark feature of DN is the derangement of the architecture of podocytes and glomerular endothelial cells participate in initiation and progression of nephropathy and have significant effect on kidney function (Toyada *et al*., 2007; Patalunan *et al*., 1997). Podocyte detachment (PD), (Figure 5.5) and structural changes in DN have previously been described in T1DM with similar results to the findings of this study (Meyer *et al*., 1999; Lemley *et al*., 2000; Dalla *et al*., 2003; Toyada *et al*., 2007; Diez-Sampedro *et al*., 2011; Siddiqi & Advani, 2013).

Caspase-3 increases in STZ-induced T1DM kidneys

Furthermore, increased apoptosis, mediated by caspase-3 immunoreactivity has been highlighted in this study. STZ-induced diabetic rats at 2 and 4 months presents with increased apoptotic cells compared to respective age-matched control groups. Apoptosis has been documented in the course of various renal diseases and more frequently in DN (Shimizu *et al*., 1996; Kitamura *et al*., 1998; Susztak *et al*., 2006; Verzola *et al*., 2007). Cell death by apoptosis is believed to be involved in the process of mesangial cell loss in the late stage of DN (Dalla *et al*., 2001). In addition, apoptosis is considered to be one of the underlying causes of podocyte loss, which contributes to the development of albuminuria in DN (Verzola *et al*., 2007; Susztak *et al*., 2006). STZ-induced diabetic rats at 2 and 4 months displayed signs of tubular as well as interstitial apoptosis compared to respective control groups and these results are in correlation with previously published study in STZ-diabetic rat kidney (Kumar *et al*., 2004). They postulated that this effect can be reversed by insulin therapy. Furthermore, the effects of type 1 (AT_1) and type 2 (AT_2) Ang II receptor blockade suggest that Ang II is involved in mediating the process of apoptosis in the diabetic kidney and deserves therapeutic interventions (Sanz *et al*., 2008).

TGFβ1 in kidney remodelling

The early changes in incipient diabetic kidney disease are characterised by an increase in kidney size, glomerular volume and kidney function, and later on by the development of mesangial cell proliferation, accumulation of glomerular extracellular matrix, increased urinary albumin excretion (UAE), glomerular sclerosis, and tubular fibrosis. Later stage overt DN is clinically characterised by proteinuria, hypertension, and progressive renal insufficiency (Mason & Wahab, 2003; Maric *et al*., 2004). The search for the significant pathogenic mechanisms in onset of diabetic kidney disease has focused on the early events, at the point in time when these early pathophysiological changes take place.

Due to their potential roles in inducing cellular differentiation and/or proliferation, growth factors such as TGFβ1 have attracted much attention in diabetes research as explained in Chapter 1 and 4. The present study supports the previous observations from this and other laboratories that TGFβ1 is up-regulated in the diabetic kidney and that this upregulation is associated with glomerulosclerosis and tubulointerstitial fibrosis (Ziyadeh *et al*., 1993; Mason & Wahab, 2003; Maric *et al*., 2004; Wolf, 2003). Numerous studies have demonstrated that TGFβ1 promotes renal cell growth, stimulates synthesis of key ECM proteins including, type I and type II collagen, laminin and fibronectin and inhibits ECM degradation via decreasing the activity of MMPs (Border *et al*., 1996; Chen *et al*., 2001; Hill *et al*., 2000; Hong *et al*., 2001). These results are consistent with findings from this study having shown marked elevations in ECM components (Col 1α, Col 3α, elastin and fibronectin) together with glomerusclerosis in the STZ-induced diabetic kidney at 2 and 4 months post STZ-induction compared to age-matched control animals.

Numerous studies have demonstrated the importance of TGFβ1 in the pathophysiology of renal disease, including DN. Furthermore, the present study showed an overall increase in TGFβ1 activity in left kidney of 2 and 4 months after STZ-induction compared to respective age-matched controls (Figure 5.9A-C). Elevated TGFβ1 activity was correlated with parallel findings of increased TGFβ1 gene expression that is consistent with previous findings with correlations to fibrosis in animals (Hong *et al*., 2001; Benigni *et al*., 2006) and in humans (Border *et al*., 1996; Yamamoto *et al*., 1993). A previous study confirmed the finding that TGFβ1 is over expressed in glomerular

mesangial cells, proximal and distal tubules in the STZ-induced diabetic rat after 9 weeks of diabetes (Mankhey *et al*., 2005). They postulated that supplementation with 17β-estradiol (E2) for 8 weeks following a 9-week duration of diabetes attenuates TGFβ1 protein expression, suggesting that one of the mechanisms by which E2 exerts its renoprotective effects in the diabetic kidney is by through regulating the expression of locally active cytokines, such as TGFβ1. Increasing evidence suggests that TGFβ1 exerts its profibrotic effect through activation of Smad2/3 which then forms a complex with Smad4 that is then translocated into the nucleus to up-regulate transcription of profibrotic genes (Nakagawa *et al*., 2004: Wells *et al*., 2005). Other studies have also reported increases in renal cortical Smad2/3 and Smad4 in the diabetic kidney (Furuse *et al*., 2004; Huang & Preisig, 2000; Isono *et al*., 2002). A recent study examined TGFβ1 gene expression and protein expression in kidneys of STZ-diabetic rats (Hill *et al*., 2013). Collectively, the results indicated that TGFβ1 protein was seen to be decreased in the kidney glomerulus in the acute phase (14-30 days) of STZ-induced diabetic disease and an increase in tubular TGFβ1 protein was detected by immunohistochemistry. These increases were reflected in increased TGFβ1 protein detected by Western blotting between days 30–90. Conversely, TGFβ1 mRNA showed a clear increase in the amount of message transcribed during the acute phase period, an observation that confirms previous reports of changes in the mRNA. This apparent paradox of protein *vs.* mRNA levels indicates that, in addition to the compartmentalisation of the TGFβ1 protein, there may be some posttranscriptional modifications or protein degradation occurring during disease progression in the remodelling glomerulus (Dixon & Maric, 2007).

In addition, CTGF is another pro-sclerotic cytokine that has been shown to be involved in both the early and later stages of DN. CTGF expression is seen to be increased in experimental diabetic glomerulosclerosis (Riser *et al*., 2000; Twigg *et al*.,2002). Elevated CTGF levels in glomeruli of NOD mice appear to correlate with the duration of diabetes (Wahab *et al*., 2001). Elevated CTGF expression has also been detected in human DN (Twigg *et al*., 2002; Ito *et al*., 1998; (Wahab *et al*., 2001). Gromerular CTGF levels have been found to be elevated in diabetic patients with microalbuminuria as well as overt nephropathy (Umezono *et al*., 2006). Several *in vitro* studies have shown that CTGF is induced in renal cells by both high glucose and AGE (Riser *et al*., 2000), as well as ROS (Park *et al*., 2001), which they generate. CTGF is one of the TGFβ1 inducible immediate early genes and has shown to be induced by TGFβ1 (Blom

et al., 2001). Several studies have highlighted the role of TGFβ1 in inducing CTGF gene expression via Smad binding elements (SBE) and a unique TGFβ1 response element in the CTGF promoter (Chen *et al*., 2002). CTGF is a crucial mediator for TGFβ1 stimulated matrix protein expression. Additionally, CTGF has been shown to mediate TGFβ1 induced increases in fibronectin and collagen type I (Yokai *et al*., 2002). Collectively, these observations are consistent with the findings of this study and correlate to the fact that although all these factors likely interact in the pathogenesis of DN, the driving force behind the cytokine expression is most likely to be HG, directly or indirectly.

ECM proliferation in the kidney

In addition to the structural changes described above, DN is associated with an excessive accumulation of ECM proteins in the mesangial cells, reffered to as glomerulosclerosis, which narrow the glomerulus lumen. These ECM depositions are closely related with loss of kidney function and reduced survival rates (Kato *et al*., 2007). The thickening of the glomerular basal membrane is associated with increases in collagen type IV, laminin, and proteoglycans (Burns *et al*., 2006; Wan *et al*., 2010). Similarly, increases in collagen types IV, V, VI, fibronectin, and laminin, as well as proteoglycans have been identified in the mesengium (Wang *et al*., 2010, Wang *et al*., 2011; Sengupta *et al*., 2008). In latter stages of glomerulosclerosis, increases in types I and III collagens occur (Sengupta *et al*., 2008) similar to the results presented in this study where increased collagen expression was concomitant with increasing age. Animal models of diabetes mirror structural changes observed in human kidneys (Kato *et al*., 2007). Increases in the deposition of ECM proteins can be the result of enhanced production and/or decreased degradation. Experimental data support causative roles for altered ECM turnover as assessed through changes in messenger ribonucleic acid and/or protein levels for ECM proteins, serine proteases (e.g. plasmin), MMPs, or tissue inhibitors of MMPs, (TIMPS) (Kato *et al*., 2007; Sekiuchi *et al*., 2012).

The role of metalloproteinases in DN

MMPs are major determinants of extracellular matrix degradation and turnover in the glomerulus. Hence, the changes in either MMP expression or activity can influence

intra-renal ECM composition (Matsuda *et al*., 2001; McLennan *et al*., 2002). Renal hypertrophy is prognostic of the development of microalbuminuria in type 1 DM (Metcalf & Meldrum, 2006; Nakagawa *et al*., 2004). Since abnormal extracellular matrix deposition is the hallmark of diabetic nephropathy, it is to be expected that altered MMP expression or activation also contributes to diabetic nephropathy, and specifically to the onset of this characteristic renal hypertrophy.

A number of studies have demonstrated a strong correlation between MMPs expression and the degree of albuminuria (hallmark of DN) or the severity of clinical symptoms. Interestingly, a study that MMP9 expression was concentrated in the mesangial stalk of the glomerulus in patients with DN, as delineated by the immunohistochemical studies, signifying that MMP9 may play a critical role in the turnover of the mesangial matrix in DN (Sekiuchi *et al*., 2012). Another study reported that MMP9 was dramatically increased in the glomeruli of diabetic mice, and MMP9 deficiency attenuates diabetic nephropathy by modulation of podocyte function and dedifferentiation. Collectively, these results suggest MMP9 play a role in the development of diabetic nephropathy (Li *et al*., 2014), as portrayed by the findings in this study. In addition, they revealed elevated MMP9 levels had strong correlations with age, body mass index (BMI) and HbA1c levels as well as progression of diabetes (van der Zijl *et al*., 2010). On the other hand, MMP2 gene expression levels were found to be significantly reduced at 2 and 4 months after STZ-induction compared to age-matched controls. Previous studies in humans have also found circulating TIMP1, TIMP4 and MMP2 to be decreased in patients with DN (Rysz *et al*., 2007). Furthermore, Del Prete and colleages demonstrated a dramatic decrease in MMP2 gene expression in glomeruli of patients with type 2 diabetes (Del Prete *et al*., 1997). However, another study showed that MMP2 protein and related enzyme activity were up-regulated in kidneys of patients with diabetes, as assessed by Western blot analysis and ELISA methods (Romanic *et al*., 2001). Similarly, there are variations in the renal tissue expression of MMP2 in biopsy specimens from patients with DN. Sekiuchi *et al.* reported that MMP2 is weakly expressed in the glomerular capillary loops and Bowman's capsules in the mesangial area, suggesting that MMP2 most likely is involved in the turnover of glomerular basement membrane (Sekiuchi *et al*., 2012).

The MMPs have long been identified as critical mediators of ECM degradation and turnover, but increasing evidence suggests that they, in conjunction with TIMPs play an

important role in the progression of diabetic nephropathy. Additionally, TIMP4 is involved in suppressing the activity of MMP1, MMP2, MMP3, MMP7 and MMP9 (Skiles *et al.*, 2001). Furthermore, besides having an inhibitory effect on MMPs, the TIMPs are endowed with other biological activities, including cell growth, migration, invasion, anti-angiogenesis, anti- and pro-apoptosis (Brew *et al*., 2010; Bond *et al*., 2000; Hoegy *et al*., 2001). Conversely, TIMP4 expression in this study was found to be elevated and this was more in regards to age progression. Taken together, MMPs and TIMPs expression in DN patients is somewhat variable, and their role in kidney pathology seems to be still very much confounding. But one can safely assume that the imbalance in MMP-TIMP expression or activation could lead to abnormal ECM deposition which decidedly remains as one of the hallmarks of DN.

Additionally, gene expression analysis of Cx43 revealed marked decreases in Cx43 levels of 2 and 4 months STZ-induced diabetic rat kidney compared to age-matched controls and this change was more severe with age. Previous studies in human kidney cells in culture have highlighted the possibility of a protective effect of Cx43 in preventing renal damage (Hillis, 1997; Guo & Barajas, 1998; Hills *et al*., 2006). Specifically, studies in human collecting duct cell lines found that as glucose concentrations increased, there was a time-dependant increase in levels of Cx43 that is opposite to the observations made in this study (Hills *et al*., 2006). The increase in Cx43 and gap junctional communication correlated with functional acceleration of calcium transients between cells. Furthermore, levels of Cx43 have also been studied in human DN as a predictive marker of disease progression and severity (Sawai *et al*., 2006). Another study found that down-regulation of Cx43 within podocytes was closely associated with disease progression in established DN and correlated with the degree of future decline in renal function (Wright *et al*., 2012). Additionally, vimentin was found to be elevated in STZ-induced diabetic rat kidney at 2 and 4 months of STZ-induced DM. Vimentin is a major intermediate filament (IF) protein of the mesenchymal cells and is physiologically important as it shows dynamically altered expression patterns during different developmental stages (Ivaska *et al*., 2007).

Major functions of vimentin involve the maintenance of cellular integrity and provide resistance against stress (Satelli & Li, 2011). A number of studies have found the role of TGFβ1 in response element within the activated protein complex-1 region of the vimentin promoter to be involved in regulation of vimentin expression (Satelli & Li,

2011; Wu *et al*., 2007). Thus, the increased gene expression of vimentin may be closely related to the increased TGFB1 activity observed in this study. Furthermore, this may also be an age related effect as the expression of TGFβ1 and vimentin both increased with age as shown in the present study. Additionally, vimentin has been also been shown to play important role in the regulation of cell to cell contacts, similar to the role integrins play in cell to cell interactions (Kim *et al*., 2003; Pellinen *et al*., 2006).This may partly explain the increased expression of Integrin 5α in this study. Nevertheless, these modifications are cell- and tissue-specific in nature and suggest an important role in regulation of vimentin's function.

Concluding Remarks

It cannot be emphasised enough that DM is a growing cause of end stage renal disease in developed countries and that DN develops in 35–40% of diabetic patients as the result of intrarenal metabolic, haemodynamic and structural changes (Wolf, 2004; Rossing, 2006). As explained in this study, DN is a complex phenotype caused by the combined effects of susceptibility alleles and environmental factors which contribute to poor glycaemic control and hypertension (Rossing, 2006).

In its entirety, this study represents an exploration of a remodelling process that is based upon hypertrophy, apoptotic cell death, elevated GBM size, glomerusclerosis and tubular fibrosis accompanied by marked elevations in gene expression of mediators and regulators as well as hypertrophic biomarkers all of which may be linked to the upregulation of TGFβ1. Nevertheless, the association between such events requires further clarification before prognosis of TGFβ1 can be determined. With regards to the results presented in chapter 3 and 4 on structural and functional remodelling of the LV in STZ-induced diabetes, can correlate to some of the changes presented here. Firstly, correlations can be conceptualised with a similar type of structural remodelling that is occurring in both the heart and the kidney. Secondly, HG can be regarded as being the principle maker of DM in studies conducted in both organs. This work emphasises the importance of specifically defining disease severity in studies of the heart and the kidney. Finally, the role of TGFβ1 as a major mediator of fibrosis within the two organs is pivotal in this HG milieu and holds great importance for further investigation.

Nonetheless, data presented here do not allow to conclude that kidney hypertrophy, ECM deposition, altered gene expression are events in the development or progression of HG-induced nephropathy. The present study lacks the functional changes associated with DN and requires further investigations into the functional aspects of the disease to make correlations with the structural remodelling observed in this study.

CHAPTER 6

A COMPARITIVE STUDY SHOWING THE STRUCTURAL AND MOLECULAR CHANGES OBSERVED IN THE HEART AND KIDNEY IN STZ-INDUCED TYPE 1 DIABETIC RAT

6.1 Introduction

The field of adult vs young adult research has undergone a number of significant changes in the past few decades. While knowledge gleaned from autopsy-based studies has formed an indispensible foundation for our understanding of the adult vs young adult process, there has been an inherent difficulty in separating the effect of age per se from those of the comorbid illnesses that caused a subject's death. Consequently, it is important that clinicians and researchers understand the physiologic changes that occur with age if new approaches to disease identification and treatment and health maintenance are to be devised that not only increase longevity, but also improve the quality of life at advanced ages.

With this said, as described extensively in the preceding chapters, DM is a multifactorial disorder which affects many organs of the body including the heart (DCM) and the kidney (DN). To a large extent, it has been emphasised that DM leads to functional, structural and molecular alterations in these organs that together correspond to dysfunction of either the heart or the kidney. Previously, major difficulties have arisen when studying DM-related complications in the adult vs young adult heart and kidney. Nevertheless, after many years of research, a magnificent number of studies regarding the heart and the kidney have somewhat come to an imperative finding that there may be a link between the complications observed within the two major organs of the human body that are associated with DM. Recently clinical and experimental research conducted along a broad range of departments have identified the emergence of a new type of syndrome reffered to as the Cardio-Renal Syndrome (CRS). CRS are disorders of the heart and the kidney in which acute or chronic dysfunction in one organ may induce either acute or chronic dysfunction of the other (Cruz *et al*., 2011). A significant number of patients are hospitalized for HF experience with an increase of serum creatinine during their hospital stay (Liang *et al*., 2008, Nohira *et al*., 2008). The mechanisms underlying renal impairment and poor outcome in HF patients are complex and still uncertain. It is postulated that worsening of the renal function could contribute to the poor outcome or it could simply be a marker of advanced hemodynamic and neuro-hormonal impairment (Cruz *et al*., 2011). Interaction between heart and kidney involves several pathways including renal hypoperfusion, neurohormonal derangements, intraglomerular hemodynamic changes, altered tubule-glomerular feedback, and decreased renal blood flow and GFR and inflammation (Liang *et al*., 2008).

Thus, the main aim of this study was to present a comparative analysis of the findings that have been described in the preceding chapters, explaining the structural and molecular alterations observed in the heart and the kidney in STZ-induced T1DM at 2 and 4 months post STZ-induction compared to age-matched controls. This study has provided substantial evidence and fundamental addition to the ongoing research on the CRS and provides essential targets for future therapy in regards to targeting ECM accumulation. TGFβ1 activity may represent a key intermediary in these processes.

6.2 Methods

Methods are described in Chapter 2

6.3 Results

The data described in graphs below are from young hearts and kidneys (2 months) and old hearts and kidneys (4 months) taken from STZ-induced diabetes and age-matched control animals as described in Chapter 2 and elaborated in Chapters 4 and 5, respectively. Statistical analysis was performed using One-way ANOVA followed by Bonferroni corrected t-tests for multiple comparisons. Level of significance is set at *p<0.05, **p<0.01, and '#' indicates significant differences between the heart and kidney at 2 or 4 months of STZ-treatment.

Represented in figure 6.1 is the mean organ weight (A), revealing significant (p<0.05) differences between heart weight and kidney weight along with organ weight/body weight ratio (B). Heart weight was significantly (p<0.05) decreased while kidney weight was significantly (p<0.05) increased at 2 and 4 months after STZ-induction compared to controls. Respectively, organ weight/body weight ratios in the heart and kidney were significantly (p<0.05) increased at 2 and 4 months after STZ-induction compared to age-matched control representing hypertrophy in both organs. Fibrosis area fraction represented in figure 6.1C showed no significant (p<0.05) differences between the heart and kidney. Interestingly, the extent of fibrosis remained almost the same in both organs at 2 and 4 months after STZ-induction highlighting the fact that fibrosis affects the heart and kidneys together and at the same level. Figure 6.1D represents immunoreactivity of active caspase-3 in heart and kidneys. Surprisingly, the results revealed a significant (p<0.05) difference between the young heart and kidney at 2 months after STZ-induction, highlighting a significant (p<0.05) increase in the extent of apoptotic cells, while no significance (p<0.05) was revealed at 4 months between the two organs.

Figure 6.2 represents mechanisms that underlie remodelling changes in heart and kidneys that were also compared to determine organ specific interactions. Total TGFβ1 (Figure 6.2A) revealed significant (p<0.05) differences between young/old heart and kidney. Total TGFβ1 was significantly (p<0.05) increased in hearts and kidney at 2 and 4 months after STZ-induction compared to age-matched control. However, these differences were significantly (p<0.05) lower in the kidney compared to the heart. On the other hand, older heart and kidneys also revealed significant (p<0.05) decrease between the organs, with the kidney having a low level of total TGFβ1content in both

age groups. Conversely, active TGFβ1 was significantly (p<0.05) increased at 2 and 4 months after STZ-induction compared to age-matched controls. However, active TGFβ1 was significantly (p<0.05) higher in young and old kidneys compared to young and old heart tissue. These results reveal surprising changes between the level of active and total TGFβ1 levels in heart and kidneys. Figure 6.1C represents the mRNA gene expression of TGFβ1 in young/old heart and kidney tissue. The level of TGFβ1 gene expression remained almost the same across the age of organ, with exceptions to older heart and kidney which showed significant (p<0.05) reductions in TGFβ1 expression in the kidneys compared to the heart.

Figure 6.3 show data for gene expression for ECM components and regulators of young/old hearts and kidneys after STZ-induction compared to age match controls. Figure 6.3A represents gene expression for collagen 1α highlighting similar expression across the age of the organ. However, a significant (p<0.05) decrease can be seen in the young heart and kidney collagen 1α expression. Similarly, figure 6.3B represents collagen 3α gene expression which can be seen to be significantly (p<0.05) increased at 2 and 4 months after STZ-induction compared to age-matched control. However, no significant (p<0.05) differences can be observed between the hearts and kidneys overall. Fibronectin gene expression (Figure 6.3C) was observed to be overall significantly (p<0.05) increased in both heart and kidneys at 2 and 4 months after STZ-induction compared to age-matched controls. However, a significant (p<0.05) reduction was observed in the young kidneys compared to heart STZ-treated tissues and this difference levelled after 4 months of STZ-induction. A similar trend was observed for elastin (Figure 6.3D). However, this time a significant (p<0.05) increase in the younger kidneys was observed in relation the expression observed within the heart. MMP2 (Figure 6.3E) and MMP9 (Figure 6.3F) levels within the hearts and kidneys remained almost the same with significant (p<0.05) up-regulation in MMP9 levels and a significant (p<0.05) down regulation in MMP2 levels at 2 and 4 months after STZ-induction compared to age-matched controls. Nevertheless, a significant (p<0.05) down-regulation was seen in MMP9 in the old kidneys compared to the heart expression. Conversely, tissue inhibitor (TIMP4) expression revealed parallel changes within the heart and kidneys. Gap junction protein connexin43 revealed an overall decrease (p<0.05) in expression after 2 and 4 months of STZ-induction compared to

age-matched control. However, this decrease was significantly (p<0.05) more in the older kidneys compared to the older heart (4 months after STZ-induction).

Figure 6.4 represents gene expression of hypertrophy biomarkers ANP (Figure 6.4A) and BNP (Figure 6.4B). The results revealed a significant (p<0.05) increase in the expression of ANP within the heart and kidney after 2 and 4 months of STZ-induction compared to age-matched control. This increase was (p<0.05) higher in the kidneys compared to the heart which was expected since the kidney weighed more than the heart at 2 and 4 months showing hypertrophied kidneys. BNP expression, on the other hand, remained same across age and organ with significant (p<0.05) increases observed after 4 months of STZ-induction compared to control representing an age-related change in both organs.

Altogether, a variety of age-related and organ-related changes have been observed throughout the expression analysis of ECM components, regulators, *and natriuretic* peptides. Some organ specific similarities have also been observed revealing similar organ interactions and hence function-related changes. This study provides new insight into developing treatments to cover such changes in both organs in order to discover a positive outcome overall.

Figure 6.1

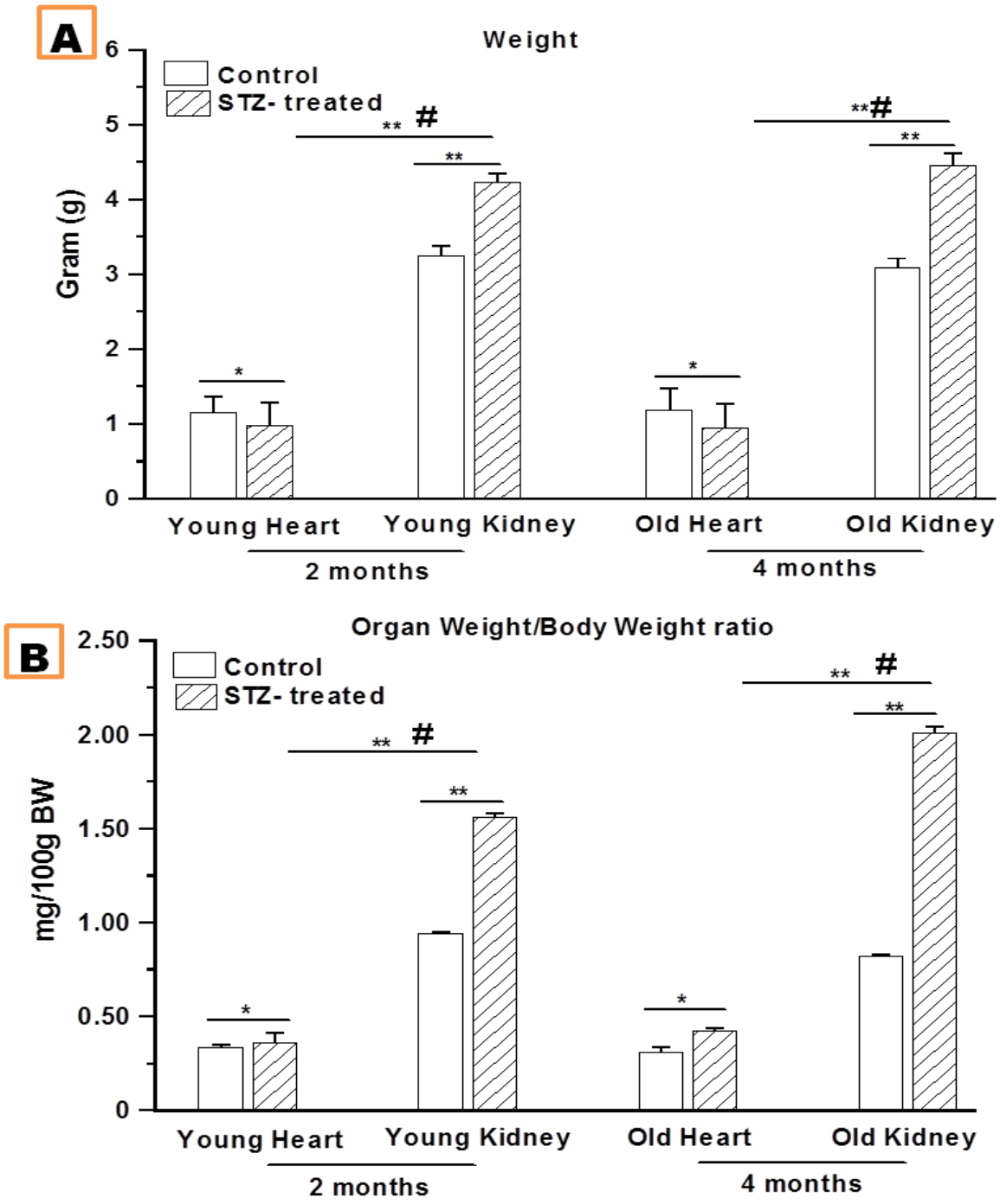
A
Weight
Control
STZ- treated
Gram (g)
0
1
2
3
4
5
6
*
**
#
Young Heart
Young Kidney
Old Heart
Old Kidney
2 months
4 months
B
Organ Weight/Body Weight ratio
mg/100g BW
0
0.50
1.00
1.50
2.00
2.50

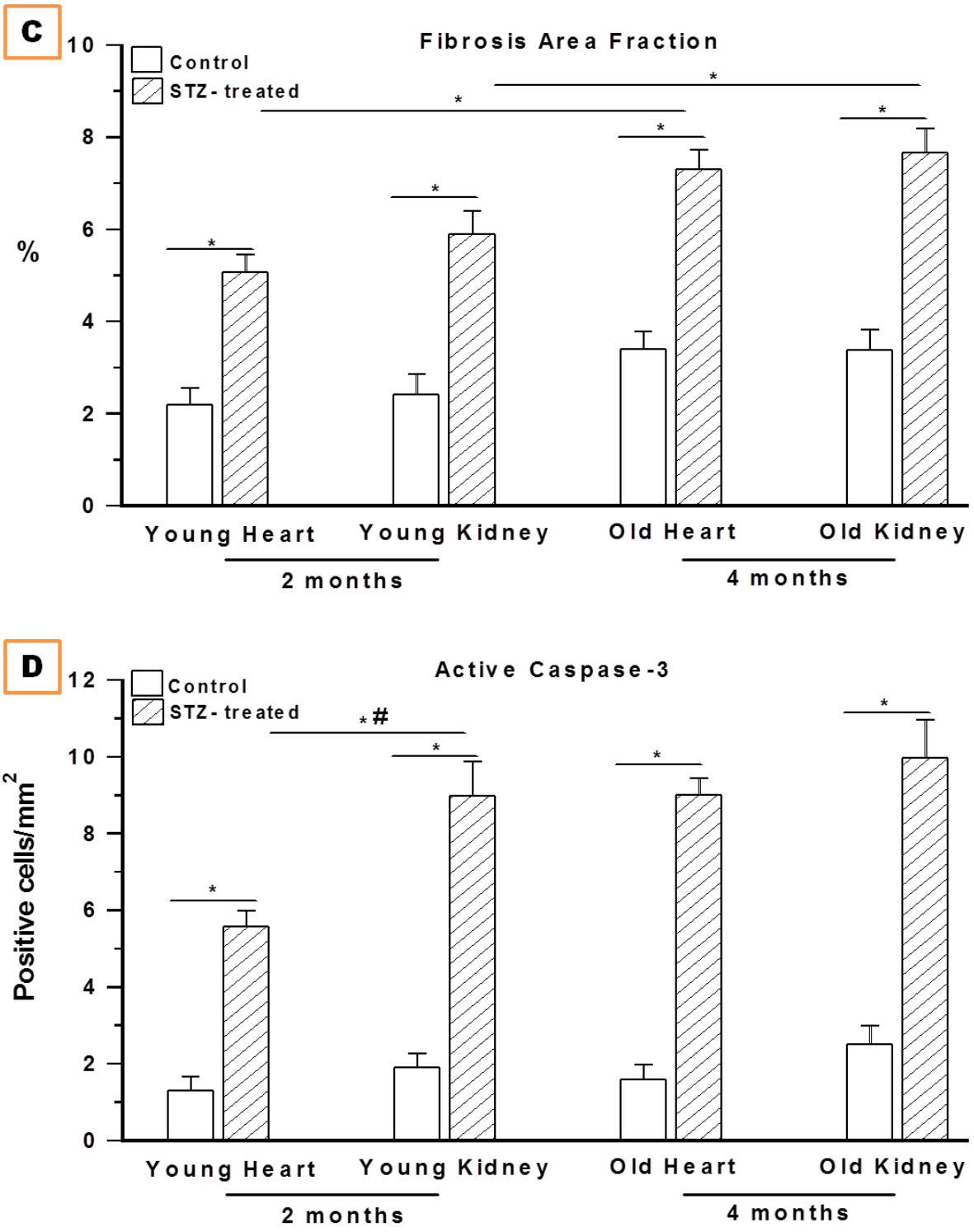

Figure 6.1: Comparison of the organ specific remodelling changes observed in heart and kidney at 2 and 4 months of STZ-treatment and age-matched controls, respectively. Weight **(A)**, Organ weight/body weight ratio **(B)**, Fibrosis quantification **(C)** and Active Caspase-3 activity **(D)**. n=6-8 in each group. Data are Mean±S.E.M, **p*< 0.05, ***p*< 0.01 '#' indicates significant difference between the heart and the kidney. One-way ANOVA followed by Bonferroni corrected t-tests for multiple comparisons.

Figure 6.2

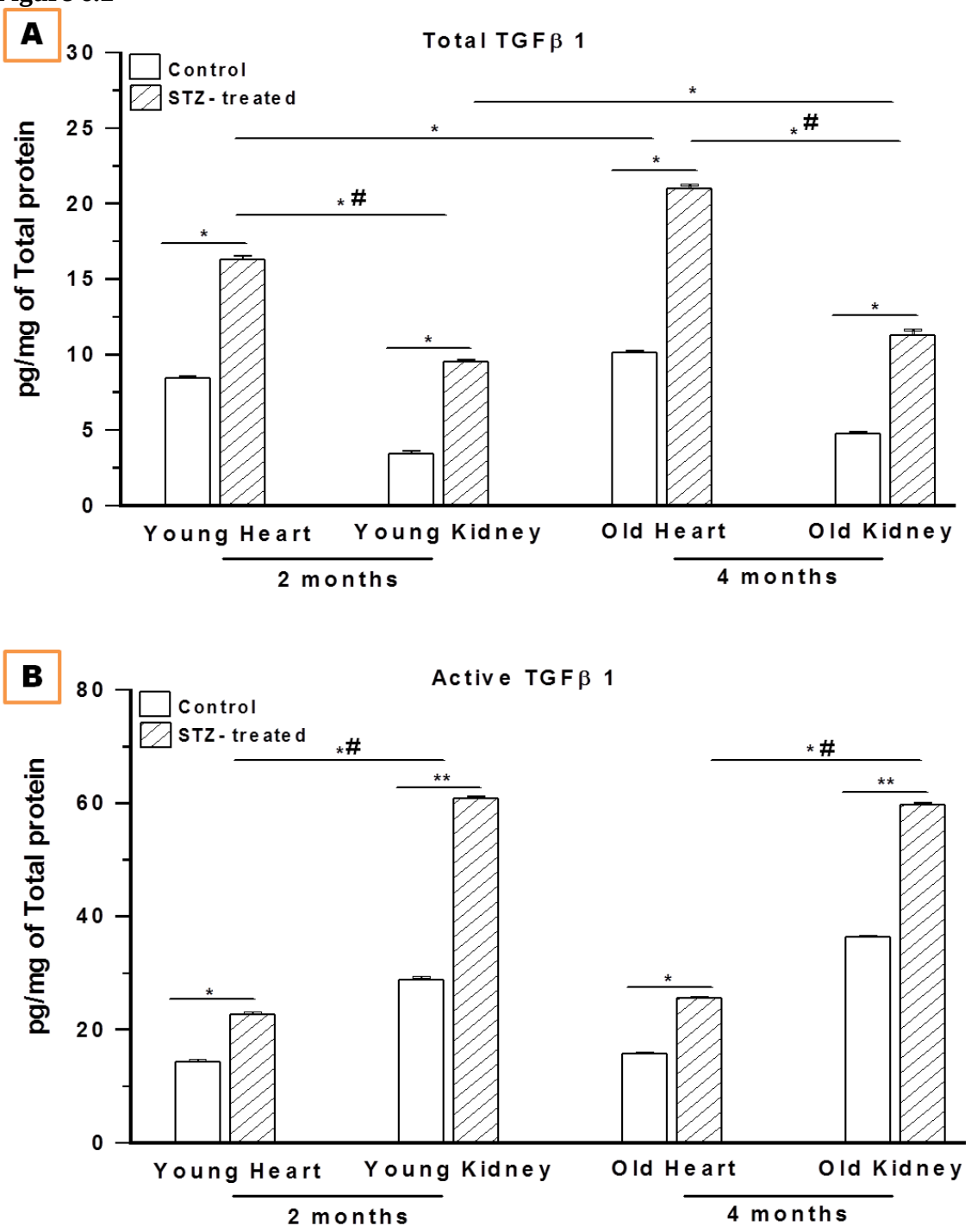
A
Total TGFβ 1
Control
STZ- treated
pg/mg of Total protein
0
5
10
15
20
25
30
Young Heart
Young Kidney
Old Heart
Old Kidney
2 months
4 months
B
Active TGFβ 1
Control
STZ- treated
pg/mg of Total protein
0
20
40
60
80
Young Heart
Young Kidney
Old Heart
Old Kidney
2 months
4 months

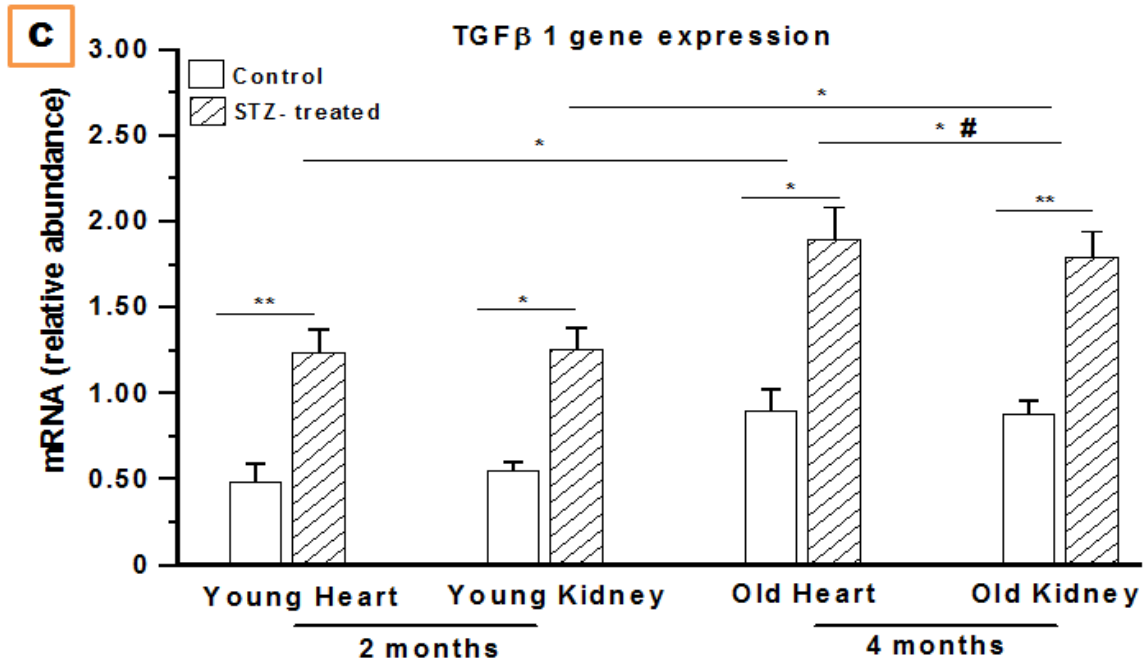

Figure 6.2: Comparison of the organ specific effects on TGFβ1 concentration in heart and kidney at 2 and 4 months after STZ-treatment and age-matched controls, respectively. Total TGFβ1 protein **(A)**, Active TGFβ1 protein **(B)** and TGFβ1 mRNA gene expression **(C).** The results of both ELIZA and qRT-PCR are representative of 3 individual experiments conducted in triplicate. RT-PCR amplification was normalised to that of GAPDH. n=6-8 in each group. Data are Mean±S.E.M, *p< 0.05, **p< 0.01, '#' indicates significant difference between the heart and the kidney. One-way ANOVA followed by Bonferroni corrected t-tests for multiple comparisons.

Figure 6.3

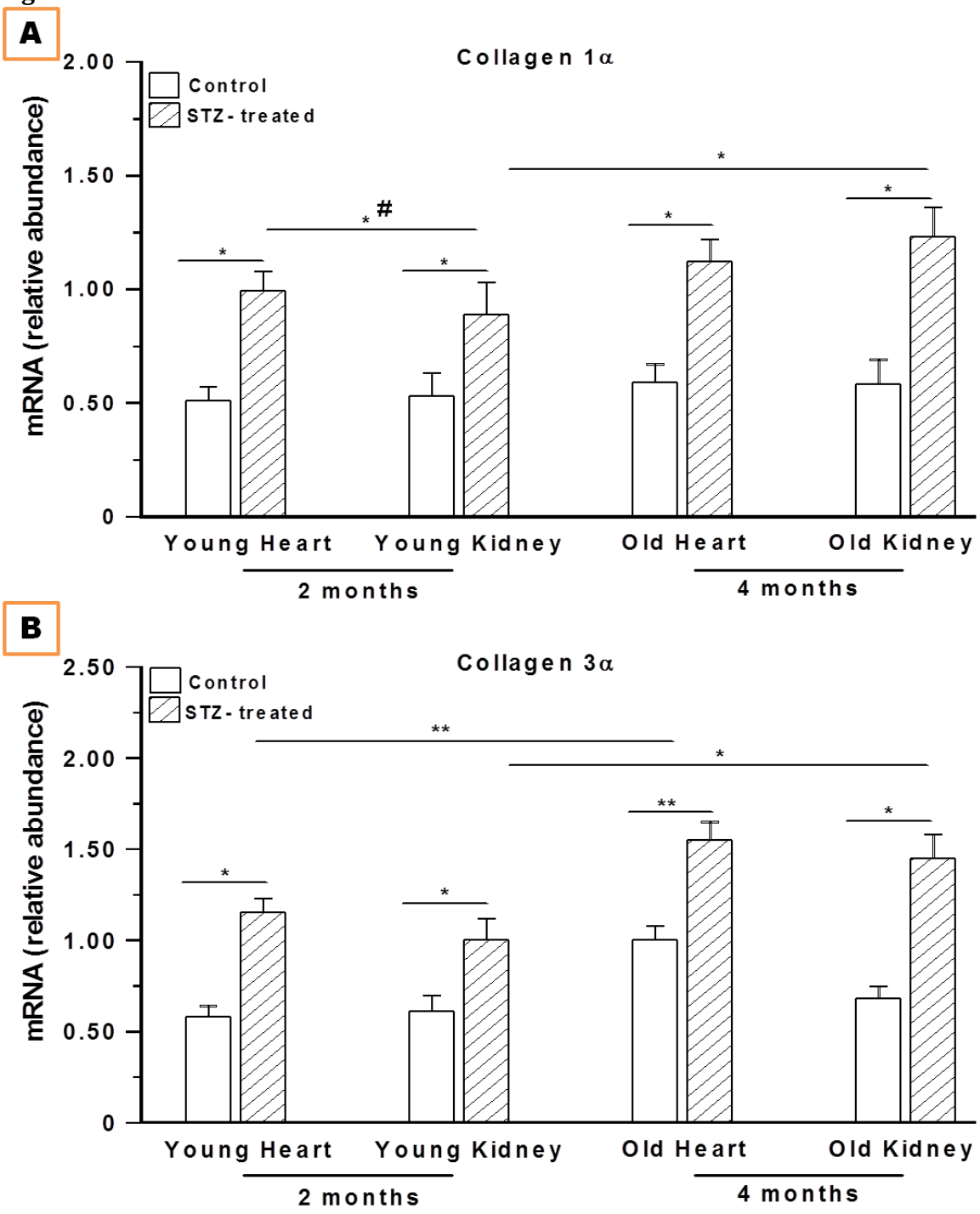
A
Collagen 1α
Control
STZ- treated
mRNA (relative abundance)
2.00
1.50
1.00
0.50
0
*
*
*#
*
*
*
Young Heart
Young Kidney
Old Heart
Old Kidney
2 months
4 months
B
Collagen 3α
Control
STZ- treated
mRNA (relative abundance)
2.50
2.00
1.50
1.00
0.50
0
**
*
*
*
**
*
Young Heart
Young Kidney
Old Heart
Old Kidney
2 months
4 months

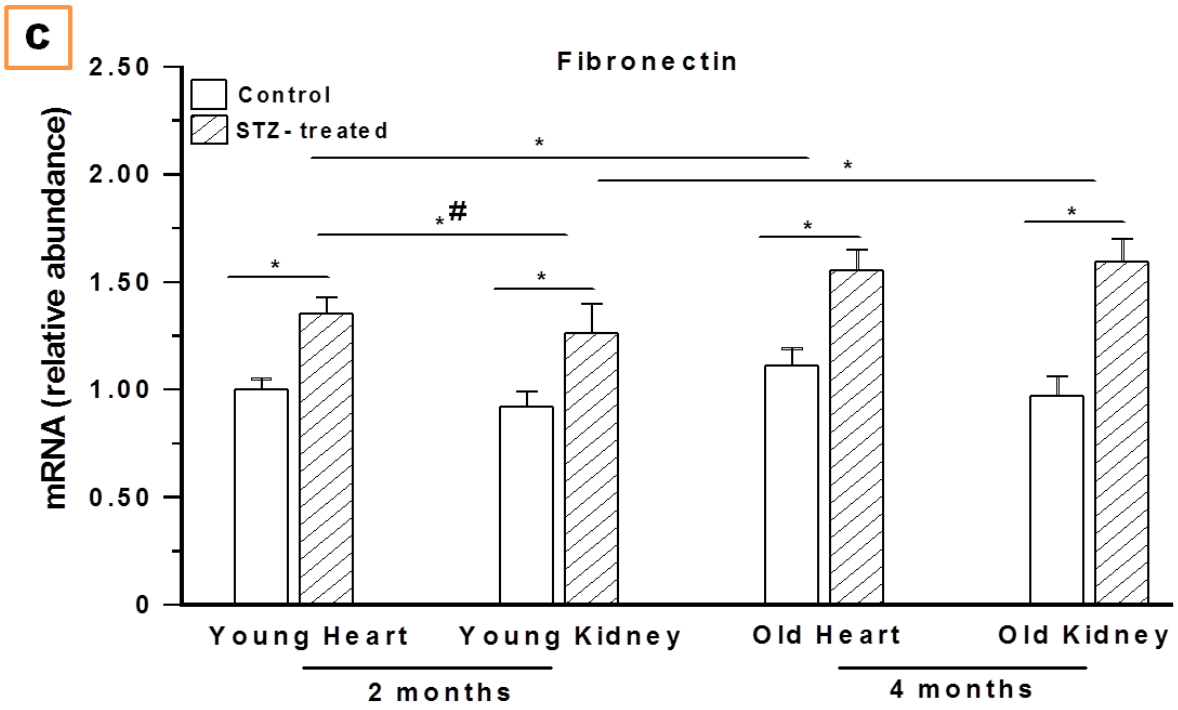
C
Fibronectin
Control
STZ- treated
mRNA (relative abundance)
2.50
2.00
1.50
1.00
0.50
0
*
*
*#
*
*
*
*
Young Heart
Young Kidney
Old Heart
Old Kidney
2 months
4 months

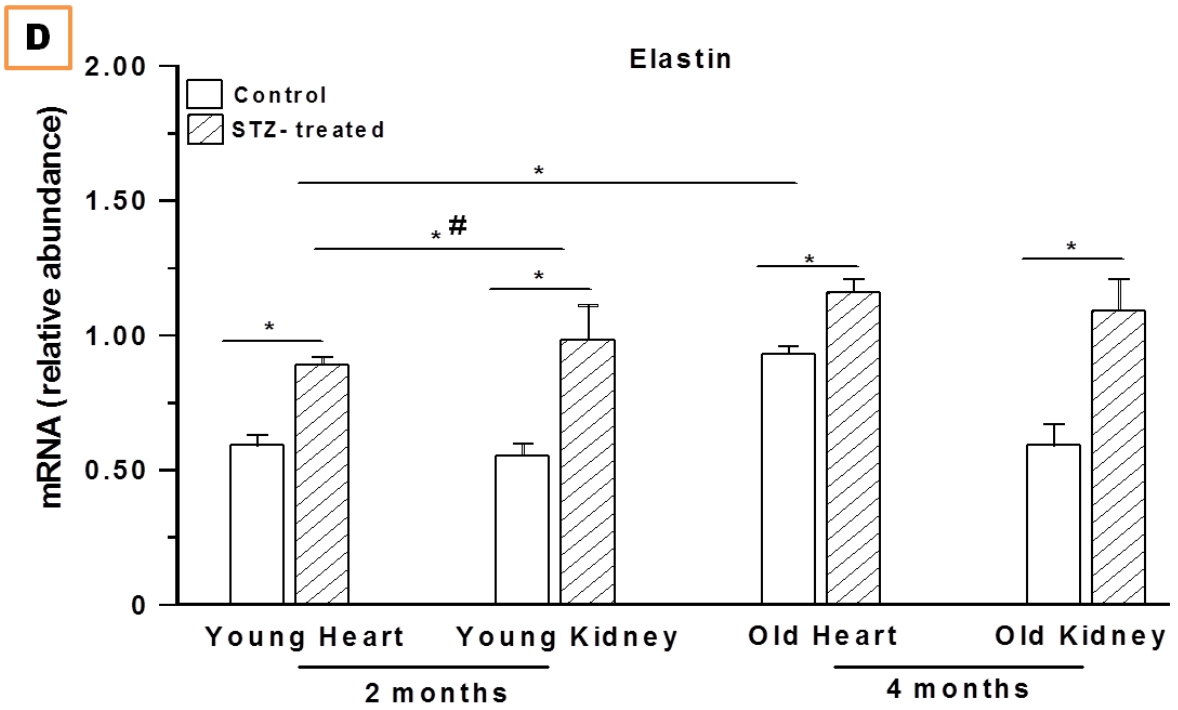
D
Elastin
Control
STZ- treated
mRNA (relative abundance)
2.00
1.50
1.00
0.50
0
*
*
*#
*
*
*
*
Young Heart
Young Kidney
Old Heart
Old Kidney
2 months
4 months

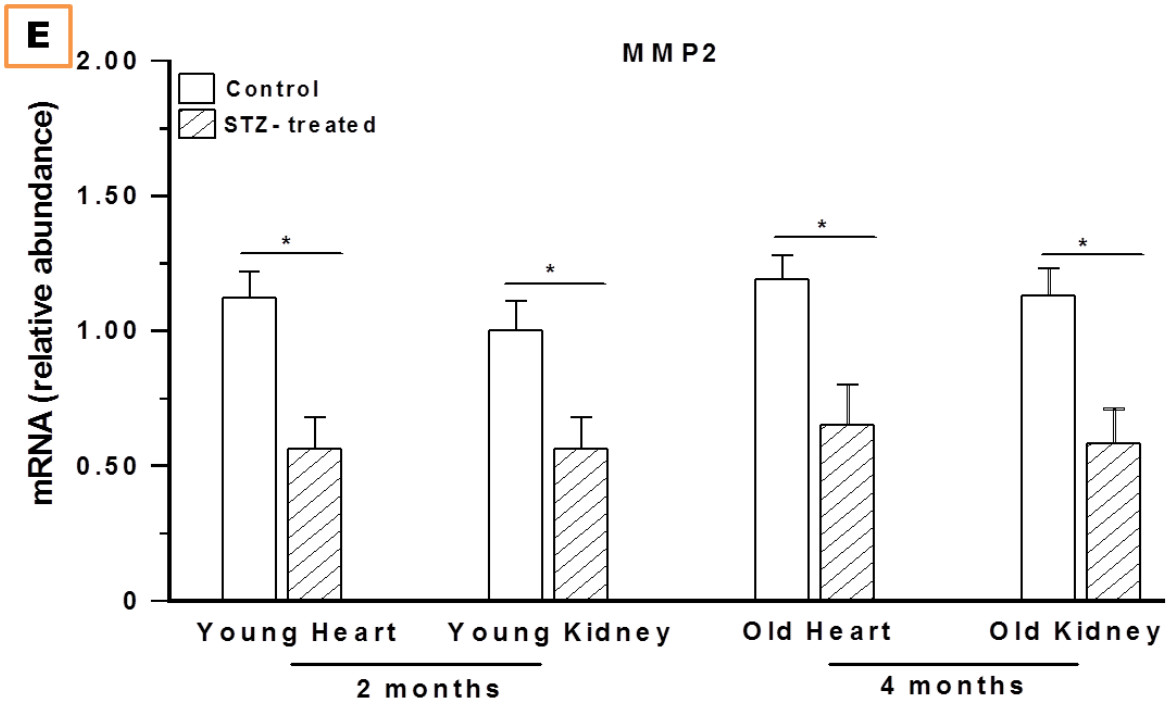
E
MMP2
Control
STZ-treated
mRNA (relative abundance)
2.00
1.50
1.00
0.50
0
*
*
*
*
Young Heart
Young Kidney
Old Heart
Old Kidney
2 months
4 months

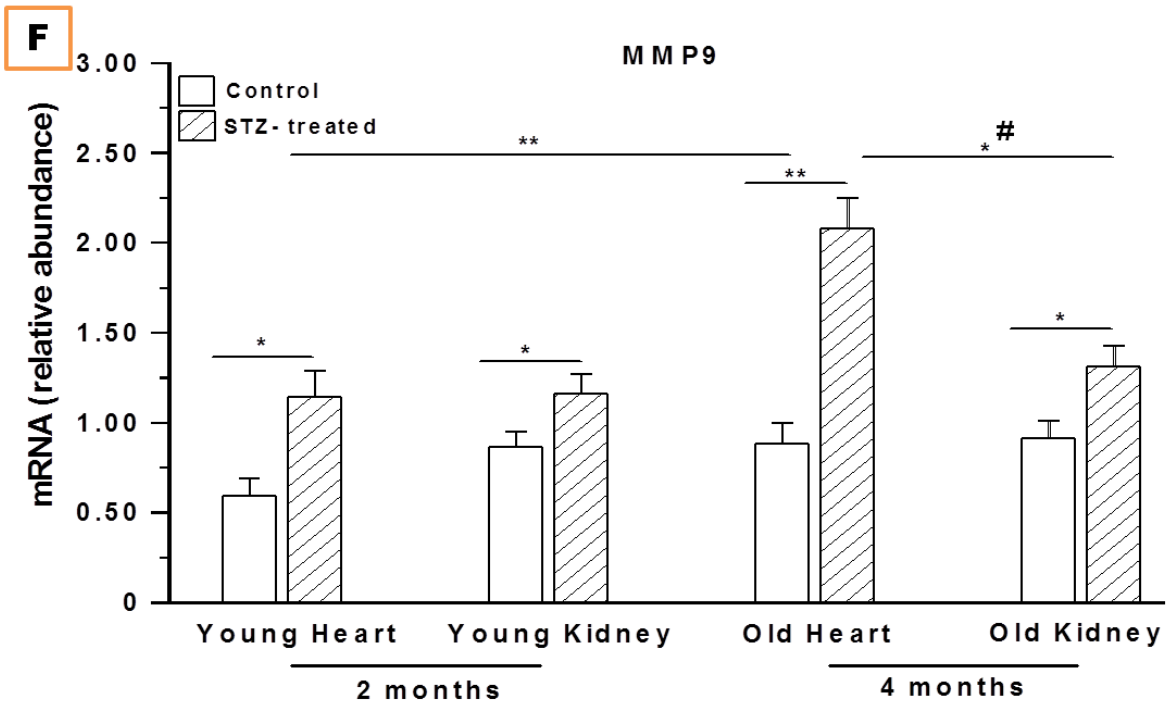
F
MMP9
Control
STZ-treated
mRNA (relative abundance)
3.00
2.50
2.00
1.50
1.00
0.50
0
**
*
#
**
*
*
*
Young Heart
Young Kidney
Old Heart
Old Kidney
2 months
4 months

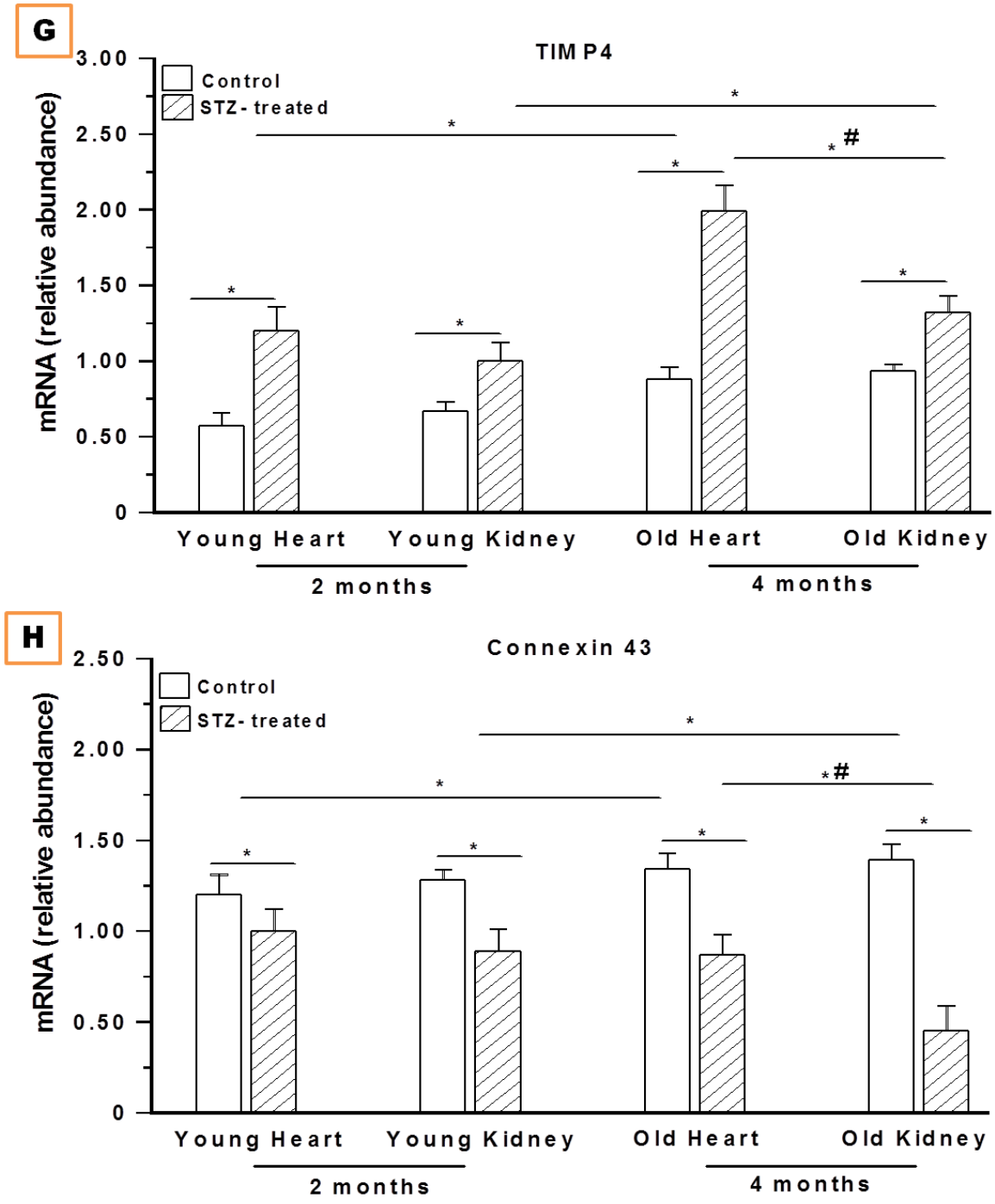

Figure 6.3: Comparison of organ specific effects on ECM components and regulators of gene expression in heart and kidneys at 2 and 4 months after STZ-treatment and age-matched controls, respectively. Collagen 1α **(A)**, Collagen 3α **(B)**, Fibronectin **(C),** Elastin **(D)** MPP2 **(E)** MMP9 **(F)** TIMP4 **(G)** and Connexin 43 **(H).** RT-PCR amplification was normalised to that of GAPDH. n=6-8 in each group. Data are Mean±S.E.M, **p*< 0.05, ***p*< 0.01, '#' indicates significant difference between the heart and the kidney. One-way ANOVA followed by Bonferroni corrected t-tests for multiple comparisons.

Figure 6.4

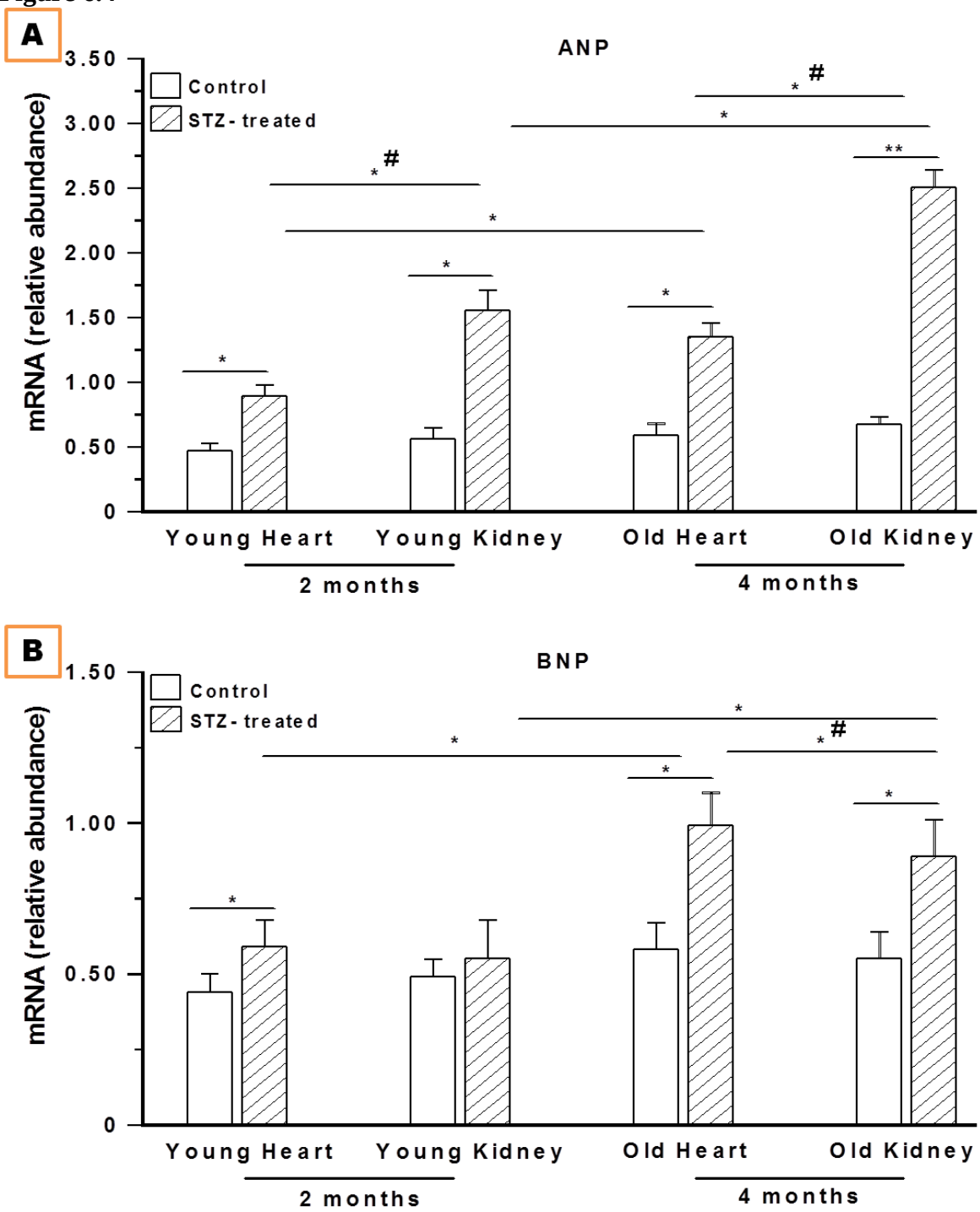

Figure 6.4: Comparison of organ specific effects on hypertrophy biomarkers in heart and kidneys at 2 and 4 months after STZ-treatment and age-matched controls, respectively, ANP **(A)** and BNP **(B).** RT-PCR amplification was normalised to that of GAPDH. n=6-8 in each group. Data are Mean±S.E.M, *$p<$ 0.05, **$p<$ 0.01, '#' indicates significant difference between heart and kidneys. One-way ANOVA followed by Bonferroni corrected t-tests for multiple comparisons.

6.5 Discussion

Summary of key findings:

1. T1DM leads to structural and molecular alterations in the heart and kidney respectively, that corresponds to the dysfunction of either organ.
2. A clear adult vs young adult comparison showing marked increases in many aspects of the remodelling process for both the heart and the kidney.
3. This study provides growing evidence for the development of a cardio renal syndrome in patients with T1DM.

Diabetes mellitus: The heart and the kidney

DM is a major metabolic disorder which can lead to multiple organ failures if left untreated. Two major organs which are affected in the body by DM are the heart (DCM) and the kidney (DN). These diabetes-induced complications are more sever with adult vs young adult. This study was designed to investigate structural and molecular processes which are occurring in the heart and the kidney following 2 and 4 months of STZ-induced DM compared to respective age-matched control groups. In concord with the combined results of this study, it can be inferred that HG-induced DM can elicit major structural and molecular alterations in both the heart and the kidney and that most of these changes are occurring parallel to each other.

Diseases and disabilities associated with adult vs young adult are of increasing global importance as longevity increases. Data from the Framingham Study show that adult vs young adult (especially in the absence of risk factors) is associated with cardiac remodelling that is characterized by a distinct pattern of increasing LV wall thickness, decreasing LV dimensions and increasing fractional shortening (Cheng *et al*., 2010). Furthermore, HF in DM appears to increase with age, paradoxically in part due to improved survival after a myocardial infarction and related cardiac disorders. Several other predisposing factors contribute to HF, including the adult vs young adult of the population on a whole and the high prevalence of traditional cardiovascular risk factors such as hypertension, hyperlipidemia and T2DM in older individuals (www.health.org; Writing Group Members, 2009). In general, the *prevalence* of HF is 3–20 per 1,000 population, nevertheless this exceeds 100 per 1,000 in those aged 65 years and over. Additionally, the annual *incidence* of HF is 1–5 per 1,000, and the relative incidence

doubles for each decade of life after the age of 45 years (Davis *et al*., 2000; Kappagoda & Amsterdam, 2012). In elderly populations, it is difficult to separate the signs and symptoms of HF from those associated with the "natural" process of adult vs young adult. Furthermore, renal impairment is frequent in aged diabetic patients resulting from a multifactorial pathogeny, particularly the combined actions of HG, hypertension and adult vs young adult (Blickle *et al*., 2007). Renal dysfunction is common in patients with HF, with a prevalence of approximately 25% (Hillege *et al*., 2006). The degree of renal dysfunction is a powerful independent risk factor for all-cause mortality in CHF patients. Nonetheless, age itself is associated with hypertension and arteriosclerosis which can decrease glomerular filtration in aged patients (Lindeman *et al*., 1984). However, even if there is a positive correlation between albuminuria and diabetes duration, the direct association between microalbuminuria or proteinuria and adult vs young adult is still debated (Wasen *et al*., 2004).

In regards to the present results, adult vs young adult has shown marked increases in many aspects of the remodelling process and this has been true for both the heart and the kidney. In particular, the elevations in ECM deposition (fibrosis) were elevated in both heart and the kidney to similar extents. Also the underlying gene expressions of ECM components and regulators showed marked elevations with age and similarities between the heart and the kidney in STZ-induced T1DM rats. Additionally, active/total TGFβ1 levels and underlying gene expression was seen to be elevated with age in the STZ-induced T1DM rats compared to age-matched control groups, respectively. However, the role of TGFβ1 in the development of a CRS is still under research; however the role of TGFβ1 in structural and molecular remodelling of the heart and the kidney has been highlighted in the preceding chapters. Nevertheless, the findings of similarities in TGFβ1 levels and expression in the heart and the kidney may well be of some importance in the near future.

Additionally, natriuretic peptides (NPs) have been validated as important cardiac biomarker for risk stratification and prognostication in HF patients either with or without chronic kidney disease (CKD) (Cruz *et al*., 2011). However, the association between NP levels and renal function is complex. In the setting of renal dysfunction, increased concentrations of NPs may stem from elevation in atrial pressure, systemic pressure, or ventricular mass. Patients with renal disease often have hypertension that results in significant LV hypertrophy, and cardiac co-morbidities are also common. The interplay between the heart and the kidney in patients with reduced renal function

accounts for one component of the increase in NP levels, thus reflecting elevated true physiologic NP levels (Daniels & Maisel, 2007). Nevertheless, the best cut-off values for each stage of CKD, including those on renal replacement therapy, are yet to be ascertained.

Concluding Remarks

Collectively, it can be stressed that there is growing evidence for the development of a CRS in patients with T1DM as well as patients with T2DM. The results from the present study have highlighted important triggers that need to be investigated in the future in order to enhance the research of the development of a CRS.

The first line of reasoning is that HG drives the pathogenesis of a diabetes specific cardiomyopathy and nephropathy. Tight glycaemic control, as well as metabolic control, may be the way forward with regards to improving the condition of the patients. In agreement with this, the study conducted with regards to addressing the nephropathy, has come to the conclusion that HG-induced oxidative stress can be prevented if good metabolic control is initiated very early, but are not easily reversed if a poor metabolic control is maintained for longer durations (Kowluru *et al*., 2004). Furthermore, glycaemic control is fundamental in the prevention of microalbuminuria and blood pressure control is equally important for the evolution from microalbuminuria to proteinuria (Constans, 2005).

In conclusion, patients hospitalised for HF experience an increase of serum creatinine and a reduction of the glomerular filtration rate, particularly those with co-morbidities or advanced age. While the predominant mechanism of renal function impairment and negative effects on outcomes in CHF are not completely understood. In the near future, this holistic view of the heart/kidney interactions should lead to a more collegial and collaborative management of the cardio-renal syndromes. Together with the findings of this study, such multidisciplinary approach will help to mitigate our ignorance and to multiply our knowledge through a serious and constructive interchange.

CHAPTER 7

EFFECT OF EXERCISE TRAINING ON LEFT VENTRICLE CARDIOMYOCYTE CONTRATILE FUNCTION AND STRUCTURAL REMODELLING IN THE GOTO-KAKIZAKI TYPE 2 DIABETIC RAT

7.1 Abstract

Background: Although, several novel forms of intervention aiming at newly identified therapeutic targets are currently being developed for DM, it is well established that physical exercise continues to be one of the most valuable forms of non-pharmacological therapy. This study tested the hypothesis that physical exercise training can be beneficial in the GK rat as a model of T2DM with regards to the functional, structural and molecular alterations observed in T2DM.

Methods: Experiments were performed in the GK and Wistar control rats aged 10-11 months following 2-3 months of treadmill exercise training. LV was isolated from control and GK groups (sedentary and exercised trained) and were used to access functional parameters (ventricular cardiomyocyte shortening and intracellular $[Ca^{2+}]_i$ transients) using video edge detection, fluorescence photometry, respectively. In another series of experiments remodelling changes were assessed in the LV employing gene expression analysis of ECM mediators and regulators, cardiomyocyte contractile proteins, hypertrophy biomarkers ANP and BNP as well as α-skeletal muscle actin intensity via confocal imaging.

Results: The results show that amplitude of shortening and $[Ca^{2+}]_i$ transients were not significantly ($p > 0.05$) altered in ventricular myocytes from GK sedentary compared to control sedentary rats or by exercise training. Gene expression for cardiac contractile proteins did not show many alterations in the T2DM sedentary GK model. Exercise training significantly reduced interstitial fibrosis, caspase-3 mediated apoptosis, and gene expressions of ECM components and regulators that underlie the extent of cardiac fibrosis compared to sedentary GK animals. Additionally, ventricular hypertrophy was reduced to some extent as represented by reduced ANP and BNP gene expressions and reduced α-skeletal actin intensity. Furthermore, TGFβ1 was significantly reduced in exercise-trained GK rat compared to sedentary GK and control groups.

Conclusions: In conclusion, the results show that ventricular myocyte shortening and Ca^{2+} transport were generally well preserved. In addition, physical exercise training significantly reduces structural remodelling observed in T2DM, suggesting exercise training to be highly beneficial in order to replace the structural and molecular remodelling that occurs in the T2DM heart.

7.2. Introduction

DM is a metabolic disorder that has reached pandemic proportions worldwide. There is increasing predictions that the number of people with diabetes will almost double within one generation from the present 380 million to 550 million in 2025 (Zimmet & Alberti, 2006). Cardiovascular disease is the major cause of morbidity and mortality in diabetic patients and hearts of diabetic patients are frequently in a compromised condition (Julien, 1997). A diversity of diastolic and systolic dysfunctions have been reported in type 2 diabetic patients and the severity of the abnormalities depend on the patients' age as well as the duration of diabetes (Dounis *et al*., 2006; Annonu *et al*., 2001; Zabalgotia *et al*., 2001; Di Binto *et al*., 1996). Although, several novel forms of interventions aiming at newly identified therapeutic targets are currently being developed for T2DM, it is well established that physical exercise continues to be one of the most valuable forms of non-pharmacological therapy. It has been shown in animal models that exercise could prevent ventricular remodelling, attenuate derangement of glucose and lipid metabolism, and improve mitochondrial function and antioxidant capacity, thus leading to ameliorated cardiac performance in the early stage of DCM (Castellar *et al*., 2011; Epp *et al*., 2013; Hafstad *et al*., 2013; Korte *et al*., 2005; Searls *et al*., 2004; Saraceni *et al*., 2007; Longnathan *et al*., 2007; Silva *et al*., 2013).

An abundance of evidence exists for prescribing exercise therapy in the treatment of a variety of diseases including metabolic syndrome-related disorders (insulin resistance, T2DM, dyslipidemia, hypertension, and obesity), heart and pulmonary diseases, muscle, bone and joint diseases and cancer, depression and asthma (Pedersen & Saltin, 2006). The benefit of exercise on the prevention and treatment of diabetes and its associated cardiac dysfunction has increasingly been reported (Bidasee *et al*., 2008; De Angelis *et al*., 2000; Li *et al*., 2003; Longnathan *et al*., 2012). Physical activity has also been reported to influence several aspects of DM, including blood glucose concentrations, insulin action and cardiovascular risk factors and long-term exercise has been repeatedly associated with lower rates of T2DM (Chipkin *et al*., 2001).

In light of the beneficial effects of regular exercise on T2DM, the present study investigated the effects of exercise training on EC coupling and expressions of mRNA encoding cardiac muscle proteins in the adult GK type 2 diabetic rats compared to age-matched Wistar control rats. Additionally, in order to study the mechanisms that underlie structural remodelling in the LV, this study has investigated the involvement of

TGFβ1, cytokine activation being a pivotal mediator in cardiac remodelling to myocardial overload injury. Much emphasis has been based on the role of HG-induced TGFβ1 as a powerful initiator of tissue repair, sustained production of which underlies myocardial fibrosis (accumulation of ECM proteins). Furthermore, a role of TGFβ1 has been identified in the myocardial during hypertrophy and HF. Nonetheless, this study will provide substantial evidence for HF pathogenesis in order to present therapeutic interventions. In addition, data in this chapter are presented to corroborate the hypothesis that exercise training may present as a beneficial therapeutic intervention in myocardial structural, functional and molecular remodelling.

7.3. Methods

Methods are described in Chapter 2

7.4. Results

1. Effects of exercise training on the general characteristics of the Goto-Kakizaki type 2 diabetic rat

Figure 7.1 represents blood glucose concentrations 120 min following a glucose tolerance challenge that was performed in the resting state at 2 months into the exercise training programme. Blood glucose concentrations in sedentary GK rats were significantly (p<0.01) higher than blood glucose in sedentary controls (236.27±15.12** mg/dl, n=15) *vs.* (93.93±2.32 mg/dl, n=15). Exercise training modestly reduced blood glucose in GK and in controls (207.36±12.13 mg/dl, n=14) *vs.* (89.60±2.78 mg/dl, n=15). However, the reduction in blood glucose with exercise did not reach significance (p<0.05). Table 7.1 represents glucometry and gravimetry data for control sedentary, GK sedentary, control exercise and GK exercise subgroups at 8 months. Body weight (443.64±7.94** *vs.* 400.33±12.17), heart weight (1.60±0.04* *vs.* 1.37±0.05) and non-fasting blood glucose (161.29±12.77** *vs.* 91.67±1.74) were significantly (p<0.01) increased in sedentary GK compared to sedentary control rats. Exercise training modestly reduced body weight, blood glucose and increased heart weight to body weight ratio in both GK and control rats although these differences did not reach significance (p<0.05). The results for the one-way ANOVA followed by Bonferroni corrected t tests for multiple comparisons are described under table 7.1.

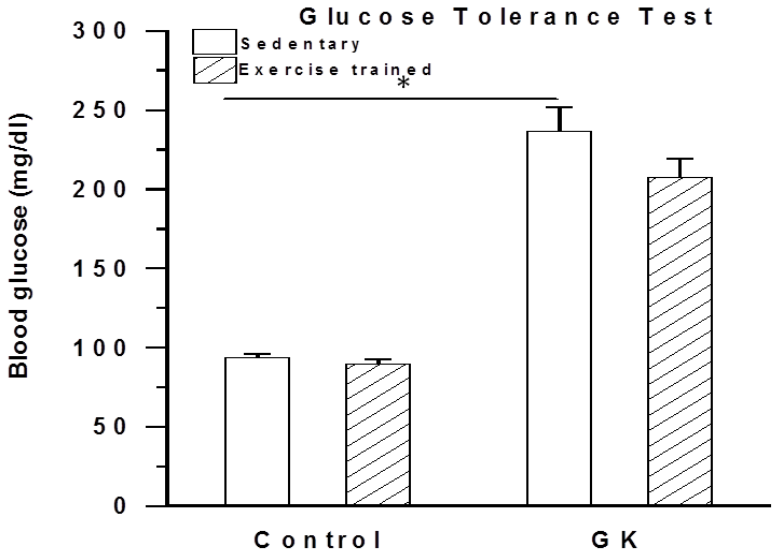

Figure 7.1: Oral glucose tolerance test. Glucose tolerance test performed at 120 minutes following glucose administration. Data are mean ± SEM and is representative of 15 animals in each group. Lines over the bars indicate significance *p< 0.05, One-way ANOVA followed by Bonferroni corrected t-tests for multiple comparisons.

Animals	Non-fasting Blood Glucose (mg/dl)	BW (g)	HW (g)	HW/BW ratio (mg/100g body weight)
Control sedentary (CS) (n=15)	91.67±1.74	400.33±12.17	1.37±0.05	3.43±0.07
Control + exercise (CEX) (n=15)	89.67±1.58	371.73±11.08	1.34±0.04	3.62±0.09
GK sedentary (GKS) (n=15)	161.29±12.77**	443.64±7.94**	1.60±0.04*	3.61±0.08*
GK + exercise (GKEX) (n=15)	133.07±9.79**	418.93±6.80*	1.64±0.04*	3.92±0.13

Non-fasting blood glucose: CS vs. GKS, CS vs. GKEX, CEX vs. GKS and CEX vs. GKEX $p<0.01$
BW: CS vs. GKS and CEX vs. GKEX $p< 0.05$; CEX vs. GKS $p< 0.01$
HW: CS vs. GKS, CS vs. GKEX, CEX vs. GKS and CEX vs. GKEX $p<0.01$
HW/BW: CS vs. GKS $p<0.01$

Table 7.1: **General glucometry and gravimetry characteristics for control sedentary, GK sedentary, control exercised and GK exercised trained subgroups at 8 months.** All data were obtained prior to the end of the treatment period. Data are given as mean±SEM, *$p<0.05$ **$p<0.01$, One-way ANOVA followed by Bonferroni corrected t-tests for multiple comparisons. Numbers in brackets indicate number of animals used for experiments.

2. Effects of exercise training on excitation-contraction coupling in the Goto-Kakizaki type 2 diabetic rat

Figure 7.2 represents the time-dependent effects of exercise on ventricular myocyte shortening for GK subgroups (8 months); control sedentary, GK sedentary, control exercise and GK exercise, treatment on resting cell length, TPK relaxation shortening, THALF relaxation shortening and amplitude of shortening (expressed as % RCL). The results indicate that TPK shortening (Figure 7.2B) was not significantly (p<0.05) different in myocytes from sedentary GK compared to sedentary control rats, however, TPK shortening was significantly (p<0.05) reduced in myocytes from exercise trained compared to sedentary control rats (110±0.19 *vs*.127±0.25) and was significantly (p<0.05) increased in myocytes from exercise trained GK compared to exercise trained control rats (137±0.23 vs. 123±0.32). THALF relaxation of shortening (Figure 7.2C) was not significantly (p<0.05) different in myocytes from sedentary GK compared to sedentary control rats. However, THALF relaxation was significantly (p<0.05) prolonged in myocytes from exercised trained GK compared to exercised trained control rats (86.1±0.29 *vs*. 80±0.35). Amplitude of shortening (Figure 7.2D) was not significantly (p<0.05) altered in myocytes from sedentary GK compared to sedentary control rats or by exercise training.

Figure 7.3 represents the time-dependent effects of exercise on ventricular myocyte calcium homeostasis in GK subgroups (control sedentary, GK sedentary, control exercise and GK exercise) treatment on resting fura-2ratio, TPK Ca^{2+} transient, THALF Ca^{2+} transient and Amplitude of Ca^{2+} transient. The results indicate that resting fura-2 ratio (Figure 7.3A) was significantly (p<0.05) increased in GK exercised trained rats compared to sedentary GK rats (0.86±0.26 *vs*. 0.74±0.32). No difference was observed for sedentary control compared to control exercised rats. TPK Ca^{2+} transient (Figure 7.3B) was not significantly (p<0.05) different in myocytes from sedentary GK compared to sedentary control rats. TPK Ca^{2+} transient was significantly (p<0.05) prolonged in myocytes from exercised trained GK compared to exercised trained control rats (72.3±3.41 *vs*. 57.4±1.96). THALF decay (Figure 7.3C) was not significantly (p<0.05) altered in myocytes from sedentary GK compared to sedentary control rats or by exercise training. The amplitude of the Ca^{2+} transient (Figure 7.3D) was not significantly (p<0.05) altered in myocytes from either sedentary GK compared to sedentary control rats or by exercise training.

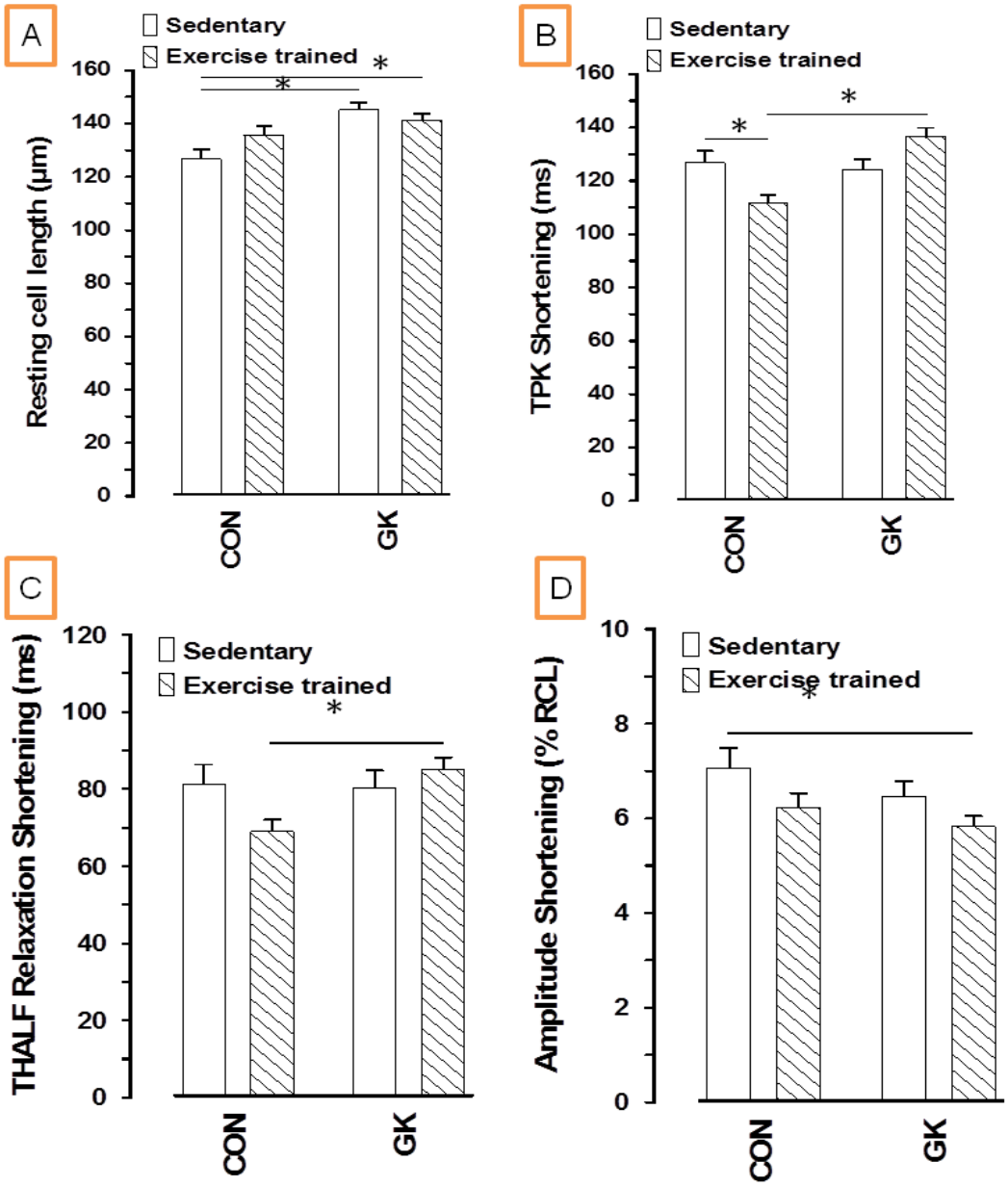

Figure 7.2: Contractility in ventricular cardiomyocytes. Time-dependent effects of control sedentary, GK sedentary, control exercised and GK exercised trained subgroups on Resting cell length **(A)**, TPK relaxation shortening **(B),** THALF relaxation shortening **(C)** and Amplitude of shortening (% RCL) **(D)** in electrically stimulated myocytes at 1 Hz. perfused at 35-37^{o}C in a solution containing 1 mM Ca^{2+}. Data are mean ± SEM and is representative of 44-67 cells from 5-6 hearts. Significance was set at *p<0.05, One-way ANOVA followed by Bonferroni corrected t-tests for multiple comparisons.

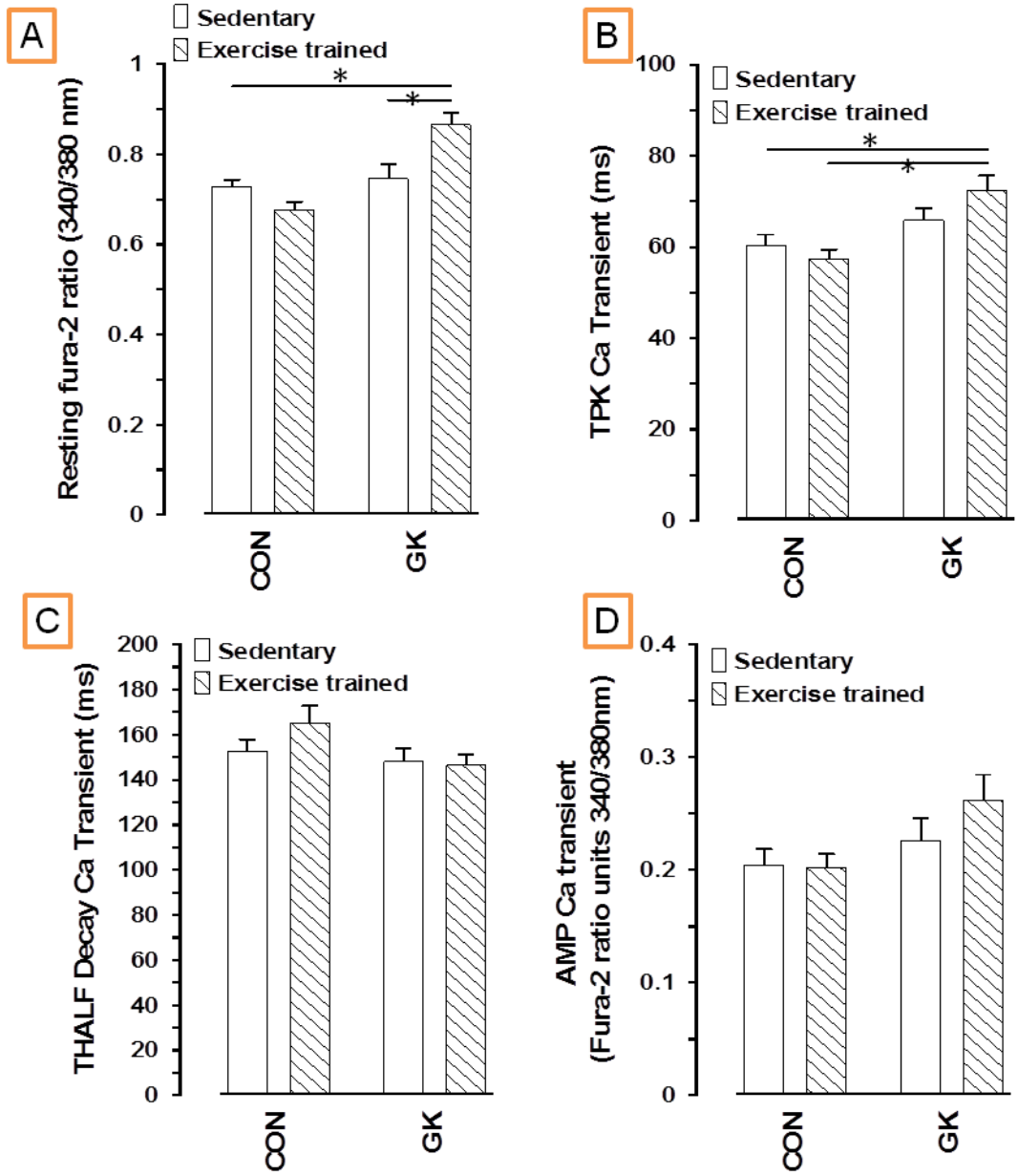

Figure 7.3: $[Ca^{2+}]_i$ transient kinetics in ventricular cardiomyocytes. Time-dependant effects of control sedentary, GK sedentary, control exercised and GK exercised trained subgroups on Ca^{2+} homeostasis, Resting Fura-2 ratio **(A)**, TPK Ca^{2+} transient **(B)**, THALF decay Ca^{2+} transient **(C)** and Amplitude of Ca^{2+} transient **(D)** in ventricular myocytes stimulated at 1 Hz and perfused with a solution containing 1 mM Ca^{2+} at 35-37^{o}C. Data are Mean±S.E.M and is representative of 40-46 cells from 5-6 hearts. Significance was set at *p<0.05, One-way ANOVA followed by Bonferroni corrected t-tests for multiple comparisons.

3. Structural investigations into effects of exercise training on LV remodelling in GK rat

LV from control sedentary and exercised trained groups revealed preserved cross-striation patterns and organised muscle fibre structure. However, GK sedentary group represented the general disorganised architecture of the myocardium characterised by hypertrophied cardiomyocytes, disarray of myofibres, irregular myofibril pattern and scared myofibrils compared to GK exercised trained group which seemed to preserve the normal striation patterns at some extent (Figure 7.4A). ECM deposition in both interstitial and perivascular regions highlighted by myocardial fibrosis showed an increase in fibrotic tissue (green staining) together with an increase in caspase-positive cells in the GK sedentary and GK exercised trained group (Figure 7.4A). Quantitative assessment (Figure 7.4B) showed a significant (*p<0.05) decrease in myocardial fibrosis in GK exercised trained group compared to GK sedentary group (5.24±0.44% *vs.*7.69±0.49%) and in control exercised trained group compared to control (2.99±0.32% vs. 3.78±0.29%). Figure 7.4C represents quantitative assessment of caspase-positive cells highlighting a significant (*p<0.05) decrease in GK exercised trained group compared to GK sedentary group (5.06±0.47 *vs.*8.05±0.42) positive cells/mm^2. Similarly, control exercised trained group compared to control (1.30±0.39 vs. 2.39±0.33) also revealed a significant (*p<0.05) decrease in caspase-3 positive cells/mm^2.

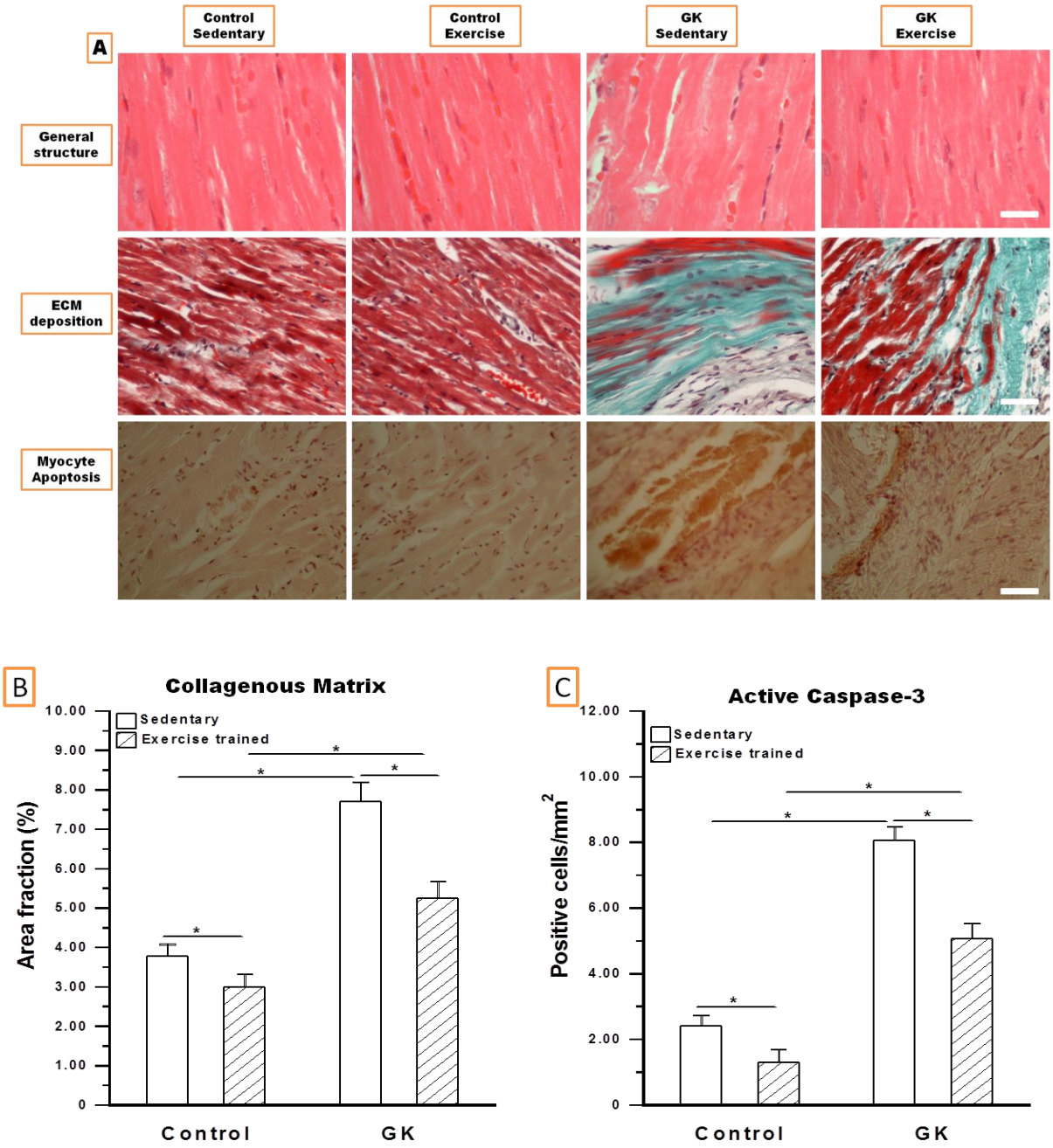

Figure 7.4: Structural remodelling of the Left ventricle in control sedentary, GK sedentary, control exercised and GK exercised trained subgroups. Representative ventricular cross-section light photomicrographs detailing LV histopathology, showing H & E stained LV myocardial sections, Masson's Trichrome stained myocardial sections and active Caspase-3 positive cells (brown staining) **(A)** Original Magnification X1000 oil immersion, X400, X400; Photomicrographs are typical of 35-45 fields/experimental groups consisting of 6-9 animals per group. Scale bar indicates 20 µm and calibration is the same for all photomicrographs. Quantitative assessment of interstitial fibrosis **(B)** and immunoreactivity **(C)** using Image J analysis tool. Bar chart data are Mean±S.E.M, *p< 0.05, **p< 0.01, One-way ANOVA followed by Bonferroni corrected t-tests for multiple comparisons.

4. Molecular events underlying effects of exercise training on left ventricular hypertrophy in GK rats

Natriuretic peptides atrial natriuretic peptide (ANP) and brain natriuretic peptide (BNP) are considered sensitive biomarkers for hypertrophy together with cellular Anti- αSKA1 labelling intensity in LV myocardium. Figure 7.5 represents an increased expression of ANP (Figure 7.5A) and BNP (Figure 7.5B) quantified by qRT-PCR in GK sedentary group compared to control sedentary group. This effect was partly attenuated by exercise training as ANP expression was significantly (*p<0.05) decreased in exercised trained GK group compared to GK sedentary group (1.00±0.12 *vs.*1.35±0.11). Similarly, ANP expression was reduced in exercised trained control group compared to sedentary control group (0.68±0.09 *vs.*0.95±010). BNP gene expression in GK exercised trained group was significantly (*p<0.05) reduced compared to sedentary GK group (1.13±0.16 *vs.*1.45±0.13). No significant change was observed between exercised trained control group and sedentary control group.

Left ventricle hypertrophy in GK rats was accompanied by increases in cellular Anti-αSKA1 intensity. Figure 7.5C represents α-skeletal actin intensity (green staining) obtained by Anti- αSKA1 labelling and confocal analysis of LV myocardial sections. An increase in Anti- αSKA1 immunostaining was significantly (*p<0.05) evident in the GK sedentary group and this appeared to be reduced in the exercised trained GK group. The distribution of αSKA1 amongst the groups was of a focal pattern but both intensity and density of fibres were greater in the GK sedentary groups compared to normal myocardium. Control sedentary group and exercised trained control group αSKA1 intensity remained almost the same. Quantitative assessment (Figure 7.5D) revealed a significant (*p<0.05) increase in α-skeletal actin intensity between GK sedentary compared to control sedentary group (18.00±1.36 *vs.*13.24±1.29). Exercise training revealed a significant (*p<0.05) decreases in α-skeletal actin intensity in GK exercised trained group compared to GK sedentary group (18.00±1.36 *vs.*29.12±1.40) and in control exercised trained group compared to sedentary control (10.07±1.22 vs. 13.24±1.29) (Figure 7.5D).

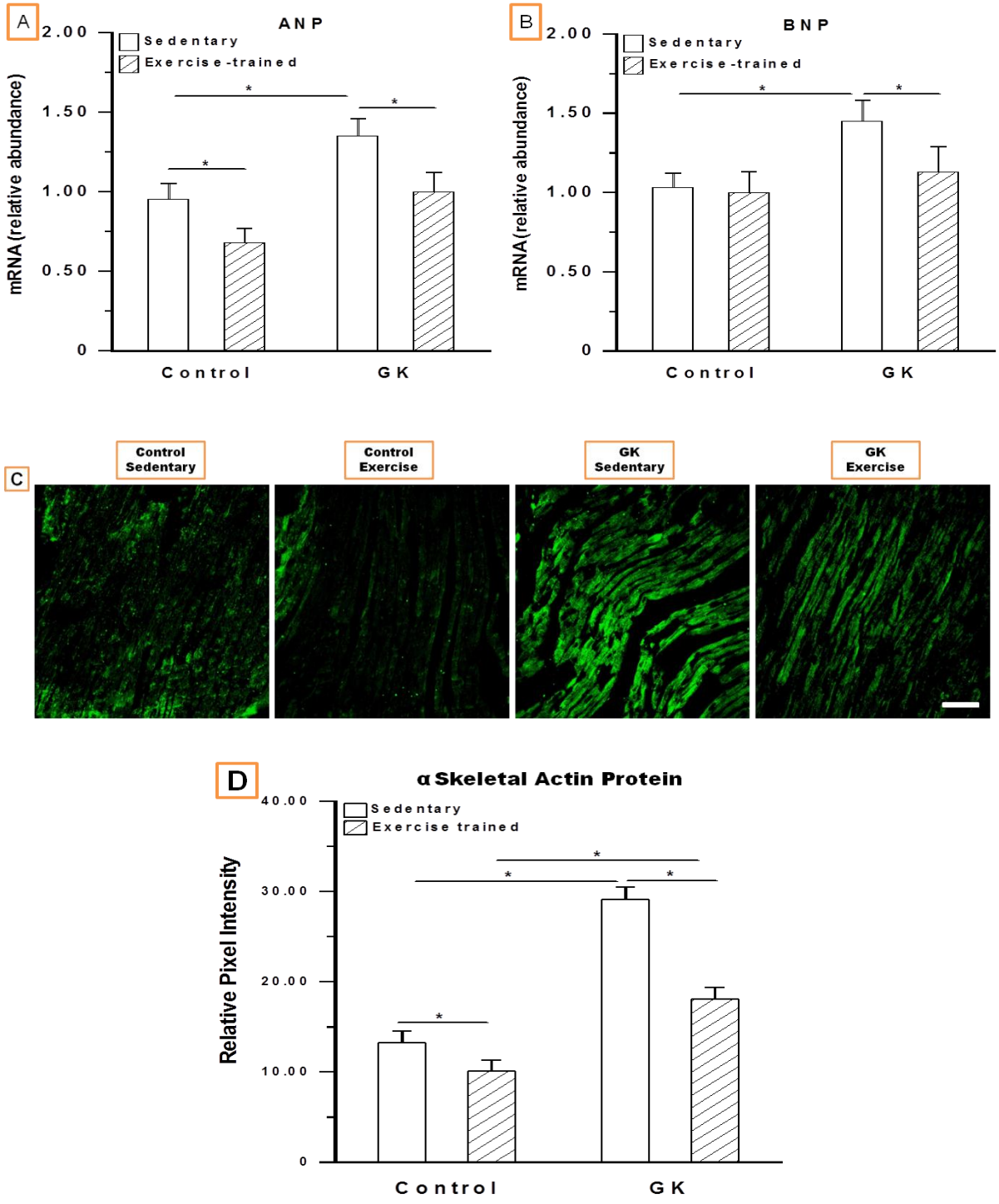

Figure 7.5: Assessment of hypertrophy in the left ventricle. Summarised data of ANP **(A)**, BNP **(B)** gene expression, confocal imaging of α-skeletal actin intensity **(C)** and quantitative assessment of relative pixel intensity measured by image J analysis tool in control sedentary, GK sedentary, control exercised and GK exercised trained subgroups. Results are representative of 6-9 animals/per group conducted in triplicate. RT-PCR amplification was normalised to that of GAPDH. Scale bar indicates 20 µm. Bar chart data are expressed as Mean±SEM. Lines over bars with asterisk indicate significance * $p<0.05$, ** $p<0.01$, One-way ANOVA followed by Bonferroni corrected t-tests for multiple comparisons.

5. Molecular events characterising effects of exercise on extracellular matrix proliferation in GK rats

a. Transcriptional profile of $[Ca^{2+}]_i$ transients

Figure 7.6A represents mRNA gene expression analysis for $[Ca^{2+}]_i$ mediators (SERCA2a, NCX, Pln, RyR2, CaV1.2, CaV1.3, Calm2 and CaMkd) in control sedentary, GK sedentary, control exercised and GK exercised trained subgroups. As expected, the calcium transient mediators were not highly affected by exercised training. Nevertheless, some genes including NCX and Calm2 revealed significant (*p<0.05) changes between sedentary GK and GK exercised trained subgroups. Gene expression for NCX revealed a significant (*p<0.05) increase in GK exercised trained group compared to GK sedentary group (1.50±0.04 *vs.* 1.10±0.03) highlighting a positive effect of exercise training on the contractility of GK rats. Exercised-trained control group and control sedentary group revealed no significant (*p<0.05) differences (1.18±0.08 *vs.*1.00±0.04). Similarly, Calm2 revealed a (*p<0.05) significant increase in GK exercise trained group compared GK sedentary group (1.32±0.03 *vs.* 0.54±0.09), highlighting a positive effect of exercise on cardiac compliance. Additionally, a significant (*p<0.05) increase was observed in control exercised trained group compared to control sedentary group (1.35±0.06 *vs*. 0.58±0.08). On the other hand, CaMkd gene expression did not reach significance (*p<0.05) between control sedentary, control exercised trained, GK sedentary or GK exercised trained subgroups. Gene expression for NCX was significantly (*p<0.05) increased in GK exercised trained group compared to GK sedentary group (1.50±0.09 *vs*. 1.10±0.03) while control exercised trained group compared to control sedentary group did not show significance (1.18±0.08 *vs*. 1.00±0.04). SERCA2a pump did not reveal any significant (*p<0.05) changes amongst control exercised trained compared to control sedentary (1.08±0.12 *vs.* 1.00±0.03) or GK exercised trained compared to GK sedentary (1.03±0.09 *vs.* 1.10±0.07) subgroups which is typical of T2DM. Similarly, no significance was recorded for RyR2 receptor gene expression in control exercised trained compared to control sedentary (1.10±0.09 *vs*. 1.12±0.06) or GK exercised trained compared to GK sedentary (1.07±0.08 *vs*. 1.09±0.03) subgroups. Phospholamban gene expression revealed a significance increase in GK exercised trained compared to GK sedentary (0.57±0.09 *vs.* 1.00±0.12) subgroups. However, no significance was recorded for control exercised trained compared to control sedentary (1.08±0.10 *vs*. 1.09±0.05) subgroup. L-type calcium channels as expected did not show much difference in the transcriptional profile of control exercised trained compared to control sedentary

(CaV1.2 (1.00±1.00 *vs.* 1.09±0.09), CaV1.3 (1.20±0.07 *vs.* 1.07±0.03)) or GK exercised trained compared to GK sedentary (CaV1.2 (1.09±0.08 *vs.* 1.15±0.07), CaV1.3 (1.09±0.03 *vs.* 1.10±0.02)) subgroups.

b**. Transcriptional profile of ECM proliferation**

Figure 7.6B represents mRNA gene expression analysis for ECM components (Col 1α, Col 3α, Fibronectin and Elastin) and regulators (MPP2, MMP9, TIMP4, CTGF, Integrin 5α and Cx43) in control sedentary, GK sedentary, control exercised and GK exercised trained subgroups. Gene expression for Collagen 1α was significantly (*p<0.05) increased in GK sedentary group compared to sedentary control group (1.45±0.11 *vs.* 1.00±0.08). This increase was reversed by exercise training as gene expression for exercised training group compared to GK sedentary group was significantly (p<0.05) decreased (0.89±0.09 *vs.* 1.45±0.11). Exercised-trained control group compared to control sedentary group revealed no significant (p<0.05) differences (1.09±0.10 *vs.*1.00±0.08). Similarly, gene expression for Collagen 3α revealed a significant (p<0.05) increase in GK sedentary group compared to control sedentary group (1.39±0.12 *vs.* 1.00±0.09) and control exercised training group (1.07±0.10). This increase was reversed by exercise training as gene expression for GK exercised training group compared to GK sedentary group was significantly (p<0.05) decreased (1.00±0.11 *vs.* 1.39±0.12). A significant increase was observed in expression for fibronectin and elastin levels in GK sedentary compared to control sedentary group (Fibronectin (1.05±0.12 *vs.* 0.55±0.06), Elastin (1.30±0.09 *vs.* 0.66±0.09)). This was reversed by exercise training in both ECM components, as a significant (p<0.05) decrease was observed in GK exercised training group compared to GK sedentary group for fibronectin (0.69±0.10 *vs.* 1.05±0.12) and elastin (1.08±0.09 *vs.* 1.30±0.09).

ECM regulators MMP2 and MMP9 were significantly (p<0.05) increased in GK sedentary group compared to control sedentary group (MMP2 (1.10±0.12 *vs.* 0.90±0.09), MMP9 (1.33±0.14 *vs.* 0.89±0.10)). This increase was reversed by exercise training as a significant (p<0.05) decrease in GK exercised trained group compared to GK sedentary group (MMP2 (0.80±0.12 *vs.* 1.10±0.12), MMP9 (1.00±0.15 *vs.* 1.33±0.14)). Gene expression for TIMP revealed a significant increase in GK sedentary group compared to control sedentary group (1.47±0.13 *vs.* 0.63±0.10) and exercise training attenuated this effect significantly (p<0.05) as compared to GK sedentary group (1.20±0.12 *vs.* 1.47±0.13). CTGF expression was also significantly (*p<0.05) increased in GK sedentary group compared to control sedentary group (1.43±0.15 *vs.* 0.67±0.09)

and control exercised trained group (0.63±0.13). Interestingly, exercise training significantly reduced CTGF expression in GK exercised trained group compared to GK sedentary group (1.12±0.12 *vs.* 1.43±0.15). Integrin 5α expression was significantly (p<0.05) increased in GK sedentary group compared to control sedentary group (1.34±0.13 *vs.* 0.53±0.09) and exercised trained group (0.50±0.10). Exercise training significantly reduced this expression compared to GK sedentary group (1.10±0.14 *vs.* 1.34±0.13). Finally, Cx43 expression was significantly increased in GK sedentary group compared to control sedentary group (1.34±0.10 *vs.* 1.00±0.07). However, exercise training had no beneficial effect on Cx43 expression in LV of GK rat heart (1.35±0.09 *vs.* 1.34±0.10).

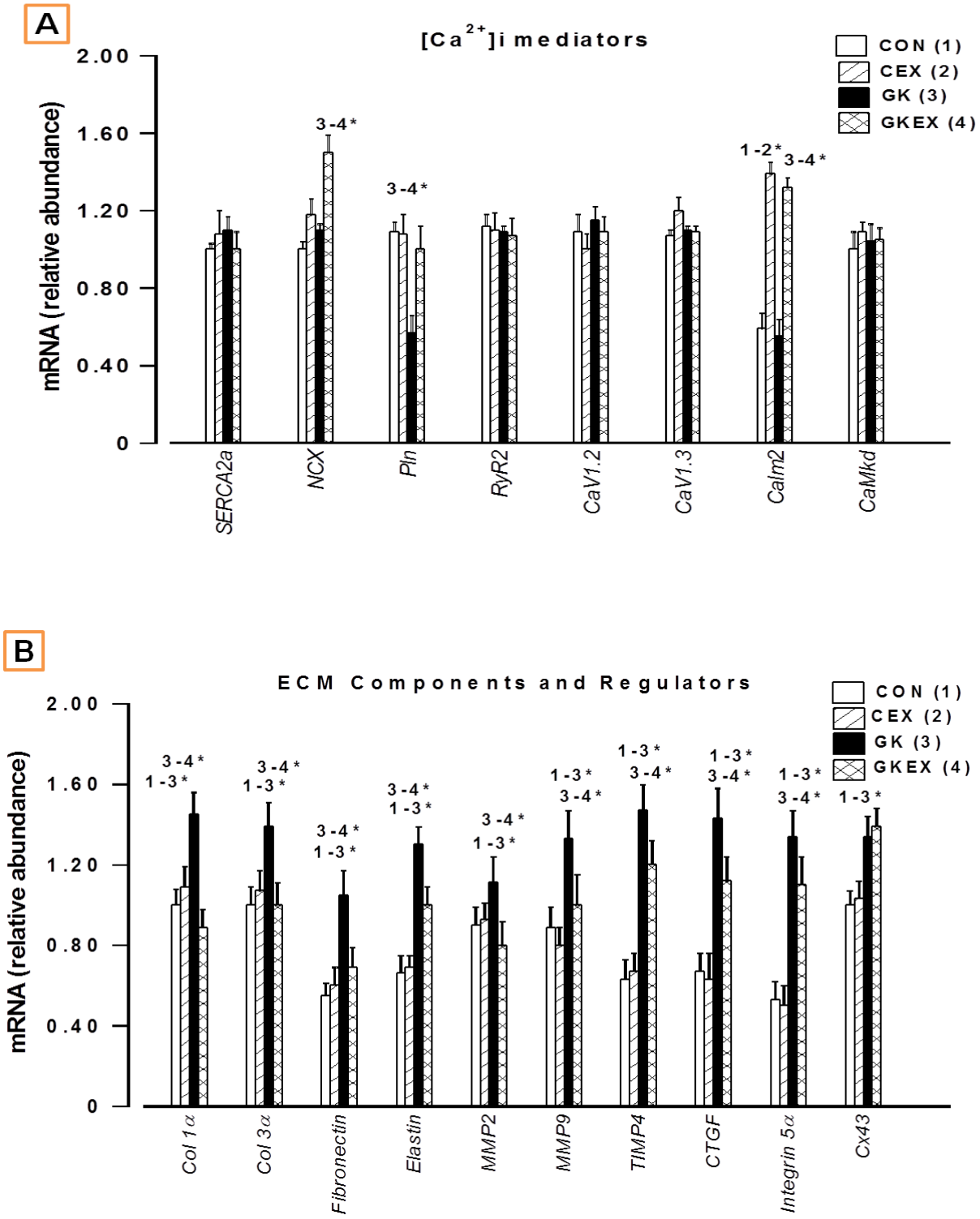

Figure 7.6: Transcriptional profile of the left ventricle. Relative abundance of mRNA for $[Ca^{2+}]_i$ mediators **(A)** and ECM components and regulators **(B)** in control sedentary, GK sedentary, control exercised and GK exercised trained subgroups. Results are representative of 6-9 animals/per group conducted in triplicate. RT-PCR amplification was normalised to that of GAPDH. Data are expressed as Mean±SEM. Numbers signify group identity and asterisk indicate significance * $p<0.05$, One-way ANOVA followed by Bonferroni corrected t-tests for multiple comparisons.

c. Transcriptional profile and activity of TGFβ1

Figure 7.7 represents TGFβ1 mRNA gene expression and active TGFβ1 levels in plasma and LV samples from rats in control sedentary, GK sedentary, control exercised and GK exercised trained subgroups. Active TGFβ1 levels were significantly ($p < 0.05$) increased in plasma in GK sedentary group compared to control sedentary group (2.69±0.10 *vs.* 1.09±0.05) (Figure 7.7A). This was reduced by exercise training as TGFβ1 levels for exercised training group compared to GK sedentary group was significantly ($p<0.05$) decreased (2.10±0.12 *vs.* 2.69±0.10). Exercised-trained control group compared to control sedentary group revealed no significant ($p<0.05$) differences (0.99±0.09 *vs.* 1.09±0.05). Total TGFβ1 levels were significantly ($p < 0.01$) increased in GK sedentary group compared to control sedentary group (49.70±1.50 *vs.* 25.03±1.20 pg/mg of total protein) (Figure 7.7B). This was potentially reduced by exercise training as TGFβ1 levels for exercised training group compared to GK sedentary group was significantly ($p<0.05$) decreased (26.09±1.40 *vs.* 49.70±1.50 pg/mg of total protein). Exercised trained control group compared to control sedentary group revealed no significant ($p<0.05$) differences (22.07±1.09 *vs.* 25.03±1.20 pg/mg of total protein). Similarly, active TGFβ1 levels in LV were significantly ($p < 0.01$) increased in GK sedentary group compared to control sedentary group (41.23±1.65 *vs.* 29.09±1.23 pg/mg of total protein). This was reduced by exercise training as active TGFβ1 levels for exercised training group compared to GK sedentary group was significantly ($p<0.05$) decreased (30.09±1.52 *vs.* 41.23±1.65 pg/mg of total protein). Exercised-trained control group compared to control sedentary group revealed no significant ($p<0.05$) differences (24.78±1.20 *vs.* 29.09±1.23 pg/mg of total protein). Finally, gene expression for TGFβ1 was significantly ($p<0.05$) increased in GK sedentary group compared to control sedentary group (2.00±1.30 *vs.* 1.20±0.12 ratio units). Expression was reduced by exercise training as mRNA levels for exercised training group compared to GK sedentary group was significantly ($p<0.05$) decreased (1.13±1.20 *vs.* 2.00±1.30 ratio units). Exercised-trained control group compared to control sedentary group revealed no significant ($p<0.05$) differences (1.00±0.19 *vs.* 1.20±0.12 ratio units).

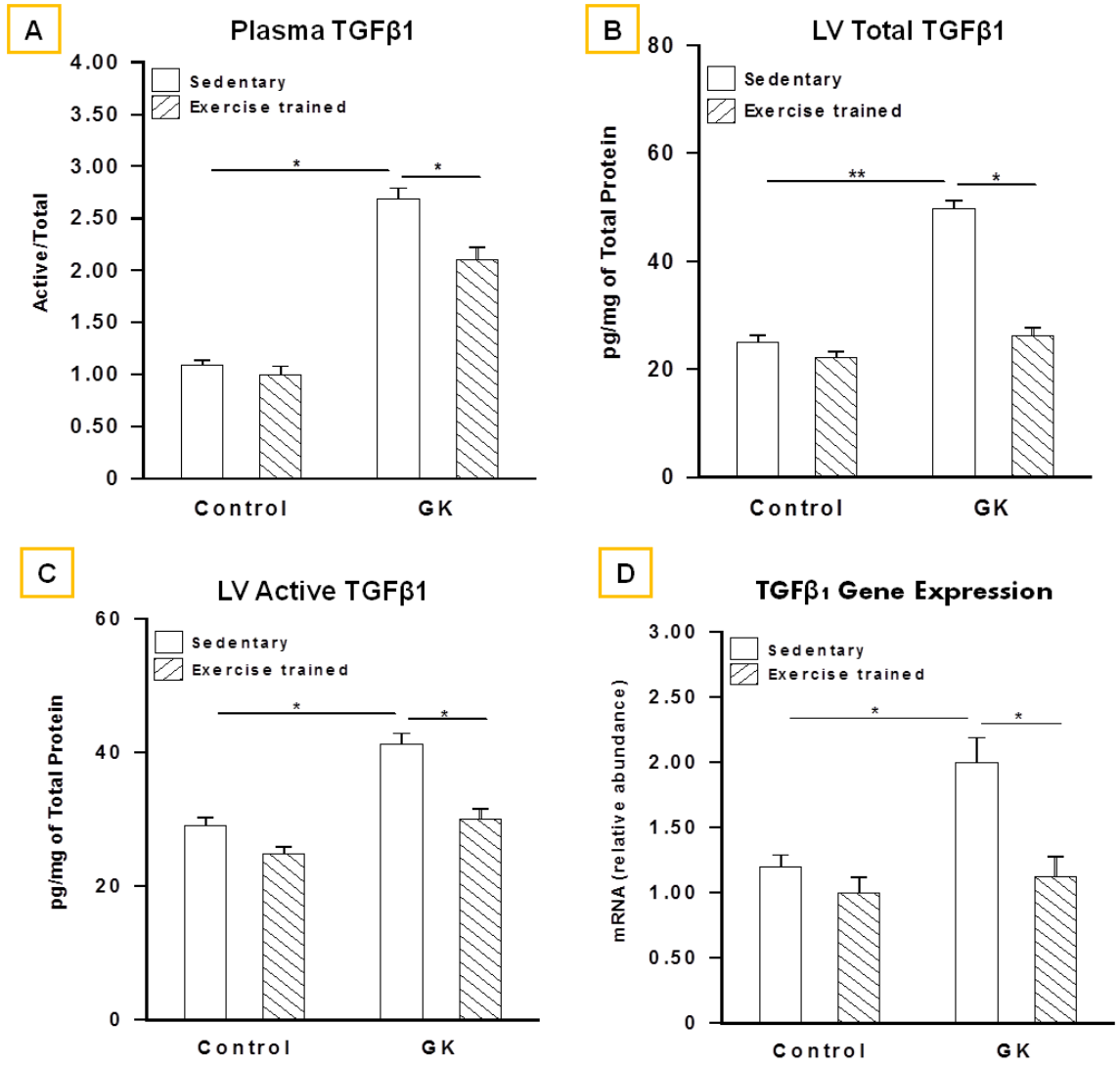

Figure 7.7: TGFβ1 protein level and gene expression profile. Summarised Data from ELIZA showing ratio of active: total TGFβ1 protein in plasma **(A)**, total TGFβ1: total extracted LV protein **(B)** and active TGFβ1: total extracted LV protein **(C)** in control sedentary, GK sedentary, control exercised and GK exercised trained subgroups (n=3/group). mRNA gene expression of TGFβ1 **(D)** (n=8/group). The results of both ELIZA and qRT-PCR are representative of 3 individual experiments conducted in triplicate. RT-PCR amplification was normalised to that of GAPDH. Data are expressed as Mean±S.E.M. Lines over bars indicate significance * $p<0.05$, ** $p<0.01$, One-way ANOVA followed by Bonferroni corrected t-tests for multiple comparisons.

7.4. Discussion

Summary of key findings:

1. LV remodelling and accompanying ECM deposition, apoptotic cell death in T2DM was reversed by exercise training.
2. Exercise training significantly reduced LV hypertrophy in T2DM accompanied by reduced α-skeletal actin protein intensity, ANP and BNP expression.
3. Molecular alterations in key ECM components and regulatory mechanisms are reversed by exercise training in T2DM compared to age-matched control animals.
4. Exercise training significantly reduced expression, activity and plasma levels of TGFβ1 in fibrotic remodelling of the myocardium in T2DM.
5. Ventricular myocyte shortening and Ca^{2+} transport were generally well preserved in T2DM and exercise training did not have a significant effect.
6. Gene expression of key calcium-cycling proteins including SERCA, Plb, NCX and Ryr2 were generally well preserved.
7. Exercise training significantly reduced structural remodelling observed in T2DM, suggesting it to be highly beneficial in T2DM.

Understanding the physiological changes underlying the altered exercise responses are fundamental to the design of therapeutic interventions aimed at helping individuals with DM, especially T2DM in order to increase their levels of fitness and reduce their cardiovascular risk (Regensteiner, 2004; Bassuk *et al*., 2005). Numerous previous studies have highlighted physical training as an effective therapeutic strategy for the management of T2DM (Lindstrom *et al*., 2006; Ellison *et al*., 2012; Tabet *et al*., 2009; Longnathan *et al*., 2012; Reusch *et al*., 2013).

With regards to the functional aspects of this study, it was revealed that exercise training was only able to reduce the characteristics of T2DM in GK rats but the differences did not reach significance. After 2 months of exercise training, the GIT was applied following an overnight fast in all four groups of rats. The results showed that 120 min following an intraperitoneal injection of glucose (2 g/kg body weight), blood glucose levels were significantly elevated in sedentary GK rats compared to sedentary controls demonstrating impaired glucose uptake in GK rats. Exercise training reduced blood glucose to a small extent in control and to a larger extent in GK rats. However,

the difference did not reach significance. Non-fasting blood glucose measured immediately before the experiments was significantly elevated in GK sedentary compared to control sedentary rats. Exercise training reduced blood glucose to a small extent in control and to a larger extent in GK rats however, the difference did not reach significance. Previous studies have shown that long term (2, 8 and 14 months of age) non-fasting serum insulin is reduced in the GK rats compared to age-matched controls whilst fasting-insulin is reduced at 2 months and increased at 8 and 14 months of age in GK rats compared to age-matched controls (Schrijvers *et al*., 2004). Conversely, exercise training for 9 weeks reduced levels of fasting insulin in exercise trained GK rats compared to age-matched controls and calculation of the insulin sensitivity index determined that training significantly increased insulin sensitivity (Grijalva *et al*., 2008). Body weight and heart weight were significantly increased in sedentary GK rats compared to sedentary controls. Collectively, these characteristics are typical of features widely displayed in T2DM (Howarth *et al*., 2008; Howarth *et al*., 2007; Salem *et al*., 2012).

Thereafter, this study investigated the effects of exercise training on EC coupling in the adult GK rat compared to age-matched Wistar control rats. The major findings were that the amplitude of shortening and the amplitude of $[Ca^{2+}]_i$ transients were not altered in ventricular myocytes from sedentary GK compared to sedentary control rats or by exercise training. This is in agreement with previously published studies performed in the GK T2DM rat (Salem *et al.*, 2013). Salem et al demonstrated no significant alterations in $[Ca^{2+}]_i$ transients as well as L-type Ca^{2+} current in ventricular myocytes from 10-11 months old GK rats compared to control sedentary rats or by exercise training. Additionally, gene expressions of key cardiac contractile proteins did not reveal any marked alterations in SERCA2a, RyR2, Calcium channel proteins (CaV1.2 and CaV1.3) and CaMK2d gene expression in regards to exercise training. This may partly be due to the fact that contractile function in the T2DM at 10-11 months is generally well preserved and hence changes in the gene underlying this are not altered to a great extent which is similar to the findings of a previous study (Salem *et al*., 2013). Previous studies have demonstrated that in embryonic cardiomyocytes altered expression of the beta-2 subunit has large effects on L-type Ca^{2+} current however, in adult cardiomyocytes the effects are well tolerated (Mangoni *et al*., 2006; Meissner *et al*., 2011). A study by Zhang and colleages also found no evidence to support the idea that altered Ca^{2+} homeostasis underlies the contractile deficit of DCM (Nemoto *et al*.,

2006; Zhang *et al*., 2010). They postulated that the slower action potential and reduced SERCA2a expression might explain the slower Ca^{2+} transient kinetics in diabetic rats, but not the contractile deficit. Instead they suggest that the observed LV remodelling may play a crucial role (D'Souza *et al*., 2011).

Effects of exercise training on the extracellular matrix

As previously stressed, it is widely accepted that DCM is characterized by a set of structural abnormalities in the heart of diabetics, including cardiomyocyte hypertrophy myocardial fibrosis and apoptosis (Huynh *et al*., 2014). A major finding of this study was that ECM proliferation and consequently myocardial fibrosis, was partly attenuated by physical exercise training. Firstly, the general morphological cross-striation patterns and organised muscle fibre structure were seen in LV from control sedentary and exercise group. In contrast the LV from GK sedentary groups were characterised by hypertrophied cardiomyocytes and disarray of microfibers. Exercise training was partly successful in preserving these morphological features. Myocardial apoptosis was elevated in the GK sedentary group as compared to control groups. Exercise training significantly attenuated this increase in apoptosis in the LV. As previously mentioned, excessive apoptosis is directly related to dysfunction and pathology in the heart exhibited with CVD, DCM and HF (Kang *et al*., 2004; Sharma *et al*., 2007; Elmore, 2007) Intriguing evidence also indicates that apoptotic signaling and caspase activation increase protein degradation and impair contractile function, independent of cell loss (Du *et al*., 2004; Ruetten *et al*., 2001). The findings of the present study are in agreement with previous studies on effects of exercise on caspase-3 mediated apoptosis (Kwak *et al*., 2006). It was also revealed in the same study that age-related apoptosis can be attenuated by exercise training and remodelling in the adult vs young adult heart. Collectively, exercise training proves to be a beneficial non-pharmacological agent in attenuating cardiomyocyte cell death by caspase-3-mediated apoptosis to some extent. However, further investigations are still necessary.

Exercise training reduces ECM deposition

Additionally, a significant proportion of the LV in GK sedentary group was accumulated by ECM depositions marked by the quantified increase in interstitial fibrosis. As mentioned previously, cardiac structural remodelling in the myocardium is widely associated with marked alterations in ECM; a widely recognised change of the failing heart (Miner and Miller, 2006). Conversely, the findings of the present study revealed that exercise training significantly ($p<0.05$) reduced ECM depositions significantly. These alterations were accompanied by marked reductions in ECM components (Col 1α, Col 3α, Elastin, and Fibronectin) following exercise training in the GK group as well as in age-matched Wistar control group following exercise training. As previously stated, the most abundant ECM fibrillar proteins in the heart are collagens, particularly the collagen type I and collagen type III phenotypes (Adeghate *et al*., 2004). A number of previous studies have found that exercise training can reduce cardiac stiffness due to collagen degradation. However, conflicting results have also been published. A study by Woodiwiss *and colleagues* found that 16 weeks of habitual voluntary wheel running reduced cardiac stiffness in young rats, without a significant change in collagen or collagen cross-linking (Woodiwiss *et al*., 1998). Conversely, a study by Thomas *and colleagues* reported that 10 week of exercise training reduced collagen cross-linking in the hearts of old Fischer-344 rats, but not in young rats (Thomas *et al*., 2000; Thomas *et al*., 2001). Furthermore, it was found that exercise training protected against a decline in systolic function, related to an attenuation of decreased solubility of collagen (Choi *et al*., 2009). Data from a study by Xu et al (2008) suggested that early exercise training may attenuate myocardial fibrosis in the infracted heart. This was due to the fact that collagen volume fraction was found to be significantly lower in the exercise trained MI group compared to sedentary MI group, indicating a beneficial role of exercise in MI as well as in attenuating myocardial fibrosis. From the results presented in this study together with previously published findings, it can be concluded to some extent that exercise training may be a beneficial therapy by declining the ventricular remodelling observed in T2DM rats. In turn, this may provide furthermore help for patients who are suffering from this disease.

Exercise training reduces metalloproteinase expression

Conversely, gene expressions of ECM regulators (MMP2, MMP9, TIMP4, CTGF and Cx43) were significantly elevated in the GK sedentary groups compared to control sedentary groups. Interestingly, these were markedly reduced by exercise training. The roles of TGFβ1 and MMPs in cardiac remodelling may be intertwined. In fact, both proteins may be part of one complex pathway for fibrosis. It has been noted that levels of MMP2 are higher in terminally failing hearts, in consistent with TGFβ1 expression increase (Hein *et al*., 2003). The imbalance between MMP and TIMP expression appears to be responsible for the increased MMP activity observed in CHF, which is associated with myocardial matrix collagen disruption and ventricular remodelling (Khan & Shepard, 2006). The results of the present study are in agreement with previous studies on beneficial roles of exercise training in reducing fibrosis and MMP dysregulation (Kwak *et al*., 2011). It was suggested that TGFβ1 is an upstream regulator of TIMP1 and it increases with age, but it is also attenuated by exercise training. Therefore, exercise training could protect the aging heart against dysregulation of MMPs and fibrosis by suppressing elevation of TIMP1 and TGFβ1 (Kwak *et al*., 2011). In addition, Cx43 gene expression level was increased in the GK sedentary groups whereas exercise training could not reduce the expression. Connexins are the pore forming subunits of gap junction channels and these channels regulate membrane permeability in individual cells or couple between adjacent cells to form gap junctions thereby providing a pathway for regulated intercellular communication. Furthermore, Cx43, which is encoded by Gja1, is a major protein of gap junctions in the heart and is vital to the synchronicity of contraction in the heart. Mutations in various connexin proteins including Cx43, are known to be associated with cardiac arrhythmias (Delmar & Makita, 2012). Altered expression of the gene encoding Gja1, if accompanied by a reduction in Cx43 protein, might partly underlie the low heart rates which have been previously reported in GK rat heart (Howarth *et al*., 2008).

TGFβ1 expression is reduced by exercise training

The results of the present study found elevated levels of active TGFβ1 and increased gene expression of TGFβ1 in the GK sedentary group compared to control sedentary group. Interestingly, exercise training significantly reduced active and total levels of TGFβ1 and gene expression in the GK exercised trained group. Conflicting data exist on the regulation of TGFβ1 by physical exercise. Previous study on acute bout of strenuous exercise caused a 2-3 fold increase in serum levels of TGFβ1 in healthy young sportsmen (Paczek *et al*., 2006). They suggested that this increased level of TGFβ1 could be involved in the process of adaptation of humans to physical training. Conversely, in another study, the expression of TGFβ1 is similar in both the exercise and sedentary MI groups 9 weeks after MI, indicating that exercise training does not affect cardiac TGFβ1 expression (Xu *et al*., 2008). Additionally, the transcriptional factor NF-kB signalling pathway has been proposed to be involved in the increase of pro-inflammatory cytokines that occurs during acute exercise (Petersen & Pedersen, 2005) However, it is suggested that exercise training may attenuate this response (Lira *et al*., 2008; Lira *et al*., 2009). In another study, measuring TGFβ1 expression levels in Wistar rats treated with Isoprenaline and exercise training found that the use of it prevented LV hypertrophy, improved myocardial contractility and conversely, attenuated the increase of TGFβ1 mRNA (Serra *et al*., 2010). Thus, concluding that exercise training in a model of beta-adrenergic hyperactivity, can avoid the adverse remodelling of the LV and inhibit inflammatory cytokines. Moreover, the cardioprotection is related to beneficial effects on myocardial performance. Another study highlighted that a combined strength and aerobic exercise program has a potential anti-atherogenic and anti-inflammatory impact which most likely reduces the risk of CVD and consequently, improves the health status in patients with T2DM (Touvra *et al*., 2011). Collectively, discrepancies exist in literature regarding the role of TGFβ1 in attenuating ECM deposition and the resultant structural remodelling of the LV. Further investigations are necessary before it can be concluded that exercise training may reduce levels of TGFβ1 and conversely, improve LV remodelling in T2DM.

Coupled with ECM deposition, it is established that left ventricular hypertrophy is an independent and powerful predictor of HF and mortality (Lips *et al.* 2003; Reichek *et al.* 2009; Van Heerebeek *et al*., 2007). A great deal of evidence has extended the regulatory portfolio of HG-up-regulated TGFβ1 to induce this cellular hypertrophy in T2DM. The results of the present study revealed marked elevations in ANP and BNP

gene expression in the GK sedentary group compared to control sedentary group. Surprisingly, the expression of these peptides was significantly reduced by exercise training indicating that exercise may have a potential role in reducing ventricular hypertrophy. A recent study has shown a long-term benefit of BNP in reversing cardiac hypertrophy in vivo with simultaneous down regulation of TGFβ1 signalling (He *et al*., 2010). Additionally, an increased LV cellular α-SKA intensity (marker for hypertrophy) was observed in the GK sedentary group and this was significantly reduced in the exercise trained GK group. However, LV wall thickness was not measured in this study. It would be of great interest to see if reductions in ANP/BNP levels and α-SKA intensity correlate with reduced LV size after exercise training. As found in this study, TGFβ1 overexpression resulted in increased cardiac hypertrophy that was characterised by both interstitial fibrosis and increased expressions of ANP and BNP. TGFβ1 is thought to be an important trigger of fibrosis in the hypertrophied heart. Expression levels of TGFβ1 in hypertrophic obstructive cardiomyopathy were 2-5 times higher than in non-hypertrophied hearts (Li *et al*., 2002).

Concluding Remarks

Taken together, the results on the functional aspect of this study did not show a significant effect of physical exercise training in the GK rats. Physical exercise was useful to some extent, but results did not show major changes in contraction and $[Ca^{2+}]_i$ transients homeostasis. This was reflected in the gene expression analysis of the key Ca^{2+} handling proteins which showed no significant changes in regards to physical exercise training. Conversely, ECM proliferation and TGFβ1 activity was markedly reduced by exercise training along with TGFβ1 activity. Exercise training was also able to reduce ventricular hypertrophy and actin intensity in the GK exercise trained group. Together, these results represent a beneficial role of exercise training in reversing structural remodelling in T2DM characterised by ECM proliferation, cardiac apoptosis, LV hypertrophy, and TGFβ1 activity. Furthermore, exercise training represents a non-pharmacological therapeutic strategy for T2DM patients and should be extensively applied.

CHAPTER 8

GENERAL DISCUSSION

8.1 Collective discussion

DM is a major metabolic disorder which is currently affecting more than 380 million people worldwide. In terms of expense, it costs about £850 billion to diagnose, treat and care for DM patients worldwide. The disease appears in mainly two forms, T1DM and T2DM. Over 90-95 % of all diabetic patients suffer from T2DM and 5-10% suffer from T1DM. T1DM is a lifelong metabolic disorder characterised mainly by a deficiency in endogenous insulin where the patient becomes dependent on exogenous insulin administration (Thorve *et al*., 2003). On the other hand, T2DM is characterised by insulin resistance and can develop at any age but is most commonly diagnosed after the fourth decade of life (Bergman, 2009). T2DM patients are treated with life style changes including physical exercise, diet and glycaemic control. If left untreated, both T1DM and T2DM can lead to long term complications which become more severe with time. Two major complications of DM include DCM and DN. Generally, most diabetic patients will eventually die as a result of either one or both complications.

Cardiac dysfunction and kidney disease are well-known consequence of DM, with sustained HG leading to the development of DCM and DN that are independent of CVD or hypertension. Animal models of diabetes are commonly used to study the pathophysiology of DCM and DN, with the hope that increased knowledge will lead ultimately to the development of better therapeutic strategies. This study was designed to investigate the effect of STZ-induced DM on the functional, morphological and molecular changes which are occurring in the heart and the kidney during DM, employing two time points of STZ-treatment, namely 2 months and 4 months. A fundamental rationale of this study was to investigate if adult vs young adult had a more adverse effect on severity of DM compared to untreated healthy age-matched control rats. In addition, this study investigated the beneficial effects of physical exercise on cardiac function, structure and molecular alterations employing the GK rat as a model of T2DM compared to sedentary animals both diabetic and control groups. This discussion will now be focused on the results obtained from the STZ-induced T1DM study employing the heart and kidney (chapter 3-6), and the study on exercise in the GK rat of T2DM.

As discussed in the preceding chapters, it is widely accepted that DM via the elevated HG can elicit adverse long term damage to both the heart and the kidney either similarly

or differently over time. Numerous studies have been performed investigating either the heart or the kidney at any one time, but no study as yet has investigated both organs at the from same animal, time, conditions and duration of DM. As such, the novelty of this study was to employ both organs from the same animals and at the same time investigating the severity of DM over time, at 2 months and 4 months of development of DM compared to age-matched controls. Generally, both groups (2 and 4 months) of diabetic rats developed more or less similar characteristics regarding blood glucose levels, organ weights and body weights. The changes in the different measured parameters were more sever or worsened with time. The data have clearly demonstrated that the diabetes if left untreated, can lead to time-dependant changes in the two organs of the body. Regarding the morphology of the heart and the kidney, the present results have shown that diabetes-induced HG can elicit more or less similar damage to the organs at cellular levels. These, however were accompanied by marked cell death mediated by caspase-3 mediated mechanisms. Both the heart and the kidney showed signs of apoptosis, which were more severe with age. It is established that apoptotic cells display a number of biochemical modifications such as protein cleavage, protein cross-linking, DNA breakdown, and phagocytic recognition that collectively result in the distinctive structural pathology described in the study (Hengartner, 2000). These processes are occurring simultaneously in both organs and therefore deserve attention in the future.

Furthermore, in regards to the heart, the initial stages of ventricular remodelling, the heart responds to iterations in the haemodynamic workload, allowing for the normalisation of wall stress and preservation of diastolic and systolic function. Progressive remodelling of the heart's muscular, vascular and ECM components leads to changes in ventricular wall and chamber dimensions. If the sustained increase in wall stress exceeds that of the compensatory capacity of the heart, subsequent degradation of the ECM and alterations of the collagen network will progressively result in alterations of LV morphology and function. In correlation with many previous studies on contraction and cellular Ca^{2+} homeostasis, the present study found that T1DM can elicit the development of cardiac disease that is characterised by alterations in contractility of ventricular cardiomyocytes and Ca^{2+} homeostasis. The present study measured the relevant contractile calcium channel proteins which were in correlation with the dysfunction of the contractile apparatus. Thus, highlighting the finding that contractile

dysfunction is occurring at the cellular level in T1DM, in conjunction with dysfunction of the cardiac contractile pump, and these changes were more severe with age.
However, this study did not measure any functional parameters of the kidney, which may also reflect similar findings.

A major finding of this study was the ECM deposition in the heart and the kidney that was occurring in parallel at the same time during DM. Collagen deposition and ECM alterations are accepted as hallmarks of the diabetic heart as well as the kidney (Brownlee *et al*., 2001). Together with, marked elevations in MMPS, TIMPS and Cx43 highlighted that the ECM deposition is regulated by such important genes. Various mechanisms have been suggested via which HG and its biochemical pathways contribute towards pathological remodelling of the heart and the kidney (Elmore, 2007). This is of fundamental importance, as while the heart is being undergoing structural remodelling, the kidney is undergoing structural remodelling as well. These findings were made imperative when the pro-fibrogenic cytokine TGFβ1, expression and levels were found to be elevated in both the heart and the kidney similarly. From the present study it was evaluated that TGFβ1 played a fundamental role in the development of cardiac and glomerular fibrosis, which is in harmony with numerous previous studies (Xiao & Zhang, 2008; Desmouliere et al., 1993; Kuwahara *et al*., 2002; Ziyadeh *et al*., 1993; Mason & Wahab, 2003; Maric *et al*., 2004; Wolf, 2003). TGFβ1 played a potent stimulus for the collagen synthesis, matrix accumulation and organisation that was found to be up-regulated for both the heart and the kidney. Several lines of evidence confirm that continuous over expression of TGFβ1 within the heart and the kidney is likely to contribute to the hypertrophy, fibrosis and cell death (Dai *et al*., 2004).

Following the concourse of these findings, chapter 6 combined the correlative results of the heart and the kidney and presented a comprehensive comparative analysis of the relationship between age, and the occurrence of T1DM complications that have been extensively elaborated in chapter 3, 4 and 5, respectively. While the findings of both organs were in a correlative nature, it became fundamental to investigate the possibility for the existence of such an entity that can be related to both of these organs. Thus, it was discovered that major research departments have identified the emergence of a new type of syndrome reffered to as the cardio renal syndrome (CRS). CRS are disorders of the heart and the kidney in which acute or chronic dysfunction in one organ may induce acute or chronic dysfunction in another (Cruz *et al*., 2011). In the light of the former, it

was suggested that TGFβ1 activity may represent a key intermediary in the onset of these processes in both, the heart and the kidney. The role of TGFβ1 in the development of a CRS is still under research; however the role of TGFβ1 in structural and molecular remodelling of the heart and the kidney has extensively been highlighted in the preceding chapters. Nevertheless, the findings of similarities in TGFβ1 levels and expression in the heart and the kidney may well be of some importance in the near future. In addition, T1DM highlights the importance of understanding the consequences of adult vs young adult on TGFβ1. Furthermore, dissection of relative roles of TGFβ1 and receptor subtypes (β2, β3) and their activation effects on different cell types in cardiac and glomerular remodelling processes will further determine if inhibition of TGFβ1 signalling proves to be an effective failure in DM. With this said, it will be of fundamental importance to study the roles of TGFβ1 in the development of CRS and the development of potential therapeutic targets.

The CRS with regards to the kidney, early diagnosis of renal involvement in patients with cardiac disease is of paramount importance (Soni *et al*., 2009). However, currently available clinical and biochemical tools are unable to diagnose renal injury immediately after the insult to the kidney. Serum creatinine (sCr), a marker of glomerular filtration, is insensitive and unreliable to diagnose renal tubular injury in the absence of significant reduction in GFR. Its concentration increases only after half of the kidney function is lost which may be days after the renal insult has occurred (Soni *et al*., 2009). Delay in detection also means delay in intervention in the early periods of renal injury where appropriate management strategies can be instituted before irreversible renal damage occurs. Therefore, finding newer biomarkers for early diagnosis of kidney injury has been declared a top research priority. Conversely, CRS in regards to the heart, NPs have been validated as an important cardiac biomarkers for risk stratification and prognostication in HF patients with or without chronic kidney disease (CKD) (Cruz *et al*., 2011). However, the best cut-off values for each stage of CKD, including those on renal replacement therapy, are yet to be ascertained. Nevertheless, work with NPs has also shown that they are not to be used as ‘‘stand-alone’’ tests; rather they are best used as adjuncts to everything else the health care provider brings to the table. Thus, it is critical to validate new biomarkers in multicenter and prospective studies encompassing a broad spectrum of patients. Furthermore, since we live in an age where complex patients are the rule of the day, panels of multiple biomarkers will be needed in evaluation, risk stratification, and ultimately treatment initiation and follow-up.

The final section of the study employed GK rat as a model of T2DM compared to sedentary animals both diabetic and control groups, in order to investigate the beneficial effects of physical exercise on cardiac function, structure and molecular alterations observed in T2DM. The results of the present study have provided potential non-pharmacotherapy of physical exercise in reversing the remodelling that is characterised in part by TGFβ1. Numerous studies have highlighted physical training as an effective therapeutic strategy for the management of T2DM (Lindstrom *et al*., 2006; Ellison *et al*., 2012; Tabet *et al*., 2009; Longnathan *et al*., 2012; Reusch *et al*., 2013). The reductions in ECM accumulation, fibrosis, cardiac hypertrophy, apoptosis and TGFβ1 have further highlighted the significance of physical exercise in T2DM. However, exercise training was not significantly beneficial in terms of cardiac functional parameters, but highlights a significant role for improvement in the contractile performance in T2DM.

8.2 Limitations of the study

In addressing the limitations of the results reported in this thesis, the following points are due, that give rise to several questions worthy of further experimental quest.

Firstly, the investigations performed in this study are primarily descriptive by design. The overall outcome assesses the interactive effects of adult vs young adult and chronic uncontrolled HG on remodelling in the LV and the kidney. While the study has demonstrated HG-related, molecular and cellular perturbations provide an insight into the nature of the disease. However, data presented here do not allow us to conclude that extracellular matrix deposition, altered gene expression and apoptotic cell death are the only events involved in the progression or development of altered ventricle function in diabetes mellitus, excluding traditional cardiovascular events.

Secondly, showcasing the absence of an interventional approach, this study is highly correlative in nature. The finding that myocardial bioactive TGFβ1 is up-regulated in T1DM and T2DM, can potentially result in many features of myocardial remodelling associated with HF (e.g., interstitial fibrosis and induction of a foetal gene expression pattern) suggests that TGFβ1 signalling imitates a fundamental role in the pathophysiology of myocardial failure and kidney failure. However, at present it remains to be determined whether myocardial TGFβ1 mediates (or modulates) remodelling of the myocardium and kidney in response to a dysglycaemic environment.

An important question that arises here is, whether TGFβ1 represents one of several peptides activated in response to HG, or does it occupy a central position as a distal meeting point for other pathways? Maybe, relative roles of TGFβ1, β2 and β3 and receptor subtypes and their activation effects on different cell types in the myocardial and renal remodelling process may further determine if TGFβ1 signalling inhibition will provide to be an effective therapeutic intervention for the prevention of fibrosis in the heart and the kidney in DM.

Specifically, each chapter aims to add to the current knowledge present in the literature, but like all other studies, is limited in several aspects. Hence, the following section aims to dissect the limitations involved in each study chapter.

Firstly, the ventricle isolations performed via the Langendorff perfusion system in order to study cardiac contractile function and calcium transients' selection may be subjective in nature. Although great care was taken when selecting, there may be some chance for the selection of dead cardiomyocytes to perform the experiments. This can have a huge effect on the quantitative analysis of the data. Moreover, if time was available it would have been beneficial to measure L-type calcium current for a better understanding of the functional dysfunction observed in the study. Furthermore, the study on kidney is primarily focused on STZ-induced T1DM structural and molecular changes to kidney leading to DN. The present study lacks the functional changes associated with DN and requires further investigations into the functional aspects of the disease to make correlations with the structural remodelling observed in this study. If time was available, it would also be of great interest to look at changes in the kidney after exercise training in T2DM rats for comparison with the GK study in chapter 7. This will provide substantial evidence to identify if remodelling of the kidneys occur in T2DM as well and potentially, provide new insights for therapeutics to consider exercise training as an important factor in fighting with the complications of T2DM. Additionally, this study only investigated age-related changes employing 2 time points. If time was available, it would have been a major advantage to investigate functional, structural and molecular changes in T1DM employing older animals.

Furthermore, an important role of the cardio renal syndrome has been implicated in this study. Although much has been learned regarding cardio renal interaction in heart failure, many questions remain unanswered. Further research is needed for an updated

classification of the cardio renal syndrome, and to improve preventive and treatment strategies preserving renal function and improving outcome in heart failure patients. However, despite several limitations, the present by has provided options for intervention, and have important implications for understanding the basic mechanisms responsible for the response to of HG in the heart and the kidney, and for the development of new treatment strategies for DCM and HF.

8.3 Conclusion

The main conclusions from the present study are summarised in figure 8.1 for T1DM and figure 8.2 for T2DM and exercise. The results have clearly shown that DM, via the elevated HG, can elicit adverse long term damage to both the heart and the kidney over time and in part, TGFβ1 has a key role to play in this entity. Furthermore, exercise training can be beneficial in T2DM patients and can be used as a non-pharmacotherapy agent.

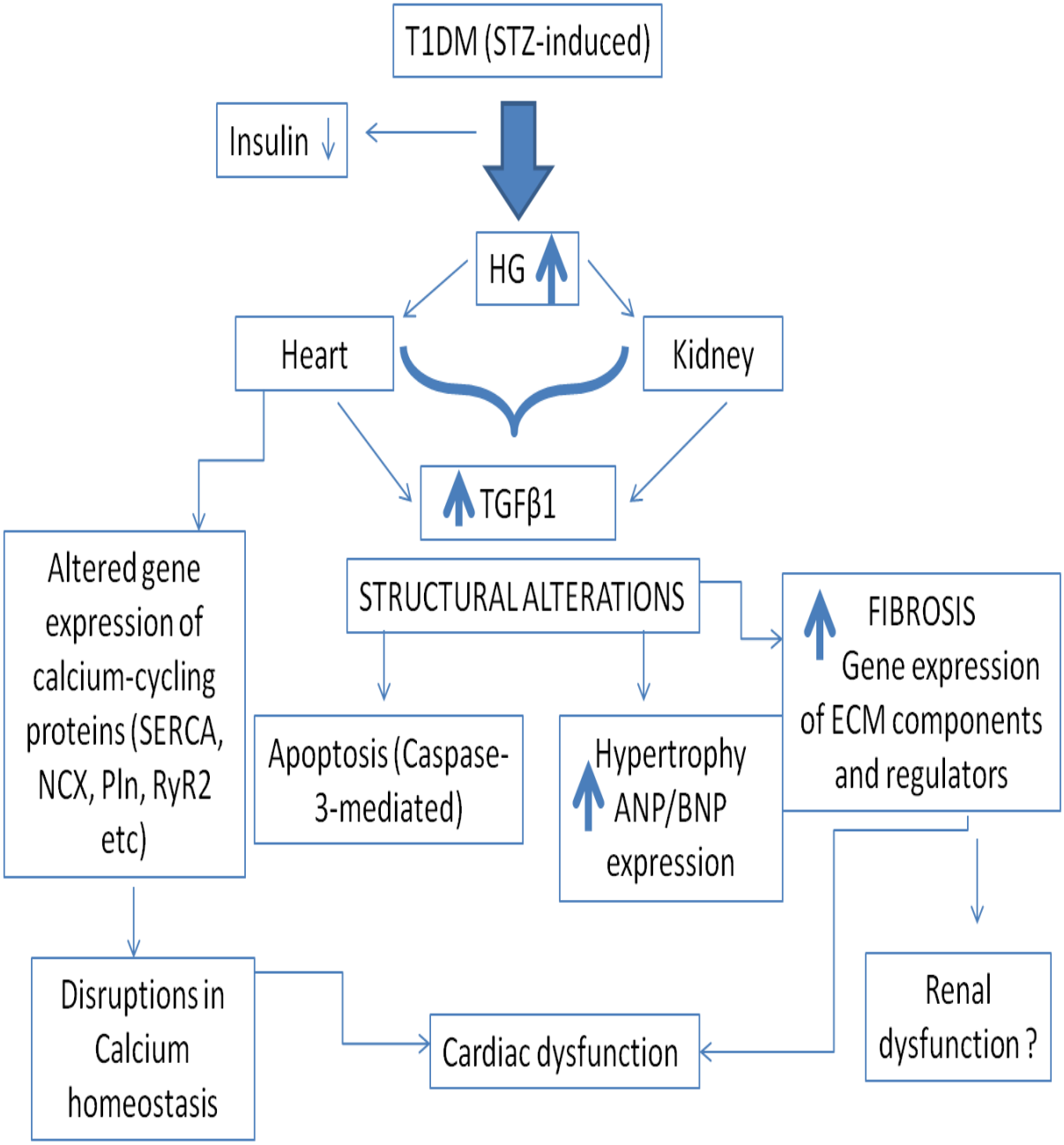

Figure 8.1: Flow diagram summarizing the main findings of the study. It is postulated that STZ-induced T1DM can lead to a decrease in blood insulin and elevation in blood glucose (HG). The HG in turn, elicits structural changes in the heart and the kidney via TGFβ1 activation leading to apoptosis, hypertrophy, upregulation in ECM components and regulators and subsequently to fibrosis in the two organs. In case of the heart, these changes lead to derangement in the cellular Ca^{2+} homeostasis which in turn, causes an alteration in the ability of the heart to contract efficiently, hence cardiac dysfunction. Whether renal dysfunction also occurs in due course is a question to be investigated.

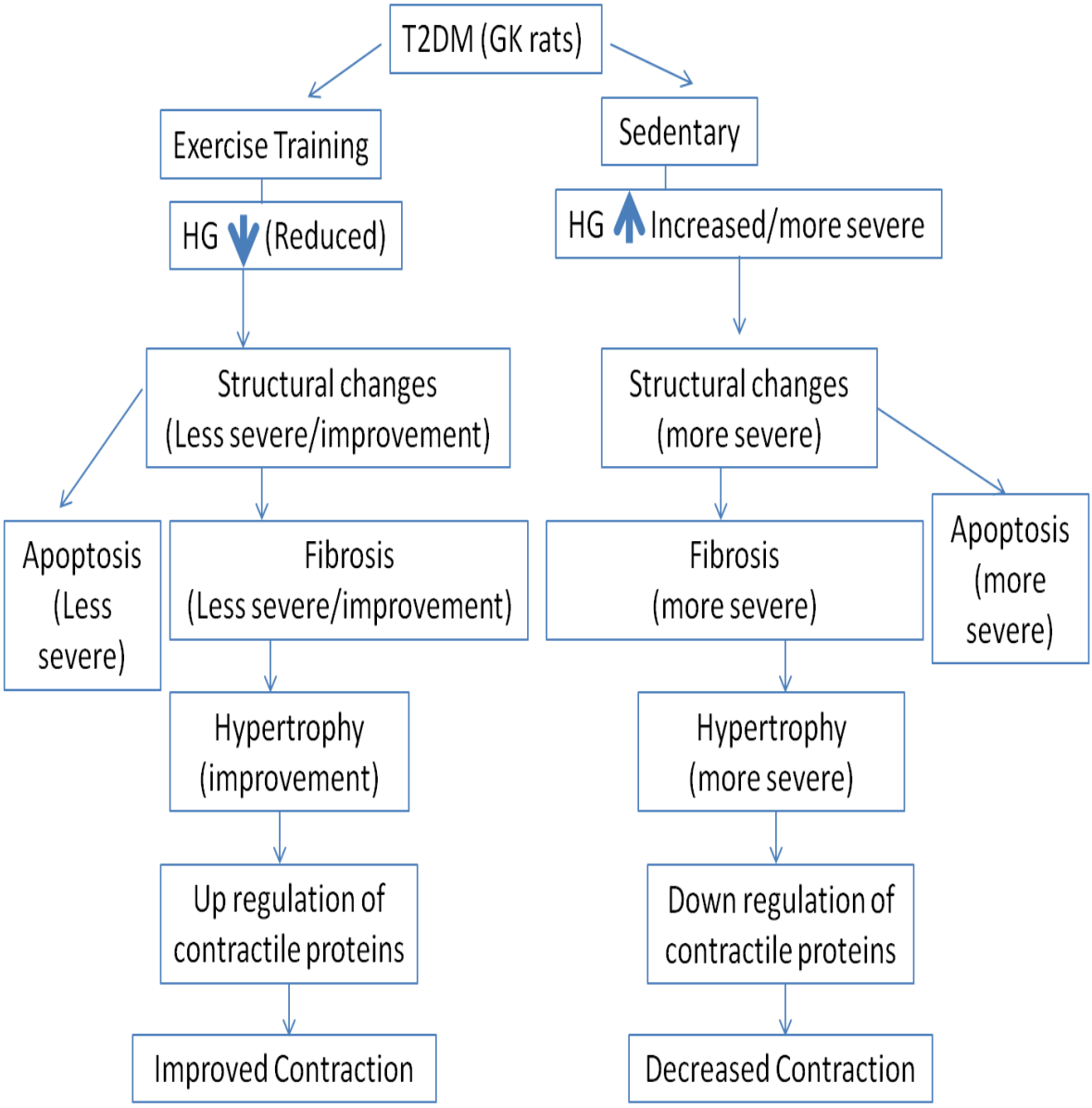

Figure 8.2: Flow diagram summarizing the beneficial effects of exercise training on cardiac function. It is postulated that exercise training can reduce HG levels which in turn leads to less severe structural changes in the heart and exercise can also reduce hypertrophy, apoptosis and fibrosis all which help in improving cellular Ca^{2+} homeostasis and cardiac function. Animals without physical exercise training display more severe dysfunction.

8.3 Scope for future studies

In addition to the parameters measured in this study, the following future work is proposed:

1. To undertake functional studies in the kidneys measuring glomerular filtration rate, albumin, creatinine and blood urea nitrogen (BUN) levels, calcium homeostasis at different time points of diabetes compared to age-matched controls. These results will provide substantial evidence for correlation with the structural remodelling observed in this study and determine if structural alterations are accompanied by functional dysfunction of the kidneys. Additionally, studies can be carried out on both the kidneys as only left kidney was employed in this study. This may provide evidence to determine if structural alterations and/or dysfunction are occurring in both kidneys.
2. Regarding the heart, it is possible to measure voltage-dependant L-type Ca^{2+} channel currents using whole-cell-patch-clamp methods using different time points of diabetes compared to age-matched controls. Calcium is the main stay in contraction and a derangement in its homeostasis with cardiac dysfunction. These results will provide substantial evidence underlying the dysfunction in contractile kinetics observed in this study.
3. Regarding the heart at the ultrastructural level, there is much evidence that dysfunction in the T-tubule occurs in cardiac disease, especially HF leading to impaired contractility. It is possible to measure these in control and STZ-induced DM in rat hearts.
4. This work so far has been conducted mainly in the LV of the heart. It is possible to repeat all these experiments using the atria and right ventricle to see if similar alterations are occurring.
5. Elevated methylglyoxal (MGO) in DM is believed to play a major role in the development of long term complications. It is possible to measure levels of MGO in serum, whole blood, heart, kidney and blood vessels. A long term study is to develop a genetic strain of rats which can express the glyoxalase enzyme which can stimulate the breakdown of MGO. The relationship between MGO and long-term complications can be measured in DM, employing different time points compared to controls.
6. To investigate structural remodelling of the kidney observed in this study, in T2DM employing the GK rat in varying age groups. This will provide

substantial evidence to identify if remodelling of the kidneys occur in T2DM as well. These experiments also need to be carried out in animals with exercise training similar to the methods adopted in this study. This will provide new insights and evidence for therapeutics to consider exercise training as an important factor in fighting with the complications of T2DM.

BIBLIOGRAPHY

Abel DE (2005) Myocardial Insulin Resistance and Cardiac Complications of Diabetes. Current Drug targets- Immune, Endocrine and Metabolic Disorders 5:219-226

Adler SG, Kang SW, Feld S, Cha DR et al (2001) Glomerular mRNAs in human type 1 diabetes: biochemical evidence for microalbuminuria as a manifestation of diabetic nephropathy. Kidney Int 60:2330-2336

Ahmed SH, Clark LL, Pennington WR, et al (2006) Matrix metalloproteinases/tissue inhibitors of metalloproteinases: relationship between changes in proteolytic determinants of matrix composition and structural, functional, and clinical manifestations of hypertensive heart disease. Circulation 113: 2089-2096

Ai X, Curran JW, Shannon TR, Bers DM, & Pogwizd SM (2005) Ca2+/calmodulin dependent protein kinase modulates cardiac ryanodine receptor phosphorylation and sarcoplasmic reticulum Ca2+ leak in heart failure. Circ Res 97:1314-1322

Alberts B, Johnson A, Lewis J, et al (2007) Molecular Biology of the Cell. London: Garland Science

Albert CM, Ma J, Rifai N et al (2002) Prospective study of C-reactive protein, homocysteine, and plasma lipid levels as predictors of sudden cardiac death. *Circulation 105*: *2595*–2599

Alsaad KO, Herzenberg AM, (2007) Distinguishing diabetic nephropathy from other causes of glomerulosclerosis: an update. J Clin Pathol;60:18-26

Aneja A, Tang WH, Bansilal S, et al (2008) Diabetic cardiomyopathy: insights into pathogenesis, diagnostic challenges and therapeutic options. Am J Med 121: 748-757

Anker SD and Haehling S (2004) Inflammatory mediators in chronic heart failure: an overview. Heart 90(4): 464–470

Annonu AK, Fattah AA, Mokhtar MS, Ghareeb S, Elhendy A (2001) Left ventricular systolic and diastolic functional abnormalities in asymptomatic patients with non-insulin-dependent diabetes mellitus. J Am Soc Echocardiogr 14(9):885-891

Aoyagi T et al (1999) The Sarcoplasmic reticulum Ca2+ ATPase gene promoter activity is decreased in response to severe left ventricular pressure- overload in hypertrophy rats. J Moll Cell Cardiol 31:919-916

Aroor AR, Mandavia C, Ren J, Sowers JR, Pulakat L (2012b) Mitochondria and oxidative stress in cardiorenal metabolic syndrome. Cardiorenal Med, 2: 87-109

Aroor AR, Mandavia CH, Sowers JR (2012a) Insulin resistance and heart failure: molecular mechanisms. Heart Fail Clin, 8(4): 609-17

Arora S, Ojha SK, Vohra D (2009) Characterisation of streptozotocin induced diabetes mellitus in swiss albino mice. Global J of Pharmaco, 3(2): 81-84

Asbun J, Villareal FJ (2006) The pathogenesis of myocardial fibrosis in the setting of diabetic cardiomyopathy. J Am Coll Cardiol 47: 693-700

Asghar O, Al-Sunni A, Khavandi K et al (2009) Diabetic cardiomyopathy. Clin Sci 116:741-760

Badylak SF (2007) The extracellular matrix as a biologic scaffold material. Biomaterials 28, 3587-3593

Ban CR and Twigg SM (2008) Fibrosis in diabetic complications: Pathogenic mechanisms and circulating and urinary markers. Vasc Health Risk Manag 4(3): 575-596

Bassuk SS, Manson JE (2005) Epidemiological evidence for the role of physical activity in reducing risk of type 2 diabetes and cardiovascular disease. *J App Physiol* 99(3):1193-1204

Bangstad HJ, Osterby R, Dahl-Jorgensen K, Berg KJ et al (1994) Improvement of blood glucose control in IDDM patients retards the progression of morphological changes in early diabetic nephropathy. *Diabetol 37:*483– 490

Belke DD, Dillmann WH (2004) Altered cardiac calcium handling in diabetes. Curr Hypertens Rep, 6:424-429

Belke DD, Swanson EA, Dillmann WH (2004) Decreased Sarcoplasmic Reticulum Activity and Contractility in Diabetic db/db Mouse Heart. Diabetes 53:3201-3208

Benigni A, Zoja C, Campana M, Corna D et al (2006) Beneficial effect of TGFbeta antagonism in treating diabetic nephropathy depends on when treatment is started. Nephron Exp Nephrol 104:158-168

Bergman M (2009) Inadequencies of absolute threshold levels for diagnosing prediabetes. Diabetes Metab Res Rev 26: 3-6

Berkowitz BA, Roberts R, Stemmler A, Luan H, Gradianu M, (2007) Impaired Apparent Ion Demand in Experimental Diabetic Retinopathy: Correction by Lipoic Acid. Investigative Ophthalmology & Visual Science 48(10):4753-4758

Bers DM (2002) Cardiac excitation-contraction coupling, Nature 415:198-205

Bers DM, Eisner DA, Valdivia HH (2003) Sarcopalsmic Reticulum Ca^{2+} Transport and Heart Failure: Roles of Diastolic Leak and Ca^{2+} Circ Res, 93:487-490

Bertoni AG, Tsai A, Kasper EK, Brancati FL (2003) Diabetes and idiopathic cardiomyopathy: a nationwide case-control study. Diabetes Care, 26: 2791-5

Bhalla, MA, ChiangA, Epshteyn, VA, Kazanegra R et al (2004) Prognostic role of b-type natriuretic peptide levels in patients with type 2 diabetes mellitus. Journal of the American College of Cardiology, 44, 1047-1052

Bidasee KR, Zheng H, Shao C-H, Parbhu SK, Rozanski GJ, Patel KP (2008) Exercise training initiated after the onset of diabetes preserves myocardial function: effects on expression of beta-adrenoceptors. J Appl Physiol Bethesda Md 1985 105:907-914

Black LS, Lee JC (1988) Effects of STZ-induced diabetes on atrial natriuretic peptide levels in rats (abstract). Am J Hypertens 1:112A

Blickle JF, Doucet J, Krummel T, Hannedouche (2007) Diabetic nephropathy in the elderly. Diabetes Metab 33(40-65)

Blom I, van Dijk A, Wieten L, Duran K et al (2001) In vitro evidence for differential involvement of CTGF, TGFbeta, and PDGF-BB in mesangial response to injury. Nephrol Dial Transplant 16:1139-1148

Bollano E, Omerovic E, Svensson H, Waagstein F, Fu M (2006) Cardiac remodeling rather than disturbed myocardial energy metabolism is associated with cardiac dysfunction in diabetic rats. Int J Cardiol [Epub ahead of print]

Bolzan, AD., and Bianchi MS (2002), Genotoxicity of Streptozotocin. Mutat Res. 512: 121-134

Bond M, Murphy G, Bennett MR, Amour A et al (2000) Localization of the death domain of tissue inhibitor of metalloproteinase-3 to the N terminus. Metalloproteinase inhibition is associated with proapoptotic activity. J. Biol. Chem 275(52):41358-41363

Border WA, Noble NA. (1994) Transforming growth factor β in tissue fibrosis. *N Engl J Med*. *331*: *1286*-1292

Border WA, Ruoslahtit E (1999) Transforming growth factor-,B in disease: The dark side of tissue repair. J. Clin. Invest.90: 1-7

Border WA, Yamamoto T, Noble NA (1999) Transforming growth factor beta in diabetic nephropathy. Diabetes Metab Rev 12:309-339

Borradaile NM, Han X, Harp JD, Gale SE, Ory DS, Schaffer JE (2006) Disruption of endoplasmic reticulumstructure and integrity in lipotoxic cell death. J Lipid Res, 47: 2726-37

Bosman, FT and Stamenkovic, I (2003) Functional structure and composition of the extracellular matrix. J. Pathol. 200, 423-428

Boudina S, Abel ED (2007). Diabetic Cardiomyopathy Revisited. Circulation 115: 3213-3223

Bowers SLK, Banerjee I, Baudino TA (2010) The extracellular matrix: At the centre of it all. J Mol Cell Cardiol 474-482

Bowker T J, Wood D A, Davies M J. *et al* Sudden, unexpected cardiac or unexplained death in England: a national survey QJM 200396269–279.279

Bracken NK, Qureshi MA, Singh J et al (2003) Mechanism underlying contractile dysfunction in streptozotocin induced type 1 and type diabetic cardiomyopathy. In: Atherosclerosis, Hypertension and Diabetes (Eds. N.S. Dhalla et al) Kluwer Academic Publishers, pp 387-408

Branton MH, Kopp JB (1999) TGF-beta and fibrosis. Microbes Infect 1:1349-1365

Brew K, Nagase H (2010) The tissue inhibitors of metalloproteinases (TIMPs): an ancient family with structural and functional diversity. Biochim. Biophys. Acta 1803(1):55-71

British Heart Foundation (2014) Cardiovascular Disease Statistics 2014 https://www.bhf.org.uk/publications/statistics/cardiovascular-disease-statistics-2014 Accessed April, 2015

Breyer JA, Bain RP, Evans JK, Nahman NS et al (1996) Predictors of the progression of renal insufficiency in patients with insulin-dependent diabetes and overt diabetic nephropathy. The Collaborative Study Group. Kidney Int 50:1651-1658

Brown R, Clark AL (2013) Reducing the cost of heart failure while improving quality of life. Br J Cardiol 20:45–6

Brownlee M (2001) Biochemistry and molecular cell biology of diabetic complications. Nature 414: 813–820

Brownlee M (2005) The Pathobiology of diabetic complications: a unifying mechanism. Nature 54:1615–1625

Bugger H, Chen D, Riehle C, Soto J (2009) Tissue-Specific Remodeling of the Mitochondrial Proteome in Type 1 Diabetic Akita Mice. Diabetes 58:1983-1997

Bujak, M., & Frangogiannis, N. G. (2007). The role of TGF-beta signaling in myocardial infarction and cardiac remodeling. Cardiovasc Res 74, 184−195

Burns WC, Twigg SM, Forbes JM, Pete J et al (2006) Connective tissue growth factor plays an important role in advanced glycation end product-induced tubular epithelial-to-mesenchymal transition: Implications for diabetic renal disease. J Am Soc Nephrol 17:2484-2494

Cagalinec M, Waczulíková I, Uličná O, Chorvat D (2013) Morphology and contractility of cardiac myocytes in early stages of streptozotocin-induced diabetes mellitus in rats. Physiol Res 62:489-501

Cai L and Kang JY (2003) Cell Death and Diabetic Cardiomyopathy. Cardio Toxicol 3(3):219-228

Cai L and Kang JY (2001) Oxidative stress and diabetic cardiomyopathy. Cardio Toxicol1 1:181-193

Cai L, Li W, Wang G et al (2002) Hyperglycemia-Induced Apoptosis in Mouse Myocardium: Mitochondrial Cytochrome c–Mediated Caspase-3 Activation Pathway. Diabetes 51:1938-1948

Cai L, Wang Y, Zhou G, et al (2006) Attenuation by metallothionein of early cardiac cell death via suppression of mitochondrial oxidative stress results in a prevention of diabetic cardiomyopathy. J Am Coll Cardiol 48: 1688-1697

Candido R, Forbes JM, Thomas MC et al (2003) A breaker of advanced glycation end products attenuates diabetes-induced myocardial structural changes. Circ Res 92: 785-792

Caramori ML, Fioretto P, Mauer M (2006) Enhancing the predictive value of urinary albumin for diabetic nephropathy. J Am Soc Nephrol 17:339-352

Castellar A, Remedio RN, Barbosa RA, Gomes RJ, Caetano FH (2011) Collagen and reticular fibers in left ventricular muscle in diabetic rats: physical exercise prevents its changes? Tissue Cell 43:24-28

Cavivell S, Gomis R (2014) Diagnosis and classification of autoimmune diabetes mellitus. Autoimmun Rev (4-5):403-7

Ceriello A, Testa R (2009) Antioxident and Anti-inflammatory treatment in Type 2 diabetes. Diabetes Care 32: S232-S236

Chareonthaitawee P, Sorajja P, Rajagopalan N, Miller TD et al (2007) Prevalence and prognosis of left ventricular systolic dysfunction in asymptomatic diabetic patients without known coronary artery disease referred for stress single-photon emission computed tomography and assessment of left ventricular function. Am Heart J 154(3):567-574

Cheng S, Xanthakis V, Sullivan L, Lieb Wet al (2010) Correlates of echocardiographic indices of cardiac remodeling over the adult life course: longitudinal observations from the Framingham heart study. Circulation 122:570-578

Chen S, Evans T, Mukherjee K, et al. (2000) Diabetes-induced myocardial structural changes: role of endothelin-1 and its receptors. J Mol Cell Cardiol 32: 1621-1629

Chen S, Hong S, Iglesias-de lCM, Isono M, Casaretto A, Ziyadeh F (2001) The key role of the transforming growth factor-beta system in the pathogenesis of diabetic nephropathy. Ren Fail 23:471-481

Chen Y, Blom IE, Sa S, Goldschmeding R, Abraham DJ, Leask A (2002) CTGF expression in mesangial cells: Involvement of SMADs, MAP kinase, and PKC. *Kidney Int 62*:*1149*-1159

Chipkin SR, Klugh SA, Chasan-Taber L (2001) Exercise and diabetes. Cardiol Clin 19(3):489-505

Choi KM, Zhong Y, Hoit BD et al (2002) Defective intracellular (Ca2+)signaling contributes to cardiomyopathy in Type 1 diabetic rats. Am J Physiol (Heart Circ Physiol) 283: H1398-H1408

Choi SW, Benzie IFF, Ma SW et al (2008) Acute hyperglycemia and oxidative stress: Direct cause and effect? Free Rad Bio and Med 44: 1217-1231

Choi S. Y., Chang H. J., Choi S. I., Kim K. I., Cho Y. S et al (2009) Long-term exercise training attenuates age-related diastolic dysfunction: association of myocardial collagen cross-linking. J Korean Med Sci 24:32-39

Chrysohoou C, Pitsavos C, Barbetseas J, et al (2009) Chronic systemic inflammation accompanies impaired ventricular diastolic function, detected by Doppler imaging, in

patients with newly diagnosed systolic heart failure (Hellenic Heart Failure Study). Heart Vessels 24: 22-26

Chuang TD, Guh JY, Chiou SJ et al (2007) Phosphoinositide 3-kinase is required for high glucose-induced hypertrophy and p21WAF1 expression in LLC-PK1 cells. *Kidney Int* 71:867-874

Chugh SS, Jui J, Gunson K, Stecker EC, John BT et al (2004) Current burden of sudden cardiac death: multiple source surveillance versus retrospective death certificate-based review in a large U.S. community. J Am Coll Cardiol 44(6):1268–75

Chugh SS, Reinier K, Teodorescu K, Evanado A, Kehr E et al (2008) Epidemiology of Sudden Cardiac Death: Clinical and Research Implications. Prog Cardiovasc Dis 51(3): 213–228

Cohen-Solal A, Beauvais F, Logeart D (2008) Heart failure and diabetes mellitus epidemiology and management of an alarming association. J Card Fail, 14: 615-625.

Cohn JN, Ferrari R, Sharpe N (2000) Cardiac remodelling– concepts and clinical implications: a consensus paper from an international forum on cardiac remodelling. J Am Coll Cardiol 35: 569-582

Connelly KA, Gilbert RE, Krum H (2007) Letter by Connelly et al regarding article, "Diastolic stiffness of the failing diabetic heart: importance of fibrosis, advanced glycation end products, and myocyte resting tension". Circu 117, e483; author reply e484

Constans T (2005) Plasma glucose goals and therapeutic management in elderly diabetic patients. Diabetes Metab 31:5S58-5S61

Colombo PC, Ganda A, Lin J, Onat D et al (2011) Inflammatory activation: cardiac, renal, and cardio-renal interactions in patients with the cardiorenal syndrome. Heart Fail Rev [Epub ahead of print]

Cosyns B, Droogmans S, Weytjens C et al (2007) Effect of streptozotocin-induced diabetes on left ventricular function in adult rats: an in vivo Pinhole Gated SPECT study. Cardiovasc Diabetol 6: 30

Cruz DN, Goh CY, Palazzuoli A, Salvin L et al (2011) Laboratory parameters of cardiac and kidney dysfunction in cardio-renal syndromes. Heart Fail Rev 16:545-551

Cruz-Munoz W and Khokha R (2008) The role of tissue inhibitors of metalloproteinases in tumorigenesis and metastasis. Crit. Rev. Clin. Lab. Sci. 45, 291-338

Damås JK, Eiken HG, Øie E, et al (2000) Myocardial expression of CC-and CXC-chemokines and their receptors in human end-stage heart failure. Cardiovasc Res 47:778–87

Dai RP, Sheen ST, He BP et al (2004) Differential expression of cytokines in the rat heart in response to sustained volume overload. Eur J Heart Fail 6 (6): 693-703

Dalla Vestra M, Saller A, Mauer M, et al (2001) Role of mesangial expansion in the pathogenesis of diabetic nephropathy. *J Nephrol* 14 Suppl 4:S51-S57

Dalla VM, Masiero A, Roiter AM, et al (2003) Is podocyte injury relevant in diabetic nephropathy? Studies in patients with type 2 diabetes. Diab ;52:1031-5

Daniels LB, Maisel AS (2007) Natriuretic peptides. J Am Coll Cardiol 50:2357-2368

Darmellah A, Baetz D, Prunier F (2007). Enhanced activity of the myocardial Na+/H+ exchanger contributes to left ventricular hypertrophy in the Goto-Kakizaki rat model of type 2 diabetes: critical role of Akt. Diabetologia 50: 1335-1344

Davis RC, Hobbs FDR, Lip GYH (2000) ABC of heart failure: history and epidemiology. BMJ 320:39-42

De Angelis KL, Oliveira AR, Dall'Ago P et al (2003) Effects of exercise training on autonomic and myocardial dysfunction in streptozotocin-diabetic rats. Braz J Med Biol Res Rev Bras Pesqui Médicas E Biológicas Soc Bras Biofísica Al 33:635-641

Declèves AE, Sharma K (2010) New pharmacological treatments for improving renal outcomes in diabetes. Nat Rev Nephrol 6:371-380

Delmar M, Makita N (2012) Cardiac connexins, mutations and arrhythmias. Curr Opin Cardiol 27(3):236-241

Del Prete D, Anglani F, Forino M, Ceol M, Fioretto P, Nosadini R, Baggio B, Gambaro G. Down-regulation of glomerular matrix metalloproteinase-2 gene in human NIDDM. Diabetol 40(12):1449-1454

Deshpande SD, Putta S, Wang M, Lai JY (2013) Transforming Growth Factor-β–Induced Cross Talk Between p53 and a MicroRNA in the Pathogenesis of Diabetic Nephropathy. Diab 62(9): 3151-3162

Desmouliere A, Geinoz A, Gabbiani F, Gabbiani G (1993) Transforming growth factor-beta 1 induces alpha-smooth muscle actin expression in granulation tissue myofibroblasts and in quiescent and growing cultured fibroblasts. J Cell Biol 122(1): 103-111

Devereux RB, Roman MJ, Paranicas M (2000) Impact of diabetes on cardiac structure and function: The Strong Heart Study. Circulation: 101:2271-2276

Dhalla NS, Pierce GN, Innes IR and Beamish RE (1985) Pathogenesis of cardiac dysfunction in diabetes mellitus. Can J Cardiol;1(4):263-281

Diabetes Control and Complications Trial Research Group (1993). The effect of intensive treatment of diabetes on the development and progression of long-term complications in insulin-dependent diabetes mellitus. N Engl J Med 329: 977-986

Diabetes UK (2007). Diabetes heartache: the hard reality of cardiovascular care for people. Report can be accessed at http://www.diabetes.org.uk/Documents/News/Heartache_report07.pdf

Di Bonito P, Cuomo S, Moio N, Sibilio G, Sabatini D, Quattrin S,Capaldo B (1996) Diastolic dysfunction in patients with noninsulin-dependent diabetes mellitus of short duration. Diabet Med13(4):321-324

Diez-Sampedro A, Lenz O, Fornoni A (2011) Podocytopathy in diabetes: a metabolic and endocrine disorder. Am J Kidney Dis 58(4): 637-646

Dobaczewski M, Chen W, Frangogiannis NG (2010) Transforming growth factor signalling in cardiac remodelling. J Mol Cell Cardiol doi: doi10.1016/j.yjmcc.2010.10.033

Dobrin JS, Lebeche D (2010) Diabetic cardiomyopathy: signaling defects and therapeutic approaches. Expert Rev Cardiovasc Ther 8: 373-391

Dokken BB (2008) The Pathophysiology of Cardiovascular Disease and Diabetes: Beyond Blood Pressure and Lipids. Diabetes Spectrum 21 (3): 160-165

Donath YM (2014) Targeting inflammation in the treatment of type 2 diabetes: time to start. Nature Reviews Drug Discovery 13: 465–476

Doron A (2003) Cross-linking of glycated collagen in the pathogenesis of arterial and myocardial stiffening of ageing and diabetes. J Hyperten 21: 3-12

Dronavalli S, Duka I, Bakris GL (2008) The pathogenesis of diabetic nephropathy. Nature Rev Endocrinol 4:444-452

Dounis V, Siegmund T, Hansen A, Jensen J, Schumm-Draeger PM, von Bibra H (2006) Global myocardial perfusion and diastolic function are impaired to a similar extent in patients with type 2 diabetes mellitus and in patients with coronary artery disease-evaluation by contrast echocardiography and pulsed tissue Doppler. Diabetologia 49(11):2729-2740

Drummond K, Mauer M (2002) The early natural history of nephropathy in type 1 diabetes:II. Early renal structural changes in type 1 diabetes. Diab;51:1580-7

D'Souza A, Howarth FC, Yanni J, Dobryznski H, Boyett MR, Adeghate E, et al (2011) Left ventricle structural remodeling in the prediabetic Goto-Kakizaki rat. Exp Physiol;96(9): 875-88

Du J, Wang X, Miereles C, Bailey JL et al (2004) Activation of caspase-3 is an initial step triggering accelerated muscle proteolysis in catabolic conditions. J Clin Invest.113:115-123

Edwards JL, Vincent AM, Cheng HT, & Feldman E.L (2008) Diabetic neuropathy: Mechanisms to management. Pharmacol Exp; Therapeut 120: 1-34

Egeblad M, Rasch MG, Weaver VM (2010) Dynamic interplay between the collagen scaffold and tumor evolution. Curr. Opin. Cell Biol. 22, 697-706

Eiken HG, Øie E, Damås JK, et al (2000) Myocardial gene expression of leukaemia inhibitory factor, interleukin-6 and glycoprotein 130 in end-stage human heart failure. Eur J Clin Invest 31:389–97

Elias D, Prigozin H, Polak N, Rapoport M, Lohse A W, Cohen I R (1994) Autoimmune diabetes induced by the b-Cell toxin STZ. Diabetes 43: 992-8

Ellison GM, Waring CD, Vicinanza C, Torella D (2012) Physiological cardiac remodelling in response to endurance exercise training: cellular and molecular mechanisms. Heart Br Card Soc 98:5-10

Elmore S (2007) Apoptosis: A Review of Programmed Cell Death. Toxicol Pathol 35(4):495-516

Elsner, M, Guldbakke, B, Tiedge M, Munday R, Lenzen S (2007) Relative importance of transport and alkylation for pancreatic beta-cell toxicity of streptozotocin. Diabetologia. 43: 1528-153

Elster SK, Braunwald E, Wood HF (1956) A study of C-reactive protein in the serum of patients with congestive heart failure. Am Heart J 51: 533-541

Epp RA, Susser SE, Morissette MP, Kehler DS, Jassal DS, Duhamel TA (2013) Exercise training prevents the development of cardiac dysfunction in the low-dose streptozotocin diabetic rats fed a high-fat diet. Can J Physiol Pharmacol 91:80-89

Esser N, Legrand-Poels S, Piett J, Scheen JA et al (2014) Inflammation as a link between obesity, metabolic syndrome and type 2 diabetes. Diab Res and Clin Prac 105: 141-150

Falcao-Pires I, Leite-Moreira AF (2012) Diabetic cardiomyopathy: understanding the molecular and cellular basis to progress in diagnosis and treatment. Heart Fail Rev 17:325-344

Falk RJ, Scheinman JI, Mauer SM, Michael AF (1983) Polyantigenic expansion of basement membrane constituents in diabetic nephropathy. *Diabetes* 32*[* Suppl 2*]:* 34-39, 1983

Fang ZY, Prins JB & Marwick TH (2004) Diabetic Cardiomyopathy: Evidence, Mechanisms, and Therapeutic Implications. Endocrine Rev 25:543-567

Fang ZY, Prins JB, Marwick TH (2005) Diabetic cardiomyopathy: evidence, mechanisms, and therapeutic implications. Endocr Rev, 25(4):543-567.

Fedak PW, Verma S, Weisel RD et al (2005) Cardiac remodelling and failure: From molecules to man (Part II) Cardiovasc Pathol 14;49-60

Feng B, Chen S, Chiu J, George B, Chakrabarti S (2008) Regulation of cardiomyocyte hypertrophy in diabetes at the transcriptional level Am J Physiol Endocrinol Metab 294: E1119-E1126

Filippo CD, Marfella R, Cuzzocrea S, et al (2006) Hyperglycemia in streptozotocin-induced diabetic rat increases infarct size associated with low levels of myocardial HO-1 during ischemia/reperfusion. Diab 54: 808-810

Foo RS, Mani K, Kitsis RN (2005) Death begets failure in the heart. J Clin Invest 115:565571

Forero MG, Pennack JA, Learte AR et al (2009) Deadeasy Caspase: Automatic Counting of Apoptotic Cells in Drosophila 4(5):e5441

Formigli L, Papucci L, Tani A, Schiavone N et al (2000) Aponecrosis: morphological and biochemical exploration of a syncretic process of cell death sharing apoptosis and necrosis. J Cell Physiol 182:41-9

Forstermann U, Munzel T (2006) Endothelial nitric oxide synthase in vascular disease: from marvel to menace. Circulation. 113:1708-1714

Frantz C, Stewart KM, Weaver VM (2010) The extracellular matrix at a glance. Journal of Cell Science 123: 4195-4200

Fredersdorf S, Thumann C, Zimmerman WH, Vetter R et al (2012) Increased myocardial SERCA expression in early type 2 diabetes mellitus is insulin dependent: In vivo and in vitro data. Cardiovas Diabetol, 11:(57)1-11

Friedl A (2010) Proteoglycans: master modulators of paracrine fibroblast-carcinoma cell interactions. Semin. Cell Dev. Biol. 21, 66-71

Fujimoto N, Prasad A, Hastings JL, Arbab-Zadeh A et al (2010) Cardiovascular effects of 1 year of progressive and vigorous exercise training in previously sedentary individuals older than 65 years of age. Circulation 122:1797-1805

Fujisawa T, Ikegami H, Kawaguchi Y (2004) Common genetic basis between type 1 and type 2 diabetes mellitus indicated by interview-based assessment of family history. Diabetes Res Clin Pract, 66: S91-S95

Furuse Y, Hashimoto N, Maekawa M, Toyama Yet al (2004) Activation of the Smad pathway in glomeruli from aspontaneously diabetic rat model, OLETF rats. Nephron Exp Nephrol 98:100-108

Ganda OP, Rossi AA, Like AA (1976) Studies on streptozotocin diabetes. Diabetes 25: 595-603

Gauguier D, Froguel P, Parent V et al (1996) Chromosomal mapping of genetic loci associated with non-insulin dependent diabetes in the GK rat. Nat Genet 12:38-43

Gattone VH (2007) The Kidney-Introduction to its Structure and Function. FASEB 21:9.4

George CH, Jundi H, Thomas NL, Fry DL et al (2007) Ryanodine receptors and ventricular arrhythmias: emerging trends in mutations, mechanisms and therapies. J Mol Cell Cardiol 42:34-50

Gerber Y, Jacobsen SJ, Frye RL, Weston SA, Killian JM et al (2006) Secular trends in deaths from cardiovascular diseases: a 25-year community study. Circulation 113(19):2285–92

Ghosh AK, Bradham WS, Gleaves LA, De Taeye B (2010) Genetic deficiency of plasminogen activator inhibitor-1 promotes cardiac fibrosis in aged mice: involvement of constitutive transforming growth factor-beta signaling and endothelial-to-mesenchymal transition. Circulation 122(12):1200-9

Giacco F, Brownlee M (2010) Oxidative stress and diabetic complications. *Circ Res* 107: 1058-1070

Goldhaber JI (2011) Role of NCX in Heart Failure, Ischemia/Reperfusion, and Arrhythmias: Lessons From NCX Knockout Mice. Session 9: NCX in the Heart Disease 1-8

Goldstein B.J (2002) Insulin resistance as the core defect in type 2 diabetes mellitus. Am J Cardiol, 90: 3-10

Gorin Y, Block K, Hernandez J et al (2005) Nox4 NAD(P)H oxidase mediates hypertrophy and fibronectin expression in the diabetic kidney. *J Biol Chem* 280*:*39616-39626

Gorman AM, Healy SJ, Jäger R, Samali A (2012) Stress management at the ER: regulators of ER stress-induced apoptosis. Pharmacol Ther, 134(3): 306-16

Goto Y, Kakizaki M and Masaki N(1975) Spontaneous diabetes produced by selective breeding of normal Wistar rats. Proc Jpn Acad 51: 80-85

Graham HK, Horn M and Trafford AW (2008) Extracellular matrix profiles in the progression to heart failure. European Young Physiologists Symposium Keynote Lecture- Bratislava. Acta Physio. (Oxf) 194: 3-21

Grant AO (2009) Cardiac ion channels, Circ Arrhythm Electrophysiol 2: 185-194

Grijalva J, Hicks S, Zhao X, Medikayala S et al (2008) Exercise training enhanced myocardial endothelial nitric oxide synthase (eNOS) function in diabetic Goto-Kakizaki (GK) rats. Cardiovasc Diabetol 19(7):34

Gupta S, Prahash AJ and Anand IS (2000) Myocyte contractile function is intact in the post-infract remodelled rat heart despite molecular alterations. Cardiovasc Res 48: 77-88

Guo R, Liu L, Barajas L (1998) RT-PCR study of the distribution of connexin 43 mRNA in the glomerulus and renal tubular segments. American Journal of Physiology - Regulatory Integrative and Comparative Physiology 275(2):R439-R447

Guo Z, Xia Z, Jiang J, McNeil JH (2007) Down-regulation of NADPH oxidase, antioxidant enzymes and inflammatory markers in the heart of streptozotocin-induced diabetic rats by N enzymes. Am J Physiol Heart Circ Physiol 292: H1728-H1736

Gutierrez C, Blanchar DG (2004) Diastolic heart failure: challenges of diagnosis and treatment. Am Fam Physc 69:2609-2616

Hafstad AD, Lund J, Hadler-Olsen E, Höper AC, Larsen TS, Aasum E (2013) High- and moderate-intensity training normalizes ventricular function and mechanoenergetics in mice with diet-induced obesity. Diabetes 62:2287-2294

Hasenfuss G, Schillinger W, (2004) Is Modulation of Sodium-Calcium Exchange a Therapeutic Option in Heart Failure? Circ Res 95:225-227

Hayashi H and Noda N (1997) Cytosolic Ca^{2+} concentration decreases in diabetic rat myocytes. Cardiovasc Res 34:99-103

Haudek SB, Taffet GE, Schneider MD, Mann DL (2007) TNF provokes cardiomyocyte apoptosis and cardiac remodelling through activation of multiple cell death pathways. J Clin Invest.117: 2692-2701

Heywood JT, Fonarow GC, Costanzo MR, Mathur VS, Wigneswaran JR, Wynne J (2007) ADHERE Scientific Advisory Committee and Investigators. High prevalence of renal dysfunction and its impact on outcome in 118,465 patients hospitalized with acute decompensated heart failure: a report from the ADHERE database. J Card Fail 13(2):422–30

Hebden RA, McNeil JH (1988) Concentration(s) of atrial natriuretic hormone in the plasma of rats with streptozotocin-induced diabetes mellitus. Life Sci 42:1789-1795

Hein S, Arnon E, Kostin S et al (2003) Progression from compensated hypertrophy to failure in the pressure-overloaded human heart:structural deterioration and compensatory mechanisms. Circulation 107:984-91

He JG, Chen YL, Chen BL et al (2010) B-type natriuretic peptide attenuates cardiac hypertrophy via the transforming growth factor-β1/smad7 pathway in vivo and in vitro. Clin Exp Pharmacol Physiol 37(3) 283-289

Hengartner MO (2000) The biochemistry of apoptosis. Nature 407:770-6

Herzog CA (2007) Can we prevent sudden cardiac death in dialysis patients? Clin J Am Soc Nephrol 2:410–412

Hilfiker-Kleiner D, Hilfiker A, Castellazzi M, Wollert KC et al (2006) JunD attenuate phenylephrine-mediated cardiomyocyte hypertrophy by negatively regulating AP-1 transcriptional activity. Card Res, 71(1):108-117

Hilfiker-Kleiner D, Landmesser U, Drexler H (2006) Molecular Mechanisms in Heart Failure. J Am Coll Cardiol 48: 56-66

Hilgemnn DW (2004) New insights into the molecular and cellular workings of the cardiac Na+/Ca2+ exchanger. Am J Physiol Cell Physiol 287(5):C1167-72

Hill C, Flyvbjerg A, Gronbaek H, Petrik J et al (2000) The renal expression of transforming growth factor-beta isoforms and their receptors in acute and chronic experimental diabetes in rats. Endocrinol 141:1196-1208

Hillege HL, Nitsch D, Pfeffer MA et al(2006) Renal function as a predictor of outcome in a broad spectrum of patients with heart failure. Circul 113:671-678

Hillis GS (1997)The expression of connexin 43 in human kidney and cultured renal cells. Nephron 75(4):458-463

Hills CE, Bland R, Wheelans DC, Bennett J et al (2006) Glucose-evoked alterations in connexin43-mediated cell-to-cell communication in human collecting duct: a possible role in diabetic nephropathy. Am J of Physiol - Ren Physiol, 291(5)1045-1051

Hobbs FDR, Kenkre JE, Roalfe AK et al (2002) Impact of heart failure and left ventricle systolic dysfunction on quality of life: a cross-sectional study comparing chronic cardiac and medical disorders and a representative adult population. Eur J Heart Fail 23:1867-1876

Hoegy SE, Oh HR, Corcoran ML, Stetler-Stevenson WG (2001) Tissue inhibitor of metalloproteinases-2 (TIMP-2) suppresses TKR-growth factor signaling independent of metalloproteinase inhibition. J. Biol. Chem. 276(5):3203-3214

Hofer T, Servais S, Seo AY, Marzetti E, Hiona A, Upadhyay SJ, et al (2009) Bioenergetics and permeability transition pore opening in heart subsarcolemmal and interfibrillar mitochondria: effects of aging and lifelong calorie restriction. Mech Ageing Dev130:297-307

Hoffman BB, Sharma K, Ziyadeh FN (1998) Potential role of TGF-β in diabetic nephropathy. Miner Electrolyte Metab 24:190-196

Hong SW, Isono M, Chen S et al (2001) Increased glomerular and tubular expression of transforming growth factor-beta1, its type II receptor, and activation of the Smad signaling pathway in the db/db mouse. Am J Pathol 158:1653-1663

Hoppel CL, Tandler B, Fujioka H, Riva A (2009) Dynamic organization of mitochondria in human heart and in myocardial disease. Int J Biochem Cell Biol; 41:1949-1956

Howarth FC, Almugaddum FA, Qureshi MA, Ljubisavljevic M (2009) Effects of heavy long-term exercise on ventricular myocyte shortening and intracellular Ca2+ in streptozotocin-induced diabetic rats. J Diabetes Complications 24(4):278-285

Howarth FC, Almugaddum FA, Qureshi MA, Ljubisavljevic M (2008) Effects of varying intensity exercise on shortening and intracellular calcium in ventricular myocytes from streptozotocin (STZ)-induced diabetic rats. Mol Cell Biochem 317(1-2):161-167

Howarth FC, Chandler NJ, Kharche S, et al (2008) Effects of streptozotocin-induced diabetes on connexin43 mRNA and protein expression in ventricular muscle. *Molecular and Cellular Biochemistry* 319(1-2):105-114

Howarth FC, Jacobson M, Shafiullah M, Adeghate E (2008) Long-term effects of type 2 diabetes mellitus on heart rhythm in the Goto-Kakizaki rat. Exp Physiol 93(3):362-369

Howarth FC, Nowotny N, Zilahi E, El Haj MA, Lei M (2007) Altered expression of gap junction connexin proteins may partly underlie heart rhythm disturbances in the streptozotocin-induced diabetic rat heart. *Mol Cell Biochem* 305(1-2):145-151

Howarth FC, Qureshi MA, Bracken NK et al (2001) Time-dependent effects of streptozotocin-induced diabetes on contraction of ventricular myocytes from rat heart. Emirates Med J 19:35-41

Howarth FC Shafiullah M, Qureshi MA (2007) Chronic effects of type 2 diabetes mellitus on cardiac muscle contraction in the Goto-Kakizaki rat. Exp Physiol 92:1029-1036

Howarth FC, Qureshi MA, White E (2002) Effects of hyperosmotic shrinking on ventricular myocyte shortening and intracellular Ca2+ in streptozotocin-induced diabetic rats. Pflugers Arch 444:446-451

Howarth FC, Qureshi A, Singh J (2004) Effects of acidosis on ventricular myocyte shortening and intracellular Ca2+ in streptozotocin-induced diabetic rats. Mol Cell Biochem 261: 227-233

Howarth FC and Singh J (1999) Altered handling of calcium during the process of excitation-contraction coupling in the streptozotocin-induced diabetic heart: a short review Int J Diab 7:52–64

Howarth FC, Adem A, Adeghate EA et al (2005) Distribution of atrial natriuretic peptide and its effects on contraction and intracellular calcium in ventricular myocytes from streptozotocin-induced diabetic rat. Peptides 26:691-700

Huang HC, Preisig PA (2000) G1 kinases and transforming growth factor-beta signaling are associated with a growth pattern switch in diabetes-induced renal growth. Kidney Int 58:162-172

Huynh K, Bernardo BC, McMullen JR, Ritchie RH (2014) Diabetic cardiomyopathy: Mechanisms and new treatment strategies targeting antioxidant signaling pathways. Pharmacol Ther 142:375-415

Huynh K, McMullen JR, Julius TL, Tan JW, Love JE, et al. (2010) Cardiac-specific IGF-1 receptor transgenic expression protects against cardiac fibrosis and diastolic dysfunction in a mouse model of diabetic cardiomyopathy. Diabetes 59:1512-1520

Hyer SL. & Shehata HA (2005) Gestational diabetes mellitus. Current Obstetrics Gynaecol.15: 368-374

Hynes RO (2009) The extracellular matrix: not just pretty fibrils. Science 326, 1216-1219

Ikebukuro K, Adachi Y, Yamada Y, Fujimoto S, Seino Y, Oyaizu H (2002) Treatment of Streptozotocin-induced diabetes mellitus by transplantation of islet cells Plus bone Marrow cells via portal vein in rats. Transplantation 73: 512-518

Inoguchi T, Yu HY, Imamura M, et al (2001) Altered gap junction activity in cardiovascular tissues of diabetes. *Medical Electron Microscopy* 34(2):86-91

Isono M, Chen S, Hong SW, Iglesias-de la Cruz MC, Ziyadeh FN (2002) Smad pathway is activated in the diabetic mouse kidney and Smad3 mediates TGF-beta-induced fibronectin in mesangial cells. Biochem Biophys Res Commun 296:1356-1365

Ito Y, Aten J, Bende RJ, Oemar BS et al (1998) Expression of connective tissue growth factor in human renal fibrosis. Kidney Int 53*:*853-861

Ivaska J, Pallari HM, Nevo J, Eriksson JE (2007) Novel functions of vimentin in cell adhesion, migration, and signaling. Exp Cell Res 313(10):2050-2062

Jacobsen IB, Henriksen JE, Hother-Nielsen O, et al (2009) Evidence-based insulin treatment in type 1 diabetes mellitus. Diabetes Res Clin Pract. 86: 1-10

James LR, Le C, Doherty H, Kim HS, Maeda N (2013) Connective tissue growth factor (CTGF) expression modulates response to high glucose. PLOS One 8:e70441

Jarvelainen H, Sainio A, Koulu M et al (2009) Extracellular matrix molecules: potential targets in pharmacotherapy. Pharmacol. Rev. 61, 198-223
Johansen JS, Harris K, Rychly DJ, Ergul A (2005) Oxidative stress and the use of antioxidants in diabetes: linking basic science to clinical practice. Cardiovasc Diabetol 4: 1-11
Julien J (1997) Cardiac complications in non-insulin-dependent diabetes mellitus. J Diabetes Complications 11:123-130

Kahn RC (2005) Ed. Joslin's Daibetes Mellitus. Lippincott Williams and Wilkins pp 89-91
Kakleas K, Kandyla B, Karayianni C, Karavanaki K (2009) Psychosocial problems in adolescents with type 1 diabetes mellitus. Diabetes and Metabolism, 35: 339-350

Kang PM, Yue P, Liu Z, Bodyak N et al (2004) Alterations in apoptosis regulatory factors during hypertrophy and heart failure. Am J Physiol 287,H72-H80

Kapoun AM, Liang A, O'Young G et al (2004) B-type natriuretic peptide exerts broad functional opposition to transforming growth factor-beta in primary human cardiac fibroblasts: fibrosis, myofibroblast conversion, proliferation, and inflammation. Circulation
Res 94:453-461

Kappagoda T, Amsterdam EA (2012) Exercise and heart failure in the elderly. Heart Fail Rev 17:92-97

Khan R, Sheppard R (2006) Fibrosis in heart disease: understanding the role of transforming growth factor-b1 in cardiomyopathy, valvular disease and arrhythmia. Immunol 118:10-24

Korte FS, Mokelke EA, Sturek M, McDonald KS (2005) Exercise improves impaired ventricular function and alterations of cardiac myofibrillar proteins in diabetic dyslipidemic pigs. J Appl Physiol Bethesda Md 1985 98:461-467

Kato M, Park JT, Natarajan R (2012) MicroRNAs and the glomerulus. Exp Cell Res 318:993-1000

Kato M, Yuan H, Xu ZG, et al (2006) Role of the Akt/FoxO3a pathway in TGF-beta1-mediated mesangial cell dysfunction: a novel mechanism related to diabetic kidney disease. J Am Soc Nephrol 17:3325-3335

Kato M, Zhang J, Wang M, Lanting L et al (2007) MicroRNA-192 in diabetic kidney glomeruli and its function in TGF-beta-induced collagen expression via inhibition of E-box repressors. Proc Natl Acad Sci USA 104: 3432-3437

Kattla JJ, Carew RM, Heljic M et al (2008) Protein kinase B/Akt activity is involved in renal TGF-β1-driven epithelial-mesenchymal transition in vitro and in vivo. *Am J Physiol Renal Physiol* 295:F215-F225

Kaul K, Tarr JM, Ahmad SI, Kohner EM, Chibber R (2012) Introduction to diabetes mellitus. Adv Exp Med Biol 771:1-11

Kawaguchi M, Asakura T, Saito F, Nemoto O et al (1999) Changes in diameter size and F-actin expression in the myocytes of patients with diabetes and streptozotocin-induced diabetes model rats. J Cardiol 34:333-339

Kim M, Carman CV, Springer TA (2003) Bidirectional transmembrane signaling by cytoplasmic domain separation in integrins. Sci 301:1720-1725

Kitamura H, Shimizu A, Masuda Y et al (1998) Apoptosis in glomerular endothelial cells during the development of glomerulosclerosis in the remnant-kidney model. *Exp Nephrol* 6:328-336

Koeppen BA and Stanton BM (2008) In: Berne and Levy Physiology with STUDENT CONSULT online access. Mosby International, London. Pp 256-267

Koplan BA and Stevenson WC (2007) Sudden arrhythmic death syndrome. Heart 93(5):

547–548

Kotsanas G, Delbridge LM, Wendt IR (2000) Stimulus interval-dependent differences in Ca2+ transients and contractile responses of diabetic rat cardiomyocytes. Cardiovasc Res 46:450-462

Kowluru RA, Abbas SN, Odenbach S (2004) Reversal of hyperglycemia and diabetic nephropathy: Effect of reinstitution of good metabolic control on oxidative stress in the kidney of diabetic rats. J Diabetes and Comp 18(5)282-288

Kumar D, Zimpelmann J, Robertson S, Burns KD (2004) Tubular and Interstitial Cell Apoptosis in the Streptozotocin-Diabetic Rat Kidney. Nephron Exp Nephrol 96:e77-e88

Kushnir AA, Betzenhauser MJ, Marks AR (2010) Ryanodine receptor studies using genetically engineered mice. FEBS Lett 584:1956-1965

Kuwahara F, Kai H, Tokuda K, Kai M, Takeshita A, Egashira K, Imaizumi T (2002) Transforming growth factor-beta function blocking prevents myocardial fibrosis and diastolic dysfunction in pressure-overloaded rats. Circulation 106(1):130-135

Kwak HB, Kim JH, Joshi K, Yeh A, Martinez DA, Lawler JM (2011) Exercise training reduces fibrosis and matrix metalloproteinasedysregulation in the aging rat heart. J FASEB 25(3):1106-1117

Kwak HB, Song W, Lawler JM (2006) Exercise training attenuates age-induced elevation in Bax/Bcl-2 ratio, apoptosis, and remodelling in the rat heart. FASEB 20(6):791-3

Lacombe, K., Massari, V., Girard, P., Serfaty, L et al (2007) Major role of hepatitis B genotypes in liver fibrosis during coinfection with HIV. AIDS 20, 419-427

LaRocca TJ, Fabris F, Chen J (2012) Na^{+}/Ca^{2+} exchanger-1 protects against systolic failure in the $Akita^{ins2}$ model of diabetic cardiomyopathy via a CXCR4/NF-κB pathway. Am J Physiol Circ Physiol 303(3): H353-H376

Lazzarini V, Bettari L, Bugatti S, Carubelli V, Lombardi C, Metra M, Dei Cas L (2011) Can we prevent or treat renal dysfunction in acute heart failure? Heart Fail Rev [Epub ahead of print]

Leask A, Holmes A, Abraham DJ (2002) Connective tissue growth factor: a new and important player in the pathogenesis of fibrosis. Curr Rheumatol Rep 4:136-142

Lebeche D, Davidoff AJ, Hajjar RJ (2008) Interplay between impaired calcium regulation and insulin signaling abnormalities in diabetic cardiomyopathy. Nat Clin Pract Cardiovasc Med, 5: 715-24

Leehey DJ, Singh AK, Alavi N et al (2000) Role of angiotensin II in diabetic nephropathy. *Kidney Int* 77 Suppl 77*:*S93-S98

Lemley KV, Abdullah I, Myers BD, et al (2000) Evolution of incipient nephropathy in type 2 diabetes mellitus. Kidney Int 58:1228-1237

Lenzen S (2008) The mechanisms of alloxan- and streptozotocin-induced diabetes. Diabetologia 51:216-226

Levine B, Kalman J, Mayer L, Fillit H M, Packer M (1990) Elevated circulating levels of tumour necrosis factor in severe chronic heart failure. N Engl J Med 323: 236-241

Liang KV, Williams AW, Greene EL, Redfield MM (2008) Acute decompensated heart failure and the cardiorenal syndrome. Crit Care Med 36:S75-S88

Li B, Zheng Z, Wei Y et al (2011) Therapeutic effects of neuregulin-1 in diabetic cardiomyopathy rats. Cardio Diabetol 10: 69-77

Li G, Borger MA, Williams WG, Weisel RD, Mickle DA, Wigle ED, Li RK (2002) Regional overexpression of insulin-like growth factor-I and transforming growth factor-beta1 in the myocardium of patients with hypertrophic obstructive cardiomyopathy. J Thorac Cardio Surg 123:89-95

Lijnen P, Petrov V (2002) Transforming growth factor-beta 1-induced collagen production in cultures of cardiac fibroblasts is the result of the appearance of myofibroblasts. Methods Find Exp Clin Pharmacol 24:333-344

Lijnen, P. J., Petrov, V. V., & Fagard, R. H. (2000). Induction of cardiac fibrosis by transforming growth factor-β1. Mol Genet Metab 71, 418-435

Lin CL, Wang LY, Huang YT, Kuo YH et al (2006) Wnt/â-catenin signaling modulates survival of high glucose-stressed mesangial cells. J Am Soc Nephrol 17: 2812-2820

Lindeman RD, Tobin JD, Shock NW. Association between blood pressure and the rate of decline in renal function with age. Kidney Int 1984;26:861-8

Lindström J, Ilanne-Parikka P, Peltonen M, et al (2006) Sustained reduction in the incidence of type 2 diabetes by lifestyle intervention: follow-up of the Finnish Diabetes Prevention Study. The Lancet 368(9548):1673-1679

Lira FS, Rosa JC, Zanchi NE, et al (2009) Regulation of inflammation in the adipose tissue in cancer cachexia: effect of exercise. Cell Biochem Fun 27:71-75

Lira F, Tavares F, Yamashita A, et al (2008) Effect of endurance training upon lipid metabolism in the liver of cachectic tumour-bearing rats. Cell Biochem Fun 26:701-708

Li RK, Li G, Mickle D et al (1997) Overexpression of transforming growth factor-beta1 and insulin-like growth factor-1 in patients with idiopathic hypertrophic cardiomyopathy. Circulation 96: 874-881

Li S, Culver B, Ren J (2003) Benefit and risk of exercise on myocardial function in diabetes. Pharmacol Res Off J Ital Pharmacol Soc 48:127-132

Li SY, Huang PH, Yang AH, Tarng DC et al (2012) Matrix metalloproteinase-9 deficiency attenuates diabetic nephropathy by modulation of podocyte functions and dedifferentiation. Kidney Int

Liu N, Colombi B, Memmi M, Zissimopoulos S, M et al (2006) Arrhythmogenesis in catecholaminergic polymorphic ventricular tachycardia: insights from a RyR2 R4496C knock-in mouse model. Circ Res 99:292-298

Loganathan R, Bilgen M, Al-Hafez B (2006) Cardiac dysfunction in the diabetic rat: quantitative evaluation using high resolution magnetic resonance imaging. Cardiovasc Diabet, 5:7

Loganathan R, Bilgen M, Al-Hafez B, Zhero SV, Alenezy MD, Smirnova IV (2007) Exercise training improves cardiac performance in diabetes: in vivo demonstration with quantitative cine-MRI analyses. J Appl Physiol Bethesda Md 1985102:665-672

Loganathan R, Novikova L, Boulatnikov IG, Smirnova IV (2012) Exercise-induced cardiac performance in autoimmune (type 1) diabetes is associated with a decrease in myocardial diacylglycerol. J Appl Physiol Bethesda Md 1985 113:817-826

Loimaala A, Groundstroem K, Majahalme S, Nenonen A, Vuori I (2006) Impaired myocardial function in newly onset type 2 diabetes associates with arterial stiffness. Eur J Echocardiogr 7(5):341-347

Lowes BC, Minobe W, Abraham WT et al (1997) Changes in gene expression in the intact human heart. Downregulation of alpha-myosin heavy chain in hypertrophied, failing ventricular myocardium. J Clin Invest 100: 2315-2324

Lowry OH, Rosebrough NJ, Farr AL et al (1951) Protein measurement with Folin phenol reagen. J Biol Chem 193(1):265-275

Lucero HA and Kagan HM (2006) Lysyl oxidase: an oxidative enzyme and effector of cell function. Cell. Mol. Life Sci. 63, 2304-2316

Lukowicz TV, Fischer M, Hense HW et al (2005) BNP as a marker of diastolic dysfunction in the general population: Importance of left ventricular hypertrophy. Eur J Heart Fail 7(4): 525-531

Mackrill JJ (2010) Ryanodine receptor calcium channels and their partners as drug targets. Biochem Pharmacol 79 (2010) 1535-1543

Macri L, Silverstein D, Clark RA (2007) Growth factor binding to the pericellular matrix and its importance in tissue engineering. Adv. Drug Deliv. Rev. 59, 1366-1381

Mac-Moune LF, Szeto CC, Choi PC et al *(2004)* Isolate diffuse thickening of glomerular capillary basement membrane: A renal lesion in prediabetes? *Mod Pathol* 17:1506– 1512

Magga J, Vuolteenaho O, Tokola H, Marttila M, Ruskoaho H (1998) Btype natriuretic peptide: a myocyte-specific marker for characterizing load-induced alterations in cardiac gene expression. Ann Med 1998;30 (Suppl. 1):39-45

Mahimainathan L, Das F, Venkatesan B et al (2006) Mesangial cell hypertrophy by high glucose is mediated by downregulation of the tumor suppressor PTEN. *Diabetes* 55:2115-2125

Manabe I, Shindo T, Nagai R (2002) Gene expression in fibroblasts and fibrosis: Involvement in cardiac hypertrophy. Circ Res. 91:1103-1113

Mangoni ME, Traboulsie A, Leoni AL, Couette B et al (2006) Bradycardia and slowing of the atrioventricular conduction in mice lacking CaV3.1/ alpha1G T-type calcium channels. Circ Res 98(11):1422-1430

Mankhey RW, Bhatti F, Maric C (2005) 17beta-Estradiol replacement improves renal function and pathology associated with diabetic nephropathy. Am J Physiol Renal Physiol 288:F399-F405

Mann DL, Bogaev R, Buckberg GD (2010) Cardiac remodelling and myocardial recovery: lost in transition? Eur J Heart Fail 12:789-796

Maric C, Sandberg K, Hinojosa-Laborde C (2004) Glomerulosclerosis and Tubulointerstitial Fibrosis are Attenuated with 17beta-Estradiol in the Aging Dahl Salt Sensitive Rat. J Am Soc Nephrol 15:1546-1556

Mason RM, Wahab NA (2003) Extracellular matrix metabolism in diabetic nephropathy. J Am Soc Nephrol 14:1358-1373

Masoudi FA, Inzucchi SE (2007) Daibetes mellitus and heart failure: epidemiology, mechanisms, and pharmacotherapy. Am J Cardiol 99:113-132

Masson S, Arosio B, Fiordaliso F, Gagliano N et al (2000). Left ventricular response to beta-adrenergic stimulation in aging rats. J Gerontol A Biol Sci Med Sci 55:B35-B41

Matsuda T, Yamamoto T, Muraguchi A, Saatcioglu F (2001) Cross-talk between transforming growth factor-beta and estrogen receptor signaling through Smad3. J Biol Chem. 2001; 276:42908-42914

Matususka H, Tomomi I, Matushima S et al (2006) Targeted deletion of matrix metalloproteinase 2 ameliorates myocardial remodelling in mice with chronic pressure overload. Hypertension 47: 711-717

Mauer SM, Steffes MW, Ellis EN, Sutherland DE et al (1984) Structural-functional relationships in diabetic nephropathy. J Clin Invest 74: 1143-1155

Maytin M and Colucci WS (2002) Molecular and cellular mechanisms of myocardial remodelling J Nucl Cardiol 9: 319-327

McDonald TJ, Ellard S (2013) Maturity onset diabetes of the young: identification and diagnosis. Ann Clin Biochem.50(Pt 5):403-15

McLennan SV, Kelly DJ, Cox AJ, Cao Z et al (2002) Decreased matrix degradation in diabetic nephropathy: effects of ACE inhibition on the expression and activities of matrix metalloproteinases. Diabetol 2002; 45:268-275

Meissner M, Weissgerber P, Londono JE et al (2011) Moderate calcium channel dysfunction inadult mice with inducible cardiomyocyte-specific excision of the cacnb2 gene. J Biol Chem 286(18):15875-15882

Metcalfe PD, Meldrum KK (2006) Sex differences and the role of sex steroids in renal injury. J Urol 176:15-21

Metra M, Voors AA (2012) The puzzle of kidney dysfunction in heart failure: an introduction. Heart Fail Rev 17:129–131

Meyer TW, Bennett PH, Nelson RG (1999) Podocyte number predicts long-term urinary albumin excretion in Pima Indians with Type II diabetes and microalbuminuria. Diabetol 42:1341-1344

Minamino T, Komuro I, Kitakaze M (2010) Endoplasmic reticulum stress as a therapeutic target in cardiovascular disease. Circ Res,107(9):1071-82

Miner JH (2003) A molecular look at the glomerular barrier. Nephron Exp Nephrol 94(4):e119-22

Miner EC and Miller WL (2006) A look between Cardiomyocytes: The Extracellular Matrix in Heart Failure. Mayo Clinic Proceedings 81(1): 71-76

Mishra R, Emancipator SN, Kern T, Simonson MS (2005) High glucose evokes an intrinsic proapoptotic signaling pathway in mesangial cells. Kidney Int 67: 82-93

Mohora M, Greabu M, Muscurel C, et al (2007) The sources and the targets of oxidative stress in the aetiology of diabetic complications. Romanian J. Biophysics, 17: 63-84

Murakami M, Elfenbein A, Simons M (2008) Non-canonical fibroblast growth factor signalling in angiogenesis. Cardiovasc Res 78, 223-231

Nagai K, Matsubara T, Mima A et al (2005) Gas6 induces Akt/mTOR-mediated mesangial hypertrophy in diabetic nephropathy. *Kidney Int* 68*:*552-561

Nakagawa T, Li JH, Garcia G, Mu W et al (2004)TGF-beta induces proangiogenic and antiangiogenic factors via parallel but distinct Smad pathways. Kidney Int 66:605-613

Nathan DM, Cleary PA, Backlund JY et al (2005) Intensive diabetes treatment and cardiovascular diabetes in patients with type 2 diabetes. N Engl J Med 353: 2643-2653

National Institute for Health and Clinical Excellence (2003). Management of chronicheart failure in adults in primary and secondary care. Clinical guideline CG5.

London:NICE; July 2003Available via: http://www.nice.org.uk/nicemedia/pdf/CG5NICEguideline.pdf

Nemoto O, Kawaguchi M, Yaoita H, Miyake K et al (2006) Left ventricular dysfunction and remodeling in streptozotocin-induced diabetic rats. Circ J 70:327-334

Nohria A, Hasselblad V, Strebbin A et al (2008) Cardio-renal interactions: insight from the ESCAPE trial. J Am Coll Cardiol 51:1268-1274

Niessner A, Hohensinner PJ, Rychli K, et al (2009) Prognostic value of apoptosis markers in advanced heart failure patients. Eur Heart J 30: 789-796

Oehrl W and Panayotou G (2008) Modulation of growth factor action by the extracellular matrix. Connect. Tissue Res. 49, 145-148

Oikonomou E, Tousoulis D, Siasos G et al (2011) The Role of Inflammation in Heart Failure: New Therapeutic Approaches. Hellenic J Cardiol 52: 30-40

Okunade GW, Miller ML, Pyne GJ, Sutliff RL et al (2004) Targeted ablation of plasma membrane Ca2_-ATPase (PMCA) 1 and 4 indicates a major housekeeping function for PMCA1 and a critical role in hyperactivated sperm motility and male fertility for PMCA4. J Biol Chem 279:33742-33750

Ortola FV, Ballermann BJ, Anderson S, Mendez RE, Brenner BM (1987) Elevated plasma atrial natriuretic peptide levels in diabetic rats: Potential mediator of hyperfiltration. J Clin Invest 80:670-674

O'Rourke B, Kass DA, Tomaselli GF, Kaab S et al (1999) Mechanisms of altered excitationcontraction coupling in canine tachycardia-induced heart failure, I: experimental studies. Circ Res 84(5):562-570

Owan TE, Hodge DO, Herges RM, Jacobsen SJ, Roger VL, Redfield MM (2006) Trends in prevalence and outcome of heart failure with preserved ejection fraction. N Engl J Med, 355: 251-9

Paczek C, Bartlomiejczyk, Przybylski J (2006) The serum levels of growth factors: PDGF, TGF-beta and VEGF are increased after strenuous physical exercise. J Physiol Pharmacol 7(2)189-197

Pagtalunan ME, Miller PL, Jumping-Eagle S, et al (1997) Podocyte loss and progressive glomerula injury in type II diabetes. J Clin Invest 99:342-348

Palmer JW, Tandler B, Hoppel CL (1986) Heterogeneous response of subsarcolemmal heart mitochondria to calcium. Am J Physiol 250:H741-H748

Pandit SV, Giles WR & Demir SS (2003) A mathematic model of the electrophysiological alterations in rat ventricular myocyte in type 1 diabetes mellitus. Biophys J 84:832–841

Parker TG, Packer SE, Schneider MD (1990). Peptide growth factors can provoke "fetal" contractile protein gene expression in rat cardiac myocytes. J Clin Invest 85: 507-514

Park SK, Kim J, Seomun Y, Choi J et al (2001) Hydrogen peroxide is a novel inducer of connective tissue growth factor. Biochem Biophys Res Commun 284:966-*971,* 2001

Pauschinger M, Knopf D, Petschauer S, et al (1999) Dilated cardiomyopathy is associated with significant changes in collagen type I/III ratio. Circulation 99: 2750-2756

Pedersen BK, Saltin B (2006) Evidence for prescribing exercise as therapy in chronic disease. Scand J Med Sci Sports 16 Suppl 1:3-63

Pellinen T, Arjonen T, Vuoriluoto T, Kallio K et al (2006) Small GTPase Rab21 regulates cell adhesion and controls endosomal traffic of beta1-integrins. J Cell Biol 173:767-780

Periasamy M & Huke S (2001) SERCA Pump Level is a Critical Determinant of Ca2+ Homeostasis and Cardiac Contractility. J Mol Cell Cardiol 33, 1053-1063

Periasamy M, and Janssen ML (2008) Molecular Basis of Diastolic Dysfunction. Heart Fail Clin 4(1):13-21

Perrin NE, Torbjornsdotter TB, Jaremko GA, Berg UB (2006) The course of diabetic glomerulopathy in patients with type I diabetes: A 6-year follow-up with serial biopsies. Kidney Int 69: 699-705

Petersen AMW, Pedersen BK (2005) The anti-inflammatory effect of exercise. J Appl Physiol 98: 1154-1162

Pichler M, Rainer PP, Schauer S, Hoefler G (2012) Cardiac fibrosis in human transplanted hearts is mainly driven by cells of intracardiac origin. J Am Coll of Cardiol 59: 1008-1016

Pires IF, Moreira LAF (2012) Diabetic cardiomyopathy: understanding the molecular and cellular basis to progress in diagnosis and treatment. Heart Fail Rev 17: 325-344

Pogwidz SM, Qi M, Yuan W, Samarel AM, Bers DM (1999) Upregulation of Na1 /Ca21 exchanger expression and function in an arrhythmo- genic rabbit model of heart failure. Circ Res 85:1009-1019

Porter KE, Turner NA (2009) Cardiac fibroblasts: At the heart of myocardial remodelling. Pharm & Ther123: 255-278

Portha B, Serradas P, Bailbe D et al (1991) Beta-cell insensitivity to glucose in the GK rat, a spontaneous nonobese model for type II diabetes. Diabetes 40:486-491

Priori SG, Napolitano C, Tiso N, Memmi M, et al. (2001) Mutations in the cardiac ryanodine receptor gene (hRyR2) underlie catecholaminergic polymorphic ventricular tachycardia. Circ 103:196-200

Qureshi MA, Bracken NK, Winlow W et al (2001) Time dependant effects of streptozotocin-induced diabetes on contraction in rat ventricular myocytes. Emirates J 19:25–41

Rahman S, Rahman T, Ismail A.A.-S., Rashid A.R (2007) Diabetes-associated macrovasculopathy: pathophysiology and pathogenesis. Diabetes Obesity Metabol 9: 767-780

Rai NK, Tripathi K, Sharma D et al (2005) Apoptosis: a basic physiologic process in wound healing. Int J Low Extrem Wounds 4:138-44

Rakieten N, Rakieten ML, Nadkarni MV (1963) Studies on the diabetogenic action of streptozotocin (NSC-37917). Cancer Chemother Rep 29:91-98

Ramos-Mondragon R, Galindo CA, Avila G (2008) Role of TGF-β on cardiac structural and electrical remodelling. Vasc Health Risk Manag 4 (6) 1289-1300

Rana JS, Nieuwdorp M, Jukema JW, Kastelein JJP (2007). Cardiovascular metabolic syndrome □Çô an interplay of, obesity, inflammation, diabetes and coronary heart disease. Diabetes, Obesity Metab 9: 218-232

Rane MJ, Song Y, Jin S et al *(2010)* Interplay between Akt and p38 MAPK pathways in the regulation of renal tubular cell apoptosis associated with diabetic nephropathy. *Am J Physiol Renal Physiol* 298:F49-F61

Raptis AE, Viberti G (2001) Pathogenesis of diabetic nephropathy. Exp Clin Endocrinol

Diabetes 109(Suppl 2): S424-S437

Reed JC, Tomaselli KJ (2000) Drug discovery opportunities from apoptosis research. Curr Opin Biotechnol 11:586-592

Regensteiner JC (2004) Type 2 diabetes mellitus and cardiovascular exercise performance. Endoc and Metab Dis 5(3)269-276

Reichek N, Devereux RB, Rocha RA, Hilkert R, Hall D, Purkayastha D & Pitt B (2009) Magnetic resonance imaging left ventricular mass reduction with fixed-dose angiotensin-converting enzyme inhibitor-based regimens in patients with high-risk hypertension. Hypertension 54:731-737

Ren J and Bode MA (2000) Altered cardiac excitation-contraction coupling in ventricular myocytes from spontaneously diabetic BB rats Am J Physiol Heart Circ Physiol 279: H238-H244

Ren J and Davidoff AJ (1997) Diabetes rapidly induces contractile dysfunctions in isolated ventricular myocytes. Am J Physiol 41: H148-H158

Reusch JEB, Bridenstine M, Regensteiner JG (2013) Type 2 diabetes mellitus and exercise impairment. Endo and Metab Dis, vol. 14(1)77-86

Riser BL, Denichilo M, Cortes P, Baker C et al (2000) Regulation of connective tissue growth factor activity in cultured rat mesangial cells and its expression in experimental diabetic glomerulosclerosis. J Am Soc Nephrol 11:25-*38*

Riva A, Tandler B, Loffredo F, Vazquez E, Hoppel C (2005), Structural differences in two biochemically defined populations of cardiac mitochondria. Am J Physiol Heart Circ Physiol, 289(2):H868-72

Rizk SM, El-Maraghy SA, Nassar, NN (2014) A Novel Role for SIRT-1 in L-Arginine Protection against STZ Induced Myocardial Fibrosis in Rats. PLoS One. 2014; 9(12): e114560

Roderick HL, Bootman MD (2007) Pacemaking, arrhythmias, inotropy and hypertrophy: the many possible facets of IP3 signalling in cardiac myocytes. J Physiol 581.3, pp 883-884

Rolo AP, Palmeira CM (2006) Diabetes and mitochondrial function: Role of hyperglycaemia and oxidative stress. Toxicol Appl. Pharmacol. 212: 167-178

Romanic AM, Burns-Kurtis CL, Ao Z, Arleth AJ, Ohlstein EH (2001) Upregulated expression of human membrane type-5 matrix metalloproteinase in kidneys from diabetic patients. Am. J. Physiol. Renal Physiol 281(2):F309-F317

Ronco C, Ronco F. Cardio-renal syndromes: a systematic approach for consensus definition and classification. Heart Fail Rev. 2011 E-pub ahead of print.

Rosca MG, Hoppel CL (2010) Mitochondria in heart failure. J Cardio Res, 88(1):40-50
Rosenkranz, S (2004) TGF-β1 and angiotensin networking in cardiac remodelling. Cardiovasc Res 63, 423-432

Rossing P (2006) Prediction, progression and prevention of diabetic nephropathy.The Minkowski Lecture 2005. Diabetol 49(1):11-19

Roy S (2000) Caspase at the heart of the apoptotic cell death pathway. Chem Res Toxicol 13:961-962

Rozario T and DeSimone DW (2010) The extracellular matrix in development and morphogenesis: a dynamic view. Dev. Biol. 341, 126-140

Ruetten H, Badroff C, Ihling C, Zeiher AM, and Dimmeler S (2001) Inhibition of caspase-3 improves contractile recovery of stunned myocardium, independent of apoptosis-inhibitory effects. J Am Coll. Cardiol 38:2063-2070

Rysz J, Banach M, Stolarek RA, Pasnik J et al (2007) Serum matrix metalloproteinases MMP-2 and MMP-9 and metalloproteinase tissue inhibitors TIMP-1 and TIMP-2 in diabetic nephropathy. J of nephrol 20(4):444-452

Ruggenenti P, Remuzzi G (2011) Worsening kidney function in decompensated heart failure: treat the heart, don't mind the kidney. Eur Heart J 32(20):2476–2478

Sabbah HN (2000) Apoptotic cell death in heart failure. Cardiovasc Res 45 (3): 704-712
Sabbah HN, Sharov VG, Lesch M (1995) Goldstein S. Progression of heart failure: a role for interstitial fibrosis. Mol Cell Biochem 147: 29-34

Salem KA, Adrian TE, Qureshi MA, Parekh K, Oz M, Howarth FC (2012) Shortening and intracellular Ca2+ in ventricular myocytes and expression of genes encoding

cardiac muscle proteins in early onset type 2 diabetic Goto-Kakizaki rats. Exp Physiol 97(12):1281-91

Sanz AB, Santamaría B, Ruiz-Ortega M, Egido J, Ortiz A (2008) Mechanisms of renal apoptosis in health and disease. J Am Soc Nephrol 19(9):1634-1642

Saraceni C, Broderick TL (2007) Cardiac and metabolic consequences of aerobic exercise training in experimental diabetes. Curr Diabetes Rev 3:75-84

Satelli A, Li S (2011) Vimentin as a potential molecular target in cancer therapy Or Vimentin, an overview and its potential as a molecular target for cancer therapy. Cell Mol Life Sci 68(18):3033-3046

Sawai K, Mukoyama M, Mori K et al (2006) Redistribution of connexin43 expression in glomerular podocytes predicts poor renal prognosis in patients with type 2 diabetes and overt nephropathy. Nephrol Dial Transpl, 21(9)2472-2477

Schaefer L and Schaefer RM (2010) Proteoglycans: from structural compounds to signaling molecules. Cell Tissue Res. 339, 237-246

Schainberg A, Riberio-Oliveira Jr A, Riberio JM (2010) Is there a link between glucose levels and heart failure? An update. Arq Bras Endocrinol Metab 54(5):488-497

Schalkwijk CG, Stehouwer CDA (2005) Vascular complications in diabetes mellitus: the role of endothelial dysfunction. Clinical Science 109: 143-159

Schena FP and Gesualdo L (2005) Pathogenetic Mechanisms of Diab Neph 16(3) suppl 1 S30-S33

Schillinger W, Janssen PML, Emami S et al (2000) Impaired contractile performance of cultured rabbit ventricular myocytes after adenovir- Aral gene transfer of Na/Ca exchanger. Circ Res 87:581-587

Schindler TH, Facta AD, Prior JO, et al (2007) Improvement in coronary vascular dysfunction produced with euglycaemic control in patients with type 2 diabetes. Heart, 93: 345-349

Schleicher ED, Weigert C (2000) Role of the hexosamine biosynthetic pathway in diabetic nephropathy. Kidney Intern 58. S-13–S-18

Schrijvers BF, De Vriese AS, Van d V et al (2004) Long-term renal changes in the Goto-Kakizaki rat, a model of lean type 2 diabetes. Nephrol Dial Transplant 19(5):1092-1097

Schultz J, Witt SA, Glascock BJ et al (2002) TGFβ1 mediates the hypertrophic cardiomyocyte growth induced by angiotensin II. J Clin Invest 109(6):787-796

Schena FP, Gesualdo L (2005) Pathogenetic Mechanisms of Diabetic Nephropathy. *JASN* 16(3) suppl 1 S30-S33

Scott JA, King GL (2004) Oxidative stress and antioxidant treatment in diabetes. Ann. N. Y. Acad. Sci 1031: 204-213

Scottish Health Survey (2012), Annual report of the Scottish Health Survey for 2011 Volume 1 focussing on adult health. http://www.gov.scot/Publications/2012/09/7854 Accessed May, 2015

Searls YM, Loganathan R, Smirnova IV, Stehno-Bittel L (2010) Intracellular Ca2+ regulating proteins in vascular smooth muscle cells are altered with type 1 diabetes due to the direct effects of hyperglycemia. Cardiovasc Diabetol 9:8

Searls YM, Smirnova IV, Fegley BR, Stehno-Bittel L (2004) Exercise attenuates diabetes-induced ultrastructural changes in rat cardiac tissue. Med Sci Sports Exerc 36:1863-1870

Seeland U, Selejan S, Engelhardt S (2007) Interstitial remodeling in beta1-adrenergic receptor transgenic mice. Basic Res Cardiol 102:183-193
Segura AM, Fraizer OH, Buja LM (2014) Fibrosis and heart failure. Heart Fail Rev 19:173-185

Sekiuchi M, Kudo A, Nakabayashi K, Kanai-Azuma M et al (2012) Expression of matrix metalloproteinases 2 and 9 and tissue inhibitors of matrix metalloproteinases 2 and 1 in the glomeruli of human glomerular diseases: the results of studies using immunofluorescence, in situ hybridization, and immunoelectron microscopy. Clin. Exp. Nephrol 16(6):863-874

Sengupta S, den Boon JA, Chen IH, Newton MA et al (2008) MicroRNA 29c is down-regulated in nasopharyngeal carcinomas, up-regulating mRNAs encoding extracellular matrix proteins. Proc Natl Acad Sci U SA 105:5874-5878

Serra AJ, Santos MH, Bocalini DS, Antônio EL (2010) Exercise training inhibits inflammatory cytokines and more than prevents myocardial dysfunction in rats with sustained beta-adrenergic hyperactivity. J Physiol 588(Pt 13):2431-42

Severs NJ, Bruce AF, Dupont E, Rothery S (2008) Remodelling of gap junctions and connexin expression in diseased myocardium. Cardiovascular Research 80(1):9-19

Sharma K, Dhingra S, Khaper N and Singal PK (2007) Activation of apoptotic processes during transition from hypertrophy to heart failure in guinea pigs. Am J Physiol (Heart Circ Physiol) 293: H1384-H1390

Sharma K, Ziyadeh FN, Alzahabi B, et al (1997) Increased renal production of transforming growth factor-beta1 in patients with type II diabetes. Diabetes 46:854-859

Shaw JE, Sicree RA, Zimmet PZ (2010) Global estimates of the prevalence of diabetes for 2010 and 2030. Diabetes Res Clin Pract 87:4-14

Sheikh AQ, Hurley JR, Huang W, Taghian T et al (2012) Diabetes Alters Intracellular Calcium Transients in Cardiac Endothelial Cells. PLoS ONE 7(5): e36840

Sherwood L (2008) Human Physiology: from cells to systems (7^{th} edition). Brooks/Cole, Belmont, USA pp 303-333

Shimizu A, Masuda Y, Kitamura H et al (1996) Apoptosis in progressive crescentic glomerulonephritis. *Lab Invest* 74:941-951

Shin SJ, Lee YJ, Tan MS, Hsjeh TJ, Tsai JH(1997) Increased atrial natriuretic peptide mRNAexpression in the kidney of diabetic rats. Kidney International 51:1100-1105

Shivakumar, K., Sollott, S. J., Sangeetha, M., Sapna, S., Ziman, B.,Wang, S., & Lakatta, E. G.(2008). Paracrine effects of hypoxic fibroblast-derived factors on the MPT-ROS threshold and viability of adult rat cardiac myocytes. Am J Physiol Heart Circ Physiol 294, H2653-H2658

Shizukuda Y, Reyland ME, Buttrick PM (2002) Protein kinase C-modulates apoptosis induced by hyperglycemia in adult ventricular myocytes. Am J Physiol Heart Circ Physiol 282: H1625-H1634

Siddiqi FA, Advani A (2013) Endothelial-Podocyte Crosstalk: The Missing Link Between Endothelial Dysfunction and Albuminuria in Diabetes. Diab 62:3647-3655

Silva E, Natali AJ, Silva MF, Gomes GJ et al (2013) Ventricular remodeling in growing rats with experimental diabetes: The impact of swimming training. Pathol Res Pract 209:618-626

Singh J, Chonkar A, Bracken N, Adeghate E et al (2006) Effect of streptozotocin-induced type 1 diabetes mellitus on contraction, calcium transient, and cation contents in the isolated rat heart. Ann N Y Acad Sci 1084:178-190

Skern R, Frost P and Nilsen F (2005) Relative transcript quantification by QPCR: roughly right or precisely wrong? BMC Mol Biology 6:10

Skiles JW, Gonnella NC, Jeng AY (2001) The design, structure, and therapeutic application of matrix metalloproteinase inhibitors. Curr. Med. Chem 8(4):425-474

Smith GL, Lichtman JH, Bracken MB, Shlipak MG, Phillips CO,DiCapua P, Krumholz HM (2006) Renal impairment and outcomes in heart failure systematic review and meta-analysis. J Am Coll Cardiol 47:1987-1996

Smith I O, Liu XH, Smith LA (2009) Nanostructured polymer scaffolds for tissue engineering and regenerative medicine. Wiley Interdiscip. Rev. Nanomed. Nanobiotechnol. 1, 226-236

Smith SB, Prior RL, Mersmann HJ (1983) Interrelationship between insulin and lipid metabolism in normal and alloxan-diabetic cattle. J Nutr 113:1002-1015

Soetikno V, Sari FR, Veeraveedu PT, Thandavarayan RA , et al (2011) Curcumin ameliorates macrophage infiltration by inhibiting NF-kappaB activation and proinflammatory cytokines in streptozotocin induced-diabetic nephropathy. Nutr Metab 8:35

Somaratne JB, Whalley GA, Poppe KK, et al (2011) Screening for left ventricular hypertrophy in patients with type 2 diabetes mellitus in the community. Cardiovasc Diabetol 10:29

Song P,Wu Y, Xu J (2007) Reactive nitrogen species induced by hyperglycemia suppresses Akt signaling and triggers apoptosis by upregulating phosphatase PTEN

(phosphatase and tensin homologue deleted on chromosome 10) in an LKB1-dependent manner. Circulation 116:1585-1595

Soni SS, Fahuan Y, Ronco C, Cruz DN (2009) Cardiorenal syndrome: biomarkers linking kidney damage with heart failure. Biomark Med 3:549-560

Soni SS, Ronco C, Katz N, Cruz DN (2009) Earlydiagnosis of acute kidney injury: the promise of novel biomarkers. Blood Purif 28:165-174

Sovari AS and Dudley SC (2010) Using Serum transforming growth factor- β to predict myocardial fibrosis. Circ Res 106:e3

Sperandio S, de Belle I, Bredesen DE (2000) An alternative, non- apoptotic form of programmed cell death. Proc Natl Acad Sci USA 97:14376-81

Spinale FG (2007) Myocardial matrix remodelling and the matrix metalloproteinases: influence of cardiac form and function. Physiol Rev 87:1285-1342

Steffes MW, Osterby R, Chavers B, Mauer SM (1989) Mesangial expansion as a central mechanism for loss of kidney function in diabetic patients. Diabetes 38:1077-1081

Steffes MW, Schmidt D, McCrery R, et al (2001) Glomerular cell number in normal subjects and in type 1 diabetic patients. Kidney Int 59:2104-13

Sun LP, Wang L, Wang H, Zhang YH, Pu JL (2010) Connexin 43 remodeling induced by LMNA gene mutation Glu82Lys in familial dilated cardiomyopathy with atrial ventricular block. *Chinese Medical Journal* 123(8):1058-1062

Susztak K, Raff AC, Schiffer M et al (2006) Glucose-induced reactive oxygen species cause apoptosis of podocytes and podocyte depletion at the onset of diabetic nephropathy. *Diab* 55*:*225-233

Swedberg K, Cleland J, Dargie H et al (2005) Guidelines for the diagnosis and treatment of chronic heart failure: Executive summary (Update 2995). Eur Herat J 26: 1115-1140

Swynghedauw B, Delcayre C, Samuel JL et al (2010) Molecular mechanisms in evolutionary cardiology failure. Ann NY Acad Sci 1188:58-67

Szkudelski T (2001) The mechanism of alloxan and streptozotocin action in B cells of the rat pancreas. Physiol Res 50(6):537-546

Tabet JY, Meurin P, Driss AB, Weber H et al (2009) Benefits of exercise training in chronic heart failure. Arch Cardiovasc Dis102:721-730

Takeda N, Dixon IC, Hata T et al (1996) Sequence of alterations in subcellular organelles during development of heart dysfunction in diabetes. Diab Res Clini Prac 30:S-S

Tamada A, Hattori Y, Houzen H, Yamada Y et al (1998) Effects of beta adrenoceptor stimulation on contractility, intracellular calcium and calcium current in diabetic rat cardiomyocytes. Am J Physiol 43:H1849-H1853

Tejada T, Catanuto P, Ijaz A et al (2008) Failure to phosphorylate Akt in podocytes from mice with early diabetic nephropathy promotes cell death. *Kidney Int* 73:1385-1393

Tervaert TW, Mooyart AL, Amann K, Cohen AH (2010) Pathologic Classification of Diabetic Nephropathy. JASN (2)4 556-563

The Diabetes Control and Complications (DCCT) Research Group: Effect of intensive therapy on the development and progression of diabetic nephropathy in the Diabetes Control and Complications Trial. Kidney Int 47:1703 –1720

Thorve VS, Kshirsagar AD, Vyawahare NS (2003) Diabetes-induced erectile dysfunction: epidemiology, pathophysiology and management. J Diabetes Complicat, 25: 129-136

Thomas D, McCormick R, Zimmerman S et al (1992) Aging and training induced alterations in collagen characteristics of rat left ventricle and papillary muscle. Am J Physiol Heart Circ Physiol 32(263) H778-H783

Thomas D. P., Cotter T. A., Li X., McCormick J., Gosselin L. E (2001) Exercise training attenuates aging-associated increases in collagen and collagen crosslinking of the left but not the right ventricle in the rat. Eur J Appl Physiol 85:164-169

Thomas DP, Zimmerman SD, Hansen TR, Martin DT, McCormick RJ (2000) Collagen gene expression in rat left ventricle: interactive effect exercise training. J Appl Physiol 89:1462-1468

Thompson EW (1988) Structural manifestations of diabetic cardiomyopathy in the rat and its reversal by insulin treatment. Am J Anat 182:270-282

Tirziu D, Giordano F J, Simons M (2010) Cell communications in the Heart. Circulation 122:928-937

Touvra AM, Volaklis KA, Spassis AT, Zois CE, Douda HD et al (2011) Combined strength and aerobic training increases transforming growth factor-β1 in patients with type 2 diabetes. Hormones (Athens) 10(2):125-30

Toyoda M, Najafian B, Kim Y, et al (2007) Podocyte detachment and reduced glomerular capillary endothelial fenestration in human type 1 diabetic nephropathy. Diab 56:2155-2160

Tsang K Y, Cheung, MC, Chan, D (2010) The developmental roles of the extracellular matrix: beyond structure to regulation. Cell Tissue Res. 339, 93-110

Tuttle K.R (2005) Linking Metabolism and Immunology: Diabetic Nephropathy Is an Inflammatory Disease. Am J Society Nephr 16:1537-1538

Twigg SM, Cao Z, McLennan SV, Burns WC et al (2002) Renal connective tissue growth factor induction in experimental diabetes is prevented by aminoguanidine. Endocrinoly *143*:*4907*-4915

Tziakas DN, Chalikias GK, Kaski JC (2005) Epidemiology of the diabetic heart. Coron Artery Dis, 16 Supplement 1:S3-S10

UK Prospective Diabetes Study (UKPDS) Group (1998) Effect of intensive bloodglucose control with metformin on complications in overweight patients with type 2 diabetes (UKPDS 34) Lancet 352:854-654

Umezono T, Toyoda M, Kato M et al (2006) Glomerular CTGF, TGF-beta 1 and type IV collagen in diabetic nephropathy. J Nephrol 19;751-7

USRDS Annual Data Report (2005) National Institutes of Health, National Institute of Diabetes and Digestive and Kidney Diseases; Bethesda

Valen G, Yan ZQ, Hansson GK (2001) Nuclear factor kappa-B and the heart. J Am Coll Cardiol 38:307–14

Vander AJ, Sherman JH, Luciano DS (2007) Human physiology: the mechanisms of body function. McGraw Hill, Columbus, OH, USA, pp701-830

Van Heerebeek L, Hamdani N, Handoko L et al (2008) Diastolic Stiffness of the Failing Diabetic Heart Importance of Fibrosis, Advanced Glycation End Products, and Myocyte Resting Tension Circulation, 117:43-51

Van Linthout S, Seeland U, Riad A, Eckhardt O et al (2008) Reduced MMP-2 activity contributes to cardiac fibrosis in experimental diabetic cardiomyopathy. Basic Res Cardiol 103(4):319-27

Van Melle JP, Bot M,De Jonge P et al (2010) Diabetes, Glycemic Control, and New-Onset Heart Failure in Patients with Stable Coronary Artery Disease: Data from the Heart and Soul Study. 33(9)2084-2089

Vander Zijl NJ, Hanemaaijer R, Tushuizen ME, Schindhelm RK et al (2010) Urinary matrix metalloproteinase-8 and -9 activities in type 2 diabetic subjects: A marker of incipient diabetic nephropathy? Clin. Biochem 43(7-8):635-639

Verzola D, Gandolfo MT, Ferrario F et al (2007) Apoptosis in the kidneys of patients with type ii diabetic nephropathy. *Kidney Int* 2007*;*72*:*1262-1272

Voulgari C, Papadogiannis D, Tentolouris N (2010) Diabetic cardiomyopathy: from the pathophysiology of the cardiac myocytes to current diagnosis and management strategies. Vasc Health Risk Manag, 6: 883-903

Wahab NA, Yevdokimova N, Weston BS et al (2001) Role of connective tissue growth factor in the pathogenesis of diabetic nephropathy. Biochem J 359*:*77-87

Walker AC, Spinale FG (1999) The structure and function of the cardiac myocyte: a review of fundemenatl concepts. J Thorac Cardiovasc Surg 118: 375-382

Wang B, Herman-Edelstein M, Koh P, Burns W et al (2010) E-cadherin expression is regulated by miR-192/215 by a mechanism that is independent of the profibrotic effects of transforming growth factor-beta. Diabetes 59:1794-1802

Wang B, Koh P, Winbanks C, Coughlan MT et al (2011) miR-200a prevents renal fibrogenesis through repression of TGF-β2 expression. Diabetes 60:280-287

Wang B, Omar A, Angelovska T, Drobic V, Rattan SG, Jones SC, Dixon IM (2007) Regulation of collagen synthesis by inhibitory Smad7 in cardiac myofibroblasts. Am J Physiol Heart Circ Physiol 293:H1282-H1290

Wang J, Song Y, Wang Q et al (2006) Causes and Characteristics of Diabetic Cardiomyopathy Rev Diabet Stud 3(3):108-117

Ward ML, Crossman DJ (2014) Mechanisms underlying the impaired contractility of diabetic cardiomyopathy. World J Cardiol 6(7): 577-584

Wasén E, Isoaho R, Mattila K, Vahlberg T, Kivelä SL, Irjala K (2004) Renal impairment associated with diabetes in the elderly. Diabetes Care 27:2648-53

Way KJ, Isshiki K, Suzuma K, Yokota T, Zvagelsky D, et al. (2002) Expression of connective tissue growth factor is increased in injured myocardium associated with protein kinase C beta2 activation and diabetes. Diabetes 51:2709-2718

Weiss RB (1982) Streptozotocin: A review of its pharmacology, efficacy and toxicity. Canc Treat Rep 66: 427-438

Wells C and Gordon E (2008) Geographical variations in premature mortality inEngland and Wales. Health Statistics Quarterly 2008. In Office for National Statistics. Available via http://www.statistics.gov.uk/downloads/theme_health/HSQ38 Accessed: 19th April 2010

Wells CC, Riazi S, Mankhey RW, Bhatti F, Ecelbrager C, Maric C (2005) Diabetic nephropathy is associated with decreased circulating estradiol levels and imbalance in the expression of renal estrogen receptors. Gender Medicine 2:227-237

Wencker D, Chandra M, Nguyen K et al (2003) A mechanistic role for cardiac myocyte apoptosis in heart failure. J Clin Invest 111: 1497-1504

Westermann D, Rutschow S, Jager S, Linderer A, Anker S, et al (2007) Contributions of inflammation and cardiac matrix metalloproteinase activity to cardiac failure in diabetic cardiomyopathy: the role of angiotensin type 1 receptor antagonism. Diabetes 56:641-646

Westermann D, Walther T, Savvatis K, Escher F, Sobirey M, et al (2009) Gene deletion of the kinin receptor B1 attenuates cardiac inflammation and fibrosis during the development of experimental diabetic cardiomyopathy. Diab 58:1373-1381

White KE, Bilous RW (2000) Type 2 diabetic patients with nephropathy show structural-functional relationships that are similar to type 1 disease. J Am Soc Nephrol 11: 1667-1673

Winer N, Sowers J. R (2004). Epidemiology of diabetes. J. Clinical. Pharmacol 44: 397-405

Willemsen S, Hartog JW, Heiner-Fokkema MR et al (2011) Advanced glycation end-products, a pathophysiological pathway in the cardiorenal syndrome. Heart Fail Rev [Epub ahead of print]

Willerson JT & Ridker PM (2004) Inflammation as a Cardiovascular Risk Factor. Circulation 109[suppl II]:II-2–II-10

Wolf G (2003) Growth factors and the development of diabetic nephropathy. Curr Diab Rep 3:485-490

Wolf G (2004) New insights into the pathophysiology of diabetic nephropathy: from haemodynamics to molecular pathology. Eur J Clin Invest 34(12):785-796

Wolf G, Reinking R, Zahner G, et al (2003) Erk 1,2 phosphorylates p27Kip1: functional evidence for a role in high-glucose-induced hypertrophy of mesangial cells. Diabetol 46:1090-9

Wong AKF, Donnelly L, Doney A et al (2010) Glycaemic control and the development of heart failure and its importance in diabetic patients with established heart failure. Abstracts from the European Society of Cardiology 2010 Congress.

Woodcock EA & Matkovich SJ (2005) Cardiomyocytes structure, function and associated pathologies. The Inter J of Biochem & Cell Bio 37: 1746-1751

Woodiwiss AJ, Oosthuyse T, Norton GR (1998) Reduced cardiac stiffness following exercise is associated with preserved myocardial collagen characteristics in the rat. Eur J Appl Physiol 78:148-154

Writing Group Members, Lloyd-Jones D, Adams R, Carnethon M, De Simone G et al (2009) Heart disease and stroke statistics-update: a report from the American heart association statistics committee and stroke statistics subcommittee. Circul 119(3):e21-181

Wright JA, Richards J, Becker DL (2012) Connexins and Diabetes. Cardiol Res and Prac, vol. 2012, Article ID 496904, 8 pages

Wu L, Derynck R (2009) Essential role of TGF-β1 Signalling in glucose-induced cell hypertrophy. Develop Cell 17: 35-48

Wu SQ, Kwan CY & Tang F 1998 Streptozotocin-induced diabetes has differential effects on atrial natriuretic peptide synthesis in the rat atrium and ventricle: a study by solutionhybridization-RNase protection assay. Diabetologia 6:660-665

Wu Y, Zhang X, Salmon M, Lin X, Zehner ZE (2007) TGFbeta1 regulation of vimentin gene expression during differentiation of the C2C12 skeletal myogenic cell line requires Smads, AP-1 and Sp1 family members. Biochim Biophys Acta 1773:427-39

Xiao H, Zhang YY (2008) Understanding the role of transforming growth factor-beta signalling in the heart: overview of studies using genetic mouse models. Clin Exp Pharmacol Physiol 35(3):335-341

Yabluchanskiy A,Yonggang MA, Iyer RP, Hall ME, Lindsey MA (2013) Matrix Metalloproteinase-9: Many Shades of Function in Cardiovascular Disease. Physiology (Bethesda) 28(6): 391-403

Yamamoto T, Nakamura T, Noble NA, Ruoslahti E, Border WA (1993) Expression of transforming growth factor beta is elevated in human and experimental diabetic nephropathy. Proc Natl Acad Sci USA 90:1814-1818

Yanni J, Tellez JO, Sutyagin PV et al (2010) Structural remodelling of the sinoatrial node in obese old rats. J Mol Cell Cardoil 48(4):653-662

Yao A, Su Z, Nonaka A et al (1998) Abnormal myocyte Ca homeostasis in rabbits with pacing-induced heart failure. Am J Physiol 275:H1441-H1448

Yaras N, Ugur M, Ozdemir S, Gurdal H, Purali N et al (2005) Effects of diabetes on ryanodine receptor Ca release channel (RyR2) and Ca2+ homeostasis in rat heart. Diabetes 54:3082-3088

Yasushi A, Tomoda M, Murata Y, Inui H et al (2007) Antidiabetic effect of long-term supplementation with Siraitia grosvenori on the spontaneously diabetic Goto-Kakizaki rat. Br J Nutr 97:770-775

Yndestad A, Damas JK, Oie E, Ueland T et al (2006) Systemic inflammation in heart failure – The whys and wherefores. Heart Fail Rev 11:83–92

Yokoi H, Mukoyama M, Sugawara A, Mori K et al (2002) Role of connective tissue growth factor in fibronectin expression and tubulointerstitial fibrosis. Am J Physiol Renal Physiol 282*:*F933-*F942*

Young LH, Wackers FJ, Chyun DA, et al (2009) DIAD Investigators. Cardiac outcomes after screening for asymptomatic coronary artery disease in patients with type 2 diabetes: the DIAD study, a randomized controlled trial. JAMA, 301: 1547-1555

Yu W, Wu J, Cai F, Xiang J, Zha W, et al (2012) Curcumin alleviates diabetic cardiomyopathy in experimental diabetic rats. PLoS One 7:e52013

Yu Z, Tibbits GF, McNeill JH (1994) Cellular functions of diabetic cardiomyocytes: contractility, rapid-cooling contracture, and ryanodine binding. Am J Physiol 266:H2082-H2089

Zabalgoitia M, Ismaeil MF, Anderson L, Maklady FA (2001) Prevalence of diastolic dysfunction in normotensive, asymptomatic patients with well-controlled type 2 diabetes mellitus. Am J Cardiol 87(3):320-323

Zarain-Herzberg A, Yano K, Elimban V, Dhalla NS (1994) Cardiac sarcoplasmatic reticulum Ca2+− ATPase expression in streptozotocin-induced diabetic rat. Biochem Biophys Res Comm 203:113-120

Zhang H, Chen X, Gao E et al (2010) Increasing Cardiac Contractility After Myocardial Infarction Exacerbates Cardiac Injury and Pump Dysfunction. Circ Res 107: 800-809

Zhang L, Cannel MB, Phillips AJ et al (2008) Altered calcium homeostasis does not explain the contractile deficit of diabetic cardiomyopathy. Diab 8:2158-2166

Zhang L, Ward ML, Phillips AR, Zhang S et al (2013) Protection of the heart by treatment with a divalent-copper-selective chelator reveals a novel mechanism underlying cardiomyopathy in diabetic rats. Cardiovasc Diabetol 12:123

Zhang T, Maier LS, Dalton ND, Miyamoto, S et al (2003) The deltaC isoform of CaMKII is activated in cardiac hypertrophy and induces dilated cardiomyopathy and heart failure. Circ. Res 92:912-919

Zhang Y, Kanter EM, Laing JG, Aprhys C et al (2010) Connexin43 expression levels influence intracellular coupling and cell proliferation of native murine cardiac fibroblasts. Cell Commun Adhes 15(3): 289-303

Zhong Y, Ahmed S, Grupp IL, Matlib MA (2001) Altered SR protein expression associated with contractile dysfunction in diabetic rat heart. Am J Physiol Heart Circ Physiol 281:H1137-H1147

Zhou YP, Ostenson C, Ling ZC and Grill V (1995) Deficiency of pyruvate dehydrogenase activity in pancreatic islet cells of diabetic GK rats. Endocrinology 136:3546-355

Zimmet PZ, Alberti KG (2006) Introduction: globalization and the non-communicable disease epidemic. Obesity (Silver Spring)14(1):1-3

Ziyadeh FN (1993) The extracellular matrix in diabetic nephropathy. Am J Kidney Dis 22:736-744

COMMUNICATIONS

Papers

K. A. Salem, M. A. Qureshi, V. Sydorenko, K. Parekh, P. Jayaprakash, T. Iqbal, M. Oz, T. E. Adrian and F. C. Howarth (2013) Effects of exercise training on excitation-contraction coupling and related mRNA expression in hearts of Goto-Kakizaki type 2 diabetic rats. Molecular and Cellular Biochemistry, 380(1-2):83-96

T. Iqbal, P. J. Welsby, F. C. Howarth, K. R. Bidasee, E. Adeghate, J. Singh (2014) Effects of Diabetes-Induced Hyperglycemia in the Heart: Biochemical and Structural Alterations. Diabetic Cardiomyopathy, Advances in Biochemistry in Health and Disease 9:77-106

T. Iqbal, F. C. Howarth, K. R. Bidasee, E. Adeghate, J. Singh (2015) Hyperglycemia-Induced Cardiac Contractile Dysfunction in the Diabetic Heart (Submitted to Journal of Physiology)

Abstracts in conference proceedings

T. Iqbal, F. C. Howarth, K. R. Bidasee, E. Adeghate and J. Singh Left Ventricle structural remodelling and cardiomyocyte contractile function in the streptozotocin-induced type 1 diabetic rat. Physiology 2012, Edinburgh, UK, July 2012

T. Iqbal, F. C. Howarth, K. R. Bidasee, E. Adeghate and J. Singh Left ventricle structural remodelling in the Streptozotocin-induced type 1 diabetic rat. International Congress of Physiological Sciences 2013, Birmingham, UK, July, 2013

T. Iqbal, A. D'Souza, F. C. Howarth, E. Adeghate and J. Singh Cardiomyocyte contractile function and structural remodelling in the left ventricle of streptozotocin-induced type 1 diabetic rat, Physiology 2014, London, UK, July 2014

S.S Kappala, **T. Iqbal**, J. Espino, A. Rodriguez, J.A. Pariente, K.R Bidasee and J. Singh Dysregulation of intracellular Ca^{2+} in lymphocytes and neutrophils in type 2 diabetic patients, Experimental Biology 2014 meeting in San Diego. USA, April, 2014

T. Iqbal and J. Singh Hyperglycaemia –induced fibrosis in the diabetic heart: A need for early pharmacological intervention, The Indian Pharmaceutical meeting 2014, Noida, Delhi, December, 2014

T. Iqbal, A. D'Souza, K.R Bidasee and J. Singh Impact of age-induced hyperglycaemia on structural remodelling in the left ventricle of the type 2 diabetic Goto-Kakizaki rat, Abstract submitted for Experimental Biology, Boston, March 2015

T. Iqbal, F. C. Howarth, K. R. Bidasee, E. Adeghate and J. Singh Chronic Type 1 diabetes mellitus induces structural changes, fibrosis and hypertrophy in the rat kidneys (Abstract accepted for poster presentation to Physiology 2015, 6-8 July, 2015